Dynamics and interactions in natural resources economics : land use, soil pollution and renewable energy

Alexandre Cornet

UNIVERSITÉ PARIS 1
PANTHÉON SORBONNE

UNIVERSITE PARIS I PANTHÉON SORBONNE
UFR d'économie
Laboratoire de rattachement : Centre d'Economie de la Sorbonne

THÈSE
Pour l'obtention du titre de Docteur en économie
Présenté(e) et soutenu(e) publiquement
le 24 novembre 2020 par

Alexandre Cornet

Dynamiques et interactions en économie des ressources naturelles : usages des sols, pollution des terres et énergies renouvelables

Sous la direction de M. Professeur Antoine Mandel

Membre du Jury
M. Prof. Antoine d'Autume, Examinateur, Université Paris 1
M. Prof. Raouf Boucekkine, Rapporteur, Université d'Aix-Marseille
M. Prof. Lucas Bretschger, Examinateur, ETH Zurich
M. Prof. Antoine Mandel, Directeur, Université Paris 1
Mme. Prof. Aude Pommeret, Rapporteuse, Université de Savoie
Mme. Prof. Katheline Schubert, Examinatrice, Université Paris 1

UNIVERSITÉ PARIS 1
PANTHÉON SORBONNE

UNIVERSITE PARIS I PANTHÉON SORBONNE
UFR d'économie

Laboratoire de rattachement : Centre d'Economie de la Sorbonne

THÈSE
Pour l'obtention du titre de Docteur en économie
Présenté(e) et soutenu(e) publiquement
le 24 novembre 2020 par

Alexandre Cornet

Dynamiques et interactions en économie des ressources naturelles : usages des sols, pollution des terres et énergies renouvelables

Sous la direction de M. Professeur Antoine Mandel

Membre du Jury
M. Prof. Antoine d'Autume, Examinateur, Université Paris 1
M. Prof. Raouf Boucekkine, Rapporteur, Université d'Aix-Marseille
M. Prof. Lucas Bretschger, Examinateur, ETH Zurich
M. Prof. Antoine Mandel, Directeur, Université Paris 1
Mme. Prof. Aude Pommeret, Rapporteuse, Université de Savoie
Mme. Prof. Katheline Schubert, Examinatrice, Université Paris 1

Résumé

Cette thèse propose une analyse théorique des interactions entre les politiques économiques concernant l'utilisation et la préservation des ressources naturelles et le cadre technologique, environnemental et géographique dans lequel elles sont implémentées.

Le premier chapitre porte sur les dynamiques optimales de décarbonation du pic de consommation via le stockage d'énergies renouvelables intermittentes. Le processus de stockage est modélisé dans un cadre Markovien pour prendre en compte le caractère incertain de la disponibilité en énergies renouvelables intermittentes. Nous considérons du progrès technique à la fois en efficacité et en capacité de stockage ce qui nous permet d'étudier les politiques optimales de stockage selon leur coût, mais aussi selon le coût du carbone et de la disponibilité en énergie renouvelable. Nous appliquons notre modèle à l'analyse de la décarbonation du pic de consommation au Portugal.

Outre le caractère intermittent des énergies renouvelables et leur coût de stockage, leur usage des sols est aussi une limite à leur développement à grande échelle. Dans le deuxième chapitre, nous développons un modèle macrodynamique de la transition énergétique en prenant en compte la contrainte d'usage des sols. Le sol et l'énergie sont considérés comme les ressources nécessaires à la production agricole et le développement d'énergies renouvelables peut alors interférer avec la production agricole et l'activité de dépollution d'éventuelles zones forestières. Nous étudions théoriquement ces arbitrages en termes d'usages des sols entre la production agricole, le développement des énergies renouvelables et les politiques de dépollution, puis nous appliquons notre modèle à l'étude du développement d'une filière biodiesel à base d'huile de palm au Brésil et des enjeux que cela soulève concernant la préservation de la forêt Amazonienne.

Le dernier chapitre de cette thèse s'intéresse aux sols agricoles mais du point de vue de l'impact de la pollution agricole sur la fertilité des terres. Nous nous intéressons plus précisément à la pollution diffuse des sols agricoles. Un modèle macrodynamique et spatial d'une économie agricole est ainsi développé en tenant compte du caractère diffusif de la pollution dans les terres agricoles. Nous montrons analytiquement que l'économie peut alors atteindre un équilibre spatial avec une région fertile et une région polluée, et que la région polluée peut soit stagner à des bas niveaux de fertilité soit rattraper le niveau de la région fertile. Une étude numérique est enfin menée pour illustrer nos résultats ainsi que pour étudier la résilience de l'économie à divers chocs de pollution.

Mots-clés : Economie de l'énergie et des ressources naturelles ; Economie spatiale et géographique ; Macroéconomie dynamique ; Méthodes numériques.

Summary

This thesis focuses on the interplay between dynamic economic policies concerning the use and preservation of natural resources and the technological, environmental and geographical frameworks in which they are implemented.

The first chapter proposes an analysis of optimal peak load decarbonation pathways when back-up fossil fuels are being gradually substituted by stored intermittent renewable energy. We model the process of intermittent renewable energy storage under renewable energy surplus uncertainty in a Markovian framework and consider technical progress in both storage efficiency and capacity. This allows us study the optimal storage policies with respect to carbon and storage costs, as well as the renewable energy surplus distribution. We analytically solve this problem under specific assumptions and use a value function iteration algorithm to investigate numerically on the optimal energy storage policies for peak load decarbonation in Portugal.

Along with intermittency and storage costs, land use is another limitation to the development of renewable energy. In the second chapter of this thesis, we develop a macrodynamic growth model of the energy shift integrating land use constraints. Land is considered as a resource for agricultural production along with energy. Developing renewable energy uses space and thus interferes with the agricultural sector. Moreover, pollution abatement policies, such as forests preservation policies, also compete with renewable energy for land in order to reduce pollution from the use of fossil fuels. We theoretically study the competition in land use between agriculture, pollution abatement and renewable energy production and apply our model to study the development of a palm oil biodiesel sector in Brazil, along with the issues it rises regarding the Amazon forest preservation.

The last chapter of this thesis also focuses on agricultural land, but this time to asses the impact of the agriculture activity on soil fertility. More precisely, we focus our analysis on a specific externality from the agricultural sector being diffuse soil pollution. Hence, we develop in this chapter a spatial growth model for an agricultural economy, in which pollution diffuses across space. We analytically show that, due to diffuse soil pollution, the economy can reach a long-term spatial equilibrium with a fertile region and a polluted region, and that the polluted region can either stagnate at low levels of fertility, or catch up with the fertile region. Our results are numerically illustrated, including the resiliency of the economy to recover from pollution shocks.

Keywords: Natural resources and energy economics ; Spatial and geographic economics ; Macrodynamics ; Numerical methods.

UNIVERSITÉ PARIS 1 PANTHÉON-SORBONNE

Thèse
pour obtenir le grade de
Docteur de l'Université Paris 1 Panthéon-Sorbonne
Discipline : Économie
présentée par
Alexandre Cornet

Dynamiques et Interactions en Economie des Ressources Naturelles : Usages des Sols, Pollution des Terres et Energies Renouvelables

Thèse soutenue publiquement le 24 novembre 2020
devant le jury composé de

M. Antoine d'Autume	Professeur à l'Université Paris 1	Examinateur
M. Raouf Boucekkine	Professeur à l'Université d'Aix-Marseille	Rapporteur
M. Lucas Bretschger	Professeur à l'ETH Zurich	Examinateur
M. Antoine Mandel	Professeur à l'Université Paris 1	Directeur
Mme. Aude Pommeret	Professeur à l'Université de Savoie	Rapporteuse
Mme. Katheline Schubert	Professeur à l'Université Paris 1	Examinatrice

CALIGULA. Oui. Enfin ! Mais je ne suis pas fou et même je n'ai jamais été aussi raisonnable. Simplement, je me suis senti tout d'un coup un besoin d'impossible. *(Un temps.)* Les choses, telles qu'elles sont, ne me semblent pas satisfaisantes.

HÉLICON. C'est une opinion assez répandue.

CALIGULA. II est vrai. Mais je ne le savais pas auparavant. Maintenant, je sais. *(Toujours naturel.)* Ce monde, tel qu'il est fait, n'est pas supportable. J'ai donc besoin de la lune, ou du bonheur, ou de l'immortalité, de quelque chose qui soit dément peut-être, mais qui ne soit pas de ce monde.

HÉLICON. C'est un raisonnement qui se tient. Mais, en général, on ne peut pas le tenir jusqu'au bout.

CALIGULA, *se levant, mais avec la même simplicité.* Tu n'en sais rien. C'est parce qu'on ne le tient jamais jusqu'au bout que rien n'est obtenu. Mais il suffit peut-être de rester logique jusqu'à la fin.

Albert CAMUS, *Caligula*, 1945, acte I, scène 4.

Aknowledgments

I would like to thank Prof. Antoine Mandel for his follow-up, advices and trust throughout my PhD thesis. A warm thank you to Prof. Carmen Camacho with whom I worked during the last two years of my PhD. I would also like to thank the members of my thesis committee for their feedbacks and kindness, Prof. Katheline Schubert and Prof. Antoine d'Autume, as well as Prof. Aude Pommeret and Prof. Raouf Boucekkine who kindly accepted to be the referees of my thesis and for their relevant reactions on my research. I am also very grateful to Prof. Lucas Bretschger who accepted to be part of my defense jury.

Thank you to the Centre d'Economie de la Sorbonne, to Prof. Michel Grabish and Prof. Agnieszka Rusinowska. I would also like to thank Prof. Jerome Lallement and Prof. Annie Cot for their very insightful class of epistemology of social sciences which I had the chance to follow during my PhD. Thank you also to all the professors who trusted me and welcomed me into their pedagogic team throughout the years of my PhD, from both the Economics and Mathematics departments of Université Paris 1 Panthéon-Sorbonne: Prof. Katheline Schubert, Prof. Gulven Rubin, Prof. Corinne Perraudin, Prof. Christophe Prechac, and Prof. Mohamed Bachir.

Last but not least, a warm thank you to the people who helped me in making my mobility at the Université Libre de Bruxelles, Prof. Gany Aldasehev, Nancy de Munck, and to the PhD students and post-doctoral fellows with whom I had the pleasure to discuss during my PhD thesis, Vipin, Brian, Emmanuel, Quentin, Alessandro, Kirstin, Frederico, Fernando, Mathieu, Gilles and Marie.

To my family, friends and *the ones who newer yawn.*

Summary

This thesis focuses on the interplay between dynamic economic policies concerning the use and preservation of natural resources and the technological, environmental and geographical frameworks in which they are implemented.

The first chapter proposes an analysis of optimal peak load decarbonation pathways when back-up fossil fuels are being gradually substituted by stored intermittent renewable energy. We model the process of intermittent renewable energy storage under renewable energy surplus uncertainty in a Markovian framework and show the existence of a limiting distribution for stored intermittent renewable energy for a given storage technology. Moreover, considering technical progress in storage technology through investments in both charging efficiency and storage capacity allows us to study the sensitivity of optimal storage policies with respect to carbon and storage costs, as well as the renewable energy surplus distribution. We analytically solve this problem under specific assumptions and use a value function iteration algorithm to investigate numerically on the optimal energy storage policies for peak load decarbonation in Portugal.

Along with intermittency and storage costs, land use is another limitation to the development of renewable energy. In the second chapter of this thesis, we develop a macrodynamic growth model of the energy shift integrating land use constraints. Land is considered as a resource for agricultural production along with energy. Developing renewable energy uses space and thus interferes with the agricultural sector. Moreover, pollution abatement policies, such as forests preservation policies, also compete with renewable energy for land in order to reduce pollution from the use of fossil fuels. Under specific assumptions on the price of fossil fuels we prove the existence of land use saddle path stable steady states and study the competition in land use between agriculture, pollution abatement and renewable energy production. Finally, our model is applied to study the development of a palm oil biodiesel sector in Brazil, along with the issues it rises regarding the Amazon forest preservation.

The last chapter of this thesis also focuses on agricultural land, but this time to asses the impact of the agriculture activity on soil fertility. More precisely, we focus our analysis on a specific externality from the agricultural sector being diffuse soil pollution. Hence, we develop in this chapter a spatial growth model for an agricultural economy, in which pollution diffuses across space. Here, in order to produce, the economy needs

fertile soil, naturally bounded by the amount of available land at each location. When regions have not yet reached their maximal soil fertility, they can locally invest in abatement in order to reduce soil pollution. Once a location reaches this maximum of fertile land, the economy is split in two: a fertile region and a polluted region. We analytically show that due to diffuse pollution, the polluted region can either stagnate at low levels of fertility, or catch up with the fertile region. Our results are numerically illustrated, including the resiliency of the economy to recover from pollution shocks.

Contents

Introduction

1. Natural resources in economics

The integration of natural resources in economics dates back to the early days of the discipline. Among others, let us mention the work of Malthus, sometimes considered as the father of natural resource economics, and in particular for his seminal work *Essay on the Principle of Population* (1798). In his work, Malthus already captured some of the essence of agricultural land which he took as limited, raising therefore the question of its scarcity. Later on, Ricardo reconsidered the scarcity of agricultural land, not as a limited resource, but by introducing the notion of decreasing returns to scale, that is the more exploited is land, the less marginally productive it becomes (Ricardo, 1815). As economics can be defined as the field of scarce resources allocation, natural resources therefore belong entirely to the scope of the discipline. Moreover, natural resources are at the center of human activity and nations' wealth and development, motivating therefore many research in economics from the question raised by the harvesting and production of fossil or renewable energy (Tahvonen and Salo, 1999; Greiner et al., 2013; Pommeret and Schubert, 2019), to the issues of food supply from fisheries and aquaculture (Hannesson, 2003; Regnier and Schubert, 2017) or agricultural lands (Ustaoglu et al., 2016; Martinho, 2019). Yet, economic mechanisms are necessary but not always sufficient to understand the complexity of the use, and sometimes the abuse, of natural resources, which often calls for interdisciplinary works (Ewel, 2001; MacMynowski, 2007).

Indeed, many issues raised by the use of natural resources are inherently at the frontier of other disciplines from either natural sciences, such as ecology or biophysics, (Knowler, 2002; Kroetz and Sanchirico, 2015; Castro et al., 2018) but also from other social sciences such as geography or political science (Wilson, 2017; González-Val and Pueyo, 2019). Hence, the interdisciplinary issues raised by the economics of natural resources requires and motivates researchers to reach out and explore beyond their own discipline, integrating tools and concepts from other fields. It is, for instance, the case of current researches on the economics of climate change in which economists must work closely with climate models (Golosov et al., 2014; Lemoine and Rudik, 2017; Gerlagh and Liski, 2018; Dietz et al., 2020), or on pollution accumulation which integrate concepts from ecology such as pollution damage thresholds and irreversibility

(Tahvonen and Withagen, 1996; Brock et al., 1999; Prieur, 2009; Le Kama et al., 2014). In today's context of ever-growing pressure on natural resources due to population growth or global industrial development, natural resources are now at the center of public debates and policies, and the need for analyzing the interaction between the economic activity and their use has never been greater.

This thesis analyzes precisely three aspects of such interactions by focusing more particularly on the use of intermittent renewable energy storage as a mean to decarbonize energy supply, by assessing new land use trade-offs raised by today's on-going development of climate change mitigation policies, and by studying the environmental concerns regarding diffuse soil pollution due to inappropriate agricultural practices. In the remaining of this introduction, we describe how the existing literature contributes to our analysis across three dimensions: the interactions between socio-economic activity and land use changes, the growing pressure on ecosystem services and the natural limits to the development of renewable energy production. We then highlight the key problematic addressed in each of the chapter of this thesis and put forward our main results.

1.1. Land use changes and the environment

Over the course of human development, many societal evolutions have led to complex land uses changes, altering consequently and substantially Earth's landscape (Foley et al., 2005). Among others, let us mention contemporary land use dynamics such as the extension of agricultural practices on forested land therefore leading to deforestation (Peres and Schneider, 2012; Curtis et al., 2018; Abman and Carney, 2020), or the ongoing growth of urban areas interfering directly with agricultural lands often located near city surroundings (Hatab et al., 2019; Peerzado et al., 2019). Hence, societal changes including demographic growth (Vesterby and Heimlich, 1991; Meyer and Turner, 1992; Li et al., 2015), urbanization (Wu et al., 2011; Dadashpoor et al., 2018) or even technological progress (Villoria et al., 2019) are important drivers for land use changes. Reciprocally, land use changes can also trigger new social or environmental challenges (Delphin et al., 2016; Zhang et al., 2020). The complex interactions between land use and societal changes led research in economics to focus more on the spatial distribution of the economic activity, as shown by the emergence of new spatial theories wether it is the New Economic Geography (Krugman, 1992), or more recently with the development of spatially explicit growth models (Boucekkine et al., 2018). Note that along

with economics, issues raised by land use changes also concern other social sciences such as geography (Meyer et al., 1996), evidently, but also sociology (Dijk et al., 2009) or anthropology (James and Fay, 2008). Yet, with the development of spatially explicit models, land use analysis in economics focus more particularly on understanding and identifying the forces that shape the spatial arrangement of the economic activity.

Among the various issues raised by land use changes, this thesis focuses more particularly on the interaction between land uses changes and the environment. Indeed, an important part of contemporary environmental problems are deeply rooted in land use changes such as air and water pollution (Sun et al., 2016; Camara et al., 2019), habitat destruction and biodiversity loss (Newbold et al., 2015; Garcia-Vega and Newbold, 2019; Yin et al., 2020), or even climate change (Kalnay and Cai, 2003; Feddema et al., 2005; Mahmood et al., 2014). For instance, the development of agricultural activities on former forested land can affect subtile ecological process leading to the depletion of forests' priceless ecosystem services such as natural habitats for biodiversity (Dudley and Alexander, 2017), flood mitigation and water purification (Bradshaw et al., 2007; Tan-Soo et al., 2014; Rogger et al., 2017) or pollution abatement services (Kindermann et al., 2008; Pugh et al., 2019). Such disturbance in complex ecological equilibria due to alterations in natural land uses can lead, in the long-term, to devastating environmental damages, and with today's ever-growing land use pressure on natural assets, the need for analyzing such potential repercussions is all the more important.

Such interplays between land use changes and the environment has been assessed in the economic literature in various streams. On the one hand, the environment can itself be responsible for the emergence of land use patterns. For instance, in Camacho and Pérez-Barahona (2015), the authors analyse how the spatial-dynamics of atmospheric pollution, responsible for local and global production damages, can lead to the emergence of land use patterns by providing with the optimal land use allocation between production, housing and abatement sites. In the same vein, Xepapadeas and Kyriakopoulou (2017) studies land use patterns emerging in industrial cities from developing economies. Here, employees tend to live away from the industrial areas because of local pollution emitted nearby. Yet, employees must work at such areas therefore if they locate too far away from the industrial sites they will suffer from high commuting costs. Hence, the emergence of land use patterns comes here from the trade-off between environmental quality preferences and commuting costs, which consequently shapes households' residential location decisions. Reciprocally, changes in

land use can be responsible for damaging the environment and the ecosystem services it provides. Among others, Denise et al. (2018) analyses the destruction of natural habitats due to agricultural production, as well as the negative feedbacks for agriculture from such destruction due to the loss of biodiversity-dependent ecosystem services. The authors derive the tax on agricultural land which internalizes biodiversity loss and increases both the carrying capacity of the environment and welfare. More recently, the interplay between land use and the environment has also been analyzed in a differential game approach in order to study strategic competition in land use. For instance, in Augeraud-Véron et al. (2020), farmers can allocate their land either to agricultural production or to biodiversity conservation according to others' decisions. The authors therefore study the strategic interactions among farmers and provide with the resulting land use decisions by finding explicitly the Nash equilibrium characterizing the overall portion of land allocated to agriculture, and the portion for biodiversity preservation.

1.2. Ecosystem services under pressure

Wether it is the competition in land use between forested land and agricultural land (Peres and Schneider, 2012; Curtis et al., 2018; Abman and Carney, 2020), or the ongoing urban sprawl interfering with the agricultural areas near city surroundings (Hatab et al., 2019; Peerzado et al., 2019), agricultural land is subject to many geographical pressures around the world (Jayne et al., 2014; Sun et al., 2016; Meyer and Früh-Müller, 2020). Yet, agricultural land is also subject to environmental pressures, and in particular due to the agricultural activity itself (Zalidis et al., 2002; Söderström et al., 2014). Agricultural yield depends strongly on soils quality and fertility, and in case of inappropriate agricultural practices, soils can loose some of their biological properties, endangering therefore the ecosystem services they provide (Lal, 2014; Drobnik et al., 2020). Indeed, soils are the complex and fragile mixture of air, water, mineral and organic components sitting on Earth's top layer and besides providing with 99% of food supply (Kopittke et al., 2019), soils are also responsible for many other ecosystems services such as carbon sequestration (Novara et al., 2017; Abbas et al., 2020; Bell et al., 2020), biodiversity habitats (Aksoy et al., 2017; Geisen et al., 2019; Mujtar et al., 2019) or flood mitigation (Ming et al., 2007; Watson et al., 2016). The value of such soils' functions and ecosystems services is tremendous. In the US, this value has been estimated to reach $11.4 trillion in 2017 (McBratney et al., 2017). Yet, such ecosystems services are very fragile as they depend greatly on subtile ecological equilibria, and with

today's expansion of industrial agricultural practices, these services are becoming more and more threatened. For instance, in 2017, the United Nations Convention to Combat Desertification (UNCCD) estimated that 24 billon tonnes of fertile soil are loss every year only due to inappropriate agricultural practices (UNCCD, 2017).

One of the main threat to soil quality and fertility is the intensive and ever-growing use of fertilizers (Savci, 2012; Alamri et al., 2018). Indeed, in 1980, the use of nitrate fertilizers around the world reached 60 million tonnes, and it almost doubled in 40 years as in 2014 it reached 110 million tonnes (FAO, 2015). The use of fertilizers and the resulting environmental pressures on soils depends strongly on local regulations regarding agricultural practices. For instance, after an important growth in the use of fertilizers in Europe, the European Union set the Nitrate Directive in 1991, (EU Commission, 1991) in order to reduce their use, which resulted in a decrease by half in Europe's fertilizers consumption (FAO, 2015). Yet, in Asia, and particularly in China, the use of fertilizers is still growing, and today, the Chinese Environmental Protection Ministry estimates that 19% of Chinese soils are polluted (CCICED, 2015). Moreover, the use of fertilizer is responsible for a very specific pollution called diffuse pollution (Li and Zhang, 1999; Campbell et al., 2005; Wang, 2006). Unlike classic point source pollution, diffuse pollution does not have a single or easily identified source and can spread over very wide areas while it accumulates in soil, making its analysis very complex (Xepapadeas, 2002). Hence, the global increase in the use of fertilizers and the complex nature of its diffusive and spatially distributed pollution call for new analysis regarding the environmental pressures applied on soils and their ecosystems services.

The diffusive dynamics of pollution has been studied in the economic literature in a broader research program on transboundary pollution, mostly applied to diffuse air and atmospheric pollution (Arnott et al., 2008; Camacho and Pérez-Barahona, 2015; Kyriakopoulou and Xepapadeas, 2017) as well as water pollution (Brock and Xepapadeas, 2008; Grass and Uecker, 2017; Augeraud-Véron et al., 2017). In such research program are developed spatial macrodynamic models in which pollution is not considered as point-source but as a negative externality which diffuses across the spatial domain of the economy. For instance, in La Torre et al. (2019) the authors analyse the case of diffuse air pollution responsible for local and global accumulation of pollutant in the atmosphere and show how the coordination at the local level of environmental policies are essential to reduce the global level of pollution. Here, the optimal policies are determined by a social planner acting as a central intergovernmental policy maker which

determines and imposes its policies to the local policymakers. Similarly, Augeraud-Véron et al. (2017) studies the problem of underground water pollution due to the use of fertilizers from agricultural production in which a central planner determines the optimal fertilizer policy. The transboundary pollution dimension here comes from the diffusion of pollutant through groundwater along with the convection dynamics of pollutant directly transported by groundwater flow. Finally, transboundary pollution has also been studied within dynamic games frameworks in which decisions are not only taken by a single central policy maker (as in most of this literature) but where several decision makers are considered along with the strategic interactions between them (De Frutos and Martìn-Herràn, 2019a; 2019b). In either case, with or without strategic interactions, the consideration of transboundary pollution leads inevitably to the use of parabolic partial differential equations within macrodynamic models (Boucekkine et al., 2013) which raises new technical challenges in order to capture the complexity of transboundary pollution, suggesting therefore new research for a better understanding of its impact on the environment (Augeraud-Véron et al., 2019).

1.3. Natural limits to the development of renewable energy

In order to reduce the global environmental pressures caused by the use of traditional pollutant fossil fuel on natural assets, the development of renewable energy (RNE) quickly became one of the main climate change mitigation policy. Indeed, the scenario of reaching carbon-free energy mix in less than two or three decades is now a reasonable objective for many countries, yet without raising new local challenges such as their intensive land needs and the management of their intermittent availability.

Indeed, compared to traditional fossil fuels, land intensities for RNE, that is the ratio of energy produced by land used, are three orders of magnitude smaller (Behrens and Zalk, 2018). This question of land requirements for RNE production raises new challenges at the political, environmental or economical level. For instance, the development of RNE power plants becomes inherently political when the acquisition of land disturbs, and sometimes deteriorates, the livelihood of vulnerable communities (Yenneti et al., 2016; McEwan, 2017; Korfiati, 2020). At the environmental level, the land allocated to massive energy projects can also be done at the expense of natural areas such as forests, at the risk of threatening natural ecosystems services or natural habitats resulting in a loss of biodiversity (Katzner et al., 2013; Hastik et al., 2015; Gasparatos et al., 2017). Finally, land acquisition for RNE production can cause

economic tensions with other land intensive activities such as the agricultural sector (Chakravorty et al., 2008; Bahel et al., 2013; Amigues and Moreaux, 2019) already pressured by the expansion of urban areas. In order to face land use pressures from RNE production, technological research now focus on the densification of energy production from renewable sources, leading to significant increases in power densities over time (Behrens and Zalk, 2018).

An other intrinsic limitation of RNE production is their intermittency. Such intermittency in the production of renewable energy is particularly noticeable in Germany in which the total wind energy capacity installed in 2017 reached 35.92 GW, while the average production was of 5.85 GW the same year (Sinn, 2017). Hence, the development of RNE carries a risk of energy shortage if the demand for electricity cannot be met by the production of intermittent renewable energy. In such case the need for back-up fossil fuels in order to produce dispatchable, yet pollutant, energy becomes necessary, even for countries which are already able to produce more RNE than it consumes. For instance, in March 2018, Portugal managed to produce 103% of its monthly electricity consumption from only renewable energy production. Yet, even with a volume of RNE produced exceeding Portugal's monthly consumption by 3%, the country still needed to use fossil fuels (APREN, 2018). Indeed, in contrast with conventional fossil fuels, renewable energy production is not dispatchable, meaning that such source of electricity cannot always provide on demand to meet the energy needs of the population as it is subject to the local climate conditions and its fluctuations.

Two ways of thinking about renewable energy intermittency have risen in the economic literature : a deterministic and predictable approach on the one hand, and an unpredictable and stochastic one on the other hand (Baker, 2013; Heal, 2016; Pommeret and Schubert, 2019). The predictable approach to model intermittency is often called variability and corresponds to a deterministic change in renewable primary energy. This is particularly useful to model the variation in solar radiation due to the interchange between night and daytime or to seasonal effects leading to predictable variations in wind availability (Heal, 2016; Helm and Mier, 2018; Pommeret and Schubert, 2019). Yet, such deterministic modelling of variation in primary renewable energy cannot cope with unpredictable weather events such as the passing of clouds over solar panels, or wind turbulence affecting wind turbine energy production. The second approach models availability of primary renewable energy as a random variable due to weather uncertainties. Indeed, even if major progress have been done regarding

weather forecasting in the last decades (Alley et al., 2019), owing to the non-linear physics of climate dynamics, weather conditions can only be known with some uncertainty. To that extent, it is more natural and general to model primary renewable energy availability in a stochastic framework. However, most of the research considering stochastic availability in renewable energy focus on the optimal design of energy mix in a static framework (Ambec and Crampes, 2012; 2017), and therefore do not consider the dynamic aspect of the on-going energy shift. In Pommeret and Schubert (2019) a dynamic model of the energy shift is presented while considering stochastic intermittent renewable energy and storage capacities but without technical progress on storage. Yet, in order to reach a carbon-free era with using intermittent RNE, the technological solution gathering the most attention today is the development of storage paired with a peak shifting mechanism (Heal, 2016; Helm and Mier, 2018). Hence, the development of energy storage is now a priority for decarbonizing energy supply and the integration of storage technical progress in dynamic models of the energy shift is required for sharper planning and decision making towards a carbon free era.

2. Thesis outline

Each chapter of this thesis focuses on the dynamics and interactions between economic policies on the one hand, and extra-economic dynamics on the other hand being, technological dynamics, geographic dynamics and environmental dynamics as illustrated and summarized in the following diagram.

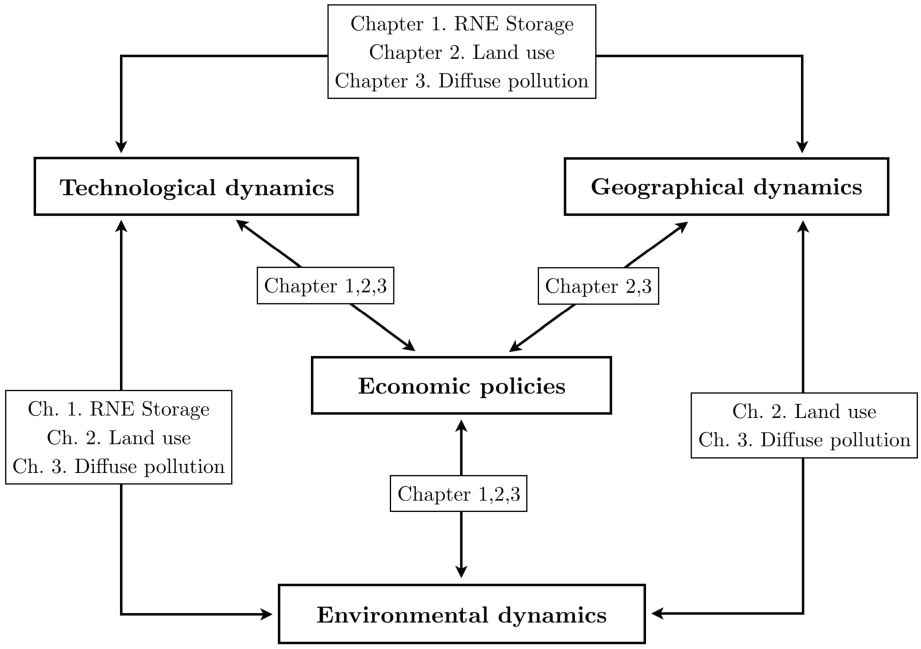

Chapter 1 studies optimal peak load decarbonation dynamics when using intermittent renewable energy storage. Storage is characterized by its efficiency and capacity levels and we analyse the optimal storage policies to reach a zero-carbon energy mix. Hence, both environmental dynamics, through the stochastic availably of renewable energy, and technological dynamics through storage technical progress are involved in this chapter, along with the optimal dynamics for energy storage policies.

Chapter 2 analyses the trade-offs in land use involved in the development of renewable energy production from land intensive technologies such as biomass. Here, all the dimensions are linked together as the geographical dynamics depends on the development of the land intensive renewable energy technology, which itself is developed as a response to the accumulation of pollution and the resulting environmental damages.

Finally, Chapter 3 analysis the stakes of diffuse soil pollution in an agricultural economy. Here pollution diffuses through soil and is therefore responsible for natural linkages between the different agricultural production sites of the economy. Hence, the geographical dynamics due to the spatially distributed soil quality depends on the environmental dynamics from soil pollution diffusion, as well as on the local technological levels of soil pollution abatement and the optimal agricultural policies maximizing welfare.

2.1. Chapter 1 : A Markov chain model for intermittent renewable energy storage and its application to peak load decarbonation

2.1.1. Problematic and method

The first chapter of this thesis focuses on intermittent renewable energy storage and answers the following question : what are the optimal peak-load decarbonation and storage policies when using intermittent renewable energy storage, with respect to the cost of storage, carbon prices, and the stochastic availability of renewable energy ?

We study the substitution dynamics of back-up fossil fuels used during peak-load by stored intermittent renewable energy. Three channels of energy supply are therefore considered: renewable energy and stored renewable energy which we consider to be free of use, yet with a stochastic availability, and back-up fossil fuels which have a cost on usage, but are dispatchable. Out from peak-load, storage capacities can store the

stochastic excess of renewable energy that is not directly consumed, which then can be destored during peak demand through a peak-shifting mechanism in order to reduce the use of pollutant back-up fossil fuels during peak load.

Splitting energy supply during peak demand between fossil fuels and stored renewable energy reduces the use of pollutant energy sources but implies a risk of energy shortage as the process of renewable energy storage is stochastic due to renewable energy intermittency. We model the process of intermittent renewable energy storage due to weather uncertainties in a Markovian framework and show that there exists an invariant distribution of stored intermittent renewable energy for a given storage technology. From this invariant distribution we define the risk of energy shortage involved during peak demand, and define the optimal mix between back-up fossil fuels and stored renewable energy which minimizes the use of pollutant fossil fuels while controlling the risk of energy shortage bellow a specific risk threshold. The model's framework can therefore be illustrated and summarized in the following diagram with the governing variables and parameters.

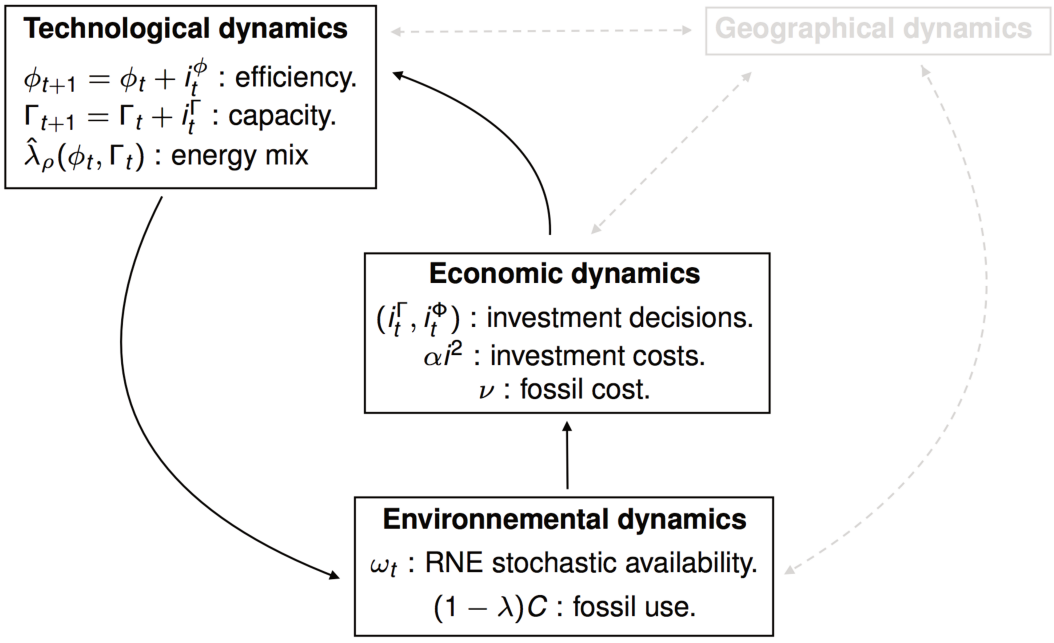

Finally, our model is applied to study Portugal's optimal peak load decarbonation pathways by considering technical progress in storage technology through both investment in charging efficiency and capacity. We calibrate our model by considering as the main source of fossil fuels used during peak load in Portugal combined cycle gas turbine (CCGT) characterized by a Levelized Cost of Energy (LCOE) of 100$/MWh (IEA, 2015).

2.1.2. Results

Within such framework we provide with the optimal storage policies and decarbonation time horizons with respect to Levelized Costs of Storage (LCOS), carbon prices, and the stochastic availability of renewable energy surplus.

At constant LCOE for CCGT, an increase in LCOS leads to a decrease in peak load decarbonation time horizon. Results are given considering three scenario of LCOS from Schmidt et al. (2019) being LCOS_{low} = 200\$/MWh, LCOS_{mean} = 600\$/MWh and LCOS_{high} = 1000\$/MWh. For LCOS_{low} = 200\$/MWh, peak load decarbonation is reached in 11 years, whereas for the mean LCOS scenario (600\$/MWh) transition time reaches 26 years, up to 37 years in the case of high LCOS (1000\$/MWh). Hence, the costs of energy storage has an important impact on transition time, and in average a reduction in 31 \$/MWh in LCOS accelerates full peak load decarbonation by one year, making LCOS a central metric for peak load decarbonation planning when using renewable energy storage.

For each LCOS scenario, as the cost of carbon emissions increases, the time for reaching full peak load decarbonation decreases. Moreover, the higher the LCOS, the more sensitive are peak load decarbonation time horizons to carbon costs variations. Indeed, the time horizons difference between a carbon price of 0 \$/tCO2 and 300 \$/tCO2 for LCOS = 1000 \$/MWh is 13 years, for LCOS = 600 \$/MWh it is 11 years and for LCOS = 200 \$/MWh it drops to 5 years. In average, an increase of 37\$ in the price of carbon emissions leads to a decrease of 1 year in peak load transition time, when a decrease in 31\$/MWh in LCOS leads to the same results.

Note that the previous results are given while considering the same benchmark distribution for the stochastic availability of renewable energy. This leads us to study how variations in the mean or variance of renewable energy availability affects the optimal storage policies and peak load decarbonation time horizons. In average, an increase of 2 GWh in renewable energy surplus mean leads to a decrease in decarbonation time horizon by one year, while investments in storage technology are being more allocated to capacity rather than to efficiency. Yet, time horizon for peak load decarbonation and storage policies show less sensitivity to the energy surplus dispersions, making therefore the energy surplus mean value a more practical statistic for peak load decarbonation planning, compared to its dispersion.

2.2. Chapter 2 : Land use and the energy shift

2.2.1. Problematic and method

The second chapter examines the trade-off in land use for an agricultural economy when different land intensive climate change mitigation policies are applied. More precisely, we focus on two land intensive climate policies being the development of renewable energy providing carbon free energy and forest preservation policies for pollution abatement. Hence, the central question in this chapter is: how do land intensive climate mitigation policies compete with each other for land, along with an agricultural sector which itself requires land, while being sensitive to pollution ?

The specificity of our analysis is to consider that renewable energy plants and abatement take a non-negligible space on agricultural production land. This trade-off in land use is studied within a macrodynamic growth model, with two productivity factors being land allocated to agricultural production and energy supplied by both fossil fuels, that have a cost, pollute, but take negligible space on production land, and renewable energy, that is free, does not pollute, but takes considerable space on agricultural production land. Here the model's framework can therefore be illustrated and summarized in the following diagram with the governing variables and parameters.

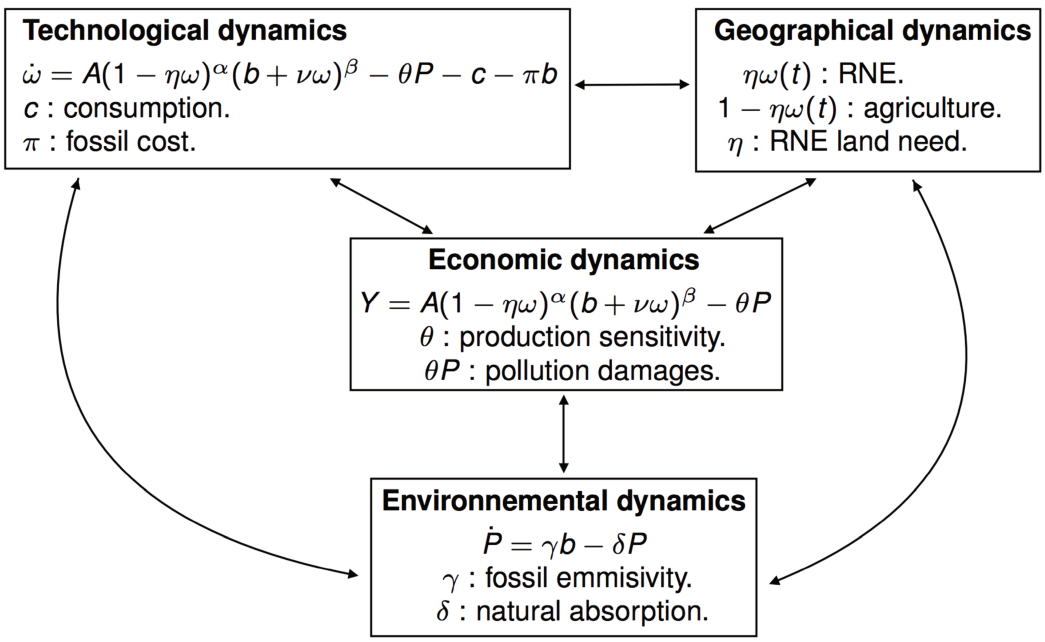

We first study the impact of renewable energy policies without abatement. A benchmark model is introduced in which social planner does not account for pollution

emissions from the use of fossil fuels. We show that the economy converges towards a steady state and prove its saddle-path stability. We then examine a model in which social planner integrates pollution emissions and prove similarly the existence of a unique saddle-path stable steady state towards which the economy converges. We describe the two steady states and derive the tax on fossil fuels which must be applied in the benchmark model for the two equilibrium to coincide.

In the final section, both renewable energy and abatement policies are considered. As these two mitigation measures compete for land, we study the optimal land use policies between abatement and renewable energy production with respect to agricultural production sensitivity to pollution. Moreover, we apply our model to study the development of a palm oil biodiesel sector in Brazil and the questions it raises regarding Amazon forest preservation policies (Villela et al., 2014).

2.2.2. Results

In the case of renewable energy production as the only land intensive mitigation policy, the more dense is energy production, the more land shall be allocated towards renewable energy production rather than towards agriculture. This result can be seen as a case of comparative advantage. Indeed, as energy production and agriculture compete for land to produce output, social planner allocates more land to the more productive sector. Hence, the denser is the renewable energy production, the more land must be allocated to its activity. Moreover, the more sensitive is the agricultural sector to pollution, the more land shall be allocated to renewable energy production as well, in order this time to assure the continuity of output production while limiting environmental damages.

In the case of both mitigation policies available, that is renewable energy production and afforestation for abatement, social planner's strategy for land use reallocation depends on the level of the agricultural production sensitivity to pollution. For low sensitivity, as agriculture becomes more sensitive to pollution, agricultural land must be reallocated towards both renewable energy (for mitigation purposes and compensation of production losses) and abatement (only for mitigation). Yet, for high sensitivities, along with agricultural land, it is also best to sacrifice renewable energy production land and reallocate exclusively land to abatement in order to save output from important pollution damages.

Finally, we apply our model to the stakes of preserving the Amazon forest in Brazil.

More particularly, we focus on the emerging market of palm oil production for biodiesel in Brazil in Amazonia and on the resulting opportunity cost for Brazil of preserving the Amazon forest. Within a wide range of pollution sensitivities, the price of carbon for preserving the Amazon forest's surface area at its current size lies in-between 300 $/tCO2 and 760 $/tCO2 which is 2 to 5 times greater than actual carbon prices (World Bank, 2020). Hence, in order to restrain the on-going Amazon deforestation and maintain the forest's current surface area for preserving its global GHG abatement services, the international community must accept to pay higher compensation through financial transfers to Brazil due to ever-growing land use pressures on the Amazon forest, which, in our case, comes from the development of palm oil biodiesel in Brazil.

2.3. Chapter 3 : Soil pollution diffusion in a spatial agricultural economy

2.3.1. Problematic and method

In the third chapter we answer the following question : how diffuse pollution from agricultural practices affects soils' ecosystems services, and what are the feedback mechanisms leading to spatially heterogenous productivities in agricultural land ?

To answer such question we study an agricultural economy using a spatial growth model and analyse diffuse soil pollution occurring in the agricultural sector. Here each location needs fertile soil to produce but production locally pollutes and transforms fertile soil into polluted soil, useless for production. The economy can either use its production for consumption or for depolluting soil that has been affected by the production process. Moreover, we allow the pollution to diffuse across locations and we model the diffusion process using Fick's law of motion. This means that the activity at one location depends and has an impact on its surrounding locations as the pollution of one location's surroundings can reach this location and reciprocally.

To provide with the explicit solutions for the optimal agricultural policies across space and time which maximize welfare, we make use of dynamic programming in order to transpose a spatio-temporal optimization problem to an eigenvector/eigenvalue problem that we solve using Sturm-Liouville theory as in Boucekkine et al. (2018). As the problem is specified in a spatio-temporal framework, planner's objective becomes an inter-temporal and intra-spatial optimization problem for a time and space dependent

utility function which can be generically written as:

$$\max_{c} \int_0^{\infty} e^{-\rho t} \left(\int_0^{2\pi} u(c(t,\theta)) d\theta \right) dt, \tag{1}$$

where $t \geq 0$ is the time component, $\theta \in [0, 2\pi]$ the space component from a 2π-periodic spatial domain, and $c(t,\theta)$ local consumption. Yet, in order to use such method, the state equation for the spatio-temporal productivity factor, here $F(t,\theta)$, must be written in the following linear form:

$$\frac{\partial F}{\partial t}(t,\theta) = \mathcal{L}F(t,\theta) + f(c(t,\theta)),$$

where $\mathcal{L}$ is a linear operator in the productivity factor and f a linear function in consumption. Under such specification, the optimal consumption path $c^*(t,\theta)$ solution to (1), can be written as:

$$c^*(t,\theta) = h(\lambda_0, e_0, F_0),$$

where λ_0 is the smallest eigenvalue of the problem $\mathcal{L}u = \lambda u$ associated to the eigenvector e_0, $F_0 = F(0,\theta)$ the initial distribution of the productivity factor, and h some function of these quantities and the remaining exogenous variables of the problem. Hence, in this chapter, the model's framework can be illustrated and summarized in the following diagram with the governing variables and parameters.

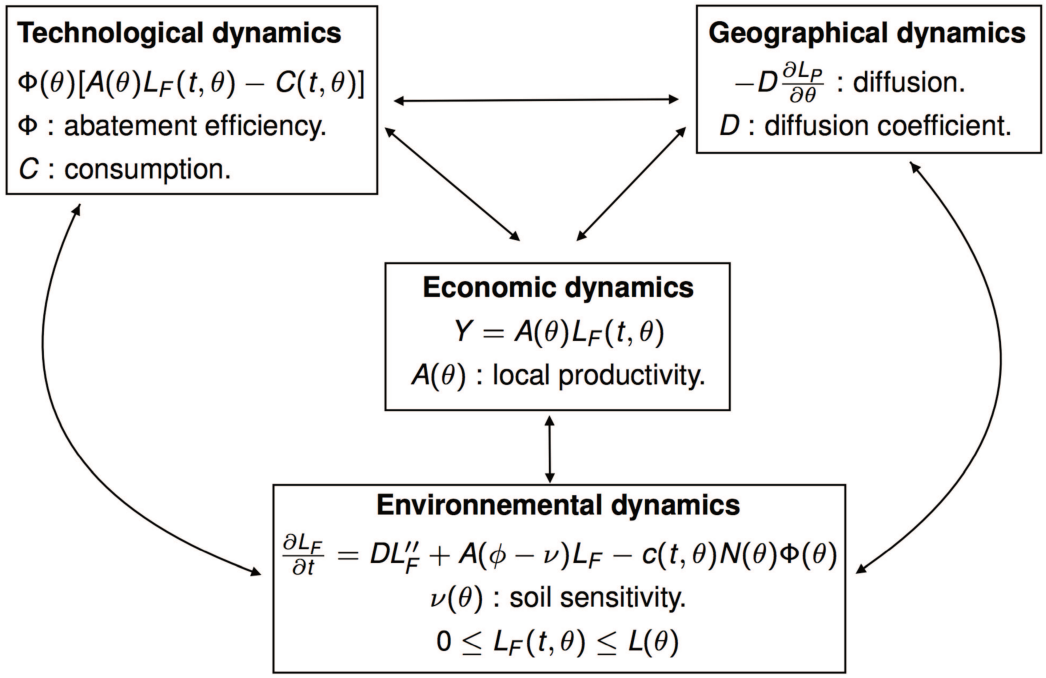

2.3.2. Results

The optimal agricultural policies and the resulting spatial-dynamics of fertile soils are described along two phases. In the first phase, during which no location have reached their maximal soil fertility level, the optimal policies are solved in the most general way, allowing for heterogeneity in productivity, population and soil characteristics. We give the optimal path for consumption as well as soil fertility distribution along the optimal consumption path that maximizes welfare. We prove that under specific assumptions on the model's parameter, the detrended fertile soil distribution converges and that its mean value is conserved throughout the optimal consumption path. We also study the transfert in consumption and in soil fertility due to diffusion and show that soil pollution diffusion tends to transfert consumption from the region that was initially more allocated in fertile soil to the region that was initially less allocated in fertile soil.

Once the economy reaches Phase 2, that is when at least one location has reached its maximal soil fertility level, the economy is thereafter divided in two regions: one fertile region, in which locations succeeded in making fertile all their land, and a polluted region, in which locations has not yet reached their upper boundary in fertile soil. The two regions are therefore separated by a pollution frontier which evolves over space and time, according to the optimal decisions taken in both the polluted and fertile region. We investigate on the evolution of such dynamic pollution frontier between the two regions, and prove the possible emergence of two distinct and permanent regions respectively polluted and fertile in the long-run steady state.

We finally investigate numerically on the economy's resiliency to pollution shocks by performing numerical "pollution stress tests". Overall, we show that if the economy uses a sufficiently advanced production technology, then the pollution shock can be absorbed with time by the economy through optimally localized investment decisions in pollution abatement. In such cases, the economy progressively relaxes back to its initial fully fertile state. However, if technology is not sophisticated enough, then the rather local initial pollution shock can diffuse all across the economy, at the risk of affecting a too large area of the economy above which the shock can no longer be contained, leading therefore to global collapse.

References

[1] Abbas, F., Hammad, H. M., Ishaq, W., Farooque, A. A., Bakhat, H. F., Zia, Z. and Cerdà, A. (2020), "A review of soil carbon dynamics resulting from agricultural practices", *Journal of Environmental Management*, 268, 110319.

[2] Abman, R. and Carney, C. (2020), "Agricultural productivity and deforestation: Evidence from input subsidies and ethnic favoritism in Malawi", *Journal of Environmental Economics and Management*, 103, 102342.

[3] Abu Hatab, A., Cavinato, M. E. R., Lindemer A. and Lagerkvist C.-J. (2019), "Urban sprawl, food security and agricultural systems in developing countries: A systematic review of the literature", *Cities*, 94, 129-142.

[4] Aksoy, E., Louwagie, G., Gardi, C., Gregor, M., Schröder, C. and Löhnertz, M. (2017), "Assessing soil biodiversity potentials in Europe", *Science of The Total Environment*, 589, 236-249.

[5] Alamri, S. and Khan, M. (2018), "Fertilizers and Their Contaminants in Soils, Surface and Groundwater", *Reference Module in Earth Systems and Environmental Sciences*.

[6] Alley, B. R., Kerry, A. E. and Zhang, F. (2019), "Advances in weather prediction", *Science*, 363(6425), 342-344.

[7] Ambec, S. and Crampes, C. (2012), "Electricity provision with intermittent sources of energy", *Resource and Energy Economics*, 34, 319-336.

[8] Ambec, S. and Crampes, C. (2017), "Decarbonizing electricity generation with intermittent sources of energy", *TSE Working Paper, 15, 603.*

[9] Amigues, J.-P. and Moreaux, M. (2019), "Competing land uses and fossil fuel, and optimal energy conversion rates during the transition toward a green economy under a pollution stock constraint", *Journal of Environmental Economics and Management*, 97, 92-115.

[10] APA (2019), "Roadmap for Carbon Neutrality 2050 : Long-term Strategy for Carbon Neutrality of the Portuguese Economy by 2050".

[11] APREN (2018), "Boletim Energias Renovaveis Edicao Mensal 1".

[12] Arnott, R., Hochman, O. and Rausser, G. C. (2008), "Pollution and land use: Optimum and decentralization", *Journal of Urban Economics*, 64(2), 390-407.

[13] Augeraud-Véron, E., Fabbri, G. and Schubert, K. (2020), "Volatility-Reducing Biodiversity Conservation Under Strategic Interactions", *Preprint (No. 2020011). Université catholique de Louvain, Institut de Recherches Economiques et Sociales (IRES).*

[14] Augeraud-Véron, E., Boucekkine, R. and Veliov, V. M. (2019), "Distributed optimal control models in environmental economics: a review", *Mathematical Modelling of Natural Phenomena*, 14(1).

[15] Augeraud-Véron, E., Choquet, C. and Comte, E. (2017), "Optimal control for a groundwater pollution ruled by a convection-diffusion-reaction problem", *J. Optim. Theory Appl.*, 173, 941-966.

[16] Bahel, E., Marrouch, W. and Gaudet, G. (2013), "The economics of oil, biofuel and food commodities", *Resource and Energy Economics*, 35(4), 599-617.

[17] Baker, E., Fowlie, M., Lemoine D. et Reynolds S. S. (2013), "The economics of solar electricity", *Annual Review of Resources Economics*, 5, 387-426.

[18] Behrens, P. and Zalk, V. J. (2018), "The spatial extent of renewable and non-renewable power generation: A review and meta-analysis of power densities and their application in the U.S.", *Energy Policy*, 123, 83-91.

[19] Bell, S. M., Barriocanal, C., Terrer, C. and Rosell-Melé, A. (2020), "Management opportunities for soil carbon sequestration following agricultural land abandonment", *Environmental Science and Policy*, 108, 104-111.

[20] Boucekkine, R., Camacho, C. and Fabbri, G. (2013), "On the optimal control of some parabolic partial differential equations arising in economics", *Serdica Mathematical Journal*, 39(3), 331-354.

[21] Boucekkine, R., Camacho, C. and Zou, B. (2009), "Bridging the gap between growth theory and the new economic geography: the spatial Ramsey model", *Macroeconomic Dynamics*, 13(1), 20-45.

[22] Boucekkine, R., Fabbri, G., Federico, S. and Gozzi, F. (2018), "Growth and agglomeration in the heterogeneous space: a generalized AK approach", *Journal of Economic Geography*, 19(6), 1287-1318.

[23] Bradshaw, C. J. A., Sodhi, N. S., Peh, K. S.-H. and Brook, B. W. (2007), "Global evidence that deforestation amplifies flood risk and severity in the developing world", *Global Change Biology*, 13(11), 2379-2395.

[24] Brock, W. and Xepapadeas, A. (2008), "Diffusion-induced instability and pattern formation in infinite horizon recursive optimal control", *Journal of Economic Dynamics and Control*, 32(9), 2745-2787.

[25] Camacho, C. and Pérez-Barahona, A. (2015), "Land use dynamics and the environment", *Journal of Economic Dynamics and Control*, 52, 96-118.

[26] Camara, M., Jamil, N. R. and Abdullah, A. F. B. (2019), "Impact of land uses on water quality in Malaysia: a review", *Ecological Processes*, 8(1).

[27] Campbell, N., D'Arcy, B., Frost, A., Novotny, V. and Sansom A. (2005), "Diffuse Pollution", *IWA Publishing*.

[28] Carpenter, S. R., Ludwig, D. and Brock, W. A. (1999), "Management of eutrophication for lakes subject to potentially irreversible change", *Ecol. Appl.*, 9, 751-771.

[29] Castro, L. M., Härtl, F., Ochoa, S., Calvas, B., Izquierdo, L. and Knoke, T. (2018), "Integrated bioeconomic models as tools to support land-use decision making: A review of potential and limitations", *Journal of Bioeconomics*, 20, 183-211.

[30] CCICED (2015), "CCICED 2015 Work Report".

[31] Chakravorty, U., Magné, B. and Moreaux, M. (2008), "A dynamic model of food and clean energy", *Journal of Economic Dynamics and Control*, 32(4), 1181-1203.

[32] Curtis, P. G., Slay C. M., Harris N. L., Tyukavina A and Hansen M. C. (2018), "Classifying drivers of global forest loss", *Science*, 361(6407), 1108-1111.

[33] Dadashpoor, H., Azizi, P. and Moghadasi, M. (2018), "Land use change, urbanization and change in landscape pattern in a metropolitan area", *Science of The Total Environment*, 655, 707-719.

[34] De Frutos, J. and Martín-Herrán, G. (2019), "Spatial effects and strategic behavior in a multiregional transboundary pollution dynamic game", *Journal of Environmental Economics and Management*, 97, 182-207.

[35] De Frutos, J. and Martín-Herrán, G. (2019), "Spatial vs. Non-Spatial Transboundary Pollution Control in a Class of Cooperative and Non-Cooperative Dynamic Games", *European Journal of Operational Research*, 276(1), 379-394.

[36] Delphin, S., Escobedo, F. J., Abd-Elrahman, A. and Cropper, W. P. (2016), "Urbanization as a land use change driver of forest ecosystem services", *Land Use Policy*, 54, 188-199.

[37] Denise, G., Lafuite, A.-S. and Loreau, M. (2018), "Sustainable Land-use Management Under Biodiversity Lag Effects", *Ecological Economics*, 154, 272-281.

[38] Dietz, A., Van der Ploeg, F., Rezai, A. and Venmans, F. (2020), "Are economists getting climate dynamics right and does it matter ?", *Discussion Paper No. 900, Department of Economics, University of Oxford.*

[39] Dijk, V. T. and Beunen, R. (2009), "Laws, People and Land Use: A Sociological Perspective on the Relation Between Laws and Land Use", *European Planning Studies*, 17(12), 1797-1815.

[40] Drobnik, T., Schwaab, J. and Grêt-Regamey, A. (2020), "Moving towards integrating soil into spatial planning: No net loss of soil-based ecosystem services", *Journal of Environmental Management*, 263, 110406.

[41] Dudley, N. and Alexander, S. (2017), "Agriculture and biodiversity: a review", *Biodiversity*, 18(2), 45-49.

[42] El Mujtar, V., Muñoz, N., Prack Mc Cormick, B., Pulleman, M. and Tittonell, P. (2019), "Role and management of soil biodiversity for food security and nutrition; where do we stand ?", *Global Food Security*, 20, 132-144.

[43] EU Commission (1991), Directive 91/676/EEC, "Council Directive of 12 December 1991 concerning the protection of waters against pollution caused by nitrates from agricultural sources", *Official Journal of European Community L375: 1-8.*

[44] Ewel, K. C. (2001), "Natural resource management: the need for interdisciplinary collaboration". *Ecosystems*, 4, 716-722.

[45] Fay, D. and James, D. (2010), "The anthropology of land restitution: An introduction". In: Fay, D, James, D (eds) The Rights and Wrongs of Land Restitution: Restoring what was Ours, *London: Routledge*, 1-24.

[46] Feddema, J. J. (2005), "The Importance of Land-Cover Change in Simulating Future Climates", *Science* 310(5754), 1674-1678.

[47] Foley, J. A. (2005), "Global Consequences of Land Use", *Science*, 309(5734), 570-574.

[48] Food and Agriculture Organization of the United Nations and Intergovernmental Technical Panel on Soils Status (2015), *Status of the World's Soil Resources Main Report.*

[49] García-Vega, D. and Newbold, T. (2019), "Assessing the effects of land use on biodiversity in the world's drylands and Mediterranean environments", *Biodiversity and Conservation*, 29, 393-408.

[50] Gasparatos, A., Doll, N.H.C., Esteban, M., Ahmed, A. and Olang, A. T. (2017), "Renewable energy and biodiversity: Implications for transitioning to a Green Economy", *Renewable and Sustainable Energy Reviews*, 70, 161-184.

[51] Geisen, S., Wall, D. H., Van der Putten, W. H. (2019), "Challenges and Opportunities for Soil Biodiversity in the Anthropocene", *Current Biology*, 29(19), 1036-1044.

[52] Gerlagh, R. and Liski, M. (2018), "Consistent climate policies", *Journal of the European Economic Association*, 16(1), 1-44.

[53] Ricardo, D. (1815), "Essay on the Influence of a Low Price of Corn on the Profits of Stock".

[54] González-Val, R. and Pueyo, F. (2019), "Natural resources, economic growth and geography", *Economic Modelling*, 83, 150-159.

[55] Grass, D. and Uecker, H. (2017), "Optimal management and spatial patterns in a distributed shallow lake model", *Electron. J. Differ. Equ.*, 2017, 1-21.

[56] Greiner, A., Gruene, L. and Semmler, W. (2013), "Economic Growth and the Transition from Non-renewable to Renewable Energy", *Environment and Development Economics*, 19(4), 417-439.

[57] Hannesson, R. (2003), "Aquaculture and fisheries", *Marine Policy*, 27, 169-178.

[58] Hastik, R., Basso, S., Geitner, C., Haida, C., Poljanec, A., Portaccio, A. and Walzer, C. (2015), "Renewable energies and ecosystem service impacts", *Renewable and Sustainable Energy Reviews*, 48, 608-623.

[59] Heal, G. (2016), "Notes on the economics of energy storage", *NBER Working Paper.*

[60] Helm, C. and Mier, M. (2018), "Subsidising Renewables but Taxing Storage? Second-Best Policies with Imperfect Carbon Pricing", *Oldenburg Discussion Papers in Economics.*

[61] IEA (2015), *Projected Costs of Generating Electricity.*

[62] Jayne, T. S., Chamberlin, J. and Headey, D. D. (2014), "Land pressures, the evolution of farming systems, and development strategies in Africa: A synthesis", *Food Policy*, 48, 1-17.

[63] Kalnay, E. and Cai, M. (2003), "Impact of urbanization and land-use change on climate", *Nature*, 423(6939), 528-531.

[64] Katzner, T., Johnson, J. A., Evans, D. M. et al. (2013), "Challenges and opportunities for animal conservation from renewable energy development", *Animal Conservation*, 16, 367-369.

[65] Kindermann, G., Obersteiner, M., Sohngen, B., Sathaye, J. andrasko, K., Rametsteiner, E. and Beach, R. (2008), "Global cost estimates of reducing carbon emissions through avoided deforestation", *Proceedings of the National Academy of Sciences*, 105(30), 10302-10307.

[66] Knowler, D. (2002), "Review of selected bioeconomic models with environmental influences in fisheries", *Journal of Bioeconomics*, 4, 163-181.

[67] Kopittke, P.M., Menzies, W.N., Wang, P., McKenna, B.A. and Lombi, E. (2019), "Soil and the intensification of agriculture for global food security", *Environment International*, 132.

[68] Korfiati, I. P. (2020), "Classifying Like a State: Land Dispossession on Eastern Crete"s Contested Mountains", *Antipode*, 52(5), 1331-1350.

[69] Kroetz K., Sanchirico J. N. (2015), "The bioeconomics of spatial-dynamic systems in natural resource management", *Annu. Rev. Resour. Econ.*, 7, 189-207.

[70] Krugman, P. (1992), "Geography and Trade", *MIT Press Books, The MIT Press.*

[71] Kyriakopoulou, E. and Xepapadeas, A. (2016), "Atmospheric pollution in rapidly growing industrial cities: spatial policies and land use patterns", *Journal of Economic Geography*, 17(3), 607-634.

[72] Kyriakopoulou, E. and Xepapadeas, A. (2017), "Atmospheric pollution in rapidly growing industrial cities: spatial policies and land use patterns", *Journal of Economic Geography*, 17(3), 607-634.

[73] La Torre, D., Liuzzi, D. and Marsiglio, S. (2019), "Transboundary pollution externalities: Think globally, act locally ?" *arXiv preprint arXiv:1910.04469.*

[74] Lal, R. (2014), "Soil conservation and ecosystem services", *International Soil and Water Conservation Research*, 2(3), 36-47.

[75] Le Kama, A.A., Pommeret, A. and Prieur, F. (2014), "Optimal Emission Policy under the Risk of Irreversible Pollution", *Journal of Public Economic Theory*, 16(6), 959-980.

[76] Lemoine, D. and Rudik, I. (2017), "Steering the climate system: using inertia to lower the cost of policy", *American Economic Review*, 107(10), 2947-57.

[77] Li, F., Zhang, S., Bu, K., Yang, J., Wang, Q. and Chang, L. (2015), "The relationships between land use change and demographic dynamics in western Jilin province", *Journal of Geographical Sciences*, 25(5), 617-636.

[78] Li, Y. and Zhang, J. (1999), "Agricultural diffuse pollution from fertilisers and pesticides in China", *Water Science and Technology*, 39(3).

[79] MacMynowski, D. P. (2007), "Pausing at the brink of interdisciplinary: power and knowledge at the meeting of social and biophysical science", *Ecology and Society*, 12(1).

[80] Mahmood R. (2014), "Land cover changes and their biogeophysical effects", *Int. J. Climatol.*, 34, 929-952.

[81] Malthus, R. T. (1798), "An Essay on the Principle of Population".

[82] Martinho, V. J. P. D. (2019), "Best management practices from agricultural economics: Mitigating air, soil and water pollution", *Science of The Total Environment*, 688, 346-360.

[83] Mc Ewan, C. (2017), "Spatial processes and politics of renewable energy transition: Land, zones and frictions in South Africa", *Political Geography*, 56, 1-12.

[84] McBratney, A., Morgan, C. and Jarrett, L. (2017), "The Value of Soil's Contributions to Ecosystem Services", *Global Soil Security*, 227-235.

[85] Meyer, M. A., and Früh-Müller A. (2020), "Patterns and drivers of recent agricultural land-use change in Southern Germany", *Land Use Policy*, 99.

[86] Meyer, W. B. and Turner, B. L. (1992), "Human population growth and global land-use/cover change", *Annual Review of Ecology and Systematics*, 23, 39-62.

[87] Meyer, William B. and Turner, B. L. (1996), "Land-use/land-cover Change: Challenges for Geographers." *GeoJournal*, 39(3), 237-40.

[88] Golosov, M., Hassler, J., Krusell, P. and Tsyvinski, A. (2014), "Optimal taxes on fossilfuel in general equilibrium", *Econometrica*, 82(1), 41-88.

[89] Ming, J., Xian-guo, L., Lin-shu Xu, Li-juan Chu and Shouzheng, T. (2007), "Flood mitigation benefit of wetland soil ? A case study in Momoge National Nature Reserve in China", *Ecological Economics*, 61(2), 217-223.

[90] Newbold, T., Hudson, L. N., Hill, S. L. L., Contu, S., Lysenko, I., Senior, R. A. and Purvis, A. (2015), "Global effects of land use on local terrestrial biodiversity", *Nature*, 520(7545), 45-50.

[91] Nitzbon, J., Heitzig, J. and Parlitz, U. (2017), "Sustainability, collapse and oscillations of global climate, population and economy in a simple World-Earth model", *Environ. Res. Lett.*, 12.

[92] Novara, A., Gristina, L., Sala, G., Galati, A., Crescimanno, M., Cerdà, A. and La Mantia, T. (2017), "Agricultural land abandonment in Mediterranean environment provides ecosystem services via soil carbon sequestration", *Science of The Total Environment*, 576, 420-429.

[93] Peerzado, M. B., Magsi, H. and Javed Sheikh, M. (2019), "Land use conflicts and urban sprawl: conversion of agriculture lands into urbanization in Hyderabad, Pakistan", *J. Saudi Soc. Agric. Sci.*, 18, 423-428.

[94] Peres, C. A. and Schneider, M. (2012). "Subsidized agricultural resettlements as drivers of tropical deforestation". *Biological Conservation*, 151, 65-68.

[95] Pommeret, A. and Schubert, K. (2019), "Energy Transition with Variable and Intermittent Renewable Electricity Generation", *CESifo Working Paper.*

[96] Prieur, F. (2009), "The environmental Kuznets curve in a world of irreversibility", *EconomicTheory*, 40(1), 57-90.

[97] Pugh, T. A. M., Lindeskog, M., Smith, B., Poulter, B., Arneth, A., Haverd, V. and Calle, L. (2019), "Role of forest regrowth in global carbon sink dynamics", *Proceedings of the National Academy of Sciences*, 116(10).

[98] Regnier, E. and Schubert, K. (2017), "To what extent is aquaculture socially beneficial ? A theoretical analysis", *American Journal of Agricultural Economics*, 99(1), 186-206.

[99] Rogger, M., Agnoletti, M., Alaoui, A., Bathurst, J. C., Bodner, G., Borga, M. and Blöschl, G. (2017), "Land use change impacts on floods at the catchment scale: Challenges and opportunities for future research", *Water Resources Research*, 53(7), 5209-5219.

[100] Savci, S. (2012), "An Agricultural Pollutant: Chemical Fertilizer", *International Journal of Environmental Science and Development*, 3(1).

[101] Schmidt, O., Melchior, S., Hawkes, A. and Staffel, I. (2019), "Projecting the Future Levelized Cost of Electricity Storage Technologies", *Joule*, 3(1), 81-100.

[102] Schmutzler, A. (1999), "The New Economic Geography". *Journal of Economic Surveys*, 13, 355-379.

[103] Sinn, H. W. (2017), "Buffering volatility: a study on the limits of Germany's energy revolution", *European Economic Review*, 99, 130-150.

[104] Sun, L., Wei, J., Duan, D. H., Guo, Y. M., Yang, D. X., Jia, C. and Mi, X. T. (2016), "Impact of Land-Use and Land-Cover Change on urban air quality in representative cities of China", *Journal of Atmospheric and Solar-Terrestrial Physics*, 142, 43-54.

[105] Söderström, B., Hedlund, K., Jackson, L. E., Kätterer, T., Lugato, E., Thomsen, I. K. and Bracht Jørgensen, H. (2014), "What are the effects of agricultural management on soil organic carbon (SOC) stocks ?" *Environmental Evidence*, 3(1).

[106] Tahvonen, O. and Salo, S. (1999), "Economic growth and transitions between renewable and nonrenewable energy resources", *European Economic Review*, 45, 1379-1398.

[107] Tahvonen, O., Withagen, C. (1996), "Optimality of irreversible pollution accumulation", *Journal of Economic Dynamics and Control*, 20, 1775-1795.

[108] Tan-Soo, J.-S., Adnan, N., Ahmad, I., Pattanayak, S. K. and Vincent, J. R. (2014), "Econometric Evidence on Forest Ecosystem Services: Deforestation and Flooding in Malaysia", *Environmental and Resource Economics*, 63(1), 25-44.

[109] United Nations Convention to Combat Desertification (2017), *The Global Land Outlook, first edition.*

[110] Ustaoglu, E., Castillo, C. P., Jacobs-Crisioni, C. and Lavalle, C. (2016), "Economic evaluation of agricultural land to assess land use changes", *Land Use Policy*, 56, 125-146.

[111] Vesterby, M. and Heimlich, R. (1991), "Land use and demographic change: results from fast-growing counties", *Land Economics*, 67(3), 279-291.

[112] Villela, A., Jaccoud, A., Rosa, P. L., Freitas, M. V. (2014), "Status and prospects of oil palm in the Brazilian Amazon", *Biomass and Bioenergy*, 67, 270-278.

[113] Villoria, N. B. (2019), "Technology Spillovers and Land Use Change: Empirical Evidence from Global Agriculture", *American Journal of Agricultural Economics*, 101(3), 870-893.

[114] Wang, X. (2006), "Management of agricultural non-point source pollution in China: current status and challenges", *Water Science and Technology*, 53(2), 1-9.

[115] Watson, K. B., Ricketts, T., Galford, G., Polasky, S. and O'Neil-Dunne, J. (2016), "Quantifying flood mitigation services: The economic value of Otter Creek wetlands and floodplains to Middlebury, VT", *Ecological Economics*, 130, 16-24.

[116] Wilson, J. D. (2017), "International Resource Politics in the Asia-Pacific: The Political Economy of Conflict and Cooperation", *Edward Elgar, Cheltenham.*

[117] World Bank (2020), "State and Trends of Carbon Pricing 2020".

[118] Wu, J. and Duke, J. M. (2014), *The Oxford Handbook of Land Economics*, Oxford University Press, USA.

[119] Wu, Y., Zhang, X. and Shen, L. (2011), "The impact of urbanization policy on land use change: A scenario analysis", *Cities*, 28(2), 147-159.

[120] Xepapadeas, A. (2002). "Non-point source pollution control", in *Handbook of environmental and resource economics* ed. Van den Bergh J. C. J. M.

[121] Yenneti, K., Day, R. and Golubchikov, O. (2016), "Spatial justice and the land politics of renewables: Dispossessing vulnerable communities through solar energy megaprojects", *Geoforum*, 76, 90-99.

[122] Yin, R., Kardol, P., Thakur, M. P., Gruss, I., Wu, G.-L., Eisenhauer, N. and Schädler, M. (2020), "Soil functional biodiversity and biological quality under threat: Intensive land use outweighs climate change", *Soil Biology and Biochemistry*, 147.

[123] Zalidis, G., Stamatiadis, S., Takavakoglou, V., Eskridge, K. and Misopolinos, N. (2002), "Impacts of agricultural practices on soil and water quality in the Mediterranean region and proposed assessment methodology", *Agriculture, Ecosystems and Environment*, 88(2), 137-146.

[124] Zhang, X., Song, W., Lang, Y., Feng, X., Yuan, Q. and Wang J. (2020), "Land use changes in the coastal zone of China's Hebei Province and the corresponding impacts on habitat quality", *Land Use Policy*, 99.

Chapter 1

A Markov chain model for renewable energy storage and its application to peak load decarbonation

Abstract

This chapter studies optimal energy storage policies for shifting from the use of back-up fossil fuels during peak load, to stored intermittent renewable energy. We model the process of intermittent renewable energy storage under renewable energy surplus uncertainties in a Markovian framework and show the existence of a limiting distribution for stored intermittent renewable energy for a given storage technology. Moreover, we consider technical progress in storage technology through investments in both charging efficiency and storage capacity and study the sensitivity of the optimal energy storage policies with respect to the renewable energy surplus distribution. We analytically solve this problem under specific assumptions and use a value function iteration algorithm to investigate numerically on investment strategies leading to optimal peak load decarbonation pathways. Finally, we apply our model to study Portugal's peak load decarbonation pathways for different scenario regarding storage and carbon costs, as well as the availability in the surplus of intermittent renewable energy.

Keywords: Energy storage, Intermittency, Peak load shifting, Technical progress, Markov chains, Numerical methods.

Journal of Economic Literature: C61, Q42, C44, Q55, O13.

Contents

List of Figures

1 Introduction

Electricity production is, worldwide, the first source of greenhouse gas emissions and consequently the first cause of global warming above all other carbon intensive sectors such as agriculture or transportation (IEA, 2018). In order to stay bellow the 2°C threshold of the Paris Agreement, decarbonation of electricity production is at the core of climate change mitigation policies. Among these means of decarbonation, This chapter focuses on the shifting from using pollutant fossil fuels to renewable energy. More specifically, we will examine the terminal stage of the energy shift, when renewable energy is the main source of electricity and the remaining fossil fuels are only used as back-up generators during peak load. We consider storage technology as a third channel of energy supply and we analyse the decarbonation of back-up fossil fuels by stored intermittent renewable energy. The energy shift from pollutant fossil fuels to renewable energy has been widely studied in macrodynamic frameworks (Hoel and Kverndokk, 1996; Tahvonen, 1998; Tahvonen and Salo, 1999; Greiner et al., 2013). Yet, these dynamic models consider deterministic supply of renewable energy and thus does not take into account one crucial characteristic of renewable energy supplies and limitation to their deployment, being their intermittency. Unlike ordinary pollutant fossil fuels which have the convenience to be dispatchable, meaning they can supply energy and be activated whenever, renewable sources of energy are non-dispatchable due to their dependency to local meteorological conditions. In order to supply electricity, wind turbines need wind, and solar plants need solar radiation. In case of inadequate weather conditions renewable plants may not supply enough energy. The use of intermittent renewable energy carries a risk of energy shortage if there are no dispatchable fossil fuels in the energy mix to assure the match between demand and supply in times of low solar radiation or low wind speed.

This difference between intermittent renewable energy and dispatchable fossil fuels is crucial in order to deliberate wisely on the ongoing energy shift process. Moreover, new metrics must be designed to compare the costs and the benefits of fossil fuels and renewable energy as intermittency of the latter makes direct comparison of LCOE less relevant (Joskow, 2011). A very illustrative example regarding the stakes of intermittency is given by the renewable energy supply in Germany (Sinn, 2017). In 2017, the installed capacity of wind energy in Germany was 35.92 GW and the average production of 5.85 GW, which represents 16.3 % of installed wind capacity. Moreover, the

electricity production that was available 99.5% of the time represents 0.13 GW, thus 0.4% of installed wind capacity. The numbers are even more dramatic for solar energy as the installed solar capacity were nearly the same than wind capacity, 37.34GW, but the average production of 3.7 GW represents 9.9% of installed solar capacity. The electricity production that was available 99.5% of the time for solar energy drops to 0GW because of night time periods.

Intermittency is a central limitation in the development of renewable energy. However, theoretical literature only appeared in the seminal paper (Ambec and Crampes, 2012) in which the authors point out that previous analyses are mostly empirical and country specific (Kennedy, 2005; Cust et al., 2007; Boccard, 2010). Since then, theoretical literature on intermittent renewable energy has grew and two ways of thinking about intermittency have risen: one deterministic and predictable way of thinking the variation in primary renewable energy availability and one unpredictable and stochastic way (Baker et al., 2013; Heal, 2016). The predictable approach to model intermittency is often called variability and corresponds to a deterministic change in renewable primary energy. This is particularly useful to model the predictable change in solar radiation due to the interchange between night and daytime or to seasonal effects leading to predictable variations in wind availability (Heal, 2016; Helm and Mier, 2018; Pommeret and Schubert, 2019). Yet, deterministic modelling of variation in primary renewable energy cannot cope with unpredictable weather events such as the passing of clouds over solar panels, or wind turbulence affecting wind turbine energy production. The second approach models availability of primary renewable energy as a random variable due to weather uncertainties. Indeed, even if major progress have been done regarding weather forecasting in the last decades (Alley et al., 2019), owing to the non-linear physics of climate dynamics, weather conditions can only be known with some uncertainty. To that extent, it is more natural and general to model primary renewable energy availability in a stochastic framework as we propose in this chapter.

However, most of the research considering stochastic availability in renewable energy focus on the design of optimal energy mix and optimal policies for integrating intermittent renewable energy in a static framework (Ambec and Crampes, 2012; 2017) and do not consider the dynamic analysis of substituting pollutant fossil fuels by new decarbonized means of energy supply such as stored intermittent renewable energy. In the seminal paper by Pommeret and Schubert (2019) a dynamic model of the energy shift is presented while considering stochastic intermittent renewable energy and stor-

age capacities. Yet, the authors do not consider technical progress in storage. In this chapter, we propose a model that considers both stochastic availability of primary renewable energy and technical progress in storage to cope with renewables intermittency in a dynamic framework. Moreover, we focus on the last stage of the energy shift, that is, when energy is mostly supplied by renewable intermittent means, and when fossil fuels are only used as back-up during peak load, when the instantaneous demand for energy is greater than the instantaneous renewable energy production.

Studying this last stage of the energy shift is essential. Indeed, in the past decades, major investments and public policies in favor of a better integration of renewables, such as feed in tarifs or subsidies (Barbose et al., 2013; Baker et al., 2013), led to a massive penetration of renewables in countries. New records are now being broken in terms of renewable energy production. For instance, in March 2018, Portugal renewable energy sector produced 4812 GWh, reaching 103.6% of the country's energy consumption on the same period (4647 GWh), beating its previous record of 99.2% reached in February 2014 (APREN, 2018). More precisely, on March 11th, the renewable energy production reached 143% of the country's demand. This massive renewable energy production was possible due to Portugal's hydroelectric installations which produced 55% of the energy during this period as well as massive past investments and favorable weather conditions regarding wind energy which contributed for 42% of energy demand in this period. This remarquable performance of renewable energy in Portugal prevented 1.8 millions tons of CO2 emissions and saved 21 million euros regarding European Emission Allowances. However, according to Portugal's National Energy Networks, the country energy demand was not fully assured consecutively by renewable energy. At best, a first period of 70 consecutive hours of full renewable energy supply started on the 9th of March, and an other period of 69 hours started on the 12th of the month. Even if Portugal produced monthly more renewable energy than it consumed in March, the use of fossil fuels was still necessary. Hydraulic and wind energy produced the major quantity of energy in this period, but Portugal still needed back-up pollutant fossil fuels in order to assure energy demand during peak load. Typically, pollutant back-up fossil fuels used during peak load are either gaz or hard coal power plants because of their quick reactivity (Sinn, 2017). Thus, Portugal may have produced more renewable energy over the month but, because of its lack of energy storage facilities, the use of pollutant back-up fossil fuels was still necessary during peak load.

As storage technologies are at the core of technical solutions put forward to cope

with renewable intermittency and for substituting pollutant back-up fossil fuels used during peak load by decarbonized means of energy supply, the economics of energy storage is a growing field. Yet early seminal papers have studied the implications of energy storage, focusing on hydroelectric water storage, to characterize optimal storage policies (Little, 1955; Koopmans, 1957). Along with this literature, seminal papers on peak load management (Jackson, 1973; Gravelle, 1976) study the implications of storage for facing peak load periods. Recent researches evaluate the role of energy storage as a solution for dealing with intermittent renewable energy production (Durmaz, 2014; Steffen and Weber, 2016; Sinn, 2017) and in particular in order to match demand during peak load (Crampes and Moreaux 2009; Steffen and Weber, 2012). In Heal (2016), the author points out the two common usages of energy storage: one is to smooth out the volatil energy production from intermittent renewable energy ; the other is to shift renewable production from times of low consumption, to times of high consumption during peak load through a peak-shifting mechanism. Off-peak, when instantaneous demand for energy is low and renewable production is high, storage allows the excess of renewable energy output to be stored. During peak load, the previous stored renewable energy is now a substitute to pollutant back-up fossil fuel, and can be used as a new channel of decarbonized energy supply.

Peak-shifting mechanisms are studied in recent literature in deterministic frameworks regarding the availability of renewable energy and authors do not consider the stochastic nature of intermittent primary renewable energy (Heal, 2016; Helm and Mier, 2018). In this chapter we model peak-shifting while considering stochastic renewable energy availability and technical progress in storage. To model technical progress in storage we use the common storage technical characteristics being capacity (the maximal volume that can be stored) and efficiency (the speed at which energy is stored) as in Steffen and Weber (2016). Moreover, as we model renewable energy intermittency in a stochastic framework, the stock of stored renewable energy in the storage capacities is uncertain. The uncertainty in the stock of stored renewable energy carries a risk of energy shortage during peak load as back-up fossil fuels generators are being closed in the energy shift process. Thus, the dynamics of closing back-up fossil fuels is determined by the dynamics of technical progress in storage as the volume of back-up fossil fuels generators that can be closed must match with the corresponding amount of stored renewable energy available above a probability appointing for the risk of lost load. As an order of magnitude, the legal standard for developed countries regarding

the risk of lost load is that power supply should always be available with a probability above 99.96% (Ambec and Crampes, 2017).

This research proposes new perspective focusing on modelling the terminal stage of the energy shift process, which consists in decarbonizing peak load by substituting back-up fossil fuels by stored intermitent renewable energy through load-shifting. To our knowledge, only very recent work from Pommeret and Schubert (2019) proposes a dynamic model of the energy shift while considering stochastic intermittency and storage technology but without storage technical progress. We attempt to fill this gap using both analytical and numerical methods. We think that the full decarbonation of peak demand using stored renewable energy through peak-shifting mechanism is a long term process in which technical progress in storage will play a prominent role which calls for sharper analyses. Hence, we propose a model which takes into account both intermittency and technical progress regarding storage in order to study the trade-off between investing in either storage efficiency or capacity. By applying our model to Portugal, we provide with the optimal storage policies and decarbonation time horizons with respect to Levelized Costs of Storage (LCOS), carbon prices, and the stochastic availability of renewable energy surplus scenarios. We show that the costs of energy storage and carbon prices have important impacts on transition time, and in average a reduction in 31$/MWh in LCOS accelerates full peak load decarbonation by one year while an increase of 37$ in the price of carbon leads to the same results. Moreover, we study how the variations in the mean or variance of renewable energy availability affect the optimal storage policies and peak load decarbonation time horizons. In average, an increase of 2GWh in renewable energy surplus mean leads to a decrease of decarbonation time horizon by one year, while investments in storage technology are more allocated to capacity rather than to efficiency. Yet, time horizon for peak load decarbonation and storage policies show less sensitivity to variations in the energy surplus dispersion, making therefore the energy surplus mean value a more practical statistic for peak load decarbonation planning, compared to its dispersion.

The rest of the chapter is organized as follows. The first section presents the modelling of intermittent renewable energy storage while considering the stochastic nature of primary renewable energy in a discrete Markovian framework. The second section to define the optimal static mix between back-up fossil fuels and stored renewable energy during peak load. Finally, we study the optimal storage policies and apply our modelling to Portugal peak load decarbonation in a dynamic framework.

2 Modelling intermittent renewable energy storage

2.1 Preliminary definitions of storage dynamics

In this chapter we shall focus on the last stage of the energy shift, in which three channels of energy supply are available. Renewable energy is the main source of energy and provides all the energy out from peak demand. During peak demand, energy is supplied by both stored renewable energy and back-up fossil fuels.

We consider a model with discrete time periods. Out from peak demand, energy is fully supplied by non-stored renewable energy. The surplus of primary renewable energy which is not directly consumed can be stored during the off-peak periods, which we consider of same duration τ day to day. We denote ω_k the random surplus of renewable energy that is not directly consumed during the k^{th} off-peak charging period, and thus, which can be stored during charging periods if storage is available. As this surplus of energy is the difference between produced intermittent renewable energy and consumed energy during each off-peak period, then energy surplus $(\omega_k)_{k\in\mathbb{N}^*}$ is indeed a collection of random variables. Moreover, we neglect all seasonal effects, that is, we suppose the distribution of renewable energy surplus constant in time and thus make the following assumption:

Assumption 1. *The collection of random variables of renewable energy surplus* $(\omega_k)_{k\in\mathbb{N}^*}$ *is independent and identically distributed.*

We consider that storage technology is characterized by its *capacity* level $\Gamma \geq 0$, the maximum amount of energy that can be stored, and by its *efficiency* $\phi \in [0, 1]$, characterizing the efficiency at which the technology can store energy (a proxy for charging rate). Therefore, be E_0^k the initial level of stored renewable energy at the beginning of the k^{th} charging period, then the level E_τ^k of stored renewable energy at the end of the k^{th} charging period is $E_\tau^k = \min\{\Gamma, E_0^k + \phi\omega_k\}$ with $\phi\omega_k$ the random amount of renewable energy that has been stored during this period. Hence, in this set-up, during each off-peak charging period, storage stores a fraction $\phi\omega_k$ of energy from the random surplus of renewable energy ω_k, and capacity Γ acts like a saturation level above which no energy can be stored.

During peak demand there is, by definition, not enough primary renewable energy in order to supply for the instantaneous energy demand. Therefore, energy is supplied by alternative sources of energy available during peak demand, namely back-up fossil

fuels and the stored surplus of renewable energy through a peak-shifting mechanism. If storage is very efficient, with high capacity levels, and that the random surplus of primary renewable energy is important enough during the off-peak periods, then storage may have stored enough renewable energy to be the only energy source during peak demand. In such case, there is no need for using back-up fossil fuels. Else, both stored renewable energy and back-up fossil must provide during peak load.

Finally, for an energy demand d on storage during peak load, the stored level of renewable energy at the beginning of the $k+1^{th}$ off-peak charging period is given by $E_0^{k+1} = \max\{0, E_\tau^k - d\}$ where E_τ^k is the level of renewable energy storage at the end of the k^{th} off-peak charging period. Note that, if demand d on storage is more important than the level of stored renewable energy at the end of the k^{th} charging period E_τ^k, then the quantity $E_\tau^k - d$ becomes negative. As only positive energy values have meanings here, we shall only consider the positive part of $E_\tau^k - d$ in the definition of the storage process, that is $\max\{0, E_\tau^k - d\}$, the rest being supplied by storage.

Definition 1. *For a demand d on storage during peak load, the stochastic process of stored renewable energy is defined as:*

$$\forall k \in \mathbb{N}^* \begin{cases} E_\tau^k = min\{\Gamma, E_0^k + \phi\omega_k\}, \\ E_0^{k+1} = max\{0, E_\tau^k - d\}, \end{cases}$$

with $E_0^1 \geq 0$ the initial level of stored renewable energy at the beginning of the first off-peak charging period.

Note that, in our model, we do not explicitly consider energy leakage in the energy storage dynamics as in Pommeret and Schubert (2019). Yet, energy leakage can be thought here as a component of efficiency ϕ as higher energy leakage would be equivalent in our specifications to lower values in storage efficiency ϕ.

Building on this framework for renewable energy storage dynamics, we study in the following the optimal mix between back-up fossil fuels and stored renewable energy during peak demand. Thereby, the relevant variable in order to decide on how to split energy supply during peak load between back-up fossil fuels and stored renewable energy, is the stored renewable energy level the moment before peak load (at the end of each charging period), that is $\{E_\tau^k\}_{k\in\mathbb{N}^*}$ from Definition 1. We characterize such energy storage level before peak load in the following section using Markov chain theory within a discrete state of charge framework.

2.2 The energy storage model: a Markovian approach

2.2.1 A discrete and finite states of charge framework

We model energy storage as an aggregated charging device with a saturation level denoted Γ and a discrete states of charge (SOC) distribution. The discrete amount of energy between two states of charge is denoted δ. Therefore, the number of SOC is $N = \frac{\Gamma}{\delta} + 1$. The first state of charge, SOC_1, characterizes the empty state of storage, and the last, SOC_N, is the full state, that is, when the level of stored renewable energy is equal to $\Gamma = (N-1)\delta$. As, we consider discrete SOC, then storage can only store discrete amounts of energy, with a discretization step of δ. This means that the level of stored renewable energy will always be given as multiples of the discretization step δ, and shall always be rounded down to the nearest discretization step multiple. Therefore, if at the end of the k^{th} off-peak charging period the random stored surplus of renewable energy $\phi\omega_k \in [j\delta, (j+1)\delta]$, then the level of energy stored during this period is $j\delta$ for any given $j \in \mathbb{N}$. As a consequence, we define the following storage probability:

Definition 2. *The probability $p^{\phi}(j)$ for storing a quantity $j\delta$ of energy during any off-peak charging period for unconstrained storage device $\Gamma = \infty$ is defined as:*

$$\forall k \in \mathbb{N}\ \forall j \in \mathbb{N}\ p^{\phi}(j) = P\left(j\delta \leq \phi\omega_k < (j+1)\delta\right).$$

Therefore, for instance, if $\phi\omega_k \in [0, \delta]$ then no energy has been stored and the probability of not charging any energy is given by $p^{\phi}(0) = P\left(0 \leq \phi\omega_k < \delta\right)$. Similarly, if $\phi\omega_k \in [3\delta, 4\delta]$ then a quantity 3δ of energy has been stored during the k^{th} off-peak charging period, with a probability $p^{\phi}(3) = P\left(3\delta \leq \phi\omega_k < 4\delta\right)$, and so on. Note that the probability $p^{\phi}(j)$ depends on the efficiency ϕ of storage. Indeed, as efficiency increases, the probability of storing more energy during charging periods also increases. We use such storage probability in order to define the transition probabilities to transit from one SOC to an other in order to characterize the Markov process through its transition matrix in the following section.

2.2.2 The states of charge transition matrix

As stored energy levels are bounded by zero and by the maximum capacity Γ, we can write the dynamics of stored renewable energy before peak load, as a discrete and

bounded Markov chain. We recall that the number of states of charge is given by $N = \frac{\Gamma}{\delta} + 1$, in which δ is the discrete energy amount between two successive states of charge. In such framework, the first state of charge SOC_1 of storage device is the empty state (stored energy is zero), and the highest state of charge SOC_N is the full state (stored energy is Γ). Any intermediate state of charge is denoted in the following as SOC_i with $1 < i < N$.

In order to deliberate on the optimal mix between back-up fossil fuels and stored renewable energy used during peak demand, one must be informed on the state of charge probability distribution before peak load. Therefore, the embedded Markov process of interest here is $\{E_\tau^k\}_{k\in\mathbb{N}^*}$ from Definition 1, that is the amount of stored renewable energy reached at the end of each charging period. With the discretized SOC framework introduced above, the embedded Markov process writes as $\left\{SOC_{\lfloor\frac{E_\tau^k}{\delta}\rfloor+1}\right\}_{k\in\mathbb{N}^*}$ where $\{E_\tau^k\}_{k\in\mathbb{N}^*}$ is the stochastic process of stored renewable energy available at the end of the k^{th} charging period. In order to write the transition matrix of the embedded Markov chain $\left\{SOC_{\lfloor\frac{E_\tau^k}{\delta}\rfloor+1}\right\}_{k\in\mathbb{N}^*}$ we must provide with the following definition:

Definition 3. *A state of charge SOC_i is in the consumption trap if after peak demand, the storage device is empty, that is, if after peak demand the new state of charge is SOC_1.*

Therefore, for a demand d on storage, a state of charge SOC_i is in *consumption trap* if $i \in [1, \lceil d/\delta \rceil + 1]$ with δ the discretization step for storage. If an initial state of charge SOC_i is not in *consumption trap*, then after peak demand, the new state is $SOC_{i-\lceil d/\delta \rceil}$.

Moreover, if the initial state is in consumption trap, then after peak demand, storage reaches the empty state of charge SOC_1. From SOC_1, the probability of reaching a state of charge SOC_j bellow full charge (that is for $j < N$) at the end of the k^{th} off-peak charing period is given by the probability of storing $(j-1)\delta$ of energy, that is $p^\phi(j-1) = P\left((j-1)\delta \leq \phi\omega_k < j\delta\right)$. Therefore, the transition probability from a SOC initially in consumption trap to SOC_j is $p^\phi(j-1)$. Finally, as capacity Γ acts as a saturation level, then the probability of reaching SOC_N from an initial state of charge in consumption trap is the sum of the probability of storing more than $\Gamma = (N-1)\delta$, that is, $P(\phi\omega_k \geq (N-1)\delta) = \sum_{j=N}^{\infty} p^\phi(j-1)$. Such reasoning holds for initial states not in consumption trap. We provide with the transition matrix Π of the Markov chain in the following proposition (see Appendix E for complete proof):

Proposition 1. *The transition matrix* Π *of the Markov chain* $\left\{SOC_{\lfloor \frac{E_T^k}{\delta} \rfloor + 1}\right\}_{k \in \mathbb{N}^*}$ *writes as:*

- *if initial state is in the consumption trap:*

$$\forall i \in [1, \lceil d/\delta \rceil + 1] \begin{cases} \Pi_{i,j} = p^\phi(j-1) \ \forall j \in [1, N-1], \\ \Pi_{i,N} = \sum_{j=N}^{\infty} p^\phi(j-1). \end{cases}$$

- *if initial state is not in the consumption trap:*

$$\forall i \in [\lceil d/\delta \rceil + 2, N] \begin{cases} \Pi_{i,j} = p^\phi(j - (i - \lceil d/\delta \rceil)) \ \forall j \in [i - \lceil d/\delta \rceil, N-1], \\ \Pi_{i,N} = \sum_{j=N}^{\infty} p^\phi(j - (i - \lceil d/\delta \rceil)). \end{cases}$$

- *else,* $\Pi_{i,j} = 0$.

In order to build readers' intuition on the states of charge dynamics before peak load, we provide with the diagram of the Markov chain for specific values of parameters in Figure 1.

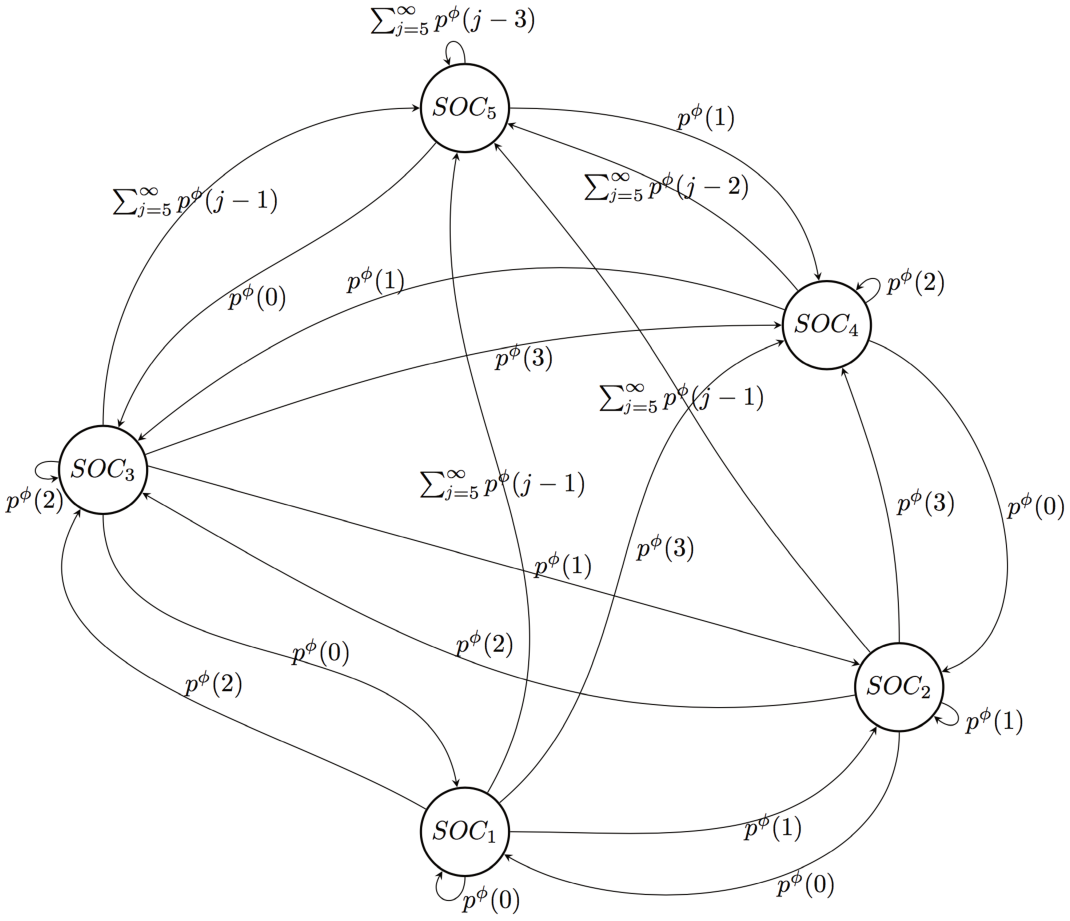

Figure 1: Markov chain diagram for $N = 5$ and $\lceil d/\delta \rceil = 2$.

Note that, the transition probabilities of the Markov chain depends on the collection of random variables of renewable energy surplus $(\omega_k)_{k\in\mathbb{N}^*}$. As from Assumption 1, the collection $(\omega_k)_{k\in\mathbb{N}^*}$ is independent and identically distributed, then the transition probabilities are constant in time and thus the Markov chain is homogeneous. Within this framework, and from homogeneous Markov chains theory, we can provide with the SOC probability distribution before each peak, and thus provide with practical information on how to split energy supply during peak load.

Indeed, let us define the probability distribution $\mu_k = (\mu_k^{(1)}, \mu_k^{(2)}, \mu_k^{(3)}, ..., \mu_k^N)$ for the N states of charge before the k^{th} peak load, where $\mu_k^{(j)}$ provides with the probability of being in SOC_j the moment before the peak, for $1 \leq j \leq N$. Then for any given initial distribution μ_0, the dynamics of the SOC probability distribution before peak load writes as $\mu_k = \Pi^k \mu_0$, for all $k \geq 0$, with Π the transition matrix defined in Proposition 1. Finally, we provide with the following claim:

Proposition 2. ***(i)*** *The Markov chain of transition matrix* Π *is irreducible.*
(ii) *The Markov chain of transition matrix* Π *is aperiodic.*
(iii) *There exists a unique stationary distribution* $\bar{\mu}$ *for the transition matrix* Π *such that* $\bar{\mu} = \lim_{k\to\infty} \Pi^k \mu_0$ *for any initial SOC distribution* μ_0*.*

From Proposition 2, we get that the Markov chain characterized by the transition matrix Π, displays all the properties so that the SOC probability distribution converges to an equilibrium distribution $\bar{\mu}$ in the long run. In the following, we shall consider that the Markov chain is always at equilibrium, which leads us to the following assumption:

Assumption 2. *We neglect the time scale for reaching* $\bar{\mu}$ *so that the states of charge probability distribution before peak load is always considered at equilibrium.*

Henceforth, the SOC probability distribution before peak load is given by $\bar{\mu}$ as we suppose the time scale for reaching $\bar{\mu}$ very small compared to the other time scales involved in the following.[1] Indeed, in the next sections, we will focus on a dynamic framework in which decisions are taken on technical progress regarding efficiency ϕ and capacity Γ through investments. A change in ϕ and Γ can therefore be seen as a shock on the Markov chain characteristics, after which the SOC probability distribution before peak load relaxes to a new steady state. Such dynamics are illustrated in Figure 2 so readers can have a representation of the different dynamics involved the

[1]From Markov chain theory, the convergence speed for the SOC probability distribution is such that $\forall k \geq 0 \ ||\mu_k - \bar{\mu}|| \leq \mathcal{O}(\hat{\rho}^k)$, where $\hat{\rho}$ is the second largest eigenvalue of Π.

following. Therefore, each line in Figure 2 represents the dynamics of the SOC probability distributions relaxing to its steady state distribution $\bar{\mu}$ after each new energy storage policy represented here by a technical state for both the efficiency level ϕ and capacity level Γ. Hence, following Assumption 2, only the last column providing with $\bar{\mu}$ for a given technical state (ϕ, Γ) shall be considered, as we suppose in the following storage at equilibrium.

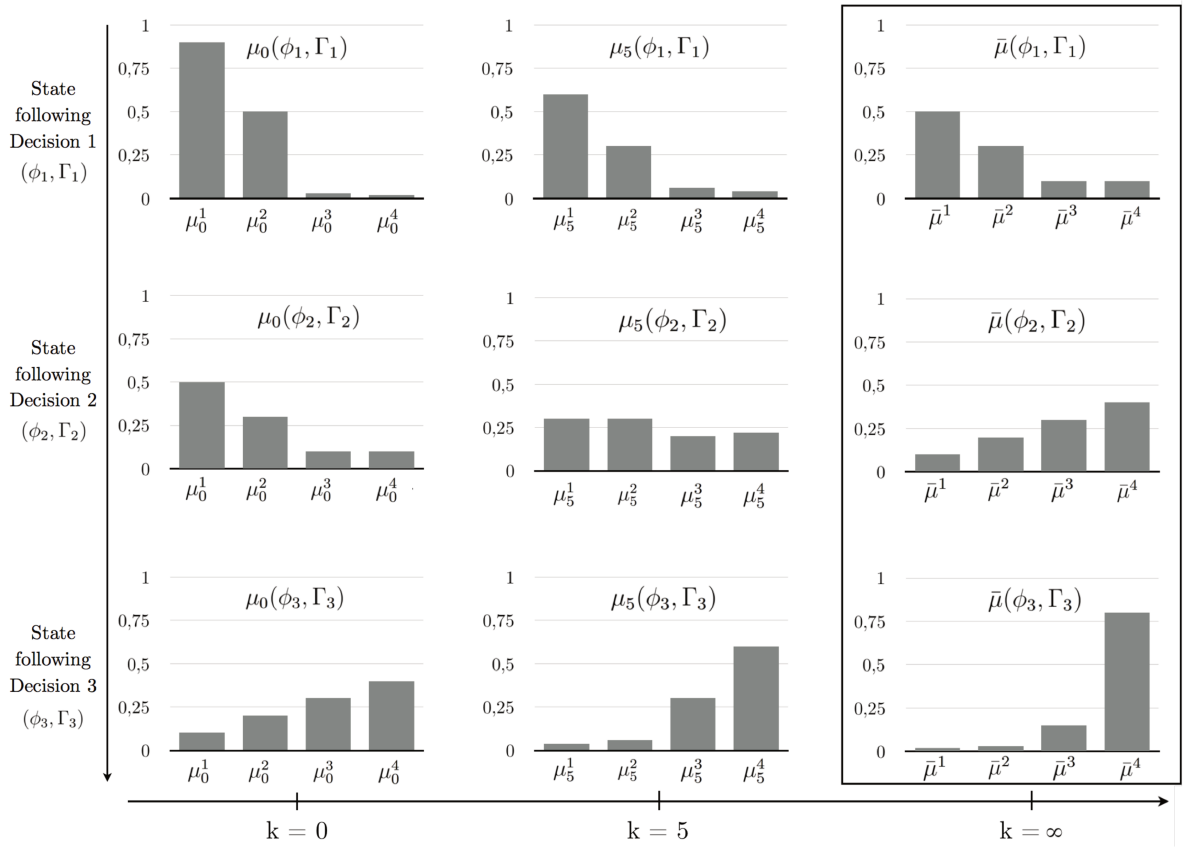

Figure 2: Illustration of SOC probability distributions relaxing to steady state $\bar{\mu}$ after each new energy storage policy (decision in ϕ and Γ).

The strong assumption here, is to suppose that each decisions in ϕ and Γ are sufficiently separated in time so that the SOC probability distribution before peak load always reaches its new equilibrium before the next decision shock/storage policy on efficiency ϕ and capacity Γ. Hence, in the following we will consider that storage is always at steady state and thus, the state of charge probability distribution before peak load is $\bar{\mu}(\phi, \Gamma)$ for a given storage technological level in both efficiency and capacity. This is convenient enough as the SOC probability distribution before peak load may now be found as solution to $\bar{\mu} = \Pi\bar{\mu}$, that we solve numerically in the following.[2]

[2]This is a well known result from Markov chain theory. In the case of few SOC, $\bar{\mu} = \Pi\bar{\mu}$ can easily

3 Static energy mix during peak load

3.1 Theoretical framework for static energy mix

We apply the previous model for stochastic storage of intermittent renewable energy to an economy with three channels of energy supply. The main energy source is provided by intermittent renewable energy (for instance photovoltaic or wind energy) and we consider that renewable energy is sufficiently developed, so that renewable sources cover most of the energy demand, except during peak demand (see example of Portugal in Introduction). We will make use of Assumption 2, that is, the SOC probability distribution before peak load is always at equilibrium, and thus solution to $\bar{\mu} = \Pi\bar{\mu}$. From this, we investigate in this section on optimal static mix strategies between back-up fossil fuels and stored renewable energy during peak load. More particularly, we will focus on the energy mix which minimizes the use of back-up fossil fuels during peak demand, while controlling the risk of energy shortage bellow a risk tolerance threshold.

We suppose that there is one peak demand at each period, period being typically a day, during which energy is provided either by back-up fossil fuels or stored renewable energy, which both only supply during peak demand. We denote C the intensity of peak demand at each period and suppose this intensity constant. Energy supply during peak demand is therefore divided between back-up fossil fuel, providing for a part $(1-\lambda)C$ of the demand during peak load, and stored renewable energy providing the remaining λC, with $\lambda \in [0,1]$. The demand on storage is therefore imposed by the energy mix during peak demand. Hence, in Definition 1, the demand d on storage during peak load writes here as $d = \lambda C$. In the following, the share λ of renewable energy will be directly referred to as the *energy mix* as it characterizes both the use of back-up fossil fuels $(1-\lambda)C$ and the demand λC on stored renewable energy during peak load.

Finally, as introduced in Section 1, storage is characterized by its efficiency ϕ and its capacity Γ. In this section, we study, for a given technical state (ϕ, Γ), the optimal energy mix λ^* between stored renewable energy and back-up fossil fuels used during peak demand that is, the mix which minimizes the use of fossil fuels while controlling the risk of energy shortage. In the following, we formally define and characterize such optimal energy mix, but beforehand, readers should get a sense of this notion of optimality regarding energy mix.

As renewable energy is intermittent, the amount of stored renewable energy before

be solved analytically. Yet, in the case of many SOC, we shall solve $\bar{\mu} = \Pi\bar{\mu}$ numerically.

peak demand is a stochastic process (as defined in Definition 1). Therefore, splitting energy mix between back-up fossil fuels and stored renewable energy during peak load induces a risk of energy shortage. Indeed, if the demand $d = \lambda C$ on storage is too high, that is, if the mix λ in favor of storage is too important ($\lambda > \lambda^*$) then the risk of energy shortage might exceed risk tolerance. Yet, if the demand $d = \lambda C$ on storage is too low, that is, if the mix λ is not important enough regarding storage ($\lambda < \lambda^*$), then back-up fossil fuels are over used. This intuition shall be analyzed and formalized by introducing risk tolerance towards energy shortage ρ and defining the following set of stored energy level.[3]

Definition 4. *For a given risk tolerance ρ, we define the set $\mathcal{A}_\rho$ as the set of stored energy level such that the probability of storing less energy is bellow risk tolerance ρ.*

With the notations from Section 2, if storage has reached its i^{th} state of charge (SOC_i) for $1 \leq i \leq N$ then the stored level of energy is δi, where δ is the discrete amount of energy between two successive SOC. As we suppose storage to be at equilibrium in Assumption 2, then the set $\mathcal{A}_\rho$ can directly be written from the SOC probability distribution before peak load given by $\bar{\mu} = (\bar{\mu}_k)_{1 \leq k \leq N}$ as:

$$\mathcal{A}_\rho = \left\{ \delta i \mid \sum_{k=0}^{i} \bar{\mu}_k \leq \rho \right\}.$$

Note that $\mathcal{A}_\rho$ is well defined as we showed in Proposition 2 the existence of the stationary distribution $\bar{\mu}$ solution to $\bar{\mu} = \Pi\bar{\mu}$, for a given technical state (ϕ, Γ) and for any demand d on storage, that is here, $d = \lambda C$. Moreover, this set depends on efficiency ϕ, capacity Γ and the energy mix $\lambda = d/C$ as the transition matrix Π from Proposition 1 and its stationary distribution $\bar{\mu}$ depends on such parameters. Moreover:

Proposition 3. ***(i)*** *For a given technical state (ϕ, Γ) and a mix λ, $\mathcal{A}_\rho$ has a supremum that we denote σ_ρ and which depends on ϕ, Γ and λ.*
(ii) *For any stored energy level above σ_ρ, the probability of storing less is greater than ρ, that is: $\forall \eta > 0 \; P(X \leq \sigma_\rho + \eta) > \rho$.*

To develop reader's representation of the set $\mathcal{A}_\rho$ and its supremum σ_ρ, we provide with the following illustration for the state of charge distribution probability distribution before peak load $\bar{\mu}$ in Figure 3.

[3]Risk tolerance ρ is typically very small. The legal standard in developed countries is 0.04% (see Ambec and Crampes (2017)).

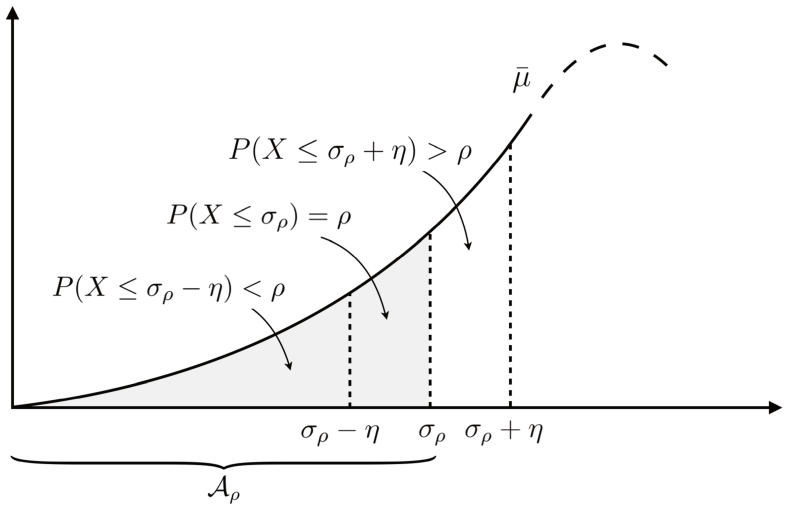

Figure 3: Illustration for $\mathcal{A}_\rho$ and σ_ρ as defined in Proposition 3.

Thereby, be X the random variable of stored and available renewable energy before peak load characterized by its SOC probability distribution $\bar{\mu}$. Energy shortage happens during peak demand if the amount of stored energy X (the offer), is less than demand λC on storage. Therefore energy shortage happens with a probability $P(X \leq \lambda C)$. Thus, if demand on storage λC is above σ_ρ then according to Proposition 3, $P(X \leq \lambda C) > \rho$, meaning that the probability of energy shortage exceeds risk tolerance ρ. In contrast, if demand λC on storage is bellow σ_ρ then the probability of energy shortage respects risk tolerance ρ.[4]

Building on this intuition, we understand that σ_ρ plays a central role on how to decide optimally on the energy mix between back-up fossil fuels and stored renewable energy in order to control the risk for energy shortage during peak load. In the following section, we formalize this intuition and analyze numerically the optimal mix between back-up fossil fuels and stored renewable energy during peak load.

3.2 Characterization of ρ-admissible mix and ρ-optimal mix

3.2.1 Theoretical characterization ρ-optimal energy mix $\hat{\lambda}_\rho$

Having defined and characterized σ_ρ in Proposition 3, the question remains on how to decide on the optimal energy mix during peak demand, between stored renewable energy and back-up fossil fuel, in order to minimize the share of fossil fuels while controlling the risk of energy shortage bellow risk tolerance ρ.

[4]Numerical experiments on the evolution of σ_ρ with respect to λ for different technical states are provided in Appendix A.

Definition 5. ***(i)*** *We define the set of ρ-admissible energy mix as:*

$$\mathcal{D}_\rho = \{\lambda \in [0,1] \mid \lambda C \leq \sigma_\rho(\phi, \Gamma, \lambda C)\}.$$

(ii) *A mix λ_ρ is said to be ρ-admissible if $\lambda \in \mathcal{D}_\rho$.*
(iii) *A ρ-admissible energy mix $\hat{\lambda}_\rho$ is said to be optimal if it minimizes the use of back-up fossil fuels during peak demand, that is:*

$$\forall \lambda_\rho \in \mathcal{D}_\rho \; F(\hat{\lambda}_\rho) \leq F(\lambda_\rho) \iff (1 - \hat{\lambda}_\rho)C \leq (1 - \lambda_\rho)C.$$

Note that, as σ_ρ depends on technical state (ϕ, Γ), then the set of ρ-admissible energy mix is defined for a given storage technology. Therefore, a ρ-admissible energy mix λ_ρ is such that the demand $\lambda_\rho C$ on storage is less than σ_ρ. Among these, we define ρ-optimal mix $\hat{\lambda}_\rho$, as the mix minimizing the use of fossil fuels. We know provide with the characterization for ρ-optimal mix:

Proposition 4. ***(i)*** *For a given technical state (ϕ, Γ) and a risk tolerance ρ, the probability of energy shortage when using a ρ-admissible energy mix λ_ρ during peak demand is less or equal to ρ.*
(ii) *$\mathcal{D}_\rho$ has a supremum $\hat{\lambda}_\rho = \sup_{\lambda \in [0,1]} \mathcal{D}_\rho(\phi, \Gamma)$ which is the ρ-optimal energy mix.*

For a tolerance $\rho = 0.04\%$ (as mentioned in Ambec and Crampes (2017) as the legal standard for developed countries) the probability for energy shortage to occur during peak load with a ρ-admissible energy mix is less than once every seven years. Moreover, as the use of back-up fossil fuels $(1 - \lambda)C$ decreases with respect to mix λ, then among the ρ-admissible energy mix, the max is the one minimizing the use of fossil fuels. Such optimal mix is denoted $\hat{\lambda}_\rho$ and depends explicitly on the level of efficiency ϕ and capacity Γ of storage as well as on the random renewable energy surplus during the charging off-peak periods $(\omega_i)_{i \in \mathbb{N}^*}$.

3.2.2 Numerical exploration of the ρ-optimal energy mix $\hat{\lambda}_\rho$

By numerically solving the equation $\bar{\mu} = \Pi\bar{\mu}$ to obtain the stationary SOC probability distribution $\bar{\mu}$ before peak load, and by solving the optimization problem $\hat{\lambda}_\rho = \sup_{\lambda \in [0,1]} \mathcal{D}_\rho(\phi, \Gamma)$, we provide in Figure 4 with the ρ-optimal energy mix $\hat{\lambda}_\rho(\phi, \Gamma)$ with respect to storage efficiency ϕ and capacity Γ.[5] As we neglect seasonal effects, the collection of random surplus of renewable energy $(\omega_i)_{i \in \mathbb{N}^*}$ are independent and identi-

[5]The optimization problem is solved using a bisection method algorithm provided in Appendix D.1.

cally distributed (Assumption 1). Moreover, the ρ-optimal energy mix $\hat{\lambda}_\rho$ is given for a benchmark renewable energy surplus distribution that is, $(\omega_i)_{i\in\mathbb{N}^*} \sim \mathcal{W}(32, 7)$ with mean 30 GWh and variance 25 GWh.[6] Finally, we consider here the parameter values $C = 10$ GWh for consumption peak intensity, and $\rho = 0.04$ for risk tolerance.

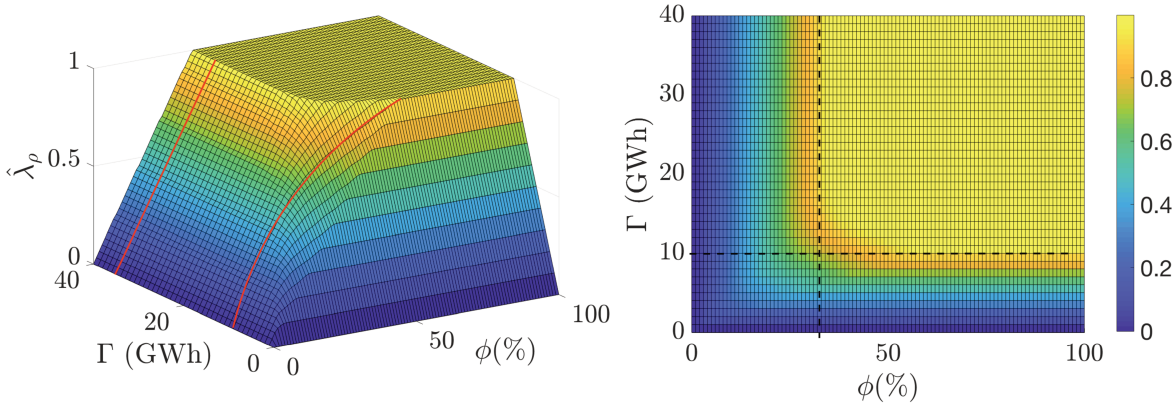

Figure 4: ρ-optimal energy mix $\hat{\lambda}_\rho$ with $(\omega_i)_{i\in\mathbb{N}^*} \sim \mathcal{W}(32, 7)$.

Intuitively enough, as long as no storage technology is available in the economy, that is capacity $\Gamma = 0$, or efficiency $\phi = 0$, then the optimal energy mix $\hat{\lambda}_\rho(\phi, \Gamma) = 0$. No decarbonation is allowed as long as one of the two technical parameter is equal to zero. In contrast, for high values in efficiency ϕ and capacity Γ, the energy mix reaches the "carbon neutral" plateau at which $\hat{\lambda}_\rho = 1$, that is, for technical states (ϕ, Γ) such that peak load can fully be decarbonated. For such technical states, the economy can directly rely on renewable energy storage during peak load, and no back-up fossil fuels shall be used during peak hours. Note that, there exists a limit value for both efficiency and capacity, that we denote $\bar{\phi}$ and $\bar{\Gamma}$, and bellow which the carbon neutral plateau cannot be reached *i.e.* $\hat{\lambda}_\rho(\phi < \bar{\phi}, \Gamma < \bar{\Gamma}) < 1$. With the benchmark distribution $\mathcal{W}(32, 7)$, the limit values in efficiency and capacity bellow which peak load cannot be fully decarbonated are $\bar{\phi} = 35\%$ and $\bar{\Gamma} = 11$ GWh. As the optimal energy mix $\hat{\lambda}_\rho(\phi, \Gamma)$ depends on the renewable energy surplus distribution, the limit values $\bar{\phi}$ and $\bar{\Gamma}$ also depends explicitly on the surplus distribution. To asses the sensitivity of the optimal energy mix $\hat{\lambda}_\rho(\phi, \Gamma)$ with respect to renewable energy surplus we provide with examples in Figure 5 and Figure 6 for two distributions $\mathcal{W}(52.3, 12.2)$ of mean 50 GWh and variance 25 GWh, and $\mathcal{W}(32.5, 5.9)$ of mean 30 GWh and variance 35 GWh, that we compare with the previous benchmark distribution $\mathcal{W}(32, 7)$ of mean 30 GWh and variance 25 GWh.

[6]We model the random renewable energy surplus $(\omega_i)_{i\in\mathbb{N}^*}$ by a Weibull distribution as it is commonly used to model random renewable energy availability in the literature. See Wais, 2017 for a complete review on the Weibull distribution.

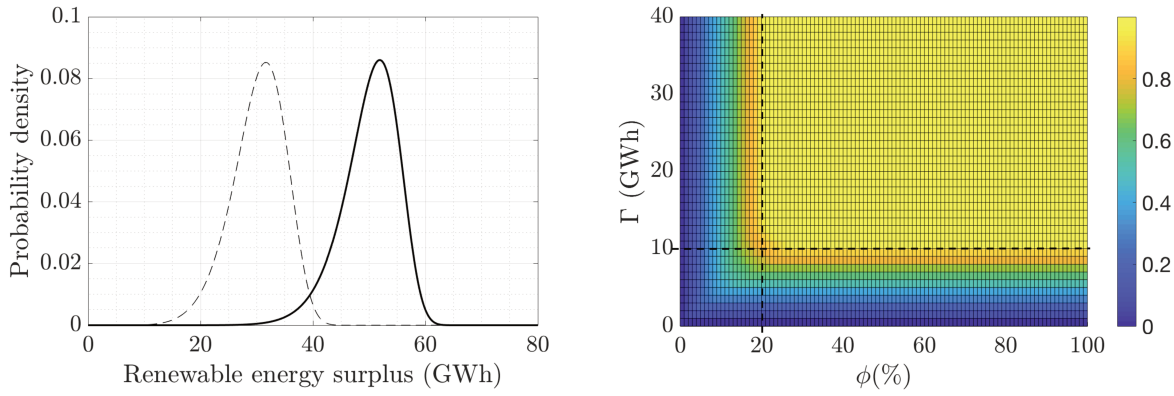

Figure 5: Renewable energy surplus distribution $(\omega_i)_{i\in\mathbb{N}^*} \sim \mathcal{W}(52.3, 12.2)$ (left) and resulting ρ-optimal energy mix $\hat{\lambda}_\rho$ (right) : increase in mean.

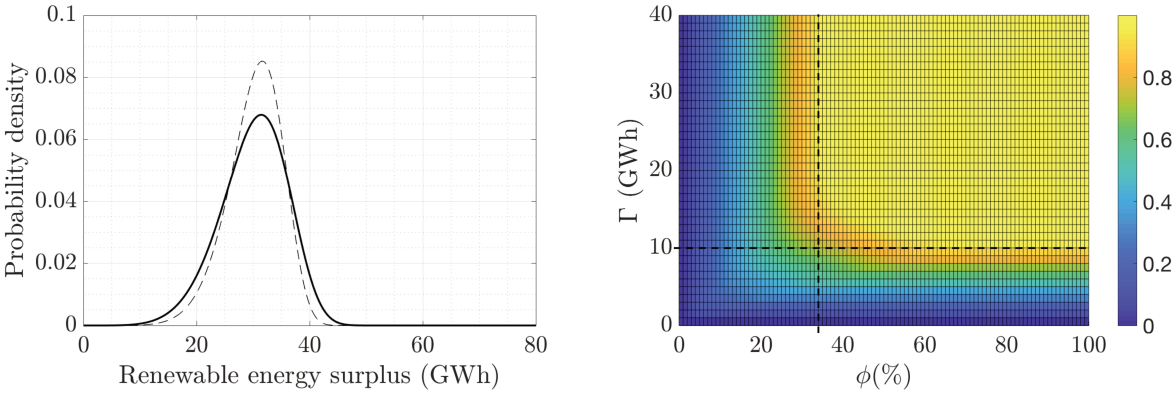

Figure 6: Renewable energy surplus distribution $(\omega_i)_{i\in\mathbb{N}^*} \sim \mathcal{W}(32.5, 5.9)$ (left) and resulting ρ-optimal energy mix $\hat{\lambda}_\rho$ (right) : increase in variance.

In Figure 5 (left) and 6 (left), the distribution in dashed line represents the benchmark distribution $\mathcal{W}(32, 7)$ from Figure 4. With the distribution $\mathcal{W}(52.3, 12.2)$, the capacity limit values remains at $\bar{\Gamma} = 11$ GWh, which is the same as for the benchmark distribution $\mathcal{W}(32, 7)$, while the efficiency limit values drops to $\bar{\phi} = 20\%$ (compared to 35% for the benchmark distribution). In contrast, with the distribution $\mathcal{W}(32.5, 5.9)$, the capacity limit values $\bar{\Gamma} = 11$ GWh is again the same as for the benchmark distribution $\mathcal{W}(32, 7)$, and the efficiency limit $\bar{\phi} = 35\%$ is also the same as for the benchmark distribution. More generally, we provide in Figure 7 with the evolution in efficiency and capacity limit values $\bar{\phi}$ and $\bar{\Gamma}$ with respect to the energy surplus distribution mean and variance. On the one hand, we find that an increase in the energy surplus mean (at constant variance) does not have an impact on the capacity limit value $\bar{\Gamma}$, yet leads to a decrease in efficiency limit values $\bar{\phi}$. On the other hand, increasing variance (at constant mean) does not have an impact on either the efficiency or the capacity limit value. Yet, an increase in variances modifies the curvature of the carbon neutral plateau's border as shown in Figure 6.

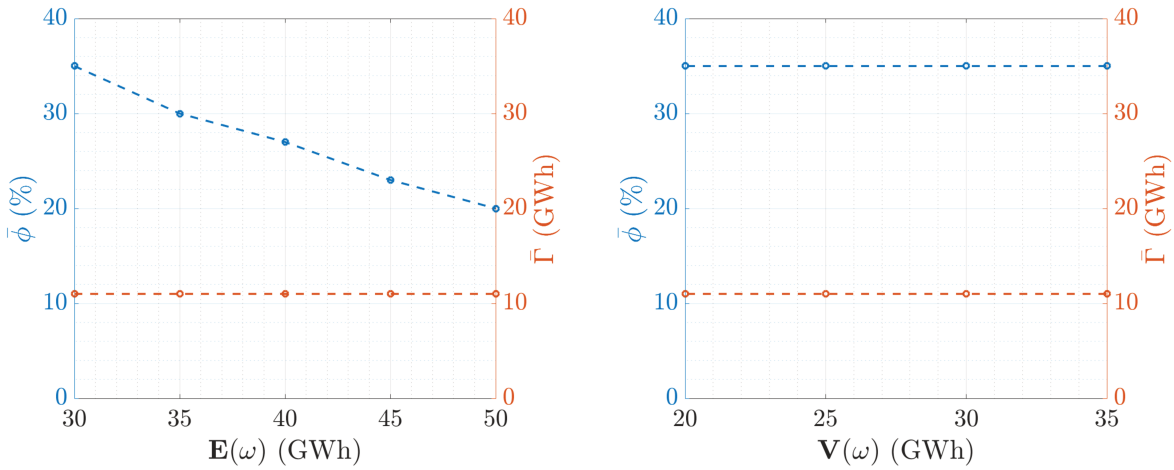

Figure 7: Evolution of $\bar{\phi}$ and $\bar{\Gamma}$ with respect to energy surplus mean at constant variance 25 GWh (left) and energy surplus variance at constant mean 30 GWh (right).

Our analysis highlights that the set of technical parameters (ϕ, Γ) for which peak load can fully be decarbonated highly depends on the renewable energy surplus distribution from which renewable energy is being stored. Thereby, the energy surplus distribution has an impact on optimal energy storage policies and the resulting peak load decarbonation dynamics that we shall analyse in the following. Beforehand, let us define two relevant regions regarding variations in the energy mix $\hat{\lambda}_\rho$ with respect to efficiency and capacity in order to study analytically peak load decarbonation in specific cases for constant capacity Γ. The first region is for high values of capacity Γ in which $\frac{\partial^2 \hat{\lambda}_\rho}{\partial \phi^2}|_{\Gamma_{high}} = 0$, which will be referred to as the *linear region* (see upper red line in Figure 4 for $\Gamma = 35$ GWh) in which energy mix $\hat{\lambda}_\rho$ evolves linearly with respect to efficiency at constant capacity. The second region is the region for low values of capacity Γ in which $\frac{\partial^2 \hat{\lambda}_\rho}{\partial \phi^2}|_{\Gamma_{low}} < 0$ which will be referred to as the *concave region* (see lower red line in Figure 4 for $\Gamma = 9$ GWh) in which energy mix can be modelled as a concave function with respect to efficiency. Thereby, in the following section, we shall study analytically optimal energy storage policies and the resulting peak load decarbonation dynamics, by making assumption regarding the expression of energy mix $\hat{\lambda}_\rho$ with respect to efficiency and capacity, and by calibrating $\hat{\lambda}_\rho$ on both the *linear region* and *concave region*.

Having characterized the ρ-optimal energy mix $\hat{\lambda}_\rho$ in such static framework, we consider in the following sections technical progress on storage regarding both efficiency ϕ and capacity Γ through investment decisions in time and study the optimal dynamics in investment decisions on storage technical progress which minimize the cost of

peak load decarbonation. More particularly, we analyse in the following the trade-offs regarding investments in efficiency ϕ and capacity Γ involved during peak load decarbonation. Indeed, as an increase in both efficiency or capacity leads to a diminution in the share of fossil fuels used during peak load, the question remains on whether it is more profitable to invest in either efficiency or capacity. We will see how optimal energy storage policies are sensitive to initial storage technology, investments costs in efficiency and capacity, fossil fuels costs, as well as on the renewable energy surplus $(\omega_i)_{i\in\mathbb{N}^*}$ supplying for the storable excess of renewable energy.

4 Dynamic energy mix with technical progress

4.1 Theoretical framework for dynamic energy mix

In the previous section, we develop a numerical method which provides, for a given efficiency ϕ and capacity Γ, the optimal energy mix $\hat{\lambda}_\rho$ between back-up fossil fuels and stored renewable energy during peak load. That is, the mix minimizing the use of fossil fuels while controlling the risk of energy shortage bellow a risk tolerance threshold. Yet, the optimal mix is obtained for a given technical state (ϕ, Γ) in a static framework. In the following, we consider that technical states (ϕ_t, Γ_t), characterizing storage technology, can evolve in time through investment decisions in both efficiency ϕ or capacity Γ so to reach peak load decarbonation.

For a given technical state (ϕ_t, Γ_t), Proposition 4 characterizes the ρ-optimal energy mix $\hat{\lambda}_\rho(\phi_t, \Gamma_t)$ that we denote in the following as $\lambda(\phi_t, \Gamma_t)$ for ease of notations. Therefore, the optimal share of fossil fuels in energy mix at time t, for a given technical state (ϕ_t, Γ_t), writes as:

$$F(\lambda(\phi_t, \Gamma_t)) = (1 - \lambda(\phi_t, \Gamma_t))C.$$

Note that the analytical expression of $\lambda(\phi, \Gamma)$ was not derived in the previous section, yet we provide with numerical experiments in Section 3.2.2 which we shall use in the following to model and calibrate the energy mix $\lambda(\phi, \Gamma)$ accordingly. We suppose that the cost of using a quantity F of fossil fuels during peak load writes as $\pi(F)$, with $\pi'(F) > 0$. As a result, the cost of using fossil fuels during peak demand for a given technical state (ϕ_t, Γ_t) at time t writes as:

$$\pi(F(\lambda(\phi_t, \Gamma_t))) = \pi[(1 - \lambda(\phi_t, \Gamma_t))C].$$

The cost of using back-up fossil fuels can here reflect different situations such as the use of a carbon tax, a cost of extracting fossil fuels or the cost from European Emission allowance as seen in Introduction.

Finally, the shift from back-up fossil fuels to stored renewable energy during peak load supposes technical progress in both efficiency and capacity through investments. We model such investments decisions at each time steps t as:

$$\begin{cases} i_t^{\phi} = \phi_{t+1} - \phi_t, \\ i_t^{\Gamma} = \Gamma_{t+1} - \Gamma_t. \end{cases}$$

Yet, technical progress on efficiency and capacity come with investment costs modelled by $\kappa(i_t^{\phi}, i_t^{\Gamma})$ with $\frac{\partial \kappa}{\partial i^{\phi}} > 0$ and $\frac{\partial \kappa}{\partial i^{\Gamma}} > 0$, that is, the more ambitious is the decision on storage technical progress, the more costly it is.

In such framework, the two state variables are the technical state, efficiency ϕ and capacity Γ of storage, and controls variable are investments decisions in ϕ and Γ, that is i^{ϕ} and i^{Γ} with the above notations. Hence, the cost minimizing problem for peak load decarbonation writes as:

$$\begin{aligned} &\min_{(i_t^{\phi}, i_t^{\Gamma})} \sum_{t=0}^{T} \beta^t \left(\pi[(1 - \lambda(\phi_t, \Gamma_t))C] + \kappa(i_t^{\phi}, i_t^{\Gamma}) \right), \\ &s.t. \begin{cases} (\phi_{t+1}, \Gamma_{t+1}) = (\phi_t, \Gamma_t) + (i_t^{\phi}, i_t^{\Gamma}), \\ \lambda(\phi_t, \Gamma_t) \leq 1, \\ (\phi_0, \Gamma_0) \in \mathbb{R}_+ \times \mathbb{R}_+ \text{ and } \lambda(\phi_T, \Gamma_T) = 1. \end{cases} \end{aligned} \tag{1}$$

where $\beta > 0$ is the time discount rate, $T \in \mathbb{R}_+ \cup \{+\infty\}$ time horizon, and (ϕ_0, Γ_0) a given initial technical state for storage.[7] The terminal condition on efficiency and capacity $\lambda(\phi_T, \Gamma_T) = 1$ implies full decarbonation at the terminal state. Yet, full decarbonation can be reached before the time horizon of the problem.

As a result to this problem, we provide with the optimal investments decisions on efficiency and capacity in order to minimize the cost of peak load decarbonation. We also obtain the optimal dynamics for efficiency ϕ_t and capacity Γ_t and thus with the optimal peak load energy mix dynamics $\lambda(\phi_t, \Gamma_t)$ between back-up fossil fuels and stored renewable energy before reaching full decarbonation. We first study analytically the

[7]Building on this model, one could study a more general specification for storage with more than two characteristics (for instance, by integrating ecological or lifetime storage characteristics to the model).

case of constant capacity, and then numerically the general problem with investments in both efficiency and capacity.

4.2 Analytical solution for constant capacity

4.2.1 The general solution

In this section we solve analytically the cost minimization problem in the case of constant capacity Γ, that is, when only investments in efficiency are considered. The control variable is thereby i_t^ϕ and state variable ϕ_t. As we do not provide with the analytical expression of energy mix with respect to ϕ in the previous section, we calibrate here the model of the energy mix λ with respect to efficiency ϕ, according to the numerical experiments from Section 3.2.2. We solve the problem in both the *linear* and *concave region* of the $\rho-$optimal energy mix as identified in Section 3.2.2 for respectively high and low capacity levels. The peak load decarbonation problem therefore rewrites as:

$$\begin{aligned} &\min_{i_t^\phi} \sum_{t=0}^{T} \beta^t \left[\pi[(1-\lambda((\phi_t))C] + \kappa(i_t^\phi)\right], \\ &s.t. \begin{cases} \phi_{t+1} = \phi_t + i_t^\phi, \\ \phi_0 \in \mathbb{R}_+ \text{ and } \lambda(\phi_T) = 1. \end{cases} \end{aligned} \tag{2}$$

We now provide with the optimal dynamics for efficiency and investments decisions, solution to the peak load cost minimization problem (2):

Proposition 5. *The optimal dynamics for efficiency ϕ during peak load decarbonation is solution to the following second order difference equation problem:*

$$\begin{cases} \beta C\pi'[(1-\lambda(\phi_{t+1}))C]\lambda'(\phi_{t+1}) - \kappa'(\phi_{t+1}-\phi_t) + \beta\kappa'(\phi_{t+2}-\phi_{t+1}) = 0, \\ \phi_0 \geq 0, \\ \lambda(\phi_T) = 1. \end{cases}$$

and the optimal investment policy in efficiency is given by $i_t^\phi = \phi_{t+1} - \phi_t$.

In this set-up, Problem (2) is not analytically solvable due to the *a priori* non-linearities in the derivative of investment costs κ', fossil fuels cost π' and energy mix λ'. Therefore we shall make the following assumptions on the cost from using back-up fossil fuels and investment decisions costs regarding storage technical progress.

Assumption 3. *The cost from using back-up fossil fuels is linear such that* $\tau(F) = \nu F$ *with* $\nu > 0$ *and investments costs are quadratic such that* $\kappa(i) = \alpha i^2$ *with* $\alpha > 0$.

Henceforth, the cost of using fossil fuels is characterized by ν, and the cost of efficiency investments, characterized by α. We suppose the cost of fossil fuels linear in the share F of fossil fuels in the energy mix. This could reflect the case of a carbon tax, or the cost from extracting the fossil fuels ressources. In either case, this cost is the main driver for investing in renewable energy storage. On the other hand, considering quadratic cost for investments allows us to capture the convexity in investment costs. That is, the cost of technical progress in efficiency marginally increases with respect to investments decisions. Finally, and conveniently enough, Assumption 3 linearizes the terms in fossil fuels and investments costs in the optimal efficiency dynamics solution to Problem (2), leading to the following claim:

Corollary 1. *Under Assumption 3, the optimal dynamics for efficiency* ϕ *during peak load decarbonation is solution to the following second order difference equation problem:*

$$\begin{cases} \phi_{t+2} - \frac{1+\beta}{\beta}\phi_{t+1} + \frac{1}{\beta}\phi_t = -\frac{C\nu}{2\alpha}\lambda'(\phi_{t+1}), \\ \phi_0 \geq 0, \\ \lambda(\phi_T) = 1. \end{cases}$$

and the optimal investment policy in efficiency is given by $i_t^\phi = \phi_{t+1} - \phi_t$.

Assuming linear fossil fuels cost and quadratic investment cost for efficiency leads to a linear left hand side in the dynamics of efficiency ϕ in Corollary 1. However the right hand side is still *a priori* non-linear in efficiency ϕ, depending on the expression of energy mix λ with respect to efficiency ϕ. We shall study the dynamics of ϕ according to the expression of λ with respect to efficiency.

Indeed, the characterization of the optimal energy mix λ and the numerical experiments from Section 3.2.2 allows us to make motivated assumptions and calibrations for energy mix $\lambda(\phi)$. More particularly we will focus on the *linear* (resp. *concave*) *region* introduced in Section 3.2.2, in which the energy mix λ can easily be modeled and calibrated as a linear (resp. concave) function in efficiency ϕ. Thereby, in the following we study the optimal dynamics in efficiency by modelling the energy mix accordingly to the numerical experiments from Section 3.2.2. We provide with the analytical optimal dynamics in efficiency and optimal investments decision using such calibrations in both the *linear* and *concave region* of energy mix λ.

4.2.2 Optimal solution in the linear region for high capacities

We solve peak load decarbonation problem in the *linear region* of energy mix λ, that is, the region for constant and high capacity in which the following assumption holds:

Assumption 4. *For high capacity, the energy mix λ is linear with respect to efficiency ϕ, that is $\lambda = \gamma\phi$ with $\gamma > 0$.*

We now provide with the optimal efficiency dynamics and investments decisions in the case of constant and high storage capacity in the *linear region* of energy mix.

Corollary 2. ***(i)*** *Under Assumption 3 and Assumption 4, the optimal dynamics for efficiency ϕ during peak load decarbonation is solution to the following second order difference equation problem:*

$$\begin{cases} \phi_{t+2} - \frac{1+\beta}{\beta}\phi_{t+1} + \frac{1}{\beta}\phi_t = -\frac{C\nu\gamma}{2\alpha}, \\ \phi_0 \geq 0, \\ \phi_T = \frac{1}{\gamma}. \end{cases} \tag{3}$$

and the optimal investment policy in efficiency is given by $i_t^{\phi} = \phi_{t+1} - \phi_t$.

(ii) *For an initial efficiency $\phi_0 = 0$, the optimal efficiency dynamics are:*

$$. \begin{cases} \phi_t^* = A\left(\left(\frac{1}{\beta}\right)^t - 1\right) + \frac{C\nu\beta\gamma}{2\alpha(1-\beta)}\ t,\ \forall t <\ T^\star, \\ \phi_t^* = \frac{1}{\gamma},\ \forall t \geq\ T^\star, \end{cases}$$

where $T^\star$ is the transition time towards decarbonation and,

$$A = C\left[\frac{1}{\gamma} - \frac{\nu\beta\gamma}{2\alpha(1-\beta)}T\right]\left[\left(\frac{1}{\beta}\right)^T - 1\right]^{-1}.$$

(iii) *If $\nu > 0$ and $\frac{ab^{d/c}ln(b)}{c} > -\frac{1}{e}$ then transition time $T^\star$ is such that:*

$$T^\star = \frac{d}{c} - \frac{1}{ln(b)}W\left(\frac{ab^{d/c}ln(b)}{c}\right),$$

with $a = A$, $b = \frac{1}{\beta}$, $c = \frac{C\nu\beta\gamma}{2\alpha(1-\beta)}$, $d = \frac{1}{\gamma} + A$ and W the Lambert W function.

Corollary 2 provides with the analytical expression of the optimal technical path regarding efficiency ϕ. Note that from the dynamics in ϕ_t, one can directly obtain the

optimal dynamics for the energy mix during peak load, that is $\lambda_t = \lambda(\phi_t)$. Figure 18 in Appendix B gives the optimal dynamics in efficiency for different fossil fuels cost ν, at constant capacity $\Gamma = 40$, starting from $\phi_0 = 0$ and thus $\lambda_0 = 0$. We get that, initially, the economy only uses back-up fossil fuels during peak load. As time evolves, the economy invests in storage technical progress, so to reduce its use of costly back-up fossil fuels, and storage efficiency ϕ increases along the optimal decarbonation path solution to (3). Back-up fossil fuels are progressively being substituted by stored renewable energy, until the mix λ reaches its upper bound at time $T^\star$, that is $\lambda(T^\star) = 1$, at which time all back-up fossil fuels have been replaced by renewable energy storage. Moreover, from Figure 18, as fossil fuels cost increases, the mix and the efficiency level reach their upper bound in a shorter time. A calibrated analysis of the evolution of transition time horizons with respect to fossil fuels costs is provided in Section 4.

4.2.3 Optimal solution in the concave region for low capacities

We now solve the decarbonation Problem (2) in the *concave region* of energy mix λ, that is, the region for constant and low capacity in which the following assumption holds:

Assumption 5. *For low capacity, the energy mix λ is concave with respect to efficiency ϕ, that is $\lambda = \eta\phi^\gamma$ with $\eta > 0$ and $\gamma < 1$.*

We provide next with the optimal efficiency dynamics and investments decisions in the case of constant and low storage capacity in the *concave region* of energy mix.

Corollary 3. *Under Assumption 3 and Assumption 5, the optimal dynamics for efficiency ϕ during peak load decarbonation is solution to the following second order difference equation problem:*

$$\begin{cases} \phi_{t+1}^{1-\gamma}\left[\phi_{t+2} - \frac{1+\beta}{\beta}\phi_{t+1} + \frac{1}{\beta}\phi_t\right] = -\frac{C\nu\eta\gamma}{2\alpha}, \\ \phi_0 \geq 0, \\ \phi_T = \left(\frac{1}{\eta}\right)^{\frac{1}{\gamma}}. \end{cases} \tag{4}$$

and the optimal investment policy in efficiency is given by $i_t = \phi_{t+1} - \phi_t$.

In contrast with the solution of the decarbonation problem in the *linear region*, Corollary 3 does not provide with the analytical expression for the optimal efficiency

dynamics ϕ_t, as assuming a concave energy mix λ with respect to efficiency ϕ leads to a non linear difference problem. Yet, the optimal efficiency dynamics in the *concave region* can be analyzed using backward shooting method. We provide in Figure 19 in Appendix C with the optimal dynamics of storage efficiency in the *concave region*, for different fossil fuels costs at constant capacity $\Gamma = 20$. With time, storage efficiency increases along the optimal path solution to (4), and back-up fossil fuels are progressively being substituted until peak load is fully decarbonated, when $\lambda(\phi_{T^\star}) = 1$. The pseudo-code used to solve (4) with a backward shooting method is given in Appendix D.2.

4.3 Numerical solution on global technical domain

4.3.1 The global peak load decarbonation problem

In the previous section, we solved analytically the problem by calibrating the ρ-optimal energy mix λ accordingly to the numerical experiments from Section 3.2.2, yet for constant value of capacity. In this section, we numerically solve the problem using a value function iteration algorithm on the global technical domain, that is for all ϕ and Γ, and with the actual ρ-optimal energy mix solution to $\lambda(\phi, \Gamma) = \sup_{\lambda \in [0,1]} \mathcal{D}_\rho(\phi, \Gamma)$, as characterized in Proposition 4. Moreover, we apply in the section 4.3.2. our numerical analysis to Portugal's peak load decarbonation.

Building on the previous assumptions, we consider therefore linear fossil fuels costs with respect to the share of fossil fuels in the energy mix, $\pi(F) = \nu F$, and the quadratic investments costs now writes $\kappa(i_t^\phi, i_t^\Gamma) = \alpha_\phi(\phi_{t+1} - \phi_t)^2 + \alpha_\Gamma(\Gamma_{t+1} - \Gamma_t)^2$. Therefore, in such framework, the peak load decarbonation cost minimization problem writes as:

$$\begin{aligned} &\min_{(i_t^\phi, i_t^\Gamma)} \sum_{t=0}^{\infty} \beta^t \left(\nu[(1 - \lambda(\phi_t, \Gamma_t))C] + \alpha_\phi(\phi_{t+1} - \phi_t)^2 + \alpha_\Gamma(\Gamma_{t+1} - \Gamma_t)^2 \right), \\ &s.t. \begin{cases} \phi_{t+1} = \phi_t + i_t^\phi, \\ \Gamma_{t+1} = \Gamma_t + i_t^\Gamma, \\ (\phi_0, \Gamma_0) \in \mathbb{R}_+ \times \mathbb{R}_+. \end{cases} \end{aligned} \tag{5}$$

Problem (5) has now four degrees of freedom. Fossil fuels cost which is still characterized by ν, investment costs in efficiency and capacity characterized by α_ϕ and α_Γ respectively, and the initial energy storage technical state (ϕ_0, Γ_0). Note that such initial technical states can potential captures pre-existing storage capacities from pre-

vious investments in storage. Problem (5) is solved using a value function iteration algorithm and we investigate on different numerical exercices in the following sections.

4.3.2 Energy storage policy sensitivity and robustness analysis

Sensitivity analysis. We study the sensitivity of energy storage optimal policies and the resulting peak load decarbonation dynamics with respect to the relative investments costs in storage efficiency α_ϕ and capacity α_Γ. Let us define the ratio of investment costs $\delta_\alpha = \frac{\alpha_\Gamma}{\alpha_\phi}$ which characterizes the relative costs of investing in either efficiency or capacity in order to substitute back-up fossil fuels by stored renewable energy. In Figure 8 are gathered the results for optimal decarbonation pathways in ϕ and Γ obtained from the value function iteration algorithm, for four scenario of relative investment costs ranging from $\delta_\alpha = 0.2$ to $\delta_\alpha = 40$.

We examine the case in which the economy has initially high storage capacities, but low efficiency, by initializing efficiency and capacity to $(\phi_0, \Gamma_0) = (0, 20)$. As δ_α decreases, investments are more directed towards capacity rather than to efficiency, as capacity becomes more profitable. However, an increase δ_α redirect investment towards efficiency, up to a point above which no investment is directed to capacity (see for $\delta_\alpha = 40$ in Figure 8).

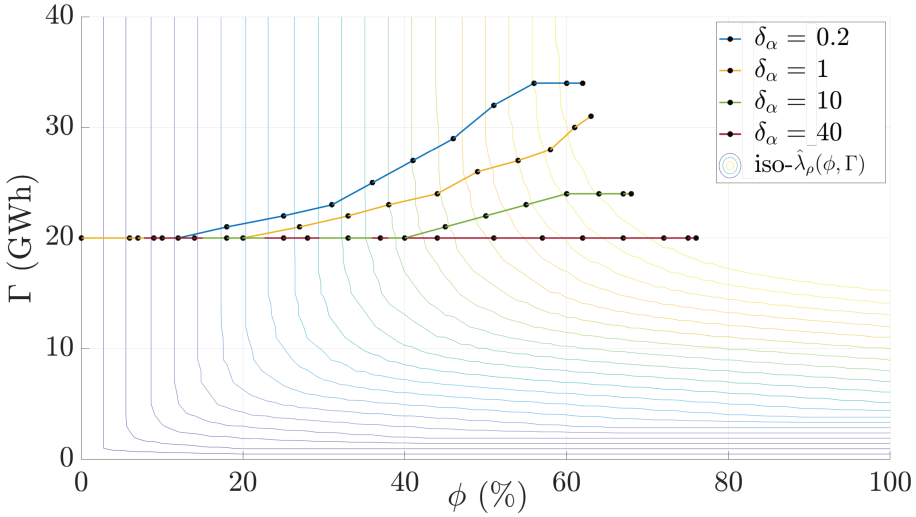

Figure 8: Optimal energy storage policy for $(\omega_i)_{i\in\mathbb{N}^*} \sim \mathcal{W}(20, 3)$ and $(\phi_0, \Gamma_0) = (0, 20)$.

Similarly, we study the evolution of the optimal decarbonation dynamics for higher initial capacity level, by initializing storage technical level to $(\phi_0, \Gamma_0) = (0, 40)$. Results are gathered in Figure 9. Starting with higher capacity values, leads to more profitable

investments in efficiency. Indeed, in this case, the economy invests more in efficiency so to catch up with the advanced technological level in capacity. Thus, the more important is initial capacity, the less investments in capacity are considered. Moreover, as previously, increasing δ_α reduces even more capacity investments until reaching the no capacity-investment pathway for $\delta_\alpha = 1$ in Figure 9. In either case, for high or low initial capacity level, the reduction in capacity level cannot be considered, as such policy has a cost while decreasing the amount of stored renewable energy.

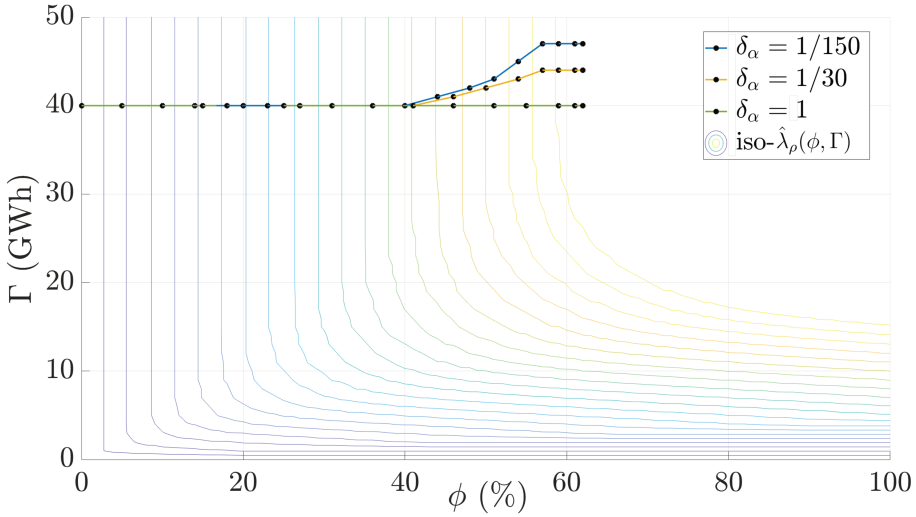

Figure 9: Optimal energy storage policy for $(\omega_i)_{i\in\mathbb{N}^*} \sim \mathcal{W}(20, 3)$ and $(\phi_0, \Gamma_0) = (0, 40)$.

Robustness analysis. Note that, on the no capacity-investment pathway (respectively for $\delta_\alpha = 40$ in Figure 8 and $\delta_\alpha = 1$ in Figure 9), the decarbonation of back-up fossil fuels by stored renewable energy is done at constant capacity. Therefore, the optimal decarbonation dynamics match with the case studied analytically in Section 4.2, when considering only investments in efficiency. Moreover, starting with high initial capacity, as in the case with $(\phi_0, \Gamma_0) = (0, 40)$ and $\delta_\alpha = 1$, then the optimal dynamics lies in the *linear region* of the energy mix introduced in Section 3.3.2. In the *linear region*, and for constant capacity, we derived an analytical solution of the optimal dynamics of efficiency in Corollary 2. We gather in Figure 10 (top) both the analytical solution and the value function iteration solution for the optimal dynamics in efficiency for $(\phi_0, \Gamma_0) = (0, 40)$, $\delta_\alpha = 1$ and fossil fuels cost $\nu = 2$.

Similarly, for initial levels in efficiency and capacity $(\phi_0, \Gamma_0) = (0, 20)$, and for $\delta_\alpha = 40$, there are no investments in capacity. The optimal decarbonation pathway considers therefore only investments in efficiency but this time for smaller capacity,

that is, in the *concave region* as introduced in Section 3.3.2. In the *concave region*, we did not derive an analytical solution, but we characterized the solution in Corollary 3. We solve the optimal decarbonation dynamics from Corollary 3 using backward shooting method and gather this solution with the value function iteration solution in Figure 10 (bottom), for fossil fuels cost $\nu = 2$.

For both scenario, in the *linear region* and in the *concave region*, the analytical approach and the value function iteration solutions match, assuring therefore the robustness of the numerical method. Moreover, we provide with similar comparisons between the analytical and the value function iteration solutions on a wider range of fossil fuels costs in Appendix B and C for both the *linear region* and the *concave region*.

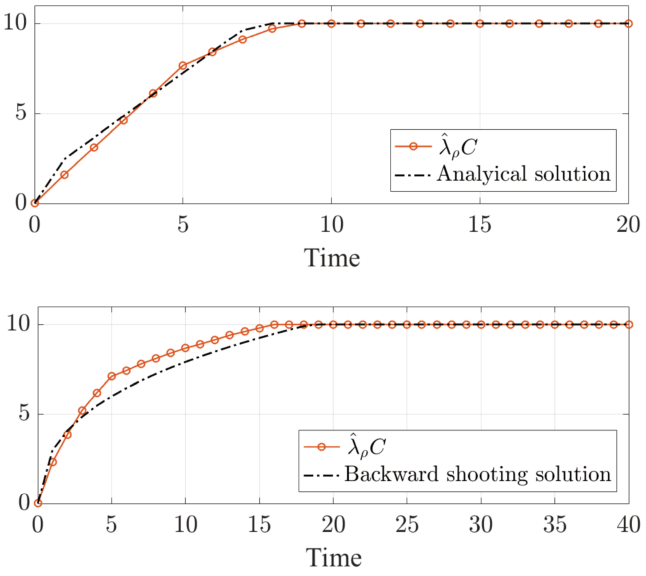

Figure 10: Peak decarbonation dynamics with $(\omega_i)_{i\in\mathbb{N}^*} \sim \mathcal{W}(20, 3)$, $(\phi_0, \Gamma_0) = (0, 40)$, $\delta_\alpha = 1$ (top) and $(\phi_0, \Gamma_0) = (0, 20)$, $\delta_\alpha = 40$ (bottom) for $\nu = 2$.

4.4 Application to Portugal's peak load decarbonation

4.4.1 Calibration of the peak load decarbonation problem

We apply our model to Portugal's peak load decarbonation through investments in renewable energy storage. Hence, we calibrate the model's parameters on Portugal's energy system and study different trajectories for peak load decarbonation in Portugal through scenario regarding the costs of fossil fuels, the cost of energy storage as well as the renewable energy surplus from which energy is stored for peak shifting. Moreover, in the following, we calibrate renewable energy production and Portugal's energy

consumption on data from March 2018, that is when Portugal produced 103% of its energy consumption with renewable energy, but still needed fossil fuels to cover the energy demand during peak load as shown in Figure 11 on March 12^{th}.

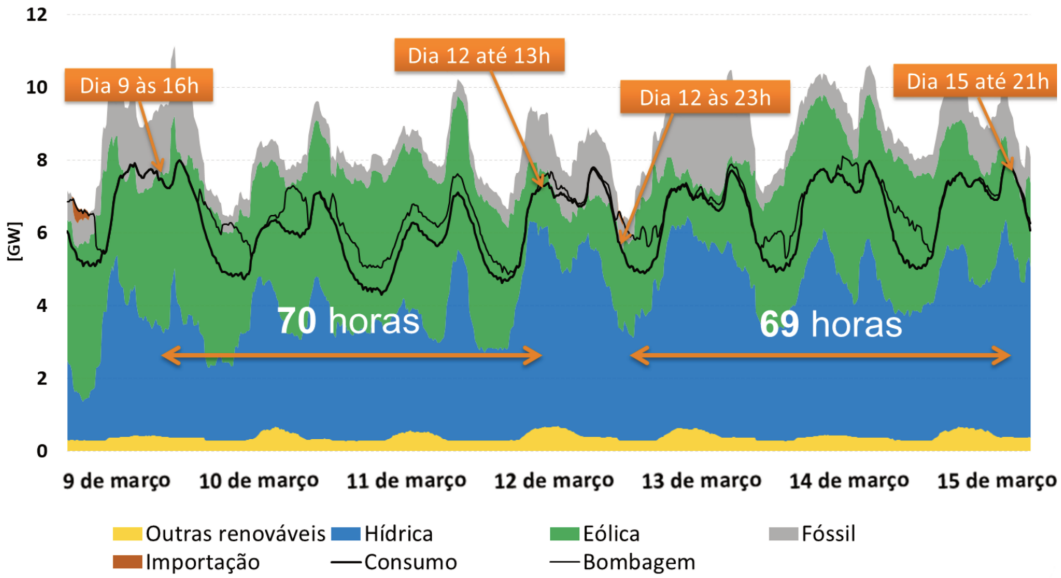

Figure 11: Portugal's energy production and consumption from March 9th to March 15 2018. Source : APREN 2018.

We calibrate the renewable energy surplus distribution $(\omega_i)_{i\in\mathbb{N}^*}$ using orders of magnitudes from the energy consumption and renewable energy production of Portugal during March 2018, leading to a mean value for the benchmark renewable energy surplus distribution of $\mathbb{E}(\omega) = 30$ GWh and a variance of $\mathbb{V}(\omega) = 25$ GWh. Such statistics lead us to consider in the following the Weibull distribution of shape parameter a = 32 and scale parameter b = 7 for the renewable energy surplus. Moreover, we calibrate the intensity of the consumption peak in Portugal from its electricity consumption during March 2018, as provided in Figure 11, leading to a peak load intensity of C = 10 GWh (see consumption peak of March 12^{th} in Figure 11).

In our model, the cost of fossil fuels ν acts as a driver for storage investments for peak load decarbonation and therefore depends on the fossil fuels used to provide electricity during peak hours. In Portugal, the main source of fossil fuels used to provide energy during peak load is combined cycle gas turbine (CCGT). Indeed, such source of energy has the benefit to be flexible and reactive, thereby adequate for peak load uses. We calibrate the cost of CCGT uses during peak load on data from IEA (2015), providing with a Levelized Cost of Energy (LCOE) for peak CCGT uses in Portugal of 100$/MWh. In the following, we shall compare energy prices using Levelized Cost

metrics of energy, therefore we calibrate costs of fossil fuels uses during peak load on such metric, hence $\nu = 100\$/\text{MWh}$. Finally, we consider typical values of $\beta = 3\%$ for discount rate as in IEA (2015) and a risk tolerance for energy shortage $\rho = 0.04\%$ as in Ambec and Crampes (2017). The calibrated parameters are gathered in Table 1.

$(\omega_i)_{i\in\mathbb{N}^*}$	RNE surplus distribution	$\mathcal{W}(32, 7)$
C	Peak demand intensity	10 GWh
ν	Fossil fuels cost (CCGT)	100 \$/MWh
β	Discount rate	3 %
ρ	Risk tolerance	0.04 %

Table 1: Calibrated parameters for Portugal.

In the following, we solve Problem (5) with the calibrated parameters from Table 1 and study the optimal energy storage policies and resulting peak load decarbonation scenarios for Portugal.

4.4.2 Optimal energy storage policy for Portugal peak load decarbonation

In this section, we numerically analyse energy storage investments policy and the resulting peak load decarbonation dynamics considering different scenario. We first study the impact of energy storage costs on decarbonation dynamics. Then we focus on carbon emissions prices due to the use of CCGT during peak load. Finally, we analyse how energy storage investments also depends on the renewable energy surplus distribution.

Levelized Cost of Storage. In this section, we provide with the optimal storage investments policies and the resulting peak load decarbonation dynamics for Portugal according to the cost of energy storage. We consider three scenarios regarding the cost of energy storage. As in Schmidt et al. (2019), we shall consider Levelized Cost of Storage (LCOS) in order to compare the costs of storage with the CCGT Levelized Cost of Energy (LCOE) used during peak load. The authors define the cost of energy storage as:

$$LCOS = \frac{Investments\ costs}{\sum_{t=0}^{T} \frac{Energy\ dischared}{(1+\beta)^t}},$$

that is, with our model's parameters:

$$LCOS = \frac{\sum_{t=0}^{T^\star} \alpha_\Gamma(\Gamma_{t+1} - \Gamma_t)^2 + \alpha_\phi(\phi_{t+1} - \phi_t)^2}{\sum_{t=0}^{T^\star} \frac{\hat{\lambda}_\rho(\phi_t, \Gamma_t)C}{(1+\beta)^t}}.$$

Note that the LCOS depends explicitly on the investments parameters α_ϕ and α_Γ, which are yet to be calibrated. Hence, we calibrate α_ϕ and α_Γ according to three different scenarios of LCOS that we shall consider in the following. Moreover, we suppose symmetric investments costs in storage efficiency and capacity that is $\alpha_\phi = \alpha_\Gamma$.[8]

In Schmidt et al. (2019), the authors provide with mean projections of LCOS according to different applications of energy storage such as energy arbitrage or congestion management. In our case, as we focus on the use of energy storage for peak load decarbonation, we thereby consider the LCOS projections from Schmidt et al. (2019) for peak replacement, leading to a mean Levelized Cost of Storage of 600 \$/MWh. Hence, the three scenario for LCOS projections that we shall consider in the following numerical analysis are $\text{LCOS}_{low} = 200\$/\text{MWh}$, $\text{LCOS}_{mean} = 600\$/\text{MWh}$ and $\text{LCOS}_{high} = 1000\$/\text{MWh}$. As a benchmark exercice, we first analyse the mean value scenario, that is $\text{LCOS}_{mean} = 600\$/\text{MWh}$. The optimal technical trajectories in energy storage investments solution to Problem (5) are provided in Figure 12 (left) along with the corresponding peak load decarbonation dynamics (right).

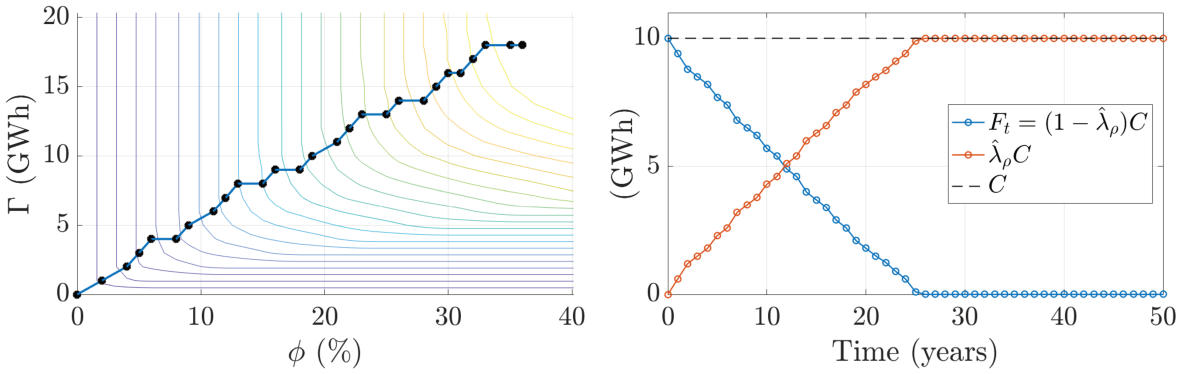

Figure 12: Optimal energy storage policy (left) and resulting peak load dynamics (right) for LCOS = 600\$/MWh.

In this case, we suppose that the economy starts with no storage capacities, that is $\Gamma_0 = 0$ and $\phi_0 = 0$. Hence, at time $t = 0$, the initial energy mix is $\hat{\lambda}_\rho(\phi_0, \Gamma_0) = 0$, and only back up CCGT supplies energy during peak demand *i.e.* $F_0 = C = 10$ GWh. Moreover, as the use of CCGT during peak load carries a costs $\nu = 100$ \$/MWh, then it is profitable to invest in storage through both capacity and efficiency in order to reduce the use of natural gas during peak hours. The full decarbonation of peak load through energy storage investments is reached in this scenario at time $T^\star = 26$

[8]For a sensitivity analysis of optimal energy storage policy and peak load decarbonation pathways with respect to relative investments costs in capacity and efficiency see Section 4.3.2.

years, that is for a cost of storage LCOS = 600\$/MWh. The final energy storage technology reached at the end of the optimal investments policy solution to the peak load decarbonation problem has a capacity of $\Gamma_{T^\star} = 18$ GWh and an efficiency of $\phi_{T^\star} = 36\%$. Note that the final capacity exceeds by 8 GWh the intensity of peak load C = 10GWh in order to respect risk tolerance of energy shortage. Similarly, we provide with the different peak load decarbonation times $T^\star$ for the two remaining LCOS scenario: $\text{LCOS}_{low} = 200$\$/MWh and $\text{LCOS}_{high} = 1000$\$/MWh. Results are gathered in Table 2.

ν (\$/MWh)	LCOS (\$/MWh)	$\alpha_\phi = \alpha_\Gamma$	$T^\star$ (years)
100	1000	$1.5 \cdot 10^4$	37
100	600	$1 \cdot 10^4$	26
100	200	$0.4 \cdot 10^4$	11

Table 2: Peak load decarbonation times for LCOS scenarios and fixed CCGT costs.

At constant CCGT costs $\nu = 100$ \$/MWh, an increase in LCOS leads to a decrease in transition time $T^\star$. For $\text{LCOS}_{low} = 200$\$/MWh, peak load decarbonation is reached in 11 years, whereas for the high LCOS scenario, that is $\text{LCOS}_{high} = 1000$\$/MWh, transition time reaches 37 years. Hence, the costs of energy storage has an important impact on transition time. In average a reduction in 31 \$/MWh in LCOS accelerates full peak load decarbonation by one year, making LCOS a central metric for peak load decarbonation planning when using of renewable energy storage.

CCGT carbon emissions costs. Providing with full peak load decarbonation times at constant CCGT costs prevents us from analyzing the effect of carbon costs on peak load decarbonation dynamics and its impact on energy storage investments policies. Indeed, the cost of carbon is internalized in the LCOE of CCGT and in 2018, the Portuguese Renewable Energy Association (APREN) estimated that the use of renewable energy during March 2018 saved 20 millions tCO2, resulting in saving of 1.8 millions euros for Portugal, leading therefore to a carbon price of carbon of 11\$/tCO_2 (consistent with the carbon prices from the EU ETS from March 2018).

In the following, we analyse the effect of carbon emissions costs due to the use of CCGT during peak load by considering an additional cost τ on the ton of carbon. Hence, considering a typical value for carbon emissivity of 0.4 tCO_2/MWh for CCGT, the costs of fossil fuel ν in the peak load decarbonation problem now writes as $\nu + 0.4 \cdot \tau$ with τ the cost of carbon expressed in \$/tCO_2. Hence, if $\tau = 0$, the cost of CCGT

during peak load is 100\$/MWh as previously, and as τ increases, the costs of using CCGT increases linearly at a rate equal to CCGT's carbon emissivity, 0.4 tCO_2/MWh. We provide with the evolution of peak load decarbonation time horizons $T^\star$ with respect to the carbon cost τ, for the three previous LCOS scenarios. Results are given for a range of carbon costs from 0\$/tCO_2 to 300\$/tCO_2 and gathered in Figure 13. For each LCOS scenario, as the cost of carbon emissions increases, the time for reaching full peak load decarbonation decreases. Note that peak load decarbonation time horizons are all the more sensitive to carbon costs for high LCOS. Indeed, the time horizons difference between the case with $\tau = 0$\$/tCO_2 and $\tau = 300$\$/tCO_2 for LCOS = 1000 \$/MWh is 13 years, for LCOS = 600 \$/MWh is 11 years and LCOS = 200 \$/MWh is 5 years. In average, an increase of 37\$ in the price of carbon emissions leads to a decrease of 1 year in peak load transition time, when a decrease in 31\$/MWh in LCOS leads to the same results.

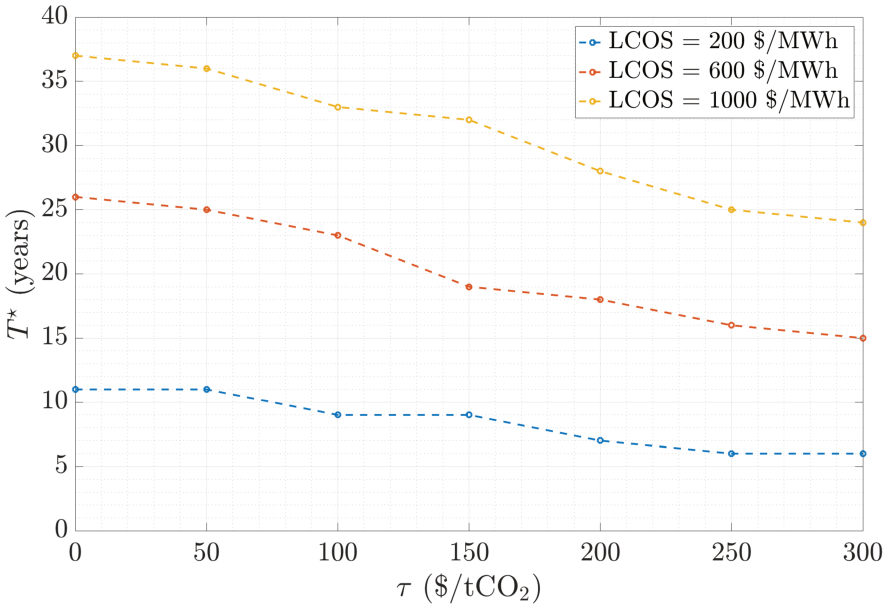

Figure 13: Peak decarbonation time horizons versus CCGT carbon emissions prices.

Hence, with important increases (resp. decreases) in the price of carbon (resp. LCOS), the policy maker can accelerate full peak load decarbonation in order to respect political objectives, such as reaching a carbon neutral electricity production by 2050 as set by the Carbon Neutrality Roadmap for Portugal (RNC2050). Note that in the case of high LCOS = 1000 \$/MWh, such objective can be reached only by increasing drastically the price of carbon emissions due to the use of CCGT during peak load, that is for $\tau > 200$ \$/tCO_2. Yet, for the mean and low projections in LCOS, full

peak load decarbonation can be reached within reasonable time horizons and CCGT carbon emissions prices.

Renewable energy surplus distribution. In the previous sections, optimal storage policies and the resulting peak load decarbonation dynamics were analyzed for a benchmark renewable energy surplus distributions $(\omega_i)_{i\in\mathbb{N}^*}$ modelled by the Weibull distribution $\mathcal{W}(32,7)$ with mean $\mathbb{E}(\omega) = 30$ GWh and variance is $\mathbb{V}(\omega) = 25$ GWh. As the energy surplus distribution is the difference between renewable energy production and energy consumption, such surplus can vary according to both renewable energy investments (leading to an increase in renewable energy production) and energy efficiency investments (leading to a decrease in energy consumption). Note that such energy surplus distribution also depends on the exogenous weather distribution providing with the natural ressources for renewable energy production (intermittent solar radiation and wind for instance), yet, not like RNE production or energy consumption, the policy maker cannot control such input.

In this section, we study the impact of such variability in the energy surplus distribution by analyzing the sensitivity of optimal peak load decarbonation pathways with respect to variations in the statistical characteristics of $(\omega_i)_{i\in\mathbb{N}^*}$. As we suppose the collection $(\omega_i)_{i\in\mathbb{N}^*}$ as independent and identically distributed (see Assumption 1), we shall henceforth consider a unique random variable ω for renewable energy surplus with the same distribution as $(\omega_i)_{i\in\mathbb{N}^*}$. Moreover, as in Campos (2018) we characterize statistical heterogeneity in the renewable energy surplus distribution by variations in its mean $\mathbb{E}(\omega)$ and variance $\mathbb{V}(\omega)$. We keep Weibull distributions as models for renewable energy surplus. Hence in the following, $\omega \sim \mathcal{W}(a,b)$ with $a > 0$, the shape parameter, and $b > 0$ the scale parameter of the distribution. Therefore, the probability distribution for renewable energy surplus is:

$$\forall \theta > 0 \; f_\omega(\theta) = \frac{a}{b}\left(\frac{\theta}{b}\right)^{a-1} e^{-(\theta/b)^a},$$

and probability theory provides with the mean and variance for the storable random renewable energy surplus ω that is:

$$\mathbb{E}(\omega) = b\Gamma\left(1+\frac{1}{a}\right) \quad \text{and} \quad \mathbb{V}(\omega) = b^2\Gamma\left(1+\frac{2}{a}\right) - \mathbb{E}(\omega)^2,$$

where Γ is the Gamma function. In the following, we shall keep as a benchmark

the energy surplus distribution $\mathcal{W}(32, 7)$ of mean $\mathbb{E}(\omega) = 30$ GWh and variance $\mathbb{V}(\omega) = 25$ GWh, and analyse the impact of an increase in its mean value at contant variance, and reciprocally, on optimal storage policies. The different energy surplus distribution used in this section and the detailed results of the analysis are gathered in in Appendix M.

We first analyse the evolution of transition time $T^\star$ for different mean values from 30 GWh to 50 GWh at a contant variance 25 GWh, for different carbon prices τ, 0\$/tCO$_2$, 100\$/tCO$_2$ and 200\$/tCO$_2$, as well as for the three LCOS projections from the previous analysis. Results are gathered in Figure 14. In both cases, that is, at constant LCOS or constant carbon price τ, the decarbonation time follows the same monotony : as the mean value $\mathbb{E}(\omega)$ of the energy surplus distribution increases, the transition time $T^\star$ decreases. Indeed, for high mean values (and constant variance), the probability of important energy surplus availability increases. Therefore, the need for highly efficient storage capacities is not necessary as the economy already benefits from important energy surplus availability, thereby accelerating peak load decarbonation. Note that for any mean values, the impacts of both carbon cost and LCOS remain the same as an increase (resp. decrease) in τ (resp. LCOS) reduces time $T^\star$ for reaching full peak load decarbonation. Finally, in average, an increase of 2 GWh in renewable energy surplus mean leads to a decrease in transition time $T^\star$ by one year, making therefore investments in both renewable energy production or energy efficiency valuable for peak load decarbonation objectives.

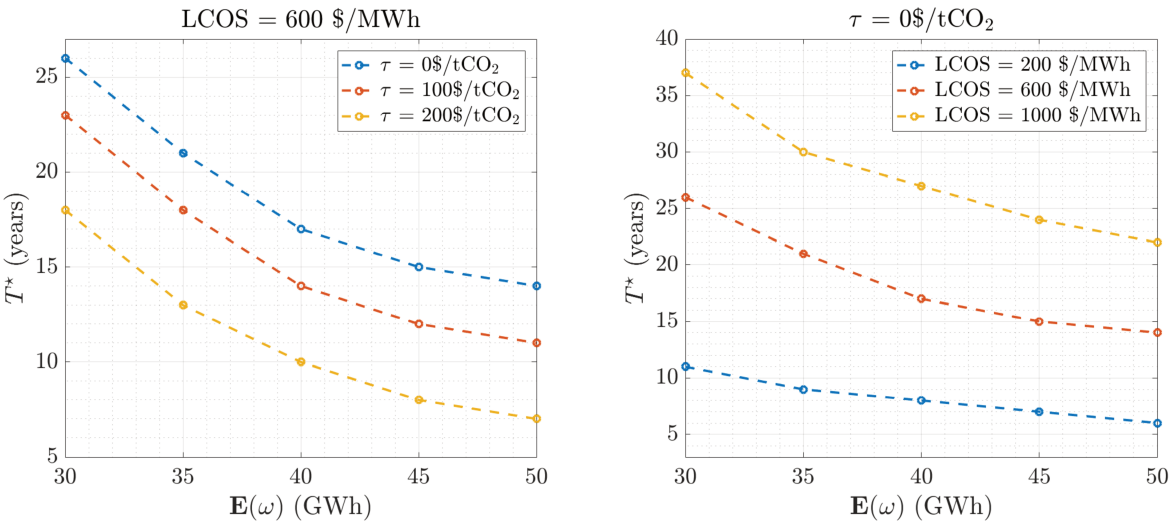

Figure 14: Transition time $T^\star$ versus the energy surplus mean at fixed variance (25 GWh) for different carbon price and LCOS scenarios.

Similarly, we study the evolution of transition time $T^\star$ for different variance of the energy surplus distribution, from 15 GWh to 35 GWh, at contant mean 30 GWh, with the same carbon prices τ and LCOS projections as from the analysis with respect to the distribution's mean. Results are gathered in Figure 15 and show that the effect of variance on transition time is less significant than variations in the energy surplus mean. As the variance of the energy surplus distribution increases, the transition time increases in a smoother way. Indeed, higher variance increases both the probability for low and high energy surplus availably. On the one hand, the effect of having higher energy surplus tends to decrease transition time, similarly to an increase in the energy surplus mean value. Yet, on the other hand, this effect is smoothed away by the increase, as well, in low energy surplus availability, in the case of wider energy surplus distribution. These two competing effects results in a smoother variation in transition time when increasing variance at fixed mean than when increasing mean value at fixed variance. Note that, the resulting smooth increase in transition time comes from the fact that Weibull distributions are not symmetric around there mean values. Here, an increase in variance gives a slight advantage to low renewable energy surplus, leading therefore to a subtle resulting increase in peak load decarbonation time $T^\star$. Hence, the time horizon for peak load decarbonation shows less sensitivity to the energy surplus dispersions than it does regarding the energy surplus mean value, making therefore the energy surplus mean value a more practical statistic for transition time horizon planning, compared to its dispersion.

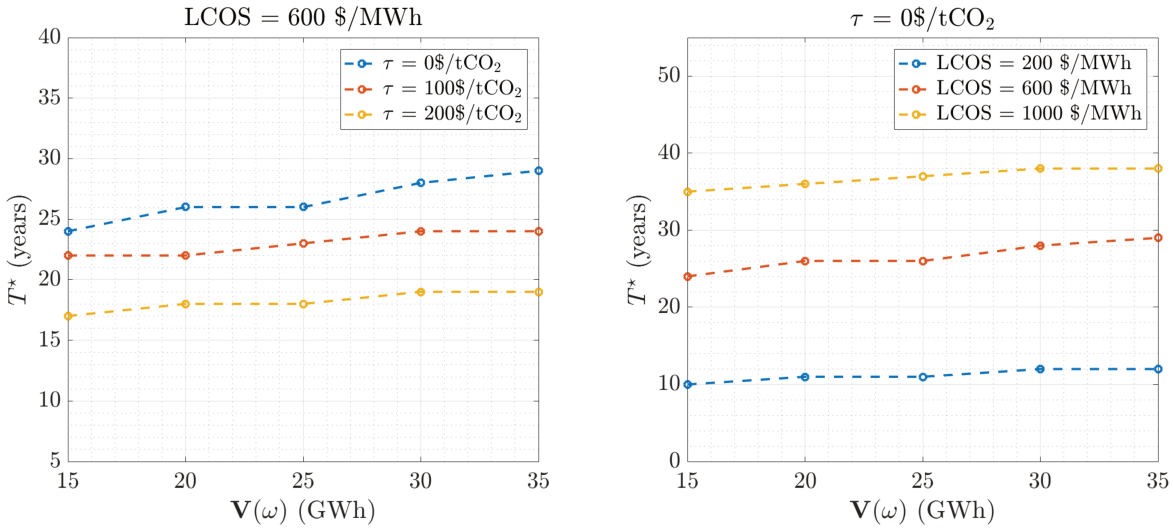

Figure 15: Transition time $T^\star$ versus the energy surplus variance at fixed mean (30 GWh) for different carbon price and LCOS scenarios.

Finally, let us introduce the investment ratio coefficient in efficiency and capacity which quantifies the relative overall expenses in efficiency and capacity investments during peak load decarbonation, defined as:

$$\xi = \frac{\sum_{t=0}^{T^\star} \alpha_\Gamma (\Gamma_{t+1} - \Gamma_t)^2}{\sum_{t=0}^{T^\star} \alpha_\phi (\phi_{t+1} - \phi_t)^2},$$

where $\sum_{t=0}^{T^\star} \alpha_\Gamma (\Gamma_{t+1} - \Gamma_t)^2$ describes the overall expenses in capacity investments during peak load decarbonation, and $\sum_{t=0}^{T^\star} \alpha_\phi (\phi_{t+1} - \phi_t)^2$ the overall expenses in efficiency investments. In Figure 16 (top) are gathered the evolution of ξ with respect to the mean value of the energy surplus distribution at fixed variance and in Figure 16 (bottom) with respect to the energy surplus variance at fixed mean.

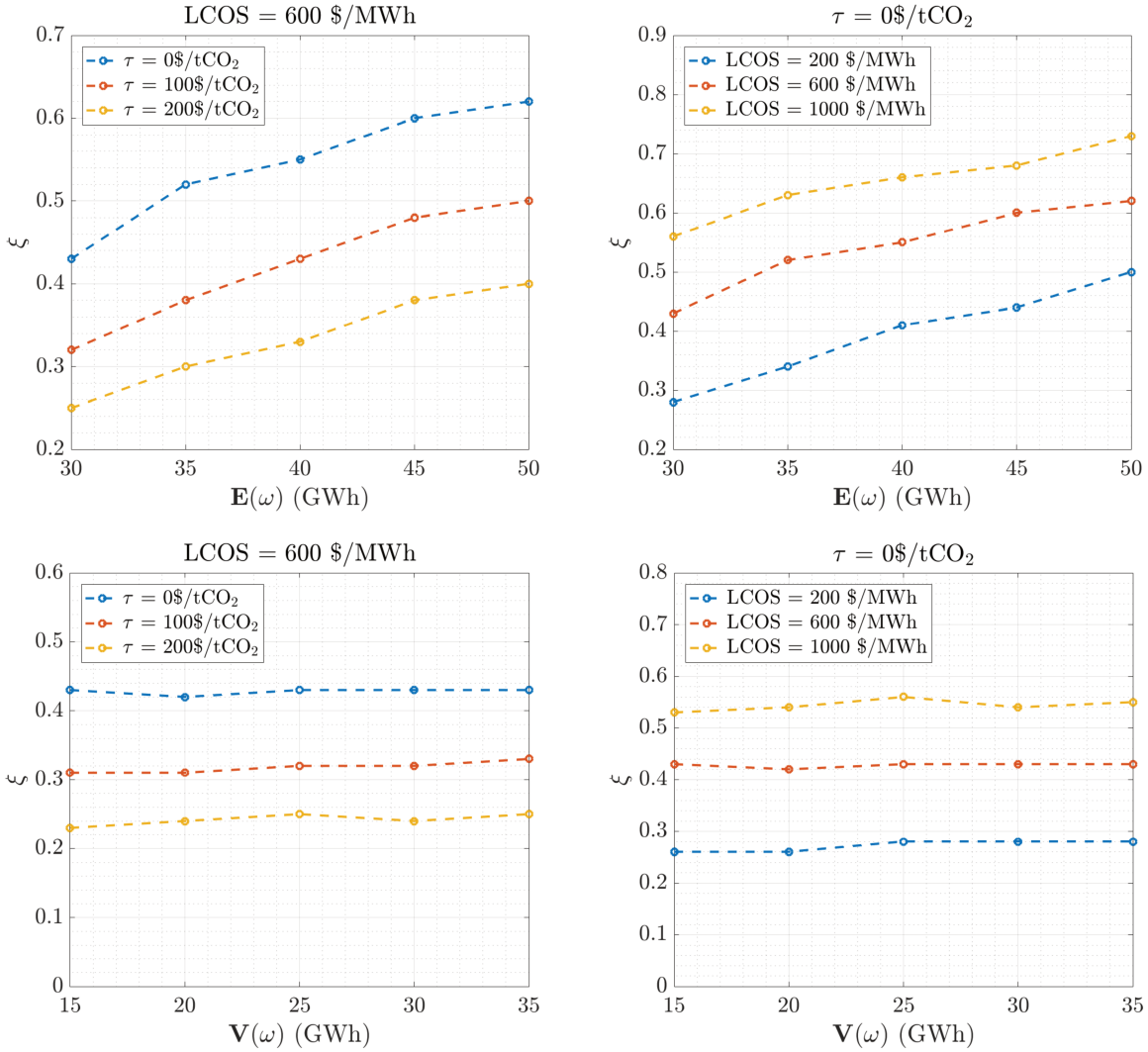

Figure 16: Investment ratio coefficient ξ versus the energy surplus mean at fixed variance 25 GWh (top) and versus the energy surplus variance at fixed mean 30 GWh (bottom).

As the mean value increases, the investment ratio coefficient gets higher, meaning that the relative overall expenses increases in favor of storage capacity Γ compared to investments in storage efficiency ϕ. Indeed, for high mean values, the probability of important energy surplus availability ω increases. For an increase of $\Delta\omega > 0$ in energy surplus availability, the efficiency term in Definition 1 of the storage process writes as $\phi(\omega + \Delta\omega) = \phi(1 + \frac{\Delta\omega}{\omega})\omega = \phi'\omega$ with $\phi' = \phi(1 + \frac{\Delta\omega}{\omega}) > \phi$. Therefore, an increase in energy availability acts as an increase in efficiency in the cost minimization problem of peak load decarbonation. Hence, investments in capacity are privileged as storage already benefits from an increase in energy surplus availability for high mean values, which has the same effect as an increase in efficiency. However, an increase in energy surplus variance does not lead to any significant variation in ξ for the same reason that an increase in variance shows very low effect on transition time $T^\star$ compared to variation in the energy surplus mean (see Figure 14 and Figure 15). Indeed, an increase in the spread of the renewable energy surplus distribution leads to both higher probabilities for having low and high renewable energy surplus, therefore resulting to two competing effects canceling one another. Finally, note that the relative investments in efficiency and capacity also depends on the LCOS and the cost of carbon emissions. As the relative cost of storage increases compared to using fossil fuels during peak load (that is, either through an increase in LCOS or a decrease in the cost of carbon) then the optimal energy storage policy promotes capacity investments (reflected here by the increase in ξ). Indeed, in either cases, the policy maker sacrifices investments in efficiency to promote investments in capacity as it offers here, a more important marginal impact on peak load decarbonation compared to technical progress in efficiency ($\bar{\Gamma} < \bar{\phi}$). Hence, the more costly are storage investments compared to using fossil fuels during peak load, the more investments shall be allocated to the technical attribute of highest marginal impact on peak load decarbonation. In conclusion, among the parameters accessible to the policy maker for peak load decarbonation planning, only the variance of the energy surplus does not have any significant impact on either peak load decarbonation time horizon $T^\star$ or on investment ratio ξ. Therefore, policy recommendations for peak load decarbonation using intermittent renewable energy storage should focus particularly on the mean value of the renewable energy surplus (by considering investments policies in either renewable energy production or energy efficiency for instance), as well as setting the right price on CCGT carbon emissions according to the Levelized Cost of Storage, the renewable energy surplus, and the political framework setting time horizons for reaching the carbon-free era.

5 Conclusion

This research proposes an approach to analyse the final stage of the energy shift, in which back-up fossil fuels used during peak load, shall be progressively substituted by stored intermittent renewable energy. We model technical progress regarding energy storage by considering both progress in storage efficiency and capacity. Thus the economy can choose to invest in either efficiency or in capacity in order to improve storage technology before reaching full peak load decarbonation.

Intermittent renewable energy storage is modelled in a Markovian framework which allows us to control the risk of energy shortage involved in the decarbonation of back-up fossil fuels by stored intermittent renewable energy. Therefore this chapter proposes a new framework of energy shift dynamic modelling, as, to our knowledge, progress in storage technology has not been yet modeled considering technical progress in both efficiency and capacity, in a dynamic and stochastic framework. This research opens new perspectives regarding decarbonation pathways involved during energy shift, and can be used to optimally plan the decarbonation of back-up fossil fuels by stored intermittent renewable energy while considering technical progress on storage technologies and the risk of energy shortage due to renewable energy intermittency.

By applying our model to Portugal, we provide with the optimal storage policies and decarbonation time horizons with respect to Levelized Costs of Storage (LCOS), carbon prices, and the stochastic availability of renewable energy surplus scenarios. We show that the costs of energy storage and carbon prices have important impacts on transition time, and in average a reduction in 31$/MWh in LCOS accelerates full peak load decarbonation by one year while an increase of 37$ in the price of carbon leads to the same results. Moreover, we study how the variations in the mean or variance of renewable energy availability affect the optimal storage policies and peak load decarbonation time horizons. In average, an increase of 2GWh in renewable energy surplus mean leads to a decrease of decarbonation time horizon by one year, while investments in storage technology are more allocated to capacity rather than to efficiency. Yet, time horizon for peak load decarbonation and storage policies show less sensitivity to variations in the energy surplus dispersion, making therefore the energy surplus mean value a more practical statistic for peak load decarbonation planning, compared to its dispersion.

References

[1] Alley, B. R., Kerry, A. E. and Zhang, F. (2019), "Advances in weather prediction", *Science*, 363 (6425), 342-344.

[2] APREN (2018), *Boletim Energias Renovaveis Edicao Mensal 1.*

[3] Ambec, S. and Crampes, C. (2012), "Electricity provision with intermittent sources of energy", *Resource and Energy Economics*, 34, 319-336.

[4] Ambec, S. and Crampes, C. (2017), "Decarbonizing electricity generation with intermittent sources of energy", *TSE Working Paper*, 15, 603.

[5] Baker, E., Fowlie, M., Lemoine D. et Reynolds S. S. (2013), "The economics of solar electricity", *Annual Review of Resources Economics*, 5, 387-426.

[6] Barbose, G., Darghouth, N., Weaver, S., and Wiser, R. (2013), "Tracking the Sun VI: An historical summary of the installed price of photovoltaics in the United States from 1998 to 2012", *Technical report, Ernest Orlando Lawrence Berkeley National Laboratory.*

[7] Boccard, N. (2010), "Economic properties of wind power: A European assessment", *Energy Policy*, 38(7), 3232-3244.

[8] Campos R.M. and Guedes Soares C. (2018), "Spatial distribution of offshore wind statistics on the coast of Portugal using Regional Frequency Analysis", *Renewable Energy*, 123, 806-816.

[9] Crampes, C. and Moreaux, M. (2009), "Pumped storage and cost saving", *Energy Economics*, 32, 325-333.

[10] Cust, J., Keats, K. and Neuhoff, K. (2007), "Implications of Intermittency and Transmission Constraints for Renewables Deployment", *University of Cambridge, February, CWPE 0711 and EPRG 0702.*

[11] Davis, M. H. A. (1984), "Piecewise-Deterministic Markov Processes: A General Class of Non-Diffusion Stochastic Models", *Journal of the Royal Statistical Society. Series B (Methodological)*, 46(3), 353-388.

[12] Durmaz, T. (2014), "Energy Storage and Renewable Energy", *NHH Discussion paper.*

[13] Durmaz, T. (2018), "The economics of CCS: Why have CCS technologies not had an international breakthrough?", *Renewable and Sustainable Energy Reviews*, 95, 328-340.

[14] Gravelle, H. S. E. (1976), "The Peak Load Problem with Feasible Storage", *The Economic Journal*, 86(342), 256-277.

[15] Greiner, A., Gruene, L. and Semmler, W. (2013), "Economic Growth and the Transition from Non-renewable to Renewable Energy", *Environment and Development Economics*, 19(4), 417-439.

[16] Heal, G. (2016), "Notes on the economics of energy storage", *NBER Working Paper.*

[17] Helm, C. and Mier, M. (2018), "Subsidising Renewables but Taxing Storage? Second-Best Policies with Imperfect Carbon Pricing", *Oldenburg Discussion Papers in Economics.*

[18] Hoel, M. and Kverndokk, S. (1996), "Depletion of fossil fuels and the impacts of global warming" *Resource and Energy Economics*, 18, 115-136.

[19] IEA (2015), *Projected Costs of Generating Electricity.*

[20] IEA (2018), *World Energy Outlook.*

[21] Jackson, R. (1973), "Peak Load Pricing Model of an Electric Utility Using Pumped Storage", *Water Resources Research*, 9(3), 556-562.

[22] Joskow, L. P. (2011), "Comparing the Costs of Intermittent and Dispatchable Electricity Generating Technology', *The American Economic Review*,101(3), 238-241.

[23] Kennedy, S. (2005), "Wind power planning: assessing long-term costs and benefits", *Energy Policy*, 33, 1661-1675.

[24] Koopmans, T. C. (1957), "Water storage policy in a simplified hydroelectric system", *Proceedings of the First international conference on operational research*, 193-227.

[25] Little, J. D. C. (1955), "The use of storage water in a hydroelectric system", *Journal of the Operations Research Society of America*, 3, 187-197.

[26] Pommeret, A. and Schubert, K. (2019), "Energy Transition with Variable and Intermittent Renewable Electricity Generation", *CESifo Working Paper.*

[27] Schmidt, O., Melchior, S., Hawkes, A. and Staffel, I. (2019), "Projecting the Future Levelized Cost of Electricity Storage Technologies", *Joule*, 3(1), 81-100.

[28] Sinn, H. W. (2017), "Buffering volatility: a study on the limits of Germany's energy revolution", *European Economic Review*, 99, 130-150.

[29] Steffen, B. and Webber, C. (2012), "Efficient storage capacity in power systems with thermal and renewable generation", *Energy Economics*, 36, 556-567.

[30] Steffen, B. and Weber, C. (2016), "Optimal operation of pumped-hydro storage plants with continuous time-varying power prices", *European Journal of Operational Research*, 252, 308-321.

[31] Tahvonen, O. (1998), "Fossil fuels, stock externalities, and backstop technology", *The Canadian Journal of Economics*, 30(4), 855-874.

[32] Tahvonen, O. and Salo, S. (1999), "Economic growth and transitions between renewable and nonrenewable energy resources", *European Economic Review*; 45, 1379-1398.

[33] Wais, P. (2017), "A review of Weibull functions in wind sector", *Renewable and Sustainable Energy Reviews*, 70, 1099-1107.

Appendices

A. Numerical illustrations for $\sigma_\rho(\phi, \Gamma, \lambda)$.

Having defined and characterized $\sigma_\rho(\phi, \Gamma, \lambda)$ in Proposition 3, the question remains on how to decide on the optimal energy mix split between stored renewable energy and back-up fossil fuels during peak demand, in order to minimize the use of fossil fuels while controlling the risk of energy shortage. In order to build readers' intuition we plot the evolution of $\sigma_\rho(\phi, \Gamma, \lambda)$ and demand λC on stored renewable energy with respect to λ for different levels of efficiency and capacity (ϕ, Γ) in Figure 17.

In this example, $\sigma_\rho(\phi, \Gamma, \lambda)$ decreases with respect to λ. Moreover there is a value $\hat{\lambda}$ such that $\lambda > \hat{\lambda} \implies \lambda C > \sigma_\rho(\lambda)$. This means that for such energy mix $\lambda > \hat{\lambda}$ (lower right of Figure 17) the choice of λ is not optimal as the demand on storage is greater than σ_ρ, therefore leading to energy shortage with a probability above risk tolerance ρ (Proposition 3). Moreover, $\lambda < \hat{\lambda} \implies \lambda C < \sigma_\rho(\lambda)$ (upper left of Figure 17). Thus, energy mix $\lambda < \hat{\lambda}$ are such that the probability of energy shortage is bellow risk tolerance ρ. We define such mix in the following as the ρ-admissible energy mix, that is, mix respecting risk tolerance for energy shortage. Yet these ρ-admissible energy mix does not necessarily minimize the use of fossil fuels $F = (1 - \lambda)C$. In order to formalize this intuition, we shall define more generally the following set.

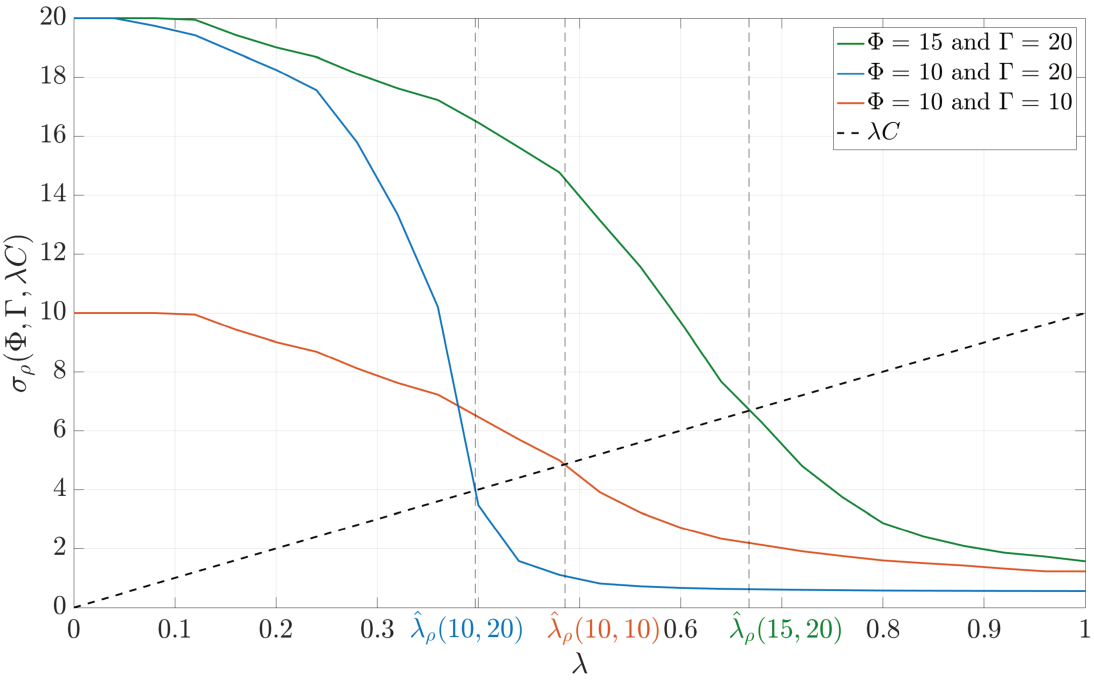

Figure 17: Numerical examples for $\rho = 0.04$, C = 10 GWh and $(\omega_i)_{i \in \mathbb{N}^*} \sim \mathcal{W}(2, 1)$.

B. Optimal dynamics in the linear region.

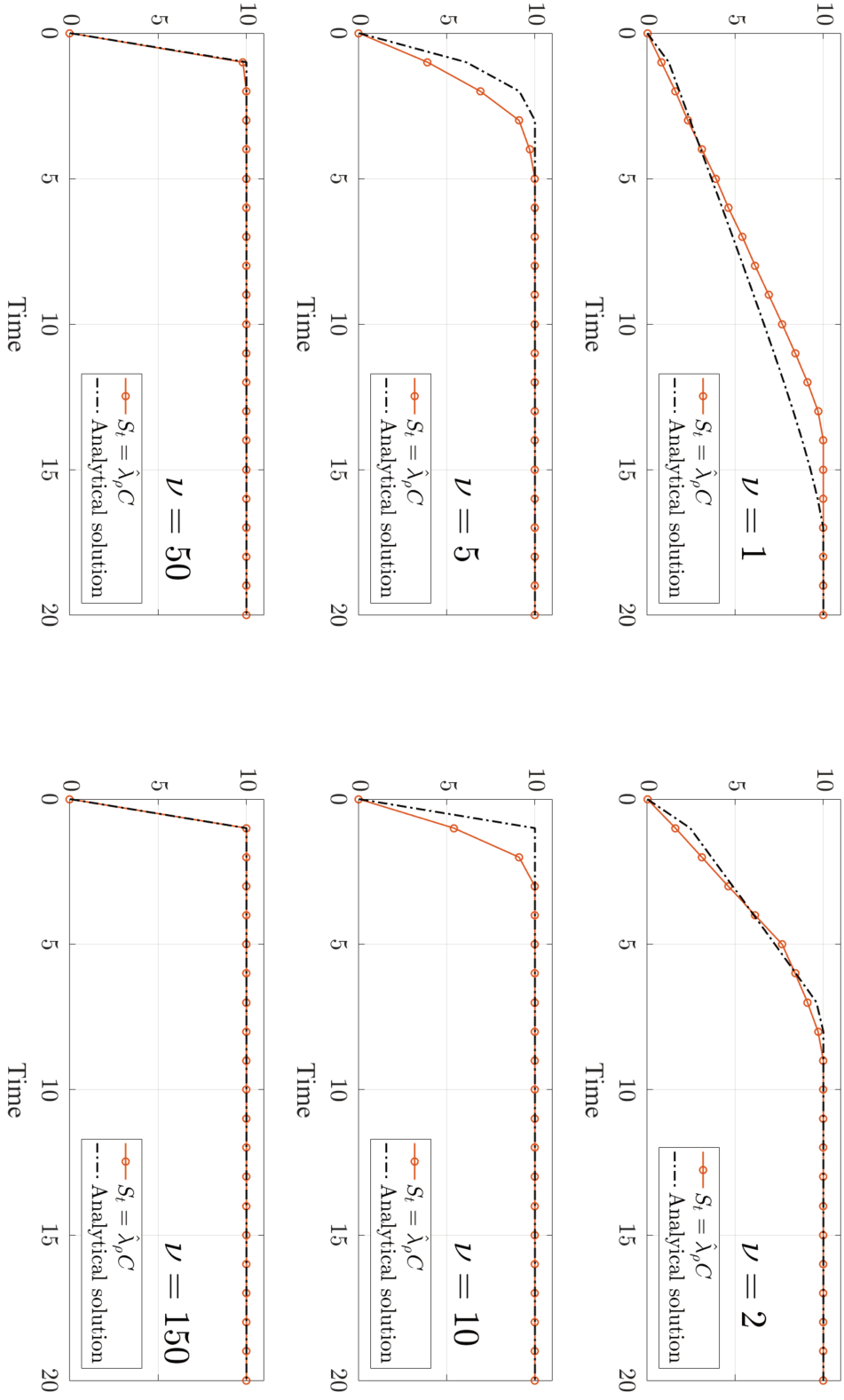

Figure 18: $(\omega_i)_{i\in\mathbb{N}^*} \sim \mathcal{W}(2,1)$, $(\phi_0, \Gamma_0) = (0, 40)$ and $\delta_\alpha = 1$.

C. Optimal dynamics in the concave region.

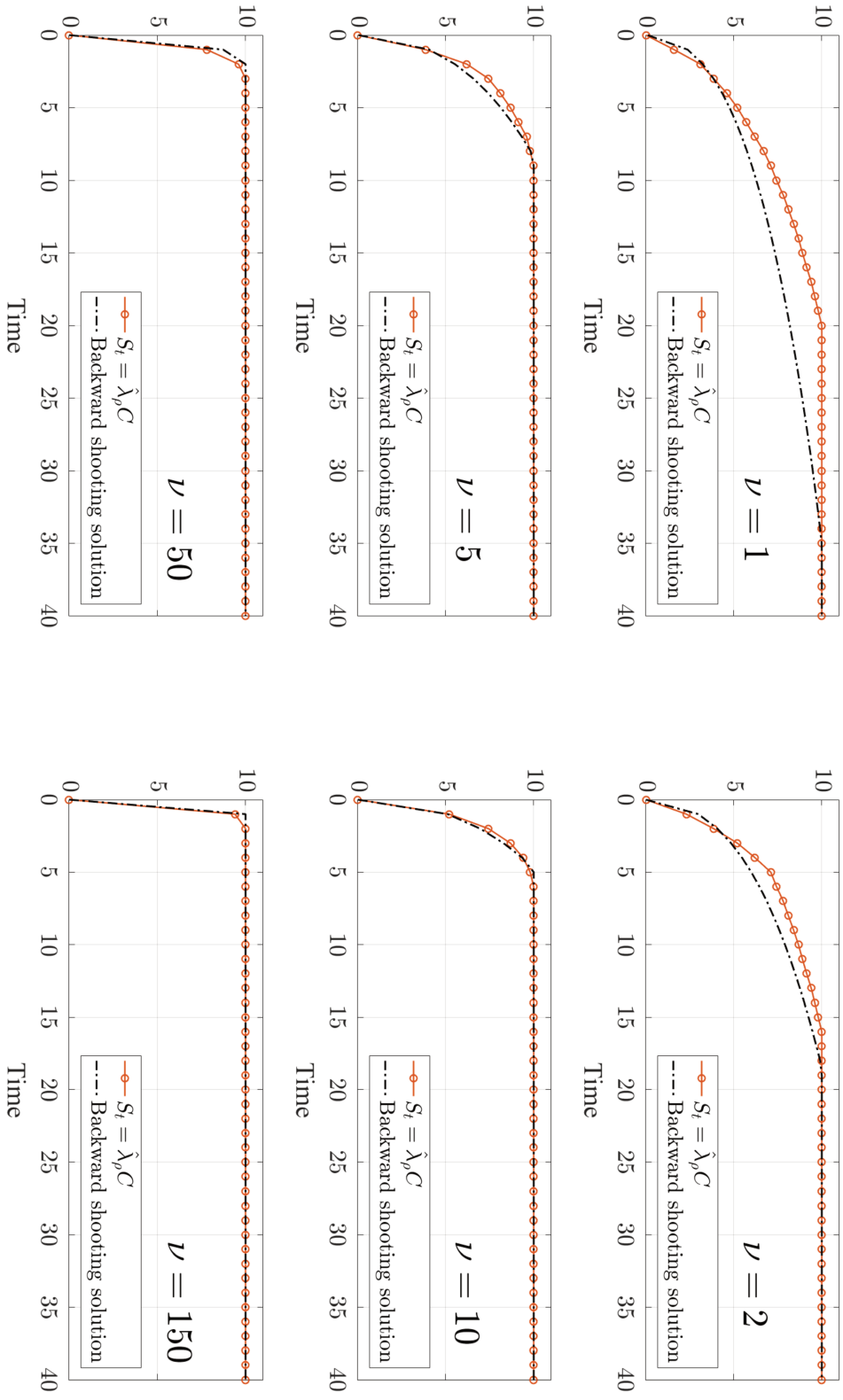

Figure 19: $(\omega_i)_{i\in\mathbb{N}^*} \sim \mathcal{W}(2,1)$, $(\phi_0, \Gamma_0) = (0, 20)$ and $\delta_\alpha = 20$.

D. Pseudo-codes.

D.1. Pseudo-code for the bisection method algorithm. Be $MAXITER$ the maximum iteration allowed and TOL the tolerance parameter for convergence.

Algorithm 1 Solves $\sigma^\rho(\phi, \Gamma, \hat{d}) - \hat{d} = 0$ for $\hat{d}$

```
I ← 1
a ← 0
b ← C
while I ≤ MAXITER do
  d ← (a+b)/2
  if σ^ρ(φ, Γ, d) − d = 0 or (b−a)/2 < TOL then
    d̂ ← d
    break
  end if
  I ← I + 1
  if sign(σ^ρ(φ, Γ, d) − d) = sign(σ^ρ(φ, Γ, a) − a) then
    a ← d
  else
    b ← d
  end if
end while
```

D.2. Pseudo-code of the backward shooting method algorithm. Be ϵ the search precision.

Algorithm 2 Solves $\phi_t = \phi_{t+1} - \frac{\beta}{2\alpha}\left[\frac{C\nu\eta\gamma}{\phi_{t+1}^{1-\gamma}} + 2\alpha(\phi_{t+2} - \phi_{t+1})\right]$

```
I ← 0
for I ← 0 : ε : MAXITER do
  S[N − 1] ← I
  for J ← N − 2 to 1 do
    S[J] ← S[J + 1] − (β/2α)[Cνηγ / S[J+1]^{1−γ} + 2α(S[J + 2] − S[J + 1])]
  end for
  if S[1] = φ_0 or |S[1] − φ_0| < TOL then
    break
  end if
end for
```

E. Proof of Proposition 1.

In order to derive the expression of the transition matrix Π, we must consider two cases: the case in which initial state is in *consumption trap*, and the case in which it is not.

- If an initial state of charge SOC_i is in the *consumption trap*, then after peak demand the current SOC_i switches to the empty SOC_1. Therefore, the probability of reaching state SOC_j from state SOC_i is the probability of reaching SOC_j from state SOC_1 that is, the probability of storing an amount $(j-1)\delta$ of energy which, according to Definition 2, is $p^\phi(j-1)$. Similarly, reaching the saturated state SOC_N from an initial state SOC_i in the *consumption trap* is given by summing the probability of storing more than $\Gamma = (N-1)\delta$, that is $\sum_{j=N}^{\infty} p^\phi(j-1)$. Therefore, the transition probabilities for an initial state SOC_i in the *consumption trap* is given by:

$$\forall i \in [1, \lceil d/\delta \rceil + 1] \begin{cases} \Pi_{i,j} = p^\phi(j-1) \ \forall j \in [1, N-1], \\ \\ \Pi_{i,N} = \sum_{j=N}^{\infty} p^\phi(j-1). \end{cases}$$

- If an initial state of charge SOC_i is not in the *consumption trap*, then after peak demand, the current SOC_i switches to $SOC_{i-\lceil d/\delta \rceil}$. Therefore, the probability of reaching state SOC_j from state SOC_i is the probability of reaching SOC_j from state $SOC_{i-\lceil d/\delta \rceil}$ that is, the probability of storing an amount $[j-(i-\lceil d/\delta \rceil)]\delta$ of energy which, according to Definition 2, is $p^\phi(j-(i-\lceil d/\delta \rceil))$. Similarly, reaching the saturated state SOC_N from an initial state SOC_i which is not in the *consumption trap* is given by summing the probability of storing more than $[N-(i-\lceil d/\delta \rceil)]\delta$, that is $\sum_{j=N}^{\infty} p^\phi(j-(i-\lceil d/\delta \rceil))$. Therefore, the transition probabilities for an initial state SOC_i not in the *consumption trap* is given by:

$$\forall i \in [\lceil d/\delta \rceil + 2, N] \begin{cases} \Pi_{i,j} = p^\phi(j-(i-\lceil d/\delta \rceil)) \ \forall j \in [i-\lceil d/\delta \rceil, N-1], \\ \\ \Pi_{i,N} = \sum_{j=N}^{\infty} p^\phi(j-(i-\lceil d/\delta \rceil)). \end{cases}$$

- Else, the SOC are not accessible one to another, therefore $\Pi_{i,j} = 0$.

F. Proof of Proposition 2.

(i) Consider the directed graph G associated to the transition matrix Π of the Markov chain. The Markov chain is irreducible if and only if G has one strongly connected component. From the definition of the transition matrix Π, all nodes $i > 1$ can directly reach node

$i-1$. Moreover, node 1 can transition to any node. Therefore, by induction, every state can be reached from any other states *i.e.* G has one strongly connected component, thus Π is irreducible.

(ii) We get from the definition of Π in equation (8) and (9) that every node has a self-loop since $\forall i \in [1, N]$ $\Pi_{i,i} > 0$. Therefore the period of each state is equal to 1 which means they are aperiodic. By definition, as all states of the Markov chain is aperiodic, the Markov chain is itself aperiodic.

(iii) From (i) and (ii) we know that Π is irreducible and aperiodic. It follows from the fundamental theorem of Markov chains stating that Π has a unique stationary distribution that we denote $\bar{\mu}$, such that $\bar{\mu} = \lim_{t\to\infty} \Pi^t \mu_0$ for any initial SOC distribution μ_0.

G. Proof of Proposition 3.

(i) As $0 \in \mathcal{A}$ therefore $\mathcal{A} \neq \emptyset$ and as A is bounded above by Γ it admits a supremum that we denote as σ_ρ.

(ii) Let $\eta > 0$ then as $\sigma_\rho = \sup \mathcal{A}_\rho$ we have that $\sigma_\rho + \eta \notin \mathcal{A}_\rho$. Thus, by definition of $\mathcal{A}_\rho$ from Definition 4 we have $P(X \leq \sigma_\rho + \eta) > \rho$, which completes the proof.

H. Proof of Proposition 4.

(i) Be X the random variable of stored renewable energy and λ a ρ-admissible energy mix. Therefore as $\lambda \in \mathcal{D}_\rho$ then from Definition 5, $\lambda C \leq \sigma_\rho$ thus, $\exists \eta \geq 0$ such that $\lambda C = \sigma_\rho - \eta$. Thereby, as $\sigma_\rho = \sup(\mathcal{A}_\rho)$ then $\lambda C = \sigma_\rho - \eta \in \mathcal{A}_\rho$ and thus from the definition of $\mathcal{A}_\rho$ in Definition 4, we get $P(X \leq \lambda C) \leq \rho$. As a result, the risk of energy shortage with a ρ-admissible energy mix is bellow risk tolerance, which proves the claim.

(ii) The energy mix during peak load with no stored renewable energy, that is $\lambda = 0$, is a ρ-admissible mix as the probability of having energy shortage is equal to 0 (back-up fossil fuels can always produce energy). Therefore $0 \in \mathcal{D}_\rho$ and thus $\mathcal{D}_\rho \neq \emptyset$. Moreover, $\mathcal{D}_\rho$ is bounded from above by 1 and as it is non empty it has a supremum $\hat{\lambda}_\rho = \sup(\mathcal{D}_\rho)$. Finally, as the use of fossil fuels writes as $F = (1-\lambda)C$, then the use of fossil fuels strictly decreases with respect to the mix λ. Therefore $\hat{\lambda}_\rho$ minimizes F on $\mathcal{D}_\rho$. As a result, the energy mix $\hat{\lambda}_\rho = \sup(\mathcal{D}_\rho)$ respects risk tolerance and minimizes the use of fossil fuels during peak load. Hence, $\hat{\lambda}_\rho$ is the *optimal* energy mix in the sense of Definition 5.

I. Proof of Proposition 5.

Writing the Lagrangian of Problem (2) leads to:

$$\begin{aligned}\mathcal{L} = &\sum_{t=0}^{T-1} -\beta^t \left[\tau(C - \lambda(\phi_t)) + \kappa(i_t)\right] + \sum_{t=0}^{T-1} \mu_{t+1}^{(1)}[\phi_t + i_t - \phi_{t+1}] \\ &+ \sum_{t=0}^{T-1} \mu_t^{(2)}[\lambda^{-1}(1) - \epsilon_t^2 - \phi_t] + \mu^{(3)}[a - \phi_0] + \mu^{(4)}[\lambda^{-1}(C) - \phi_T].\end{aligned}$$

Therefore, the F.O.C with respect to control i_t and state ϕ_t gives:

$$\forall\ 0 < t < T \begin{cases} \text{F.O.C w.r.t. } i_t : -\beta^t \kappa'(i_t) + \mu_{t+1}^{(1)} = 0, \\ \text{F.O.C w.r.t. } \phi_t : \beta^t \tau'[(1 - \lambda(\phi_t))C]C\lambda'(\phi_t) + \mu_{t+1}^{(1)} - \mu_t^{(1)} - \mu_t^{(2)} = 0, \\ \text{Stationary condition} : 2\epsilon_t \mu_t^{(2)} = 0. \end{cases}$$

If $\phi_t < \lambda^{-1}(1)$ then $\epsilon_t \neq 0$ therefore $\mu_t^{(2)} = 0$. As a result:

$$\beta^t \tau'[(1 - \lambda(\phi_t))C]C\lambda'(\phi_t) + \mu_{t+1}^{(1)} - \mu_t^{(1)} = 0.$$

Moreover, as $-\beta^t \kappa'(i_t) + \mu_{t+1}^{(1)} = 0$, we get:

$$\beta^t \tau'[(1 - \lambda(\phi_t))C]C\lambda'(\phi_t) + \beta^t \kappa'(i_t) - \mu_t^{(1)} = 0.$$

Rewriting the previous equation at time $t+1$ and with the transition equation $\phi_{t+1} = \phi_t + i_t$ leads to:

$$\beta^{t+1} \tau'[(1 - \lambda(\phi_{t+1}))C]C\lambda'(\phi_{t+1}) + \beta^{t+1} \kappa'(\phi_{t+2} - \phi_{t+1}) - \mu_{t+1}^{(1)} = 0.$$

And again, as $\mu_{t+1}^{(1)} = \beta^t \kappa'(i_t) = \kappa'(\phi_{t+1} - \phi_t)$ we get:

$$\beta^{t+1} \tau'[(1 - \lambda(\phi_{t+1}))C]C\lambda'(\phi_{t+1}) + \beta^{t+1} \kappa'(\phi_{t+2} - \phi_{t+1}) - \beta^t \kappa'(\phi_{t+1} - \phi_t) = 0.$$

As $\beta > 0$, we get after simplification:

$$\beta C \tau'[(1 - \lambda(\phi_{t+1}))C]\lambda'(\phi_{t+1}) + \beta \kappa'(\phi_{t+2} - \phi_{t+1}) - \kappa'(\phi_{t+1} - \phi_t) = 0.$$

Such dynamics are valid as long as $\phi_t < \lambda^{-1}(1)$. Else, $\phi_t = \lambda^{-1}(1)$.

As a result, $(\phi_t) = min(\phi_t^*, \lambda^{-1}(1))$ where (ϕ_t^*) is solution to:

$$\beta C \tau'[(1 - \lambda(\phi_{t+1}))C]\lambda'(\phi_{t+1}) - \kappa'(\phi_{t+1} - \phi_t) + \beta \kappa'(\phi_{t+2} - \phi_{t+1}) = 0,$$

which proves the claim.

J. Proof of Corollary 1.

From Proposition 5, the optimal dynamics in efficiency writes as:

$$\beta C\tau'[(1-\lambda(\phi_t))C]\lambda'(\phi_{t+1}) - \kappa'(\phi_{t+1}-\phi_t) + \beta\kappa'(\phi_{t+2}-\phi_{t+1}) = 0.$$

Moreover, from Assumption 3 we have $\tau(F) = \nu F$ and $\kappa(i) = \alpha i^2$. Therefore, under these assumptions in fossil fuels and investments costs, the dynamics of efficiency now writes:

$$\begin{aligned}
&\beta C\nu\lambda'(\phi_{t+1}) - 2\alpha(\phi_{t+1}-\phi_t) + \beta 2\alpha(\phi_{t+2}-\phi_{t+1}) = 0 \\
\iff &\phi_{t+2} - \phi_{t+1} - \frac{1}{\beta}\phi_{t+1} + \frac{1}{\beta}\phi_t = -\frac{C\nu}{2\alpha}\lambda'(\phi_{t+1}) \\
\iff &\phi_{t+2} - \frac{1+\beta}{\beta}\phi_{t+1} + \frac{1}{\beta}\phi_t = -\frac{C\nu}{2\alpha}\lambda'(\phi_{t+1}).
\end{aligned}$$

which proves the claim.

K. Proof of Corollary 2.

(i) In the *linear region*, energy mix is linear in efficiency, that is $\lambda(\phi) = \gamma\phi$. Moreover as from Corollary 1:

$$\phi_{t+2} - \frac{1+\beta}{\beta}\phi_{t+1} + \frac{1}{\beta}\phi_t = -\frac{C\nu}{2\alpha}\lambda'(\phi_{t+1}),$$

then, under the assumption of linear mix we have:

$$\phi_{t+2} - \frac{1+\beta}{\beta}\phi_{t+1} + \frac{1}{\beta}\phi_t = -\frac{C\nu\gamma}{2\alpha}.$$

which gives the dynamics of efficiency in the *linear region* of energy mix.

(ii) In the *linear region* of the energy mix and under Assumption 3, the dynamics of optimal efficiency for storage writes as a second order difference equation problem that is:

$$\begin{cases}
\phi_{t+2} - \frac{1+\beta}{\beta}\phi_{t+1} + \frac{1}{\beta}\phi_t = -\frac{C\nu\gamma}{2\alpha}, \\
\phi_0 \geq 0, \\
\phi_T = \frac{1}{\gamma}.
\end{cases}$$

Therefore, the characteristic equation of the homogenous second order difference equation writes:

$$X^2 - \frac{1+\beta}{\beta}X + \frac{1}{\beta} = 0,$$

for which the discriminants given by:

$$\Delta = \left(\frac{1+\beta}{\beta}\right)^2 - \frac{4}{\beta} = \frac{1-2\beta+\beta^2}{\beta^2} = \left(\frac{1-\beta}{\beta}\right)^2 > 0,$$

as $0 < \beta < 1$. Therefore, the solution for the homogenous equation are $Ar_1^t + Br_2^t$ with r_1 and r_2 roots to $X^2 - \frac{1+\beta}{\beta}X + \frac{1}{\beta} = 0$ and $(A, B) \in \mathbb{R}^2$ given by:

$$r_1 = \frac{1}{2}\left(\frac{1+\beta}{\beta} + \frac{1-\beta}{\beta}\right) = \frac{1}{\beta} \text{ and } r_2 = \frac{1}{2}\left(\frac{1+\beta}{\beta} - \frac{1-\beta}{\beta}\right) = 1.$$

Moreover, the particular solution ϕ_P for this equation is given by $\frac{\nu\beta\gamma C}{2\alpha(1-\beta)}t$ and thus, the solution writes:

$$\phi_t = A\left(\frac{1}{\beta}\right)^t + B + \frac{\nu\beta\gamma C}{2\alpha(1-\beta)}t.$$

Finally, the initial $\phi_0 = 0$ and terminal conditions $\phi_T = \frac{1}{\gamma}$ leads to:

$$A = -B \text{ and } A = \left[\frac{1}{\gamma} - \frac{\nu\beta\gamma C}{2\alpha(1-\beta)}T\right]\left[\left(\frac{1}{\beta}\right)^T - 1\right]^{-1}.$$

Thereby, we get:

$$\phi_t^* = A\left(\left(\frac{1}{\beta}\right)^t - 1\right) + \frac{C\nu\beta\gamma}{2\alpha(1-\beta)}\ t,$$

which gives the optimal dynamics of efficiency before reaching full decarbonation of peak load.

(iii) By definition of the transition time $T^\star$ we have that $\lambda(\phi_{T^\star}) = 1$ and thus in the *linear region* that $\phi_{T^\star} = \frac{1}{\gamma}$. Therefore, from the expression of ϕ_t in the *linear region* obtained as a result of Corollary 2 we have that: $A\left(\left(\frac{1}{\beta}\right)^{T^\star} - 1\right) + \frac{C\nu\beta\gamma}{2\alpha(1-\beta)}\ T^\star = \frac{1}{\gamma} \iff ab^{T^\star} + cT^\star = d$ with $a = A$, $b = \frac{1}{\beta}$, $c = \frac{C\nu\beta\gamma}{2\alpha(1-\beta)}$ and $d = \frac{1}{\gamma} + A$. As $\nu > 0$ we can divide by c and rewrite (13) as $d' - T^\star = a'b^{T^\star}$ with $d' = d/c$ and $a' = a/c$. Be $y = d' - T^\star$, $v = 1/b$ and $u = a'b'^{d'}$ then $y = a'b^{d'-y} = a'b^{d'}b^{-y} = ub^{-y} = uv^y = ue^{yln(v)}$. Finally, be $z = -yln(v)$, this gives $ze^z = -uln(v)$ therefore by definition of the Lambert W function $z = W(-uln(v))$. Rewriting, z, u and v in the initial variables leads to:

$$T^\star = \frac{d}{c} - \frac{1}{ln(b)}W\left(\frac{ab^{d/c}ln(b)}{c}\right),$$

with $a = A$, $b = \frac{1}{\beta}$, $c = \frac{C\nu\beta\gamma}{2\alpha(1-\beta)}$, $d = \frac{1}{\gamma} + A$ and W the Lambert W function.

L. Proof of Corollary 3.

(i) In the *concave region*, energy mix writes as $\lambda(\phi) = \eta\phi^{\gamma}$. Moreover as from Corollary 1:

$$\phi_{t+2} - \frac{1+\beta}{\beta}\phi_{t+1} + \frac{1}{\beta}\phi_t = -\frac{C\nu}{2\alpha}\lambda'(\phi_{t+1}),$$

then, under the assumption concave mix we have:

$$\phi_{t+2} - \frac{1+\beta}{\beta}\phi_{t+1} + \frac{1}{\beta}\phi_t = -\frac{C\nu\eta\gamma}{2\alpha}\phi_{t+1}^{\gamma-1},$$

therefore leading to:

$$\phi_{t+1}^{1-\gamma}\left[\phi_{t+2} - \frac{1+\beta}{\beta}\phi_{t+1} + \frac{1}{\beta}\phi_t\right] = -\frac{C\nu\eta\gamma}{2\alpha},$$

which gives the dynamics of efficiency in the *concave region* of energy mix.

(ii) From what precedes we have that:

$$\begin{aligned}
&\phi_{t+2} - \frac{1+\beta}{\beta}\phi_{t+1} + \frac{1}{\beta}\phi_t = -\frac{C\nu\eta\gamma}{2\alpha\phi_{t+1}^{1-\gamma}} \\
\iff &\phi_t = \beta\left[\frac{1+\beta}{\beta}\phi_{t+1} - \phi_{t+2} - \frac{C\nu\eta\gamma}{2\alpha\phi_{t+1}^{1-\gamma}}\right] \\
\iff &\phi_t = (1+\beta)\phi_{t+1} - \beta\phi_{t+2} - \frac{\beta C\nu\eta\gamma}{2\alpha\phi_{t+1}^{1-\gamma}} \\
\iff &\phi_t = \phi_{t+1} - \frac{\beta}{2\alpha}\left[\frac{C\nu\eta\gamma}{\phi_{t+1}^{1-\gamma}} + 2\alpha(\phi_{t+2} - \phi_{t+1})\right],
\end{aligned}$$

which completes the proof. The pseudo-code for the shooting method is given in Appendix E.2.

M.1. Time horizon versus energy surplus mean.

Distrib.	Mean (GWh)	Var. (GWh)	LCOS (\$/MWh)	Carbon price (\$/tCO$_2$)	$T^\star$ (years)
$\mathcal{W}(32, 7)$	30	25	600	0	26
$\mathcal{W}(32, 7)$	30	25	600	100	23
$\mathcal{W}(32, 7)$	30	25	600	200	18
$\mathcal{W}(37.2, 8.3)$	35	25	600	0	21
$\mathcal{W}(37.2, 8.3)$	35	25	600	100	18
$\mathcal{W}(37.2, 8.3)$	35	25	600	200	13
$\mathcal{W}(42.2, 9.6)$	40	25	600	0	17
$\mathcal{W}(42.2, 9.6)$	40	25	600	100	14
$\mathcal{W}(42.2, 9.6)$	40	25	600	200	10
$\mathcal{W}(47.2, 12.2)$	45	25	600	0	15
$\mathcal{W}(47.2, 12.2)$	45	25	600	100	12
$\mathcal{W}(47.2, 12.2)$	45	25	600	200	8
$\mathcal{W}(52.3, 12.2)$	50	25	600	0	14
$\mathcal{W}(52.3, 12.2)$	50	25	600	100	11
$\mathcal{W}(52.3, 12.2)$	50	25	600	200	7

Table 3: Time horizon $T^\star$ versus the energy surplus mean at fixed variance (25 GWh) and constant LCOS (600 \$/MWh).

Distrib.	Mean (GWh)	Var. (GWh)	LCOS (\$/MWh)	Carbon price (\$/tCO$_2$)	$T^\star$ (years)
$\mathcal{W}(32, 7)$	30	25	200	0	11
$\mathcal{W}(32, 7)$	30	25	600	0	26
$\mathcal{W}(32, 7)$	30	25	1000	0	37
$\mathcal{W}(37.2, 8.3)$	35	25	200	0	9
$\mathcal{W}(37.2, 8.3)$	35	25	600	0	21
$\mathcal{W}(37.2, 8.3)$	35	25	1000	0	30
$\mathcal{W}(42.2, 9.6)$	40	25	200	0	8
$\mathcal{W}(42.2, 9.6)$	40	25	600	0	17
$\mathcal{W}(42.2, 9.6)$	40	25	1000	0	27
$\mathcal{W}(47.2, 12.2)$	45	25	200	0	7
$\mathcal{W}(47.2, 12.2)$	45	25	600	0	15
$\mathcal{W}(47.2, 12.2)$	45	25	1000	0	24
$\mathcal{W}(52.3, 12.2)$	50	25	200	0	6
$\mathcal{W}(52.3, 12.2)$	50	25	600	0	14
$\mathcal{W}(52.3, 12.2)$	50	25	1000	0	22

Table 4: Time horizon $T^\star$ versus the energy surplus mean at fixed variance (25 GWh) and constant carbon cost (0 \$/tCO$_2$).

M.2. Time horizon versus energy surplus variance.

Distrib.	Mean (GWh)	Var. (GWh)	LCOS (\$/MWh)	Carbon price (\$/tCO$_2$)	$T^\star$ (years)
$\mathcal{W}(31.7, 9.3)$	30	15	600	0	24
$\mathcal{W}(31.7, 9.3)$	30	15	600	100	22
$\mathcal{W}(31.7, 9.3)$	30	15	600	200	17
$\mathcal{W}(31.9, 7.9)$	30	20	600	0	26
$\mathcal{W}(31.9, 7.9)$	30	20	600	100	22
$\mathcal{W}(31.9, 7.9)$	30	20	600	200	18
$\mathcal{W}(32, 7)$	30	25	600	0	26
$\mathcal{W}(32, 7))$	30	25	600	100	23
$\mathcal{W}(32, 7))$	30	25	600	200	18
$\mathcal{W}(32.3, 6.4)$	30	30	600	0	28
$\mathcal{W}(32.3, 6.4)$	30	30	600	100	24
$\mathcal{W}(32.3, 6.4)$	30	30	600	200	19
$\mathcal{W}(32.5, 5.9)$	30	35	600	0	29
$\mathcal{W}(32.5, 5.9)$	30	35	600	100	24
$\mathcal{W}(32.5, 5.9)$	30	35	600	200	19

Table 5: Time horizon $T^\star$ versus the energy surplus variance at fixed mean (30 GWh) and constant LCOS (600 \$/MWh).

Distrib.	Mean (GWh)	Var. (GWh)	LCOS (\$/MWh)	Carbon price (\$/tCO$_2$)	$T^\star$ (years)
$\mathcal{W}(31.7, 9.3)$	30	15	200	0	10
$\mathcal{W}(31.7, 9.3)$	30	15	600	0	24
$\mathcal{W}(31.7, 9.3)$	30	15	1000	0	35
$\mathcal{W}(31.9, 7.9)$	30	20	200	0	11
$\mathcal{W}(31.9, 7.9)$	30	20	600	0	26
$\mathcal{W}(31.9, 7.9)$	30	20	1000	0	36
$\mathcal{W}(32, 7)$	30	25	200	0	11
$\mathcal{W}(32, 7)$	30	25	600	0	26
$\mathcal{W}(32, 7)$	30	25	1000	0	37
$\mathcal{W}(32.3, 6.4)$	30	30	200	0	12
$\mathcal{W}(32.3, 6.4)$	30	30	600	0	28
$\mathcal{W}(32.3, 6.4)$	30	30	1000	0	38
$\mathcal{W}(32.5, 5.9)$	30	35	200	0	12
$\mathcal{W}(32.5, 5.9)$	30	35	600	0	29
$\mathcal{W}(32.5, 5.9)$	30	35	1000	0	38

Table 6: Time horizon $T^\star$ versus the energy surplus variance at fixed mean (30 GWh) and constant carbon cost (0 \$/tCO$_2$).

M.3. Investment ratio versus energy surplus mean.

Distrib.	Mean (GWh)	Var. (GWh)	LCOS ($/MWh)	Carbon price ($/tCO$_2$)	ξ
$\mathcal{W}(32, 7)$	30	25	600	0	0.43
$\mathcal{W}(32, 7)$	30	25	600	100	0.32
$\mathcal{W}(32, 7)$	30	25	600	200	0.25
$\mathcal{W}(37.2, 8.3)$	35	25	600	0	0.52
$\mathcal{W}(37.2, 8.3)$	35	25	600	100	0.38
$\mathcal{W}(37.2, 8.3)$	35	25	600	200	0.3
$\mathcal{W}(42.2, 9.6)$	40	25	600	0	0.55
$\mathcal{W}(42.2, 9.6)$	40	25	600	100	0.43
$\mathcal{W}(42.2, 9.6)$	40	25	600	200	0.33
$\mathcal{W}(47.2, 12.2)$	45	25	600	0	0.6
$\mathcal{W}(47.2, 12.2)$	45	25	600	100	0.48
$\mathcal{W}(47.2, 12.2)$	45	25	600	200	0.38
$\mathcal{W}(52.3, 12.2)$	50	25	600	0	0.62
$\mathcal{W}(52.3, 12.2)$	50	25	600	100	0.5
$\mathcal{W}(52.3, 12.2)$	50	25	600	200	0.4

Table 7: Investment ratio coefficient ξ versus the energy surplus mean at fixed variance (25 GWh) and constant LCOS (600 $/MWh).

Distrib.	Mean (GWh)	Var. (GWh)	LCOS ($/MWh)	Carbon price ($/tCO$_2$)	ξ
$\mathcal{W}(32, 7)$	30	25	200	0	0.28
$\mathcal{W}(32, 7)$	30	25	600	0	0.43
$\mathcal{W}(32, 7)$	30	25	1000	0	0.56
$\mathcal{W}(37.2, 8.3)$	35	25	200	0	0.34
$\mathcal{W}(37.2, 8.3)$	35	25	600	0	0.52
$\mathcal{W}(37.2, 8.3)$	35	25	1000	0	0.63
$\mathcal{W}(42.2, 9.6)$	40	25	200	0	0.41
$\mathcal{W}(42.2, 9.6)$	40	25	600	0	0.55
$\mathcal{W}(42.2, 9.6)$	40	25	1000	0	0.66
$\mathcal{W}(47.2, 12.2)$	45	25	200	0	0.44
$\mathcal{W}(47.2, 12.2)$	45	25	600	0	0.6
$\mathcal{W}(47.2, 12.2)$	45	25	1000	0	0.68
$\mathcal{W}(52.3, 12.2)$	50	25	200	0	0.5
$\mathcal{W}(52.3, 12.2)$	50	25	600	0	0.62
$\mathcal{W}(52.3, 12.2)$	50	25	1000	0	0.73

Table 8: Investment ratio coefficient ξ versus the energy surplus mean at fixed variance (25 GWh) and constant carbon cost (0 $/tCO$_2$).

M.4. Investment ratio versus energy surplus variance.

Distrib.	Mean (GWh)	Var. (GWh)	LCOS (\$/MWh)	Carbon price (\$/tCO$_2$)	ξ
$\mathcal{W}(31.7, 9.3)$	30	15	600	0	0.43
$\mathcal{W}(31.7, 9.3)$	30	15	600	100	0.31
$\mathcal{W}(31.7, 9.3)$	30	15	600	200	0.23
$\mathcal{W}(31.9, 7.9)$	30	20	600	0	0.42
$\mathcal{W}(31.9, 7.9)$	30	20	600	100	0.31
$\mathcal{W}(31.9, 7.9)$	30	20	600	200	0.24
$\mathcal{W}(32, 7)$	30	25	600	0	0.43
$\mathcal{W}(32, 7))$	30	25	600	100	0.32
$\mathcal{W}(32, 7))$	30	25	600	200	0.25
$\mathcal{W}(32.3, 6.4)$	30	30	600	0	0.43
$\mathcal{W}(32.3, 6.4)$	30	30	600	100	0.32
$\mathcal{W}(32.3, 6.4)$	30	30	600	200	0.24
$\mathcal{W}(32.5, 5.9)$	30	35	600	0	0.43
$\mathcal{W}(32.5, 5.9)$	30	35	600	100	0.33
$\mathcal{W}(32.5, 5.9)$	30	35	600	200	0.25

Table 9: Investment ratio coefficient ξ versus the energy surplus variance at fixed mean (30 GWh) and constant LCOS (600 \$/MWh).

Distrib.	Mean (GWh)	Var. (GWh)	LCOS (\$/MWh)	Carbon price (\$/tCO$_2$)	ξ
$\mathcal{W}(31.7, 9.3)$	30	15	200	0	0.26
$\mathcal{W}(31.7, 9.3)$	30	15	600	0	0.43
$\mathcal{W}(31.7, 9.3)$	30	15	1000	0	0.53
$\mathcal{W}(31.9, 7.9)$	30	20	200	0	0.26
$\mathcal{W}(31.9, 7.9)$	30	20	600	0	0.42
$\mathcal{W}(31.9, 7.9)$	30	20	1000	0	0.54
$\mathcal{W}(32, 7)$	30	25	200	0	0.28
$\mathcal{W}(32, 7)$	30	25	600	0	0.43
$\mathcal{W}(32, 7)$	30	25	1000	0	0.56
$\mathcal{W}(32.3, 6.4)$	30	30	200	0	0.28
$\mathcal{W}(32.3, 6.4)$	30	30	600	0	0.43
$\mathcal{W}(32.3, 6.4)$	30	30	1000	0	0.54
$\mathcal{W}(32.5, 5.9)$	30	35	200	0	0.28
$\mathcal{W}(32.5, 5.9)$	30	35	600	0	0.43
$\mathcal{W}(32.5, 5.9)$	30	35	1000	0	0.55

Table 10: Investment ratio coefficient ξ versus the energy surplus variance at fixed mean (30 GWh) and constant carbon cost (0 \$/tCO$_2$).

Chapter 2

Land use and the energy shift

Abstract

Along with intermittency and production costs, land use is one of the major limitation to the development of renewable energy. In this research, we develop a macrodynamic growth model of the energy shift integrating land constraints. Land is considered as a ressource for agricultural production along with energy. Developing renewable energy uses space and thus interferes with the agricultural sector. Moreover, pollution abatement policies are also analyzed in our model as they compete with renewable energy for land in order to reduce pollution from the use of fossil fuels. Under specific assumptions on the price of fossil fuels we prove the existence of land use saddle path stable steady states and study the competition in land use between agriculture, pollution abatement and renewable energy production. Finally, we apply our model to study the development of a palm oil biodiesel sector in Brazil, along with the issues it rises regarding the Amazon forest preservation.

Keywords: Land use, Renewable energy, Pollution abatement, Climate change mitigation, Macrodynamic growth model, Optimal control.

Journal of Economic Literature: C61, Q5, Q24, R14, O44, O13.

This chapter builds on the eponymous research paper co-written with Carmen Camacho. All errors remain mine.

Contents

List of Figures

1 Introduction

The on-going investments in renewable energy production raise new questions on land use as one major limitation of renewable energy development is land availability. Indeed, the land needed to produce one unit of renewable energy is much greater than the land required to produce fossil fuels energy (Smill, 2016). Land constraint and the spatial implications of renewable energy development has been widely studied in the economic, geographic and energy literature since the early days of renewable energy development. In 1991, the nuclear industry already reminded how compact is nuclear energy compared to renewable energy sources (Nuclear Forum, 1991). According to industry representatives, a nuclear plant uses 630 m^2 to produce of 1 MW of electricity compared to 100 000 m^2 for solar energy, 265 000 m^2 for hydroelectric, and 1 700 000 m^2 for wind energy. In Wintson (1979) the author estimates that, in order to meet the entire US electricity demand with the photovoltaic technology available in the early 1980's, the surface of the State of Oregon would be required.

Yet, estimating land use pressures caused by renewable energy depends drastically on who, when and how is done the estimation (Walker, 1995). For instance, estimations from Wintson (1979) must be put into perspective as solar panel would naturally be placed onto the roofs of existing buildings, which would lower considerably the need of raw land for solar energy production (Pasqualetti, 1990)[1]. Similarly, regarding wind energy, the consideration of off-shore wind energy production would also lowers the amount of raw land required to produce energy from such source (Danielsen, 1994)[2]. In Hall and House (1995), authors point out that land availability is perceived as the biggest contraint for large-scale biomass energy production. Yet, they claim that important amounts of land are not considered for biomass production such as large areas of surplus agricultural land in Europe or in North America[3], which use would also lower land use pressures due to renewable energy production.

The question of the amount of usable available land is therefore at the centre of the land use debate regarding renewable energy development and in particular near high landscape valuable sites such as national parks or protected areas (Mc Kenzie, 1995).

[1]More recent studies estimate PV roof hosting potential according to building sizes as in De Boer et al. (2011), NREL (2015) or Gagnon et al. (2016) among others.

[2]For country specific studies on off-shore wind energy see Emeksiz et al. (2019), Marafia et al. (2003), Park et al. (2019), Nassar et al. (2019), Sawulski et al. (2019) or Kim et al. (2019).

[3]For a more recent literature review on the use of surplus agricultural land for biomass energy production see Rahman et al. (2014).

Estimates for land use stress caused by the the development of renewable energy in these seminal studies depend highly on the amount of available land considered by the authors, as well as on the hypothesis being done on the technological level of renewable energy production at the time of their early development. Indeed in Behrens and Zalk (2018) the authors analyse publications from 1974 to 2016 in order to estimate the dynamics of land required for RNE production. They find that the reduction in land requirements is particularly important for solar energy, and less for wind energy, while geo-thermal, biomass or hydro show negligible or non-significant trend. With the ongoing massive development of renewable energy to fight against climate change, and with the growing demand for energy, the land use question is still at the center of the energy shift debate (Bridge et al., 2013; Fouquet, 2016; Andrews et al., 2011), and has been more recently analyzed in a country-specific and empirical literature[4] at the political, socio-cultural, environmental and economical level.

Indeed, the development of RNE becomes inherently political when the acquisition of land for massive energy projects leads to the deterioration of the livelihood of surrounding vulnerable community (Yenneti et al., 2015)[5]. At the socio-cultural level, the question of aesthetics and landscape are strong social barriers at the center of public debates and controversies regarding the development of renewable energy (Nadai et al., 2010; Pasqualetti, 2011; Tuan, 1974). The environmental implications of RNE development are particularly important regarding the conservation of biodiversity and the maintenance of ecosystems. Indeed, as RNE infrastructure needs significant amount of land, their development leads to the modification and fragmentation of natural habitats resulting in a loss of biodiversity (Gasparatos et al., 2017)[6]. Finally, land acquisition for renewable energy production causes particularly economic tensions with land-intensive industries such as the agricultural sector. The trade-off in land use between agricultural and renewable energy production has been studied theoretically in Chakravorty et al. (2008)[7]. The authors develop a model in which the exhaustible fossil fuels sees its price increases as it becomes scarcer, making renewable energy more competitive which results in a shift in land use from food production to energy production. This analytical framework has been recently extended in Bahel et al. (2013) and Amigues

[4]See Hernandez (2015), McEwan (2017), Sliz-Szkliniarz (2013) or Calvert (2015) among others.

[5]Here, the authors examine the impact of the Charanka solar park in India on population from the surrounding Charanka village by interviewing the villagers.

[6]The authors review the impact of renewable energy pathways on ecosystems and biodiversity and the specific environmental stress caused by solar, wind, hydro, ocean, geothermal and bioenergy.

[7]For country-specific analysis see Poggi (2018), Liu (2018) or Appel (2016).

and Moreaux (2019) to study respectively the competition between farmers and oil cartel to produce energy and the optimal dynamics of energy transformation rate.

In order to asses land use pressure due to the development of RNE, the common metric used in the literature is the power density of energy production, that is, the amount of energy produced per horizontal square meters. With the development of renewable energy, a wide literature on power density estimates has emerged[8]. Indeed, a better understanding regarding power densities may help policy makers to guide their decisions concerning land use trade-offs resulting in political, social, environmental or economical stresses. In the systematic study from Behrens and Zalk (2018), the authors review the power densities of nine types of energy. Among these energy sources, five are renewable energy sources (hydropower, wind power, geothermal, solar, biomass) and four are non renewable energy (natural gas, nuclear, coal and oil). Each types of energy are divided in sub-types (for instance, for solar power the authors consider photovoltaic energy and solar thermal energy) and provide median, mean and uncertainty estimates for 177 power densities from 54 publications for each energy sub-types. They find that renewable energy power densities are three orders of magnitude smaller than non-renewable energy power densities, revealing the spatial impact of renewable energy system. Yet, despite of being land use intensive and responsible for tensions at many levels, the development of renewable energy production is one of the key climate change mitigation policy. In Fritsche et al. (2017) the author study the relationship between the power density of an energy source and its green house gaz (GHG) emissivity. Results show that the most GHG emissive technologies are the one with the highest density (coal, gaz) and the least GHG emissive are the one with the lowest density (biomass, wind, solar). This positive relationship between power density and GHG emission exhibits the trade-off between negative externalities due to the use of fossil fuels and the growing spatial and geographical pressures that goes with the on-going development of land use intensive renewable energy sources.

From a theoretical perspective, few research have been developed to study the implications in land use management practices that goes along the massive development of renewable energy production, and in particular the trade-off between pollution emission and land use. In Chakravorty et al. (2008), Bahel et al. (2013) and Amigues and Moreaux (2019), the author do explore this question theoretically, yet, they do not pose

[8]See Layton (2008), Fthenakis et al. (2010), Gagnon et al. (2002), Smil (2010) or Dijkman et al. (2010) among others.

the problem using the metric of power density, making their theoretical results difficult to articulate with empirical research on that matter. We tend to fill this gap in the theoretical literature by developing a macrodynamic model of the energy shift which takes into account land use competition between renewable energy and agricultural production while characterizing energy sources by their power densities.

In this chapter, the economy is modelled as an energy-land agricultural economy, which only requires available land and energy (supplied by both renewable energy and fossil fuels) to produce. We neglect the amount of land needed to produce energy from fossil fuels ressources compared to the land used for renewable energy production and pollution abatement. Moreover, we consider that pollution emitted from the use of fossil fuels can be reduced through abatement policies which also take considerable space and therefore compete with renewable energy for land. Therefore, producing energy from fossil fuels has a cost, pollutes and takes negligible land, whereas renewable energy production is free, does not pollute but is land-intensive. Not like other theoretical approaches, we provide here with the expression of the optimal land use distribution between agricultural production, renewable energy, and pollution abatement, with respect to energy and pollution parameters such as the availability of primary renewable energy, the power density or of fossil fuels emissivity. This allows us to examine the trade-offs in land use, and provide with relevant information for policy makers regarding optimal land allocation according to the pollution sensitivity of the agricultural sector.

When renewable energy production is the only land intensive mitigation policy, the more dense is energy production, the more land shall be allocated towards renewable energy production rather than towards agriculture. This result can be seen as a case of comparative advantage. Indeed, as energy production and agriculture compete for land to produce output, social planner allocates more land to the more productive sector. Hence, the denser is the renewable energy production, the more land must be allocated to its activity. Moreover, the more sensitive is the agricultural sector to pollution, the more land shall be allocated to renewable energy production as well, in order this time to assure the continuity of output production while limiting environmental damages.

Yet, when both mitigation policies available, that is renewable energy production and afforestation for abatement, social planner's strategy for land use reallocation depends on the level of the agricultural production sensitivity to pollution. For low sensitivity, as agriculture becomes more sensitive to pollution, agricultural land must

be reallocated towards both renewable energy (for mitigation purposes and compensation of production losses) and abatement (only for mitigation). In contrast, for high sensitivities, along with agricultural land, it is also best to sacrifice renewable energy production land and reallocate exclusively land to abatement in order to save output from important pollution damages.

Finally, we apply our model to the stakes of preserving the Amazon forest in Brazil. More particularly, we focus on the emerging market of palm oil production for biodiesel in Brazil in Amazonia and on the resulting opportunity cost for Brazil of preserving the Amazon forest. Within a wide range of pollution sensitivities, the price of carbon for preserving the Amazon forest's surface area at its current size lies in-between 300 \$/tCO_2 and 760 \$/tCO_2 which is 2 to 5 times greater than actual carbon prices. Hence, in order to restrain the on-going Amazon deforestation and maintain the forest's current surface area for preserving its global GHG abatement services, the international community must accept to pay higher compensation through financial transfers to Brazil due to ever-growing land use pressures on the Amazon forest, in our case, due to the development of a palm oil biodiesel sector in Brazil.

This chapter is organized as follows. Section 2 introduces a benchmark model with renewable energy production, no abatement and no pollution externalities, in which the only incentive to invest in renewable energy is therefore fossil fuels price. We derive the steady state of the economy and show its saddle path stability. Through a comparative statics analysis we study the sensitivity analysis of the land use equilibrium regarding fossil fuels prices and renewable energy density. Section 3 integrates pollution externalities to the previous model by considering pollution emission from the use of fossil fuels. We prove saddle path stability of the steady state and give the tax on fossil fuels that internalizes pollution. Similarly, we perform a comparative statics but this time to study the land use equilibrium sensitivity with respect to the pollution-related parameters. In Section 4, land can also be allocated to abatement activities. Two mitigations policies are therefore available, being renewable energy and abatement, and compete for land in order to reduce pollution. In such framework, we study the trade-offs in land use between the two mitigation measures and apply in the last section the model to study the tensions between the development of a palm oil biodiesel sector in Brazil and the preservation of the Amazon forest. Section 6 concludes.

2 The benchmark model

2.1 Social planner's problem

We suppose that the economy disposes of one unit of land which is occupied by two activities: renewable energy production on the one hand, and agricultural production on the other hand. Thus we consider that the land needed to produce one unit of energy from fossil fuels (such as coal, gaz or oil) is negligible compared to the land needed to harvest renewable energy (such as wind, biomass or solar power plants). Therefore in this research we only focus on the amount of land required to produce renewable energy. We suppose that the economy disposes of a unique source of renewable energy, the production of which only requires primary renewable energy and a physical stock of renewable energy plants that can be accumulated in time through investments. In such framework, a stock ω of installed renewable energy plants produces a quantity $\Gamma(\nu, \omega)$ of energy where ν captures the efficiency of renewable energy production. Efficiency ν characterizes how much energy a given stock ω of renewable energy plants produces and therefore depends on the technical level of the economy as well as on the availability of primary renewable energy.

We denote $l(\omega)$ the land occupied by a stock ω of renewable energy plants. Note that in this framework, the development of renewable energy is bounded from above as available land is bounded by 1. Therefore, the stock ω of renewable energy plants that can be installed is such that $l(\omega) \leq 1$ and thus, the maximal stock of renewable plants $\hat{\omega}$ is given by $\hat{\omega} = l^{-1}(1)$. Hence, in the following $\omega \in [0, \hat{\omega}]$ and l is defined on this interval with $l(0) = 0$ and $l(\hat{\omega}) = 1$. Similarly to Greiner et al. (2014), we suppose that local production of energy can be written as the superposition of fossil fuels b and renewable energy production and therefore is given by $b + \Gamma(\nu, \omega)$.

Moreover, we consider a unique good, the production of which requires only land and energy such that $F(1 - l(\omega), b + \Gamma(\nu, \omega))$ with $1 - l(\omega)$ the remaining land not used by renewable energy production and therefore available for agriculture, and $b + \Gamma(\nu, \omega)$ the global energy supply produced by both renewable energy and fossil fuels. Finally, the use of fossil fuels has a cost π and production can either be consumed or invested in renewable energy which can be accumulated as:

$$\dot{\omega} = F(1 - l(\omega), b + \Gamma(\nu, \omega)) - c - \pi b,$$

with c the consumption level of the economy.

Before writing social planner's problem we make the following final assumptions regarding the production function of the economy, the utility function, as well as the land required to produce energy and the renewable energy production function.

Assumption 1. ***(i)*** *The production function F is a Cobb-Douglas production function in land and energy: $F(1-l(\omega), b+\Gamma(\nu,\omega)) = A(1-l(\omega))^{\alpha}(b+\Gamma(\nu,\omega))^{\beta}$ with $0 < \alpha+\beta < 1$ and $A > 0$ a productivity factor.*
(ii) *Utility function is supposed to have constant relative risk aversion: $u(c) = \frac{c^{1-\sigma}}{1-\sigma}$.*
(iii) *The land used by renewable energy production is linear in the stock of renewable energy plants: $l(\omega) = \eta\omega$ with $\eta > 0$.*
(iv) *Renewable energy production is linear in efficiency ν and in the stock of installed renewable energy plants: $\Gamma(\nu,\omega) = \nu\omega$.*

Assumption (1.i.) assures the concavity of the production function with respect to the two production factors being here land and energy. We therefore assume decreasing return to scales with respect to energy as in Greiner et al. (2014) and land as in Camacho and Pérez-Barahona (2015). Assumption (1.ii.) assures the concavity of utility with respect to consumption where σ is the risk aversion coefficient. Finally, the two last assumptions are more specific to our model. Assumption (1.iii.) supposes that the stock of renewable energy plants cannot be superposed and can only be juxtaposed side by side, resulting in the linear relation between the amount of land occupied by renewable energy production and the number of RNE power plants. Finally, the last assumption supposes a linear production function for renewable energy production, neglecting therefore potential screening effects between the installed renewable energy power plants, which could potentially lead to decreasing returns to scale.

In this section we present a benchmark model in which pollution emissions from using fossil fuels is neglected. Hence, it is as if central planner does not account for pollution in the inter-temporal optimization problem. This will allow us to asses secondly the impact of pollution on social planner's optimal land allocation policies, when emissions are internalized in the model. Thus, in the benchmark model, social planner's problem therefore writes as:

$$\max_{\{c,b\}} \int_0^{\infty} \frac{c^{1-\sigma}}{1-\sigma} e^{-\rho t} \mathrm{d}t,$$

$$\text{s.t.} \begin{cases} \dot{\omega} = A(1-\eta\omega)^{\alpha}(b+\nu\omega)^{\beta} - c - \pi b, \\ c \geq 0 \; ; b \geq 0 \text{ and } 0 \leq \omega \leq \hat{\omega}, \\ (\eta, \nu, \pi) \in \mathbb{R}_+^3 \text{ and } \sigma \in \mathbb{R}_+ \backslash \{1\}. \end{cases}$$

In the following sections, this problem will be referred to as the *market problem* as the only incentives to invest in renewable energy is the price π of fossil fuels as for now, we do not consider any pollution emission in the use of fossil fuels. We solve the *market problem* in the following and give the optimal land use distribution between the land allocated to renewable energy $l(\omega)$ and the land allocated to agricultural production $1 - l(\omega)$ at equilibrium.

2.2 Steady state analysis

2.2.1 Optimal land use policy for the market problem

Beforehand we must assume the following statement regarding fossil fuels price before analyzing the longterm equilibrium in land use for the *market problem*.

Assumption 2. *$\pi > \frac{\rho}{\nu}$ where ρ is the discount rate, ν the quantity of energy produced by one unit of renewable energy and π the price of fossil fuels.*

The quantity $\frac{\rho}{\nu}$ acts as a price threshold on fossil fuels above which social planner triggers investments and land allocation to renewable energy production. The effects of the discount rate ρ and renewable energy efficiency ν on the price threshold are discussed in the following. But before, we shall provide with the optimal land allocation towards renewable energy production in the *market problem*, that is, when the cost of fossil fuels π is the only incentives for renewable energy development.

Proposition 1. *Under Assumption 1 and Assumption 2, there exists a unique saddle-path stable interior steady state for the renewable energy land use policy l_m given by:*

$$l_m = 1 - \left(\frac{A\alpha\eta \left(\frac{A\beta}{\pi}\right)^{\frac{\beta}{1-\beta}}}{\nu\pi - \rho} \right)^{\frac{1-\beta}{1-\alpha-\beta}}.$$

The optimal land use policy for renewable energy production l_m increases w.r.t. renewable energy production efficiency ν and fossil fuels price π. Yet it decreases w.r.t. renewable land needs η and the discount rate ρ.

The equilibrium derived in Proposition 1 will be referred in the following to the *market equilibrium* as the only incentive to invest and allocate land to renewable energy is fossil fuels price π. The first information given by Proposition 1 is that the

existence of an interior steady state for the amount of land allocated to renewable energy production in the *market problem* depends on this specific price of fossil fuels π. Indeed, if Assumption 2 does not hold *i.e.* $\pi < \frac{\rho}{\nu}$ then no land shall be allocated to renewable energy production and energy is only produced by fossil fuels. Therefore, the price $\pi_m = \frac{\rho}{\nu}$ can be seen as a threshold price for the use of fossil fuels above which, if $\pi > \pi_m$, investments in renewable energy are triggered and land is allocated to renewable energy production.

Moreover, this threshold price increases with respect to the discount rate meaning that as social planner becomes less altruistic towards future generation, the threshold price triggering renewable energy investments increases. Indeed a very low altruistic planner towards future generation, will heavily weight consumption sacrifices of present generation in order to investment in renewable energy and thus only important fossil fuels prices will trigger such investments. Yet, as renewable energy production becomes more efficient *i.e.* ν increases, then the threshold price decreases as renewable energy becomes a better alternative to fossil fuels for energy production.

Moreover, be $\kappa_m = \left(\frac{A\alpha\eta\left(\frac{A\beta}{\pi}\right)^{\frac{\beta}{1-\beta}}}{\nu\pi-\rho} \right)^{\frac{1-\beta}{1-\alpha-\beta}}$ the land allocated to agriculture, then the land allocated to renewable energy production at equilibrium writes as $l_m = 1 - \kappa_m$. Therefore, discount rate ρ has a similar effect on land use equilibrium than it has on the price threshold. As the discount rate increases, the land use equilibrium shifts towards more land allocated to agriculture rather than to renewable energy production. Indeed, as social planner becomes less altruistic towards future generation, more weight is added on present consumption sacrifices for renewable energy investments, therefore reducing, in the long run, land use in renewable energy production.

On the contrary, very efficient renewable energy production with high ν, tends to push land allocation towards more renewable energy production. Note that this result is not necessarily straightforward as the economy could have relied on very efficient renewable energy to precisely reduce the land occupied by renewable energy. In our land use model, it is the exact opposite: the more efficient is renewable energy, the more land should be allocated to its production. This result can be seen as a case of comparative advantage. As energy production and agriculture compete for land to produce output, social planner allocates more land to the more productive sector. This reasoning holds regarding the amount of land η needed to produce one unit of energy. Indeed, for high land needs η, the land allocated to renewable energy production decreases. High η

means that the production of renewable energy is less efficient with respect to land use and thus, following the previous comparative advantage reasoning, less land shall be allocated to renewable energy production and more towards agriculture.

Finally, renewable energy also competes with fossil fuels in order to produce energy. As a substitute to fossil fuels, the more costly is the use of fossil fuels the more renewable energy shall be used in the energy mix. Therefore, as the price for the use of fossil fuels π increases, the land use equilibrium shifts towards more land allocated to renewable energy production.

2.2.2 On the energy mix

Having characterize the optimal land allocation towards renewable energy production and agriculture, we now give the energy mix associated to the land use distribution for the *market equilibrium*.

Proposition 2. *Under the previous assumptions there exists a unique interior saddle-path stable energy mix steady state* (ω_m, b_m) *such that:*

$$\begin{cases} \omega_m = \frac{l_m}{\eta} = \frac{1}{\eta}\left[1 - \left(\frac{A\alpha\eta\left(\frac{A\beta}{\pi}\right)^{\frac{\beta}{1-\beta}}}{\nu\pi-\rho}\right)^{\frac{1-\beta}{1-\alpha-\beta}}\right], \\ b_m = \left[\frac{A\beta(1-l_m)^{\alpha}}{\pi}\right]^{\frac{1}{1-\beta}} - \frac{\nu}{\eta}l_m. \end{cases}$$

The use of renewables (resp. fossil fuels) at steady state increases (resp. decreases) w.r.t. renewable production efficiency ν *and fossil fuels price* π *and decreases (resp. increases) w.r.t. to land occupation* η*.*

From the previous static analysis for the model's parameters with respect to land l_m allocated to renewable energy production of Proposition 1, the comparative statics study regarding the stock ω_m of renewable energy at equilibrium is very straightforward. As ω_m is directly given by $\omega_m = \frac{l_m}{\eta}$, the comparative statics interpretation for the stock of renewable energy at steady state will exactly be the same as the one for land allocation l_m, for all parameters other than land needs η. Indeed, $\frac{\partial\omega_m}{\partial X} = \frac{1}{\eta}\frac{\partial l_m}{\partial X}$ for a variable X being either fossil fuels price π, efficiency ν or discount rate ρ. Regarding land need η, as l_m decreases with respect to land need η and $l_m = \eta\omega_m$ then ω_m must necessarily decreases w.r.t. to land needs at a higher rate than land use.

Regarding the use of fossil fuels b_m in the energy mix, the more land is allocated to renewable energy production or the more costly is the use of fossil fuels, then the less the latter will provide energy in the steady state energy mix. This clearly highlights that renewable energy here acts as an alternative source of energy for costly fossil fuels.

Moreover, the term $\frac{\nu}{\eta}$ in the expression for the use of fossil fuels b_m from Proposition 2 is defined as the energy density in the literature of renewable energy land use (Behrens and Zalk, 2018).[9] In the expression for the use of fossil fuels, we see that for a given land allocation to renewable energy, the denser are renewable energy sources, the less is the use of fossil fuels in the energy mix. Therefore, fossil fuels tends to be substituted by renewable energy not only if the latter have the capacity to produce lots of energy for a given stock ω_m but also if they are able to produce this energy through limited land use. The substitutability of fossil fuels by renewable energy integrates both dimension of energy production and land needs through the metric of energy density in our model.

Finally, the overall energy production at steady state $b_m + \nu\omega_m = \left[\frac{A\beta(1-l_m)^\alpha}{\pi}\right]^{\frac{1}{1-\beta}}$ depends directly on the other factor of production $1 - l_m$, that is the land allocated to agriculture. As allocating land to renewable energy mechanically reduces the land allocated to agriculture, it also reduces energy production. Therefore, allocating land to renewable energy tends to reduce the overall production of the economy as the two production factors decreases w.r.t. renewable energy land use. Yet, it does not necessarily reduces consumption. Indeed, allocating more land to renewable energy reduces the use of fossil fuels, therefore cutting expenses in energy production due to the costs π in the use of fossil fuels. The effect of land use policy on consumption is studied in the following section.

2.2.3 Steady state consumption and discounting

We study in this section the land allocation distribution which maximizes steady state consumption for the *market problem* and discuss on the effect of the discount rate regarding the maximization of long-run consumption.

Proposition 3. *Steady state consumption c_m increases w.r.t. the land allocated to renewable energy production l_m. Moreover, the land policy l_g for renewable energy*

[9] See introduction for references on energy density literature.

production given by:

$$l_g = 1 - \left(\frac{A\alpha\eta \left(\frac{A\beta}{\pi}\right)^{\frac{\beta}{1-\beta}}}{\nu\pi} \right)^{\frac{1-\beta}{1-\alpha-\beta}},$$

maximizes steady state consumption.

In the previous section we showed how allocating land to renewable energy production reduces the overall production of the economy. Yet, according to Proposition 3 it goes the other way regarding steady state consumption. Indeed, if land use from renewable energy is important in the long run steady state, this means that consumption sacrifices were done by past generations in order to invest and develop renewable energy production. Moreover, as the only cost of renewable energy are investments cost done by previous generations then, once installed, renewable energy are cost-free sources of energy. Thus, the accumulation of renewable energy sources payed by present generation, leads to free energy production for the long run generations at steady state. Therefore, allocating land to renewable energy production increases long run consumption at steady state as costly fossil fuels were partly substituted by cost free renewable energy sources due to past investments.

Yet, the land use policy at steady state does not maximize steady state consumption. Indeed, comparing the land use policy which maximizes steady state consumption to the land use policy from Proposition 1 leads to:

$$l_g - l_m = \left(\frac{A\alpha\eta \left(\frac{A\beta}{\pi}\right)^{\frac{\beta}{1-\beta}}}{\nu\pi} \right)^{\frac{1-\beta}{1-\alpha-\beta}} \left[\underbrace{\left(\frac{\nu\pi}{\nu\pi - \rho} \right)^{\frac{1-\beta}{1-\alpha-\beta}}}_{>1} - 1 \right] > 0.$$

As the discount rate is strictly positive, then $\left(\frac{\nu\pi}{\nu\pi-\rho}\right) > 1$. Moreover as $\frac{1-\beta}{1-\alpha-\beta} > 1$ then $\left(\frac{\nu\pi}{\nu\pi-\rho}\right)^{\frac{1-\beta}{1-\alpha-\beta}} > 1$. Thus, the land use policy maximizing consumption at steady state is higher than land use at steady state derived in Proposition 1. Moreover, from Proposition 1, we know that as ρ decreases, the land allocated to renewable energy production at steady state increases and Proposition 2 shows that as $\rho \to 0_+$ l_m converges to the land use policy maximizing steady state consumption l_g. This highlights that discount rate ρ is the reason why land use policy at steady state does not maximize consumption at steady state. Indeed, in our problem, social planner puts less weight on future generation and as the accumulation of renewable energy requires

consumption sacrifices of present generations, the land policy reached at steady state must be strictly smaller than the policy maximizing steady state consumption.

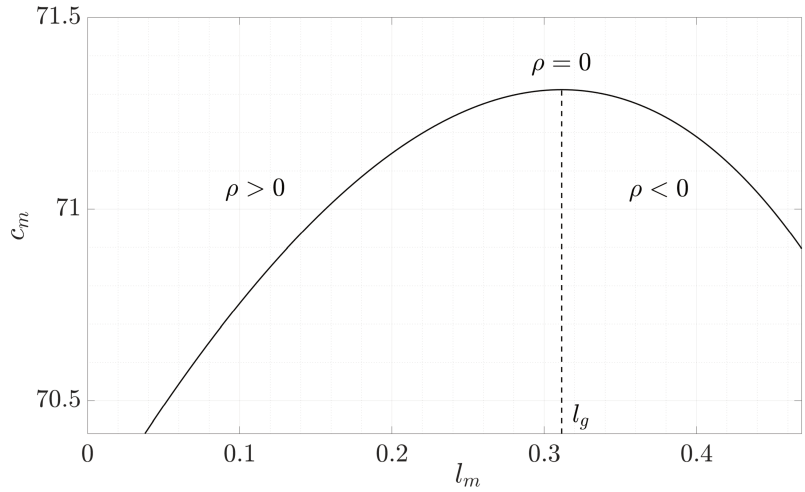

Figure 1: Steady state consumption w.r.t. steady state renewable energy land use.

2.3 Transient dynamics and stability

In the previous section we derived the land use equilibrium towards which the economy converges in the long-run and characterized the *market equilibrium* through a comparative statics analysis. Here, we analyse the transient dynamics of the problem as well as the stability of the equilibrium using the phase diagram in consumption and renewable energy. The numerical simulations are done with the set of values for parameters from Table 1.[10]

A	Technology	10
ρ	Time discount rate	0.01
α	Land productivity	0.2
β	Energy productivity	0.35
ν	Renewable efficiency	3
σ	Utility parameter	5
η	RNE land needs	0.01
π	fossil fuels price	0.1

Table 1: Parameter values.

2.3.1 Phase diagram

In order to study the phase diagram in consumption and stock of renewable energy, we provide with the optimal dynamics in renewable energy and consumption which solves the *market problem.*

[10]The parameters are taken for illustrative purposes. A calibrated analysis is proposed in Section 4.3.

Proposition 4. *Under the model assumptions there exists a unique optimal policy solution to the market problem given by:*

$$\begin{cases} \dot{\omega} = A\left(\frac{A\beta}{\pi}\right)^{\frac{\beta}{1-\beta}}(1-\eta\omega)^{\frac{\alpha+\beta-1}{1-\beta}} - \pi\left(\frac{A\beta(1-\eta\omega)^{\alpha}}{\pi}\right)^{\frac{1}{1-\beta}} + \nu\pi\omega - c, \\ \dot{c} = -\frac{c}{\sigma}\left[A\eta\alpha\left(\frac{A\beta}{\pi}\right)^{\frac{\beta}{1-\beta}}(1-\eta\omega)^{\frac{\alpha+\beta-1}{1-\beta}} + \rho - \nu\pi\right], \end{cases}$$

and where $b = \left(\frac{A\beta(1-\eta\omega)^{\alpha}}{\pi}\right)^{\frac{1}{1-\beta}} - \nu\omega$, *for all* $t \geq 0$.

Figure 2 provides with the phase diagram for the *market problem*. We study the nature of the equilibrium $(\omega_m,\ c_m)$ by analyzing the dynamics of ω and c away from equilibrium.

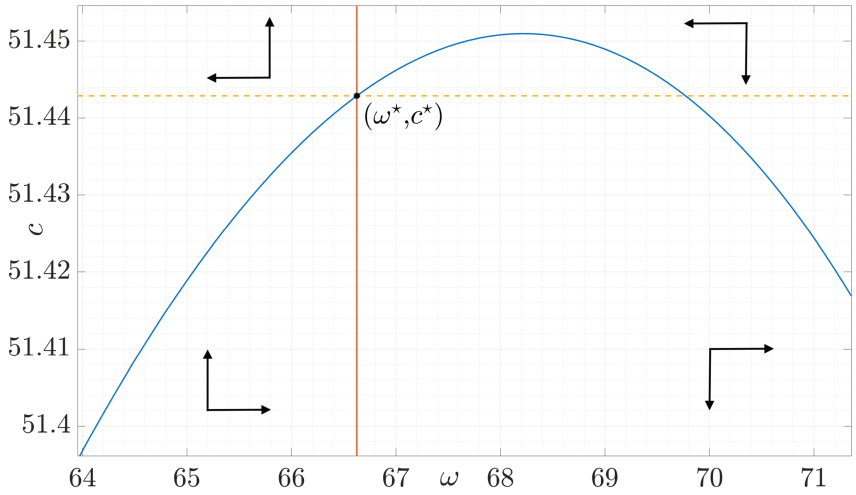

Figure 2: Phase diagram for the *market problem* in consumption and renewable energy.

- If $\dot{c} = 0$ then $A\eta\alpha\left(\frac{A\beta}{\pi}\right)^{\frac{\beta}{1-\beta}}(1-\eta\omega)^{\frac{\alpha+\beta-1}{1-\beta}} + \rho - \nu\pi = 0$. Therefore, if $\omega < \omega_m$ then $\dot{c} > 0$ and if $\omega > \omega_m$ then $\dot{c} < 0$. This means that on the left side of the quadrant of Figure 2, when the stock of renewable energy is bellow equilibrium then consumption increases (represented by the upward vertical arrows). Reciprocally, on the right side of the quadrant of the Phase diagram, if the stock of renewable energy is above equilibrium then consumption decreases (represented by the downward vertical arrows on Figure 2).

- Similarly, if $\dot{\omega} = 0$ then A $\left(\frac{A\beta}{\pi}\right)^{\frac{\beta}{1-\beta}}(1-\eta\omega)^{\frac{\alpha+\beta-1}{1-\beta}} - \pi\left(\frac{A\beta(1-\eta\omega)^{\alpha}}{\pi}\right)^{\frac{1}{1-\beta}} + \nu\pi\omega - c = 0$. Therefore, on the lower side of the quadrant of Figure 2 for $c < c_m$ we have $\dot{\omega} > 0$ meaning that the stock of renewable energy increases (represented by the right-pointing horizontal arrows in Figure 2). Reciprocally, on the upper side of Figure 2 for $c > c_m$

then $\dot{\omega} < 0$ meaning that the stock of renewable decreases (represented by the left-pointing horizontal arrows in Figure 2). Hence, the equilibrium (ω_m, c_m) is saddle path stable.

2.3.2 Numerical simulations

Figure 3 describes the dynamics of consumption c, fossil fuels use b, the stock of renewable energy ω, the land allocated to agriculture $1-\eta\omega$, the overall energy produced $b+\nu\omega$ and production with an initial stock of renewable energy $\omega(0) = 0$, that is when the economy initially disposes of only fossil fuels to produce energy and no renewable energy power plants are available. Parameters's values are given in Table 1.

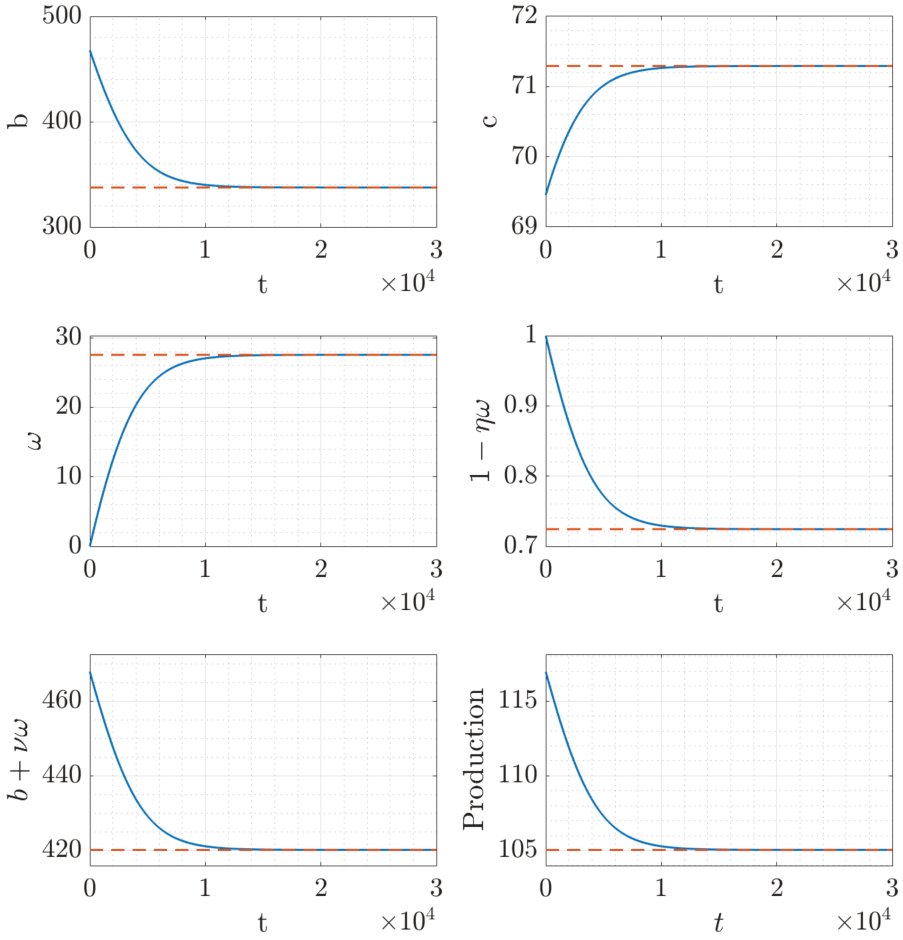

Figure 3: Stable arm converging towards steady state for initial level of renewable energy bellow equilibrium: $\omega(0) = 0 < \omega_m$.

In such case, as time evolves, the economy reduces its use of fossil fuels and invests in renewable energy. The increase in renewable energy does not compensate totally

the loss in energy production from fossil fuels, therefore the overall energy production $b + \nu\omega$ decreases. Moreover, as renewable energy is being developed, this new activity interferes with agriculture and the land allocated to agricultural production $1 - \eta\omega$ also diminishes. Thereby, the two productivity factors, being land allocated to agriculture and energy, decrease, resulting in a diminution of production. However, consumption increases before converging to its steady state value. Indeed, developing renewable through investments implies a sacrifice on consumption and reduces production, but reducing the use fossil fuels avoid the economy to spend for energy production costs. The overall dynamic resulting in an increase in the consumption level. On the long run the different variables of the problem converges to the interior steady state given in Proposition 1.

We run similar simulation but for an initial stock of renewable energy above the equilibrium level ω_m. This could reflect situations for instance in which renewable energy has improved and would therefore lead to a new equilibrium in land use. Here $\omega(0) = \frac{\hat{\omega}}{2} > \omega_m$ where $\hat{\omega}$ is the maximum amount of renewable energy that can be installed due to the land availability constraint $l(\hat{\omega}) = 1$. Results are gathered in Appendix in Figure 8. In our model we supposed reversible investments in the stock of renewable energy, meaning that $\dot{\omega}$ can be negative. Moreover, the uninstallation of renewable energy is cost free and can be directly consumed. This could for instance be the case in which biomass is fed to livestock instead of being used to produce renewable energy. Therefore, if the initial level of renewable energy is above equilibrium, the economy reduces the stock of renewable energy in order to save space for agriculture production, leading to an increase in agricultural land use. Moreover, to compensate the loss of renewable energy, the economy increases its use of fossil fuels which lead to an overall increase in energy production. Therefore, as the two productivity factor increase, production levels also increase. Yet, consumption decreases as energy production has a greater cost due to an increase in the use of fossil fuels.

3 Integrating environmental externalities

In the previous section we develop a model in which social planner does not account for pollution externalities due to the use of fossil fuels. As a result, the only incentive to invest in renewable energy in the preivous *market problem* is the price π of fossil fuels. Yet, fossil fuels' market price does not necessarily integrates the economic negative externalities due to the use of such pollutant sources of energy. We here develop a

model in which social planner accounts for pollution emission. We analyse how the land use equilibrium differs when pollution has an impact on the economy, and derive the tax that integrates pollution externalities in the *market problem* of Section 1.

3.1 Social planner's problem

We extend the framework of the *market problem* from Section 1, in which energy is produced by both renewable energy $\nu\omega$ and fossil fuels b, by considering that pollution is now emitted from the use fossil fuels. In order to simplify the analysis, we do not consider that agricultural production is responsible for any pollution emissions.[11] Therefore the only source of pollution in our model is the use of fossil fuels b. In such framework, we write the accumulation of pollution stock P in the most common description used in the literature[12] that is:

$$\dot{P} = \gamma b - \delta P,$$

where the emissivity coefficient $\gamma > 0$ captures how much the use of one unit of fossil fuels emits pollution, and the coefficient $\delta > 0$ the natural absorption of pollution into the atmosphere.

It is common to normalize the emissivity coefficient as in Farzin et al. (1996) or Chakravorty et al. (2008). Yet, in the following, we assess the impact of emissions from the use of fossil fuels on the land use distribution reached at equilibrium and therefore do not choose to normalize this coefficient. The emissivity coefficient γ depends on the nature and technology of the fossil fuels ressource used by the economy. For instance, emissions from coal-power plants in the US are, on average, around 1000g/kWh, whereas for gas, it drops to 500g/kWh.[13] Regarding, the natural absorption coefficient δ, we suppose here a linear natural decay of pollution as in the above cited literature. Such description is subject to discussion as mentioned in Farzin et al. (1996), in which the authors specify more accurately the natural decay of pollution according to climate models (Maier-Raimer et al., 1987). Yet we choose here the linear description, as a first approximation, in order to keep the model analytically tractable.

Similarly, in order to obtain a closed form formula for the land use equilibrium in

[11] We therefore neglect all pollution emissions from transports, manufacturing process, or livestock emissions from the agricultural sector.

[12] see Kverndokk (1994), Sinclair (1994), Ulph et al. (1994) or Farzin et al. (1996) among others.

[13] See Dones et al. (2003) for a more complete review on the emissivity of different energy sources.

this new framework, we suppose linear damages of pollution on production.[14] Thereby, we suppose that the stock of accumulated pollution impacts negatively agricultural production such that production net from pollution damages writes as:

$$F(1 - l(\omega), b + \Gamma(\nu, \omega)) - \theta P,$$

where $\theta > 0$ captures the agricultural production sensitivity to pollution. Hence, in our description of production damages, it is the stock of pollution that impacts production and not the flow.[15]

Therefore, under such description of pollution accumulation and agricultural production damages, and under the specifications on the model's parameters given in Assumptions 1, social planner's problem now writes as:

$$\max_{\{c,b\}} \int_0^\infty \frac{c^{1-\sigma}}{1-\sigma} e^{-\rho t} \mathrm{d}t,$$

$$\text{s.t.} \begin{cases} \dot{\omega} = A(1 - \eta\omega)^\alpha (b + \nu\omega)^\beta - \theta P - c - \pi b, \\ \dot{P} = \gamma b - \delta P, \\ c \geq 0 \; ; b \geq 0 \; ; P \geq 0 \text{ and } 0 \leq \omega \leq \hat{\omega}, \\ (\eta, \nu, \pi, \theta, \gamma, \delta) \in \mathbb{R}_+^6. \end{cases}$$

In the following, this problem will be referred to as the *environmental problem*. We solve the *environmental problem* in the following section and discuss on its solutions' steady states. More specifically, we look at the impact of pollution through the parameters γ, δ and θ on the land use distribution reached at the equilibrium. We also prove, as for the *market problem* of Section 1, that the equilibrium for the *environmental problem* is saddle-path stable.

3.2 Steady state analysis

3.2.1 Optimal land use policy for the environmental problem

Beforehand we shall make the following assumption regarding fossil fuels price before analyzing the longterm equilibrium in land use for the *environmental problem*.

[14] Non-linear damage function have been tested on this model but such specifications lead to non-tractable equilibriums.

[15] The general specification being that pollution damages on production come from both the stock and the flow of pollution as in Farzin et al. (1996) or Chakravorty et al. (2008) among others.

Assumption 3. $\pi > \frac{\rho}{\nu} - \frac{\gamma\theta}{\rho+\delta}$ *where* γ *is the emissivity of fossil fuels,* θ *agricultural production sensitivity to pollution and* δ *pollution natural absorption coefficient.*

We provide next with the optimal land allocation towards renewable energy production in the *environmental problem*, that is, when the stock of pollution P impacts agricultural production and therefore is, along with the cost of fossil fuels π, the other incentive for investing in the development of renewable energy.

Proposition 5. *Under assumptions 1 and 3 there exists a unique saddle-path stable interior steady state for land use* l_e *given by:*

$$l_e = 1 - \left(\frac{A\alpha\eta \left(\frac{A\beta}{\pi + \frac{\gamma\theta}{\rho+\delta}} \right)^{\frac{\beta}{1-\beta}}}{\nu \left(\pi + \frac{\gamma\theta}{\rho+\delta} \right) - \rho} \right)^{\frac{1-\beta}{1-\alpha-\beta}}.$$

The optimal land use policy l_e *at the environmental equilibrium increases with respect to production sensitivity to pollution* θ *and fossil fuels emissivity* γ*, and decreases with respect to atmospheric absorption* δ*.*

We denote the equilibrium derived in Proposition 5 as the *environmental equilibrium* as pollution is now, along with fossil fuels price, an incentive to development and allocate land to renewable energy. As in the *market problem*, there is a price threshold for the use of fossil fuels above which investments and land allocation to renewable energy production are triggered. The price threshold for the *environmental problem* writes as:

$$\pi_e = \frac{\rho}{\nu} - \frac{\gamma\theta}{\rho+\delta} = \pi_m - \frac{\gamma\theta}{\rho+\delta},$$

where π_m is the price threshold triggering renewable energy investments in the *market problem*. Note that as $\frac{\gamma\theta}{\rho+\delta} > 0$ then $\pi_e < \pi_m$. Therefore, the term $\frac{\gamma\theta}{\rho+\delta}$, which captures the impacts of pollution on agricultural production due to the use of fossil fuels, lowers the price threshold in the *environmental problem*. More generally, as emissivity and sensitivity increases, or as the natural absorption coefficient decreases, the price threshold diminishes. This highlights that pollution, by lowering the price threshold, acts as a new incentive to invest in the energy shift. The effect of the discount rate on the price threshold is left unchanged compared to the *market problem*, as a less altruistic planner towards future generations delays investments in energy shift by increasing π_e

as it does for π_m. Yet, the more altruistic is social planner towards future generation, the more the threshold from the *environmental problem* diverges from the one of the *market problem* as pollution accumulation lowers future generations' welfare.

Pollution not only diminishes the price threshold, but also modifies the land use equilibrium. Indeed, the land allocated to produce renewable energy is greater in the *environmental problem* than it is in the *market problem*. More generally, the more pollution has an impact on the economy through an increase of emissivity or sensitivity, or a decrease in absorption, the more land shall be allocated to renewable energy production rather than to agriculture. Integrating pollution in social planner's problem have two effects: lowering the threshold price for investments in the energy shift and shifting the land use equilibrium towards more renewable energy production at the expense of agriculture.

Note that in extreme cases, for very high θ or γ, then l_e converges to 1, that is, all land shall be allocated to renewable energy production. Yet this upper limit is never reached for finite θ and γ. In the opposite case when the economy shows little sensitivity to pollution *i.e.* $\theta \to 0$ then the price threshold and the land use policy of the *environmental problem* coincides with the one from the *market problem*. This results holds if the use of fossil fuels emits few pollution *i.e.* $\gamma \to 0$ or if natural absorption of pollution is infinite $\delta \to \infty$. Indeed, in the *market problem*, it is *as if* the economy is either not sensitive to pollution, the use of fossil fuels does not emit pollution or atmosphere absorbes pollution at an infinite rate.

A	Technology	150
ρ	Time discount rate	0.01
α	Land productivity	0.1
β	Energy productivity	0.1
ν	Renewable efficiency	3
σ	Utility parameter	5
η	RNE land needs	0.01
γ	Emissivity	5
π	Fossil fuel price	0.1
δ	Natural absorption	1

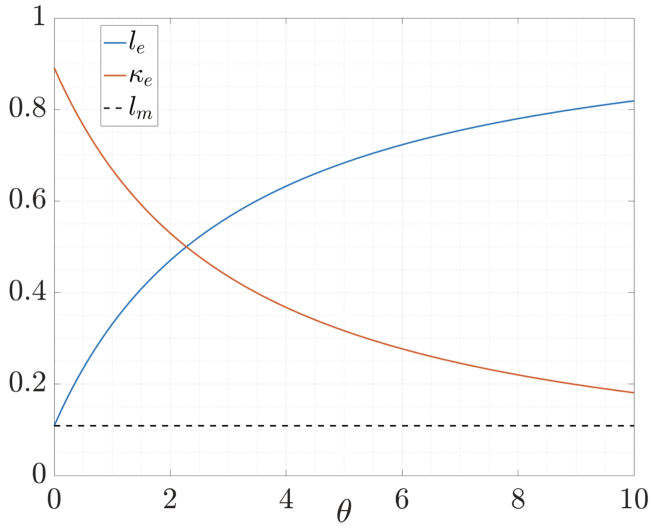

Figure 4: Land use policies from the market and the *environmental problem* diverging as pollution sensitivity increases.

Figure 4 compares the land use equilibrium from the *environmental problem* with the *market equilibrium* for different pollution sensitivities θ.[16] As stated above, the two land use equilibrium coincides when the economy of the *environmental problem* is strictly insensitive to pollution, that is when $\theta = 0$. Yet, for $\theta > 0$ the land allocated to renewable energy production in the *environmental problem* is greater than for the *market problem*, and the two policies diverge as sensitivity increases. Finally for extreme sensitivities the land allocated to renewable energy production converges towards its upper limit being all the available land, without ever reaching this limit.

3.2.2 Steady state energy mix implications

Having characterize the optimal land allocation towards renewable energy production, we now study the optimal energy mix associated to the land use distribution at the *environmental equilibrium*.

Proposition 6. *Under Assumptions 1 and Assumption 3 there exists a unique interior saddle-path stable energy mix steady state* (ω_e, b_e) *for the environmental problem such that:*

$$\begin{cases} \omega_e = \frac{l_e}{\eta} = \frac{1}{\eta}\left[1 - \left(\frac{A\alpha\eta\left(\frac{A\beta}{\pi+\frac{\gamma\theta}{\rho+\delta}}\right)^{\frac{\beta}{1-\beta}}}{\nu\left(\pi+\frac{\gamma\theta}{\rho+\delta}\right)-\rho}\right)^{\frac{1-\beta}{1-\alpha-\beta}}\right], \\ b_e = \left[\frac{A\beta(1-l_e)^{\alpha}}{\pi+\frac{\gamma\theta}{\rho+\delta}}\right]^{\frac{1}{1-\beta}} - \frac{\nu}{\eta}l_e. \end{cases}$$

The use of renewables (resp. fossil fuel) at steady state increases (resp. decreases) with respect to production sensitivity to pollution θ *and fossil fuels emissivity* γ *and decreases (resp. increases) with respect to atmospheric absorption* δ.

From the previous analysis of the effect of pollution on land use in the *environmental equilibrium*, studying the effect of pollution on the energy mix is straightforward. From the previous section, we know that pollution shifts the land use equilibrium towards more land allocated to renewable energy production. Therefore, as $\omega_e = \frac{l_e}{\eta}$, then the use of renewable energy increases as pollution impacts negatively the economy. In contrast, pollution externalities tends to decrease the use of fossil fuels as, in our model, the only source of pollution is the use of fossil fuels in the energy mix.

[16] The parameters are taken for illustrative purposes. A calibrated analysis is proposed in Section 4.3.

As, pollution damages the economy, social planner decreases the use of fossil fuels in order to spare the economy from environmental damages. Finally, the overall energy production at steady state is given by $b_e + \nu\omega_e = \left[\frac{A\beta(1-l_e)^\alpha}{\pi+\frac{\gamma\theta}{\rho+\delta}}\right]^{\frac{1}{1-\beta}}$. As pollution reduces the land allocated to agriculture $1 - l_e$, it also reduces energy production. Therefore, pollution tends to reduce the overall production of the economy as the two factors of productivity decreases as the impacts of pollution becomes more consequent through either an increase in sensitivity for high θ or an increase in the accumulated pollution for high γ or low δ.

3.2.3 Consumption and pollution

As in Section 1, we study here the land allocation distribution which maximizes steady state consumption for the *environmental problem* and discuss on the effect of the discount rate regarding the maximization of long-run consumption. Moreover, we also study the existence of an optimal land allocation policy which minimizes the stock pollution reached at the *environmental equilibrium*.

Proposition 7. *Steady state consumption c_e increases w.r.t. the land allocated to renewable energy production l_e. Moreover, the land policy l_{g_e} for renewable energy production:*

$$l_{g_e} = 1 - \left(\frac{A\alpha\eta \left(\frac{A\beta}{\pi+\frac{\theta\gamma}{\rho+\delta}} \right)^{\frac{\beta}{1-\beta}}}{\nu\left(\pi + \frac{\theta\gamma}{\delta}\right)} \right)^{\frac{1-\beta}{1-\alpha-\beta}},$$

maximizes steady state consumption.

Comparing the stock of renewable energy that maximizes consumption to the stock of renewable at steady state derived in Proposition 5 leads to:

$$l_{g_e} - l_e = \left(A\alpha\eta \left(\frac{A\beta}{\pi + \frac{\gamma\theta}{\rho+\delta}} \right)^{\frac{\beta}{1-\beta}} \right)^{\frac{1-\beta}{1-\alpha-\beta}} \underbrace{\left[\frac{1}{\left(\nu\left(\pi + \frac{\theta\gamma}{\delta+\rho}\right) - \rho\right)^{\frac{1-\beta}{1-\alpha-\beta}}} - \frac{1}{\left(\nu\left(\pi + \frac{\theta\gamma}{\delta}\right)\right)^{\frac{1-\beta}{1-\alpha-\beta}}} \right]}_{>0} > 0.$$

As social planner accounts more for present generations than for future generations, that is $\rho > 0$, we get that the level of renewable energy that would maximize long-run consumption is higher than the one reached at steady state. Thereby, the effect of

the discount rate on the stock of renewable energy ω_e is similar to the one identified and analyzed in the *market problem* from Section 1. We study next the existence of an interior land use policy which minimizes long-run pollution as for steady state consumption.

Proposition 8. *Pollution P_e at the environmental equilibrium is given by:*

$$P_e = \frac{\gamma b_e}{\delta} = \frac{\gamma}{\delta}\left(\left[\frac{A\beta\left(1-l_e\right)^{\alpha}}{\pi+\frac{\gamma\theta}{\rho+\delta}}\right]^{\frac{1}{1-\beta}} - \frac{\nu}{\eta}l_e\right).$$

The stock of pollution at equilibrium decreases w.r.t. to renewable energy land use l_e. Yet no interior renewable energy land policy minimizes steady state pollution.

In the case of steady state pollution there is no interior land allocation regarding renewable energy production that minimizes pollution. Indeed, as the land allocated to renewable energy increases then the use of fossil fuels decreases and thus pollution decreases as well. Therefore, pollution is minimal when all the available land is allocated to renewable energy. This is not a relevant land use policy as, in such case, there is no production in the economy as all land is allocated to renewable energy and none to agricultural production.

3.3 Fiscal integration of pollution in the market problem

In Section 2, we derive the land use equilibrium for the *market problem*, that is when social planner does not accounts for production damages due to pollution and when investments in renewable energy are only driven by market forces being the price of fossil fuels π. We showed in this section that, when social planner accounts for pollution damages, the land use equilibrium is shifted towards an equilibrium allocating more land to renewable energy production, and thereby less land to agriculture.

Proposition 9. *When the price of fossil fuels π in the market problem is adjusted by a tax $\tau = \frac{\gamma\theta}{\rho+\delta}$ to the price $\pi' = \pi + \frac{\gamma\theta}{\rho+\delta}$ then the land use equilibrium for the market problem coincides with the one from the environmental equilibrium.*

When taking into account pollution damages on the agricultural production in the *environmental problem*, the economy converges towards a steady state in which land allocated to renewable energy is greater than the one obtained in the *market problem*.

This means that, if the market price π of fossil fuels does not take into account the information of pollution damages on production, then the equilibrium in the *market problem* will be suboptimal as the stock of renewable energy at steady state will not be important enough to compensate for the production losses due to pollution damages.

In order to fix such market failure, Proposition 9 provides with the tax $\tau = \frac{\gamma\theta}{\rho+\delta}$ on fossil fuels such that, adjusting the fossil fuels market price π to $\pi + \tau$ redresses the *market equilibrium* to the *environmental equilibrium*. Pollution externalities are internalized in the *market problem* through the tax $\tau = \frac{\gamma\theta}{\rho+\delta}$. Finally, note that as the natural absorption coefficient δ decreases or pollution emissivity γ or sensitivity θ increases then the taxe τ increases. Indeed, as the impact of pollution on production becomes more important, then the market failure from not accounting for pollution damages in fossil fuels market price becomes more consequent, and the *market equilibrium* becomes more and more suboptimal. Therefore, the tax on fossil fuels must increase as the *market equilibrium* deviates from optimality.

4 Pollution abatement implications

In the previous sections, the only climate change mitigation measure is the development of renewable energy production through investments. In the following, we extend the previous framework of the *environmental problem* by considering a second mitigation policy that is pollution abatement. This additional mitigation policy competes with renewable energy production for land in order to reduce pollution and minimize production damages. Therefore, in this section, we study the land use distribution between, production, renewable energy and abatement, and analyse the trade-offs in land between the two mitigation measures.

4.1 Social planner's problem

The Kyoto Protocol clearly highlights the benefits of abatement activity through carbon sequestration in agricultural soil or forests. In order for countries to comply to their national commitments, the agreement allows parties to deduce from their global carbon footprint their emissions sequestered by these additional mitigation measures.[17] Among

[17]See Article 3.3 and Article 3.4 of the Kyoto Protocol for the modalities on how to include abatement activities into the accounting of national commitments.

the eligible abatement activities[18], we focus here on afforestation and reforestation, that is, the conversion of non-forest land to forests. It is estimated that between 60 to 87 Gt of carbon could be absorbed by such activities during the period between 1995 and 2050 (Brown et al., 1996), being therefore a considerable carbon sink yet to be exploited. However, the benefits from allocating land to forestry come with the cost of abandoning the opportunities of the previous activity, for instance agriculture. Moreover, if abatement is one mitigation measure among others, how should land be allocated between the different land-intensive mitigation activities ?

In this section we explore these land use trade-offs by extending the framework from the *environmental problem* with an abatement activity, which is, as renewable energy production and agriculture, land demanding. In such framework, the accumulation of pollution now writes as in Camacho and Pérez-Barahona (2015), that is:

$$\dot{P} = \gamma b - \delta P - f(\xi),$$

where $f(\xi)$ is the amount of pollution that is absorbed by an abatement site, such as a forest, occupying a quantity $0 < \xi < 1$ of land. The land allocated to renewable energy is still $\eta\omega$, and thus, the remaining land that can be allocated to agriculture is here $1 - \xi - \eta\omega$. Therefore, production net from pollution damages now writes as:

$$F(1 - \xi - \eta\omega, b + \nu\omega) - \theta P.$$

Therefore, under the specifications from Assumptions 1, and with the integration of abatement into the *environmental problem*, social planner's problem now writes as:

$$\max_{\{c,b,\xi\}} \int_0^\infty \frac{c^{1-\sigma}}{1-\sigma} e^{-\rho t} \mathrm{d}t,$$

$$\text{s.t.} \begin{cases} \dot{\omega} = A(1 - \xi - \eta\omega)^\alpha (b + \nu\omega)^\beta - \theta P - c - \pi b, \\ \dot{P} = \gamma b - \delta P - f(\xi), \\ c \geq 0 \; ; b \geq 0 \; ; P \geq 0 \text{ and } 0 \leq \omega \leq \hat{\omega}, \\ (\eta, \nu, \pi, \theta, \gamma, \delta) \in \mathbb{R}^6_+. \end{cases}$$

This extension of the *environmental problem* will be referred to as the *abatement problem*. We solve the *abatement problem* in the following section and discuss on its solutions' steady states as well as on the trade-off in land allocation between the two available mitigation policies being renewable energy and abatement.

[18]For the list of eligible activities see IPCC (2000).

4.2 Steady state analysis

4.2.1 Optimal land use policy and trade-offs

Beforehand we make the final assumption on the abatement capacity with respect to land use, as in Camacho and Pérez-Barahona (2015).

Assumption 4. *Abatement has decreasing return to scale with respect to land such that* $f(\xi) = \mu\xi^{\epsilon}$ *with* $\mu > 0$ *and* $\epsilon < 1$.

For instance, this could reflect the situation in which a forest absorbs the pollution emitted by fossil fuels ressources while occupying considerable land. In order to absorb the emitted CO_2 from the use of fossil fuels, the wood ressource needs to be exploited (without being burnt, as it would release all the absorbed pollution) by the wood sector. Yet, as the quantity of wood rises the demand for wood can no longer absorb all the exploited ressource and therefore the pace of exploitation diminishes. As a result, the abatement capacity of the forest also marginally decreases as the forest grows and occupies more land.

We provide next with the optimal land allocation for agriculture, abatement activity, and renewable energy production reached at the equilibrium and study the trade-offs in land use between the productive lands (agriculture and renewable energy) and the climate mitigation lands (abatement and renewable energy).

Proposition 10. *Under assumptions 1 and 3 and 4 there exists a unique saddle-path stable interior steady state for land use and the optimal land allocation for agriculture production is given by:*

$$\kappa_a = \left[A \left(\frac{\eta}{\nu} \cdot \frac{\alpha}{(\pi - \pi_e)} \right)^{1-\beta} \left(\frac{\beta}{\pi + \frac{\gamma\theta}{\rho+\delta}} \right)^{\beta} \right]^{\frac{1}{1-\alpha-\beta}},$$

the optimal land allocation for abatement is given by:

$$\xi_a = \left[\mu\epsilon \cdot \frac{\eta}{\nu} \cdot \frac{\theta}{(\rho+\delta)(\pi - \pi_e)} \right]^{\frac{1}{1-\epsilon}},$$

and the land allocated to renewable energy production is therefore:

$$l_a = 1 - \xi_a - \kappa_a,$$

where π_e *is the price threshold introduced in Section 2 as* $\pi_e = \frac{\rho}{\nu} - \frac{\gamma\theta}{\rho+\delta}$.

As in the previous *market problem* and *environmental problem*, renewable energy and agricultural production both compete for land to produce output. The renewable energy land use density $\frac{\nu}{\eta}$ appears in the expression of agricultural land of Proposition 10 in the same way as for the previous problems. That is, we also have in the *abatement problem* that, the more efficient is renewable energy technology, that is the more important is its energy density $\frac{\nu}{\eta}$, the less land shall be allocated to agricultural production.

Moreover, renewable energy density intervenes in a similar way in the expression of the land allocated to abatement at steady state. Indeed, renewable energy also competes for land with the abatement activity, but this time not for output production, but in order to reduce pollution emissions from the use of fossil fuels. As a result, we get that the more dense is the renewable energy production, the more land should be allocated to its production in order to avoid pollution emission rather than to the abatement activity. Yet, the efficiency μ of abatement also impacts the steady state land distribution. Indeed, for very efficient abatement activities, that is for high μ, the land allocated to abatement rises, reducing consequently the land allocated to renewable energy. Thereby the trade-off between abatement and renewable energy in order to reduce pollution is here clearly identified analytically through the balance between the term μ, characterizing abatement efficiency, and the intensity term $\frac{\nu}{\eta}$, characterizing renewable energy efficiency, in the expression of land allocated to abatement. As a result, social planner allocates more land to the most efficient mitigation measure between abatement and renewable energy production.

Finally, as in the previous *environmental problem*, the land allocated to agriculture diminishes as production becomes more damageable by pollution emissions (that is through an increase in production sensitivity θ or fossil fuels emissivity γ, the two playing symmetric roles in the expression of κ_a). Yet, in the *environmental problem*, as production sensitivity increases, the land taken from the agricultural production would be entirely reallocated to the only mitigation policy available being renewable energy. Here, in the *abatement problem*, the land taken from the agriculture can be reallocated to either pollution abatement, renewable energy production or to both with different marginal allocations as production sensitivity rises. In the following, we therefore study the land reallocation trade-offs from agricultural production to mitigation measures as production sensitivity to pollution increases.

First of all, when the economy is strictly not sensitive to pollution, that is for $\theta = 0$,

we get from the expression of abatement in Proposition 10 that $\xi_a(\theta = 0) = 0$. Indeed, in such case, pollution emissions do not damage the economy, and thus no land should be sacrificed for abatement activities. Note that even if the economy is not sensitive to pollution, we get that $\kappa_a(\theta = 0) < 1$. Indeed, land is still allocated to renewable production, yet not for mitigation purposes, but as the alternative to costly fossil fuels energy production.

We now study the case for $\theta > 0$. First of all, from the expression of the abatement policy in Proposition 10 we get that ξ_a disposes of an inflection point with respect to pollution sensitivity that we denote as $\hat{\theta}$ and make the following assumption.

Assumption 5. *The set of parameters is such that* $\forall \theta \geq \hat{\theta}\ \xi_a'(\theta) + \kappa_a'(\theta) > 0$ *with,* $\hat{\theta}$ *the inflection point of abatement policy with respect to pollution sensitivity.*

Under assumption 5 and for fossil fuels prices $\pi > \pi_m$ we claim the following statement.

Proposition 11. *The land* ξ_a *allocated to abatement activity always increases with respect to production sensitivity to pollution, whereas the land allocated to renewable energy* l_a *increases when sensitivity is bellow a threshold, and diminishes beyond.*

Hence, as the economy becomes more sensitive to pollution, social planner reduces the land allocated to the agricultural production and a part of this land shall always be reallocated to abatement activity regardless of the sensitivity level of production. Under a sensitivity threshold $\tilde{\theta}$ the remaining land is allocated to renewable energy production. Yet, above this threshold, the production sensitivity is such that social planner reduces the land allocated to both agriculture and renewable energy production and reallocates all the land to pollution abatement activities.

A	Technology	145
ρ	Time discount rate	0.01
α	Land productivity	0.05
β	Energy productivity	0.05
ν	Renewable efficiency	1.1
σ	Utility parameter	5
η	RNE land needs	0.01
γ	Emissivity	0.1
π	Fossil fuel price	0.1
δ	Natural absorption	1
μ	Abatement efficiency	20
ϵ	Abatement productivity	0.8

Table 2: Parameter values

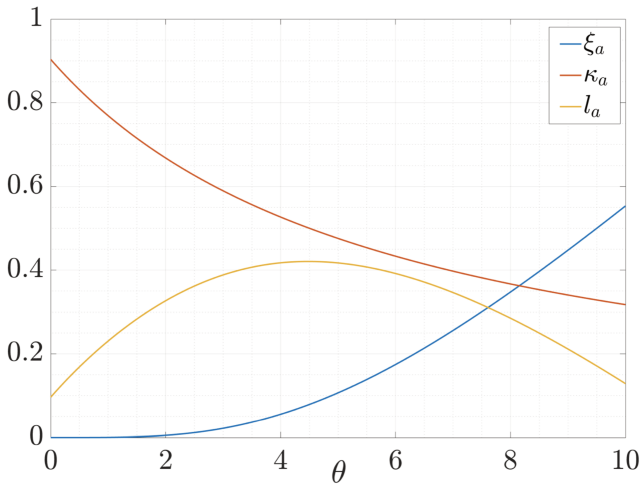

Figure 5: Reallocation of agricultural land towards the two mitigation activities.

As a result, social planner prioritizes pollution reduction measures to save the economy rather than production for extreme pollution damages as depicted in Figure 5. For instance, with the set of parameters from Table 2[19], when the economy is not sensitive to pollution, that is for $\theta = 0$, then 90% of available land is allocated to agricultural production, and the remaining 10% to renewable energy as no land is allocated to abatement. For sensitivity values in between 0 and 4.1, the land allocated to agricultural production is reallocated to the two mitigation measures, that are renewable energy production and abatement. Yet for low sensitivities, the reallocation is mostly done towards renewable energy production in order to both mitigate pollution and compensate the loss of output due to the reduction in agricultural land by increasing energy production. As sensitivity increases, pollution mitigation becomes the priority for social planner compared to the other imperative that is the conservation of production. Above the sensitivity threshold $\tilde{\theta} = 4.1$, both land allocated to agriculture and renewable energy production diminishes and land is entirely reallocated towards pollution abatement. Hence, social planner's strategy for land use reallocation depends on the level of production sensitivity to pollution. For low sensitivity, agricultural land is reallocated towards both renewable energy (for mitigation purposes and compensation of production losses) and abatement (only for mitigation). Yet, for high sensitivities, along with agricultural land, it is also best to sacrifice renewable energy production land and reallocate exclusively land to abatement in order to save output from important pollution damages.

4.2.2 Land use abatement golden rule

In this last section we study the abatement land use policies which respectively minimize steady state pollution and maximize steady state consumption and compare such abatement policies to the endogenous policy ξ_a from Proposition 10.

Proposition 12. *The abatement land use policy ξ_P minimizing steady state pollution is given by:*

$$\xi_P = \left(\frac{\eta\mu\epsilon}{\gamma\nu}\right)^{\frac{1}{1-\epsilon}},$$

and the abatement land use policy ξ_c maximizing steady state consumption is given by:

$$\xi_c = \left(\frac{\theta\eta\mu\epsilon}{\delta\nu\left(\pi + \frac{\gamma\theta}{\delta}\right)}\right)^{\frac{1}{1-\epsilon}}.$$

[19]The parameters are taken for illustrative purposes. A calibrated analysis is proposed in Section 4.3

As we found two different policies ξ_P and ξ_c respectively minimizing steady state pollution and maximizing steady state consumption, the first question is: how these two abatement policies compete with each other ? In other words, to what extent maximizing consumption can be articulated with minimizing pollution ? This question can be assessed by examining the expression of the policies from Proposition 12 and rewriting the optimal abatement policy in consumption as:

$$\xi_c = \left(\frac{\theta\eta\mu\epsilon}{\delta\nu\left(\pi + \frac{\gamma\theta}{\delta}\right)}\right)^{\frac{1}{1-\epsilon}} = \left(\frac{\eta\mu\epsilon}{\gamma\nu}\right)^{\frac{1}{1-\epsilon}} \left(\frac{\theta}{\delta\left(\frac{\pi}{\gamma} + \frac{\theta}{\delta}\right)}\right)^{\frac{1}{1-\epsilon}} = \xi_P \left(\frac{1}{1 + \frac{\delta\pi}{\gamma\theta}}\right)^{\frac{1}{1-\epsilon}}.$$

From the above equation we first see that, as $\left(\frac{1}{1+\frac{\delta\pi}{\gamma\theta}}\right)^{\frac{1}{1-\epsilon}} < 1$, we get that $\xi_c < \xi_P$. Thereby, it takes less abatement to maximize steady state consumption than to minimize steady state pollution, meaning that pollution minimization policies are more demanding in abatement land than consumption policies. Moreover as $\frac{\delta\pi}{\gamma\theta}$ goes to zero, the abatement policy maximizing steady state consumption converges to the one minimizing pollution. Indeed, as δ gets smaller or γ increases, pollution is being accumulated at a higher rate because more pollution is being emitted by the use of fossil fuels, and less is being naturally absorbed into the atmosphere. This implies an increase in pollution and thus an increase in production damages, reducing therefore consumption. Hence, as δ decreases or γ increases, maximizing consumption and minimizing pollution objectives become correlated, which conciliates the two abatement policies. Similarly as the production sensitivity θ to pollution increases, the less important will be consumption at steady state, which also conciliates the two abatement policies. Finally, as the price of fossil fuels π goes to zero, the negative impact on consumption of using fossil fuels will only be due to pollution. As a result a reduction in the price of fossil fuels as well conciliates the two abatement policies in consumption and pollution.

We now compare these abatement policies with the one from the social planner's problem ξ_a from Proposition 10. Writing the planner's abatement policy with respect to ξ_P leads to:

$$\xi_a = \left[\mu\epsilon \cdot \frac{\eta}{\nu} \cdot \frac{\theta}{(\rho+\delta)(\pi - \pi_e)}\right]^{\frac{1}{1-\epsilon}} = \xi_P \left(\frac{1}{1 + \frac{\rho+\delta}{\gamma\theta}\left(\pi - \frac{\rho}{\nu}\right)}\right)^{\frac{1}{1-\epsilon}}.$$

Thereby, the relative position of ξ_a with respect to ξ_P depends on the price π of fossil fuels relatively to the price threshold $\pi_m = \frac{\rho}{\nu}$ of the *market problem* from Section 1

and:

- if $\pi > \pi_m = \frac{\rho}{\nu}$ then $\frac{\rho+\delta}{\gamma\theta}\left(\pi - \frac{\rho}{\nu}\right) > 0$ and thus $\xi_a < \xi_P$,
- if $\pi = \pi_m$ then $\xi_a = \xi_P$,
- if $\pi < \pi_m$ then $\xi_a > \xi_P$.

Moreover, if $\rho \to 0$ then we get that $\xi_a \to \xi_P \left(\frac{1}{1+\frac{\delta\pi}{\gamma\theta}}\right)^{\frac{1}{1-\epsilon}} = \xi_c$. Thereby, As for renewable energy land use policy, the land use for abatement which minimizes steady state consumption is not reached at steady abatement because planners accounts less for future generations than for present generations as $\rho > 0$. Finally, writing the planner's abatement policy with respect to ξ_c leads to:

$$\xi_a = \xi_c \left(\frac{1}{1 + \frac{\rho}{\gamma\theta+\delta\pi}\left(\pi - \frac{\rho+\delta}{\nu}\right)}\right)^{\frac{1}{1-\epsilon}}.$$

Therefore, the relative position of ξ_a with respect to ξ_c also depends on the price π of fossil fuels, but this time relatively to the threshold $\frac{\rho+\delta}{\nu}$, such that:

- if $\pi > \frac{\rho+\delta}{\nu}$ then $\frac{\rho}{\gamma\theta+\delta\pi}\left(\pi - \frac{\rho+\delta}{\nu}\right) > 0$ and thus $\xi_a < \xi_c$,
- if $\pi = \frac{\rho+\delta}{\nu}$ then $\xi_a = \xi_c$,
- if $\pi < \frac{\rho+\delta}{\nu}$ then $\xi_a > \xi_c$.

Hence, the relative position of social planner's abatement policy ξ_a with respect to ξ_c and ξ_p depends of fossil fuels price and is summarized in Figure 6.

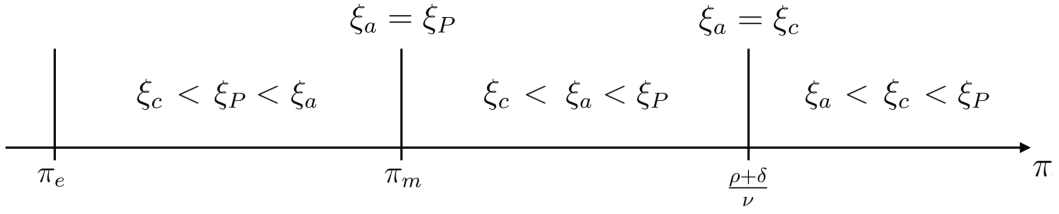

Figure 6: Abatement policies comparison for different fossil fuels prices.

As fossil fuels price increases, the use of renewable energy rises, thereby reducing the part of fossil fuels in the energy mix. As a result, pollution emissions diminishes and thus the need to allocate land to pollution abatement diminishes as well. As a result, for low fossil fuels prices, that is for $\pi_e < \pi < \pi_m$, planner's abatement policy ξ_a must be important and thus above both ξ_c and ξ_P. For intermediate fossil prices, that is $\pi_m < \pi < \frac{\rho+\delta}{\nu}$, planner abats more than the consumption maximizing policy, yet less than the pollution minimizing policy. Finally, high fossil prices, $\pi > \frac{\rho+\delta}{\nu}$, leads to few abatement activity and thereby planner shall abat less than the two policies ξ_c and ξ_P.

5 Palm oil biodiesel in Brazil and the Amazonia

In this final section, we propose an application of the *abatement problem* to the stakes of preserving the Amazon forest in Brazil. More particularly, we focus on the emerging market of palm oil production for biodiesel in Brazil and on the resulting opportunity cost for Brazil of preserving Amazonia.

5.1 The development of a sector and its limitation

Palm oil production was first introduced to the food, hygiene and chemical industries, and is still widely used today as the demand in 2013 in such industries grew up to 55.3 million tons worldwide, accounting for 40% of all vegetable oil production (USDA, 2013). Yet, since the early 2000's, a vast and new market of palm oil production for biodiesel is and has been expanding (Villela et al., 2014; Brandão et al., 2019) such that, in 2012, 5.6 millions tons of palm oil were produced as biodiesel. In Europe for instance, the part of palm oil importation used as biodiesel has continuously increased. In 2008, 90% of palm oil importation were used for the the food industry and the 10% remaining were used as biodiesel. In ten years, the trend changed radically as in 2018, 35% of imported palm oil were used in the food industry, and 65% was used for energy (among which 53% were used as biodiesel for motorized vehicles, and 12% to generate heat and electricity (Oil world, 2019)). Hence, this increase in demand for palm oil biodiesel certainly fosters its production worldwide, but also raises new questions regarding its sustainability.

Today, the majority of palm oil is produced in Indonesia and Malaysia. The two countries account for 80% of palm oil production due to the very favorable climate they offer to palm oil culture (Villela et al., 2014). Indeed, the production of palm oil needs high rain-fall throughout the year, as well as regular sunshine rate as offered in tropical areas (César and Batalha, 2013). Such tropical climate can also be found in Brazil, and even though the country holds one of the most important amount of land on which palm oil could be cultivated (Pirker et al., 2016), it is yet a minor producer of palm oil (Villela et al., 2015). Indeed, in 2015 the country accounted for 110 000 hectares of land allocated to palm oil culture (IBGE/SIDRA, 2015) whereas 31.8 million hectares of land have been identified to provide adequate soil and climate for palm oil culture (Ministério da Agricultura, Pecuária e Abastecimento, 2010). Many researches agree on

the very high potential in Brazil of palm oil culture, given the important productivity index (between 3 and 6 thousand kg of oil per hectare) as well as the vast area providing with the right climate conditions for its production (Furlan et al., 2004; Veiga et al., 2005; Villela, 2009). Even the Brazilian Government identified palm oil as the ideal crop for developing Brazil's biodiesel sector, yet the main limitation remains in that most of this land is occupied by the Amazon forest (Pirker et al., 2016). Hence, the development of a palm oil biodiesel sector in Brazil is closely related to the question of the Amazon forest preservation (Yui and Yeh, 2013).

Today, the Amazon forest covers 60% of Brazil's territory, therefore is an important reservoir for palm oil production land. Yet, the forest also participates in regulating global and local climate through its pollution abatement properties, and the emerging market and growing demand for palm oil biodiesel may increase the pressure on Amazon forest conservation. Until today, 17% of Amazonia has been deforested, most of which being in the responsibility of the state of Parà, the same state which provides with the majority of palm oil production in Brazil (INPE, 2013). Such growing pressure on the Amazon forest is likely to continue as the Brazilian Government proposed a plan for the development of palm oil biodiesel in Brazil up to 2030. Indeed, the National Biodiesel Production and Use Program (PNPB) identified the development of palm oil biodiesel as a mean to reduce the use of fossil fuels in the agricultural sector, leading to a reduction of Brazilian fossil fuels importations as well as minimizing local environmental damages (Brandão et al., 2019). More precisely, the plan exposes a domestic biodiesel production scenario in which palm oil biodiesel becomes the main biodiesel produced in Brazil by 2030, providing for 59% of Brazil's biodiesel. The detailed projection from the PNPB is gathered in Table 3 (Villela et al., 2015).

Feedstock	2005	2010	2015	2020	2025	2030
Soybeans	122	1.848	2.394	2.641	3.737	3.394
Palm oil	**5**	**137**	**408**	**1.062**	**2.571**	**5.695**
Castor bean	11	87	150	229	328	451
Sunflower	1	22	35	54	78	50
Total biodiesel production	**139**	**2.095**	**2.988**	**3.987**	**6.714**	**9.644**
Total diesel demand	35.901	41.878	49.698	56.837	67.405	80.146
% of biodiesel	0.4	5	6	7	10	12

Table 3: Brazilian Government domestic biodiesel production scenario (1000 m3).

In the following, we shall focus our analysis on how the development of a palm

oil biodiesel sector in Brazil can indeed be beneficial to Brazil, and in particular by minimizing its local environmental damages due to the use of conventional fossil fuels responsible for local air pollution such as ozone precursors emissions. Yet, such palm oil biodiesel development is done at the expense of Amazon forest land, which also provides global environmental services to the international community ; for instance, through the abatement of global greenhouse gas (GHG) emissions. Hence, in the following, we analyze how Brazilian local interests of sacrificing forested land for its palm oil biodiesel production can go against the internal community's will to preserve the Amazon forest, and how the latter can deal with such conflicting interests by setting-up financial compensation instruments.

5.2 Brazil's opportunity cost for preserving Amazonia

In this section we extend the *abatement problem* by considering two kinds of pollution, both of which can be abated by Amazon forest's preserved areas. The first kind of pollution is a local pollution in Brazil, which comes from the emissions of local pollutants due to the use of conventional fossil fuels in Brazil, typically air pollution from ozone precursors. Such pollution reduces Brazil's agricultural production, which damages are captured by the term θP in the *abatement problem*. As the Amazon forest can abate such local pollution, the forest therefore contributes indirectly to the Brazilian agricultural production by reducing local air pollution damages. Yet, Brazil could also decide to develop a palm oil biodiesel production sector, which would also contributes to the reduction of local air pollution damages by minimizing the use of fossil fuels responsible for the local ozone precursors emissions - yet such alternative can only be done at the expense of preserving forested area and its abatement properties.

Along with local air pollution from the use of fossil fuels in Brazil, we consider a second kind of pollution, being global pollution from the worldwide GHG emissions responsible for global warming. Yet the GHG stakes is a global problem and not only concerns Brazil, but also the international community. Hence, the development of a palm oil biodiesel sector in Brazil - for Brazil's self and only interest - may go against the international community's will to preserve Amazonia for the global GHG abatement services it benefits from. In this section, we consider the case in which the international community can therefore offer financial compensations to Brazil through a transfer mechanism for each hectares of preserved forested land, in order to limit the

Amazon deforestation driven by the development of a Brazilian palm oil biodiesel sector in this region. Such transfer is therefore acting as a direct financial compensation for Brazil's opportunity cost of preserving Amazonia, in the interest of the international community benefiting from global GHG abatement services, rather than developing its palm oil biodiesel sector, for Brazil's own interest.

We study such conflicting interests between Brazil and the international community regarding the preservation of the Amazon forest by adding to Brazil's agricultural production function, a linear transfer term. Hence, considering such transfer, Brazil's agricultural production net from local environmental damage θP now writes as:

$$F(1-\xi-\eta\omega, b+\nu\omega) - \theta P + \tau\xi,$$

where $\tau\xi$ represents the financial transfer due to Brazil from the international community for preserving an area ξ of forested land. Hence, τ (expressed in \$/ha) captures *in fine* Brazil's opportunity cost of conserving hectares of forested land rather than developing its palm oil biodiesel sector on such land. In other words, τ can be seen as the rent due to Brazil from the international community in order to benefit from global pollution abatement by the Amazon forest, while it could have been more beneficial to Brazil to precisely sacrifice such land for developing its palm oil biodiesel production and minimize its local environmental damages due to its local use of fossil fuels. In the following, we provide with the expression of such opportunity cost and calibrate the model on the Brazilian economy in order to evaluate the opportunity cost for Brazil of preserving Amazonia rather than exploiting this land for palm oil biodiesel production.

Proposition 13. *Under Assumptions 1 and 3, the opportunity cost for Brazil for preserving the Amazon forest and scarifying its palm oil biodiesel production writes as:*

$$\tau = \frac{\nu}{\eta}(\pi - \pi_m) + \frac{\theta}{\rho+\delta}\left(\gamma\frac{\nu}{\eta} - \frac{\mu\epsilon}{\xi^{1-\epsilon}}\right),$$

with $\pi_m = \frac{\rho}{\nu}$ is the fossil price threshold from the market problem such that $\pi > \pi_m$.

First of all, note how the opportunity cost τ, as expressed in Proposition 13, writes as the sum of two terms. The first term $\frac{\nu}{\eta}(\pi - \pi_m)$ shall be denoted in the following as the *energy component* of the opportunity cost. Indeed, this component directly reflects the cost of Brazil's missed opportunities from preserving Amazonia rather than allocating forested land to renewable energy production from palm oil biodiesel. The

second term of the opportunity cost writes as $\frac{\theta}{\rho+\delta}\left(\gamma\frac{\nu}{\eta}-\frac{\mu\epsilon}{\xi^{1-\epsilon}}\right)$ and shall be denoted as the *mitigation component* of the opportunity cost. Indeed, forest land can also be used for local mitigation measures, either by using its land for biodiesel production, or through the preservation of forested land for abatement measures. Note how the two mitigation measures compete in the *mitigation component*, and how palm oil biodiesel energy density $\frac{\nu}{\eta}$ intervenes in both the *energy* and the *mitigation component* terms as biodiesel can either be used for energy production or mitigation purposes.[20]

The energy component. The *energy component* of the opportunity cost is captured by the left term of the opportunity cost $\frac{\nu}{\eta}(\pi-\pi_m)$ where $\frac{\nu}{\eta}$ is the renewable energy density, that is the quantity of energy produced by occupied surface land, and π the cost of fossil fuels. Interpreting the *energy component* of the opportunity cost is very straightforward. Indeed, as the Amazon forest is an important potential land source for palm oil biodiesel renewable energy production, the preservation of such land would cost Brazil to continue using fossil fuels at a price π, rather than producing and using renewable energy from palm oil biodiesel culture. Hence, the *energy component* of the opportunity cost gathers all the energy parameters of the model being, the energy density of the land intensive biodiesel energy resource, as well as the price of fossil fuels. Moreover, Assumption 3 ensures that $\pi > \pi_m$, leading therefore to the strict positivity of the *energy component*. Hence, the denser is palm oil biodiesel energy production, that is the greater $\frac{\nu}{\eta}$, the higher becomes the opportunity cost for Brazil of preserving Amazonia, rather than exploiting such land for biodiesel energy production. Indeed, the less the biodiesel provided by palm oil culture is land intensive, the more valuable becomes renewable energy production in Amazonia, and thus the higher gets the opportunity cost for Brazil of preserving the Amazon forest rather than exploiting a potentially energy productive land. Similarly, as the price on fossil fuels π increases, the higher becomes the cost of not using palm oil biodiesel as a renewable energy source, therefore increases as well the opportunity cost of preserving Amazonia.

The mitigation component. The right term of the opportunity cost $\frac{\theta}{\rho+\delta}\left(\gamma\frac{\nu}{\eta}-\frac{\mu\epsilon}{\xi^{1-\epsilon}}\right)$ results from the balance between the two mitigation measures of the problem: the use of biodiesel rather than pollutant fossil fuels, captured by the term $\gamma\frac{\nu}{\eta}$, and the preservation of forested area for abatement measures, captured by the term $\frac{\mu\epsilon}{\xi^{1-\epsilon}}$. These two mitigation measures compete with each other as the substitution of pollutant fossil

[20] See discussion of Proposition 11 on that matter.

fuels through the allocation of forested land to palm oil biodiesel production leads inevitably to deforestation, and reduces mechanically the abatement capacities of the forest. Note how the first term in factor of the *mitigation component* $\frac{\theta}{\rho+\delta}$ is directly linked to production sensitivity to pollution θ. Yet, as θ increases, the *mitigation component* of the opportunity cost can either increase or decrease according to the relative efficiency of the two competing mitigations measures. Indeed, if fossil fuels are very emissive or biodiesel energy production very dense, such that $\gamma\frac{\nu}{\eta} > \frac{\mu\epsilon}{\xi^{1-\epsilon}}$, then scarifying forest land for biodiesel production becomes *in fine* the best mitigation measure for Brazil's interest. In such case, a rise in pollution sensitivity θ leads to an increase in the opportunity cost as the development of biodiesel through the allocation of forested land to palm oil culture is a more efficient pollution mitigation measure, rather than conserving forested land for abatement. On the other hand, if fossil fuels are less emissive, biodiesel energy production less dense, or if the forest abatement capacity if very important such that $\gamma\frac{\nu}{\eta} < \frac{\mu\epsilon}{\xi^{1-\epsilon}}$, then preserving forest land for abatement becomes the best mitigation measure, rather than sacrificing such land to palm oil biodiesel production. In such case, a rise in pollution sensitivity θ leads to a decrease in the opportunity cost as the development of biodiesel through forested land allocation to palm oil culture is a less valuable mitigation measure than preserving Amazonia for abatement.

5.3 Calibrating the model

We now calibrate the model using data for the Brazilian economy in order to evaluate the opportunity cost introduced in Proposition 13. Our exercices are of two kinds. First, we look at the evolution of the opportunity cost with respect to Brazil's crops sensitivity to air pollution for a given forest conservation policy. As the opportunity cost can be seen as the transfer from the international community to Brazil for carbon abatement services from the Amazon forest, we compare the opportunity cost to the price of carbon from different literature. Finally, following the previous theoretical analysis, we characterize the opportunity cost by studying the respective weights of the *energy component* and the *mitigation component* with respect to the model's parameters and pollution sensitivity.

General calibrations. In what follows, we shall use the typical time discount rate of $\rho = 0.03$ from the Interagency Working Group on Social Cost of Carbon reports (EPA, 2010). Moreover, we consider in the following a natural absorption rate for

Brazil's local air pollution of $\delta = 0.01$. The six remaining parameters are more specific to our analysis and are calibrated on the Brazilian agricultural sector as we measure the impact of local pollution damages on such sector.

Fossil fuels in Brazil and crops sensitivity to air pollution. Regarding the use of fossil fuels in Brazil, in 2018 the two main energy sources used by the Brazilian agricultural sector were diesel and electricity, accounting for 70% of the sector's energy consumption. Moreover, the share of renewable energy in Brazil's electricity mix is 82% (65% being hydro). Hence, as a first approximation, we shall consider that the only fossil fuel used for Brazil's agriculture production is diesel. We therefore calibrate the model fossil fuel's price π on Brazil's diesel price in 2019, that is $\pi = 0.6$ \$/L.

In our analysis, two different kinds of pollution are considered. The first kind of pollution is local air pollution that impacts locally Brazilian agricultural production due to the use of diesel in Brazil. The second type of pollution are GHG emissions which are responsible for global warming and concerns both Brazil and the international community. Here we shall focus on the first kind of pollution in order to calibrate how Brazil's use of diesel fossil fuels locally impacts its agricultural production. Indeed, burning diesel emits different gases that are particularly harmful to crops and thus reduces Brazil's agricultural yield. In particular, Nitrogen Oxydes (NO_x) and Carbon Monoxyde (CO), two ozone precursors, are emitted when burning diesel fuel, and are well known for threatening crops development (Wilkinson et al., 2012). Moreover, some plants are more sensitive to such air pollutants and in particular soybean, Brazil's main agricultural product (FAO, 2018). Note that, with an annual soybean production of more than 120 millions tons, Brazil is the world's most productive country and accounts for 36% of soybean world production (FAO, 2018). Hence, assessing the impact of Brazil's use of diesel on its agricultural production is crucial. In the case of soybeans, it is estimated that ozone air pollution can lead to a decrease up to 14% in crop yield (Avnery et al., 2011). For instance, the economic losses in 2000 from ozone pollution damages on crops was estimated in Europe to 6.7 bilions euros (Holland et al., 2006).

Thus, we calibrate the emissivity γ of diesel regarding ozone precursors emissions (mostly Nitrogen Oxydes and Carbon Monoxyde for diesel fuels), that is the amount of ozone precursors emitted per MJ of burnt diesel. In the following, we shall consider γ =0.5 g/MJ, which corresponds to the maximum emission limits of ozone precursors set by Brazil's Proconve P-8 emission standards adopted in 2018 and based on the Euro

VI emissions standards (ICCT, 2019). Finally, the local impact of ozone precursors air pollutants on Brazil's agricultural production is captured in our model by the term θP in the expression of Brazil's agricultural production function net from air pollutants damages $F(1-\xi-\eta\omega, b+\nu\omega)-\theta P$. Therefore, through its abatement properties, the Amazon forest benefits the Brazilian agricultural sector as, by absorbing ozone precursors, the forest also contributes to maintaining high levels of agricultural yield in Brazil. We leave θ as a free parameter as in the following exercices, we analyse the evolution of the opportunity cost with respect to Brazil's crops sensitivity to local pollution.

Palm oil as biodiesel. In our model, the two characteristics of palm oil as biodiesel are its land occupation η (in hectares), that is the surface area of land occupied by one palm tree, and its energy efficiency ν (in joules), that is the energy provided by one palm tree over a year. The ratio of these two parameters defines the energy density of palm oil, therefore measured in joules per hectare. The literature on palm oil as biodiesel provides with technical details on palm oil plantation and in particular on planting arrangements used in palm oil cultures. From four different sources we find that the optimal planting arrangements regarding palm tree lies in-between 130 and 156 trees per hectare (see Table 4).

Reference	Country	Optimal arrangement
Big Lands Brazil	Brazil	148-156 (trees/ha)
Harsono et al. (2011)	Indonesia	138-142 (trees/ha)
FAO (1981)	Surinam	150 (trees/ha)
Barcelos et al. (2015)	General	130-150 (trees/ha)
Corley and Tinker (2003)	General	138-143 (trees/ha)

Table 4: Optimal arrangement of palm tree for biodiesel production (per hectare).

Hence, in the following, we shall consider an optimal arrangement of 150 trees per hectare, leading to $\eta = 1/150$ ha.[21] Moreover, the technical literature on palm oil as biodiesel also provides with its energy density expressed in GJ/ha, that is, the energy quantity produced by palm oil biodiesel per hectare (see Table 5), and in the following, we consider an energy density $\frac{\nu}{\eta} = 180$ GJ/ha. Finally, we obtain palm oil efficiency ν, by multiplying its energy density by its land use η. For $\eta = 1/150$ ha, and with

[21] We calibrate the model on values from the industry standards. Yet, hybridations of species has been developed in order to increase the density of plantation and the highest densities found in the literature are 180-200 trees per hectare. Though hybrid species provide with denser palm trees plantations, seeds from such species are less affordable for farmers and therefore less used (Barcelos et al., 2015).

an energy density of 180 GJ/ha, this leads us to an energy efficiency of $\nu = 1.2$ GJ.

Reference	Country	Energy density
Big Lands Brazil	Brazil	182 GJ/ha
IPCC (2012)	Brazil	169 GJ/ha
Worldwatch institute (2007)	Tanzania	186 GJ/ha

Table 5: Palm oil biodiesel energy densities (GJ/ha).

Forest abatement. We calibrate the abatement properties of the Amazon forest using data on ozone precursors absorptions rates from the forest. In our model we suppose the absorption rate to be concave in forest's surface area. Hence, the remaining parameters to calibrate are $\epsilon < 1$ and μ, the forest's absorption efficiency. The abatement properties of the Amazon forest are calibrated using values from Kroeger et al. (2014), in which forests' abatement properties regarding ozone precursors are given in a range in-between 0.5 to 2.6 t/km^2/yr. Moreover, the surface area of the Amazon forest in 1970 was 5 900 000 km^2 and dropped by 19% reaching therefore 4 900 000 km^2 in 2017 (FAO, 2017). At such deforestation rate, it is estimated that the Amazon forest surface area would drop to 4 300 000 km^2 by 2050. Hence we calibrate the two abatement parameters μ and ϵ so that, for forest surface areas in-between the surface area of 1970 and the one estimated for 2050, the abatement properties of the forest lie in the range of values from Kroeger et al. (2014). In the following, we shall consider $\mu = 3.10^7$ t/yr and $\epsilon = 0.9$. Note that μ is not expressed per hectare as it is a normalized abatement efficiency in our model and thus must be expressed "per Brazil's surface area".

Land normalization. Finally, as for the abatement efficiency parameter μ, we must normalized the calibrated parameters with respect to Brazil's surface area as the land use model here is normalized to one unit of available land. Hence we shall here consider Brazil's surface area of 850 000 000 hectares (FAO, 2013). The resulting normalized calibrated parameters are gathered in Table 6.

5.4 Main results

In the following, we study the evolution of the opportunity cost with respect to sensitivity θ for the forest policy which aims at preserving the Amazon forest's surface area at its current size in Brazil, that is 60% of Brazil's territory ($\xi = 0.6$). Results

are given in Figure 7 and provide with the opportunity cost for Brazil (in \$/ha) for preserving the Amazon forest rather than developing biodiesel from palm oil culture as planned by the PNPB.

ρ	Time discount rate	0.03
δ	Natural absorption	0.01
π	Diesel price in Brazil	17 \$/GJ
γ	Diesel emissivity	5.3e-4 t/GJ
ν	Palm oil energy efficiency	1.2 GJ/yr
η	Palm tree land needs	7.84e-12
μ	Amazon forest abatement efficiency	3e7 t/yr
ϵ	Amazon forest abatement elasticity	0.9

Table 6: Normalized and calibrated parameters' values for Brazil.

The cost for preserving the Amazon forest. As analyzed in the previous section, we write the opportunity cost τ as the sum of its *energy component* $\tau_e = \frac{\nu}{\eta}(\pi - \pi_m)$ and its *mitigation component* $\tau_m = \frac{\theta}{\rho+\delta}\left(\gamma\frac{\nu}{\eta} - \frac{\mu\epsilon}{\xi^{1-\epsilon}}\right)$. Figure 7 shows the evolution of the opportunity cost τ and its two components τ_e and τ_m for a wide range of pollution sensitivities, from $\theta = 0$ to $\theta = 3000$. On such range of sensitivities the opportunity cost varies from 3000 \$/ha to 7600 \$/ha. Note that the variation of the opportunity cost is only due to the variation in its *mitigation component* τ_m as its *energy component* τ_e does not depend on θ (see Proposition 13).

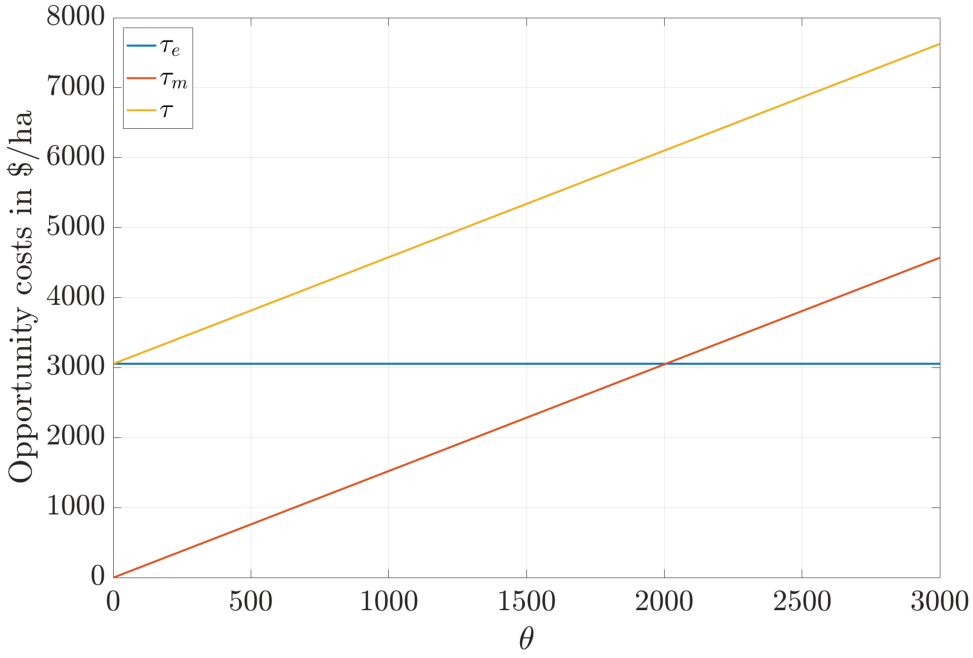

Figure 7: Opportunity cost τ (in \$/ha) with respect to sensitivity θ for $\xi = 0.6$.

Moreover, as the opportunity cost τ is here directly compensated by a financial transfer to Brazil from the international community in order to preserve the Amazon forest from the development of a palm oil biodiesel sector in Brazil, then, by dividing τ (in \$/ha) by the carbon abatement capacities of the Amazon forest (in tCO_2/ha), we provide with the price of the ton of carbon (in \$/tCO_2) that the international community must be willing to pay in order to maintain the Amazon forest at its current surface area ($\xi = 0.6$). Considering the carbon abatement capacity of the Amazon forest from Brown et al. (1996), that is 10 tCO2/ha/yr for tropical forests, we find that, within this range of sensitivities, the price of carbon lies in-between 300 \$/tCO_2 and 760 \$/tCO_2 which is 2 to 5 times greater than actual carbon prices from the literature.[22] Hence, in order to restrain the on-going Amazon deforestation and maintain the forest's current surface area for preserving its global GHG abatement services, the international community must accept to pay higher carbon prices due to ever-growing land use pressures on the Amazon forest, in our case, due to the development of a palm oil biodiesel sector in Brazil. Note however, that some underlying hypothesis of our model might lead to an over-estimation of such pressure, leading therefore to a mechanical increase in the resulting carbon prices, such as supposing all Brazilian palm oil biodiesel being exclusively produced on Amazonian land, or that such production does not also emit local air pollution along with the use of conventional fossil fuels. Yet, even with such hypothesis, the message remains the same : in the current context of ever-growing land use pressure on the Amazon forest, the promotion of ambitious Amazon preservation policies from the international community cannot go without the willingness to pay higher carbon prices.

Missed opportunities : energy production or pollution mitigation ? With the calibrated parameters from Table 6, the opportunity cost τ increases as Brazilian's crops become more sensitive to pollution. Indeed, with this set of parameter, the *mitigation component* $\tau_m = \frac{\theta}{\rho+\delta}\left(\gamma\frac{\nu}{\eta} - \frac{\mu\epsilon}{\xi^{1-\epsilon}}\right)$ of the opportunity cost is strictly positive as $\gamma\frac{\nu}{\eta} > \frac{\mu\epsilon}{\xi^{1-\epsilon}}$. This means that for Brazil, using palm oil biodiesel instead of fossil fuels is a better mitigation policy for reducing ozone precursors local emissions due to the use of the latter, rather than preserving forested land for local abatement purposes while continuing to use pollutant fossil fuels. Hence, the opportunity cost increases linearly with respect to sensitivity at the same rate as its *mitigation component*, while the *energy component* stays constant as it does not depend of θ.

[22] Carbon prices typically yield between 50 \$/tCO_2 to 150 \$/tCO_2 (World Bank, 2020).

Therefore, for low pollution sensitivities, the dominant term in the opportunity cost is the *energy component* $\tau_e = \frac{\nu}{\eta}\left(\pi - \frac{\rho}{\nu}\right)$. This means that for low crop sensitivities to local air pollution, Amazon forest conservation policies lead to higher missed opportunities in energy production rather than in mitigation opportunities. Yet, as sensitivity increases, the mitigation term increases up to a threshold above which the mitigation term τ_m becomes dominant in the opportunity cost (that is when $\tau_m > \tau_e$). The sensitivity threshold with the calibrated parameters from Table 6 is $\theta = 2000$ as shown in Figure 7, and above which the missed opportunities due forest preservation policies are mostly missed mitigation opportunities. This is quite counter-intuitive as the Amazon forest preservation is itself a mitigation policy. Yet, in our case, forest preservation policy for local air pollution mitigation purposes competes with palm oil biodiesel energy production for the mitigation purposes. And here, it is estimated that shifting from pollutant fossil fuels to biodiesel renewable energy by exploiting forest land for palm oil culture is a better mitigation policy for Brazil, than conserving its forested land for abatement.

6 Conclusion

This chapter examines the trade-offs in land use when climate change mitigation policies such as renewable energy production or reforestation for pollution abatement are applied. The specificity of our analysis being that renewable energy production and abatement take a non-negligible space and therefore interferes with agricultural production which is itself sensitive to pollution.

We develop a first benchmark model in which social planner does not account for pollution emissions from the use of fossil fuels. In such framework the economy converges towards a steady state and we prove its saddle-path stability. We then examine a model in which social planner integrates pollution emissions and prove similarly the existence of a unique saddle-path stable steady state towards which the economy converges. We describe the two steady states and derive the tax on fossil fuels that must be applied so that the two land use equilibrium coincide. When renewable energy production is the only land intensive mitigation policy, the more dense is energy production, the more land shall be allocated towards renewable energy production rather than towards agriculture. This result can be seen as a case of comparative advantage. Indeed, as energy production and agriculture compete for land to produce output,

social planner allocates more land to the more productive sector. Hence, the denser is the renewable energy production, the more land must be allocated to its activity. Moreover, the more sensitive is the agricultural sector to pollution, the more land shall be allocated to renewable energy production as well, in order this time to assure the continuity of output production while limiting environmental damages.

Moreover, we develop a second model in which are considered both renewable energy production and abatement policies such as reforestation. In such case, when both mitigation policies available, social planner's strategy for land use reallocation depends on the level of the agricultural production sensitivity to pollution. For low sensitivity, as agriculture becomes more sensitive to pollution, agricultural land must be reallocated towards both renewable energy (for mitigation purposes and compensation of production losses) and abatement (only for mitigation). In contrast, for high sensitivities, along with agricultural land, it is also best to sacrifice renewable energy production land and reallocate exclusively land to abatement in order to save output from important pollution damages.

Finally, we apply our model to the stakes of preserving the Amazon forest in Brazil. More particularly, we focus on the emerging market of palm oil production for biodiesel in Brazil in Amazonia and on the resulting opportunity cost for Brazil of preserving the Amazon forest. Within a wide range of pollution sensitivities, the price of carbon for preserving the Amazon forest's surface area at its current size lies in-between 300 \$/tCO_2 and 760 \$/tCO_2 which is 2 to 5 times greater than actual carbon prices. Hence, in order to restrain the on-going Amazon deforestation and maintain the forest's current surface area for preserving its global GHG abatement services, the international community must accept to pay higher compensation through financial transfers to Brazil due to ever-growing land use pressures on the Amazon forest, in our case, due to the development of a palm oil biodiesel sector in Brazil.

Further research could be developed at both theoretical and empirical levels. For instance, in Behrens and Zalk (2018), the authors show that the density of renewable energy is a metric that evolved in time. Thereby, further theoretical work could extend the model presented in this research in order to take into account, through technical progress, the dynamics of renewable energy production density. Also, land heterogeneity is not considered here, but of course, plays an important role regarding land use policies. A spatial model taking into account heterogeneities in land regarding abatement capacities or agricultural production could also be developed as an extension of

this present research and study the plausible emergence of land use patterns. Finally, calibrating the model from empirical land use data could allow such trade-offs to be analyzed in country-specific studies as proposed for the Brazilian case in this research. Such calibrations could bring useful insights to policy makers regarding future land use puzzles they shall meet, in the on-going development of land use intensive climate mitigation policies, such as renewable production or forests preservation.

References

[1] Al-Nassar, W. K., Neelamani, S., Al-Salem, K. A. and Al-Dashti, H. A. (2019), "Feasibility of offshore wind energy as an alternative source for the state of Kuwait", *Energy*, (169), 783-796.

[2] Amigues, J.-P. and Moreaux, M. (2019), "Competing land uses and fossil fuel, and optimal energy conversion rates during the transition toward a green economy under a pollution stock constraint", *Journal of Environmental Economics and Management*, (97), 92-115.

[3] Andrews, C. V. and Schechtman, J. (2011), "Alternative Energy Sources and Land Use", *Climate Change Policies and Land Policies*, Chapter 5, 91-121.

[4] Appel F., Ostermeyer-Wiethaup, A. and Balmann, A. (2016), "Effects of the German Renewable Energy Act on structural change in agriculture - The case of biogas", *Utilities Policy*, 41, 172-182.

[5] Avnery, A., Mauzerall, L., D., Liu, J. and Horowitz L. W. (2011), "Global crop yield reductions due to surface ozone exposure", *Atmospheric Environment*, 45(13), 2297-2309.

[6] Bahel, E., Marrouch, W. and Gaudet, G. (2013), "The economics of oil, biofuel and food commodities", *Resource and Energy Economics*, 35(4), 599-617.

[7] Barcelos, E., Rios Sara, A., Cunha Raimundo, N. V., Lopes, R., Motoike Y., Babiychuk E., Skirycz, A. and Kushnir, S. (2015), "Oil palm natural diversity and the potential for yield improvement", *Frontiers in Plant Science*, 6, 190.

[8] Behrens, P. and Zalk, V. J. (2018), "The spatial extent of renewable and non-renewable power generation: A review and meta-analysis of power densities and their application in the U.S.", *Energy Policy*, 123, 83-91.

[9] Bender, R. M. J. and Dijkman, T. J. (2010), "Comparison of renewable fuels based on their land use using energy densities", *Renewable and Sustainable Energy Reviews*, 14, 3148-3155.

[10] Big Lands Brazil, retrieved from : https://www.biglandsbrazil.com

[11] de Boer, C., Hewitt, R., Bressers, H. et al., (2015), "Local power and land use: spatial implications for local energy development", *Energ Sustain Soc*, 5(31), 1-8.

[12] Brandão, F., Castro, F. and Futemma, C. (2019), "Between structural change and local agency in the palm oil sector: Interactions, heterogeneities and landscape transformations in the Brazilian Amazon", *Journal of Rural Studies*, 71, 156-168.

[13] Bridge, G., Bouzarovski, S., Bradshaw, M. and Eyre, N. (2013), "Geographies of energy transition: Space, place and the low-carbon economy", *Energy Policy*, 53, 331-340.

[14] Brown, S., Jayant, S., Melvin, C. and Pekka, E. K. (1996), "Mitigation of Carbon Emissions to the Atmosphere by Forest Management", *The Commonwealth Forestry*, 75(1), 80-91.

[15] Calvert, K and Mabee, W. (2015), "More solar farms or more bioenergy crops? Mapping and assessing potential land-use conflicts among renewable energy technologies in eastern Ontario, Canada", *Applied Geography*, 56, 209-221.

[16] Camacho, C. and Pérez-Barahona A. (2015), "Land use dynamics and the environment", *Journal of Economic Dynamics and Control*, 52, 96-118.

[17] César, A. and Batalha, M. O. (2013), "Brazilian biodiesel: The case of the palm's social projects", *Energy Policy*, 56, 165-174.

[18] Chakravorty, U., Magné, B. and Moreaux, M. (2008), "A dynamic model of food and clean energy", *Journal of Economic Dynamics and Control*, 32(4), 1181-1203.

[19] Corley, R. H. V. and Tinker, P. B. (2003), *The Oil Palm. Oxford: John Wiley & Sons.*

[20] Danielsen, O. (1995), "Large-scale wind power in Denmark", *Land Use Policy*, 12(1), 60-62.

[21] Dones, R., Heck, T. and Hirschberg, S. (2003), "Greenhouse gas emissions from energy systems, comparison and overview", *Encyclopedia of Energy*, 3, 27-40.

[22] Emeksiz, C. and Demirci, B. (2019), "The determination of offshore wind energy potential of Turkey by using novelty hybrid site selection method", *Sustainable Energy Technologies and Assessments*, 36, 100562.

[23] EPA (2010), "Technical Support Document: Technical Update of the Social Cost of Carbon for Regulatory Impact Analysis"

[24] Feldman, D., Margolis, R., Brockway, A. and Ulrich, E. (2015), "Shared Solar: Current Landscape, Market Potential, and the Impact of Federal Securities Regulation", NREL (National Renewable Energy Laboratory), United States.

[25] Farzin, Y. H. and Tahvonen, O. (1996), "Global carbon cycle and the optimal time path of carbon tax". *Oxford Economic Papers*, 48(4), 515-536.

[26] Fritsche, U., Berndes, U., Cowie, A. and Woods, J. (2018), "Energy and land use", *Global Land Outlook.*

[27] Fthenakis, V. and Kim, H. C. (2010), "Life-cycle uses of water in U.S. electricity generation", *Renew. Sustain. Energy*, 14, 2039-2048.

[28] Furlan, J., Kaltner, F., Alves, S. and Barcelos, E. (2004), "A Utilização de Óleo de Palma como Componente do Biodiesel na Amazônia". *Comunicado técnico*, 103.

[29] Gagnon, P., Margolis, R., Melius, J., Phillips, C. and Elmore, R. (2016), "Rooftop Solar Photovoltaic Technical Potential in the United States: A Detailed Assessment."

[30] Gagnon, L., Elanger, C. B. and Uchiyama, Y. (2002), "Life-cycle assessment of electricity generation options: the status of research in year 2001", *Energy Policy*, 30, 1267-1278.

[31] Gasparatos, A., Doll, N. H. C., Esteban, M., Ahmed, A. and Olang, A. T. (2017), "Renewable energy and biodiversity: Implications for transitioning to a Green Economy", *Renewable and Sustainable Energy Reviews*, 70, 161-184.

[32] Greiner, A., Gruene, L. and Semmler, A. (2014), "Economic growth and the transition from non-renewable to renewable energy", *Environment and Development Economics*, 19, 417-439.

[33] Hall, D. O. and House, J. (1995), "Biomass: An Environmentally Acceptable Fuel for the Future." *Proceedings of the Institution of Mechanical Engineers, Part A: Journal of Power and Energy*, 209, 203-213.

[34] Harsono, S. S., Prochnow, A., Grundmann, P., Hansen, A. and Hallmann, C. (2012), "Energy balances and greenhouse gas emissions of palm oil biodiesel in Indonesia", *GCB Bioenergy*, 4, 213-228.

[35] Hedger, M. (1995), "Wind power: challenges to planning policy in the UK", *Land Use Policy*, 12(1), 17-28.

[36] Hernandez, R. (2015), "Solar energy development impacts on land cover change and protected areas", *Proceedings of the National Academy of Sciences of the United States of America*, 112(44), 13579-84.

[37] Holland, M., Kinghorn, S., Emberson, L., Cinderby, S., Ashmore, M. ,Mills, G. and Harmens, H. (2006), "Development of a framework for probabilistic assessment of the economic losses caused by ozone damage to crops in Europe". *UNECE International Cooperative Programme on Vegetation. Contract Report EPG 1/3/205.CEH Project No: C02309NEW.*

[38] Instituto Nacional de Pesquisas Espaciais TerraClass (2012), *Levantamento de Informações de uso e Cobertura da Terra na Amazônia ?"*

[39] International Council on Clean Transportation (2019), *Brazil Proconve P-8 Emission Standards*.

[40] IPCC (2000), "Land use, land-use change and forestry".

[41] IPCC (2012), "Renewable Energy Sources and Climate Change Mitigation: Special Report of the Intergovernmental Panel on Climate Change".

[42] Kim, H. J., Kim, J.-H. and Yoo, S.-H. (2019), "Social acceptance of offshore wind energy development in South Korea: Results from a choice experiment survey", *Renewable and Sustainable Energy Reviews*, 113, 109253.

[43] Kroeger, T., Hernández, J., Varela, S., Delphin, S., Fisher, J. and Waldron, J. (2014), "Reforestation as a novel abatement and compliance measure for ground-level ozone", *Proceedings of the National Academy of Sciences*, 111(40).

[44] Kverndokk, S. (1994), "Depletion of fossil fuels and the impact of global warming", *Statistics of Norway*, Discussion Paper No. 187.

[45] Layton, B. (2008), "A comparison of energy densities of prevalent energy sources in units of joules per cubic meter", *Int. J. Green. Energy*, 5, 438-455.

[46] Liu, T., McConkey, B., Huffman, T., Smith, S., MacGregor, B., Yemshanov, D. and Kulshreshtha, S. (2014), "Potential and impacts of renewable energy production from agricultural biomass in Canada", *Applied Energy*, 130, 222-229.

[47] Maier-Raimer, E. and Hasselmann, K. (1987), "Transport and storage of CO_2 in the ocean - an inorganic ocean-circulation carbon cycle model" *Climate Dynamics*, 2,63-90.

[48] Marafia, A-H. and Ashour, A. H. (2003), "Economics of off-shore/on-shore wind energy systems in Qatar", *Renewable Energy*, 28(12), 1953-1963.

[49] Mc Ewan, C. (2017), "Spatial processes and politics of renewable energy transition: Land, zones and frictions in South Africa", *Political Geography*, 56, 1-12.

[50] Ministério do Desenvolvimento Agrário (2010). *Palma de Óleo: Programa de Produção Sustentável*.

[51] Nadai, A. and Van der Horst, D. (2010), "Landscapes of energies", *Landscape Research*, 35(2), 143-155.

[52] Nuclear Forum, (1991), "A compact powerpack".

[53] Oil World (2019), *Oil World Annual 2019*.

[54] Park, J. and Kim, B. (2019), "An analysis of South Korea's energy transition policy with regards to offshore wind power development", *Renewable and Sustainable Energy Reviews*, 109, 71-84.

[55] Pasqualetti, M. (1990), "The Land Use Focus of Energy Impacts".

[56] Pasqualetti, M. (2011), "Social barriers to renewable energy landscapes", *Geographical Review*, 101(2), 201-223.

[57] Pirker, J., Mosnier, A., Kraxner, F., Havlík, P. and Obersteiner, M. (2016), "What are the limits to oil palm expansion ?", *Global Environmental Change*, 40, 73-81.

[58] Poggi, F., Firmino, A. and Amado, M. (2018), "Planning renewable energy in rural areas: Impacts on occupation and land use", *Energy*, 155, 630-640.

[59] Rahman, M. M., Mostafiz, B. S., Paatero, V. J. and Lahdelma, R. (2014), "Extension of energy crops on surplus agricultural lands: A potentially viable option in developing countries while fossil fuels reserves are diminishing", *Renewable and Sustainable Energy Reviews*, 29, 108-119.

[60] Sawulski, J., Galczynski, M. and Zajdler, R. (2019), "Technological innovation system analysis in a follower country - The case of offshore wind in Poland", *Environmental Innovation and Societal Transitions*, 33, 249-267.

[61] Sinclair, P. (1994),"On the trend of fossil fuels taxation", *Oxford Economic Papers*, 46, 869-77.

[62] Sistema IBGE de Recuperação Automática (2015), *Produção Agrícola Municipal: cereais, leguminosas e oleaginosas.*

[63] Sliz-Szkliniarz, B. (2013), "Assessment of the renewable energy-mix and land use trade-off at a regional level: A case study for the Kujawsko-Pomorskie Voivodship", *Land Use Policy*, 35, 257-270.

[64] Smil, V. (2010), "Power Density Primer: Understanding the Spatial Dimension of the Unfolding Transition to Renewable Electricity Generation (Part I - Definitions)".

[65] Smil, V. (2016), "Power Density: a Key to Understanding Energy Sources and Uses", *MIT Press.*

[66] Tuan, Y. (1974), "Topophilia: A Study of Environmental Perception, Attitudes and Values", *Prentice Hall.*

[67] Ulph, A. and Ulph, D. (1994), "The optimal path of a carbon tax", *Oxford Economic Papers*, 46, 857-68.

[68] United States Department of Agriculture (2013), *Oilseeds - World Markets and Trade.*

[69] UNFCCC (1997), Kyoto Protocol to the United Nations Framework Convention on Climate Change adopted at COP3 in Kyoto, Japan, on 11 December 1997.

[70] Veiga, A. S. (2005), "Políticas públicas na agroindústria do dendê na visão do produtor", *Documento 222. Belém: Embrapa*

[71] Villela, A. A. (2009). "O dendê como alternativa energética sustentável em áreas degradadas da Amazônia", *M.D. Thesis Rio de Janeiro: Rio de Janeiro Federal University.*

[72] Villela, A., Jaccoud, A., Rosa, P. L. and Freitas, M. V. (2014), "Status and prospects of oil palm in the Brazilian Amazon", *Biomass and Bioenergy*, 67, 270-278.

[73] Walker, G. (1995), "Energy, land use and renewables: A changing agenda", *Land Use Policy*, 12, 3-6.

[74] World Bank (2020), "State and Trends of Carbon Pricing 2020".

[75] Worldwatch Institute (2007), "Biofuels for transport 2007 : global potential and implications for energy and agriculture."

[76] Wilkinson, S., Mills, G., Illidge, R. and Davies, W. J. (2012), "How is ozone pollution reducing our food supply ?", *Journal of Experimental Botany*, 63(2), 527?536.

[77] Winston, D. C. (1979), "There goes the Sun", *Newsweek*, (35).

[78] Yenneti, K., Day, R. and Golubchikov, O. (2016), "Spatial justice and the land politics of renewables: Dispossessing vulnerable communities through solar energy mega-projects", *Geoforum*, (76), 90-99.

[79] Yui, S. and Yeh, S. (2013), "Land use change emissions from oil palm expansion in Pará, Brazil depend on proper policy enforcement on deforested lands", *Environmental Research Letters*, 8(4).

Appendices

A. Numerical exercices.

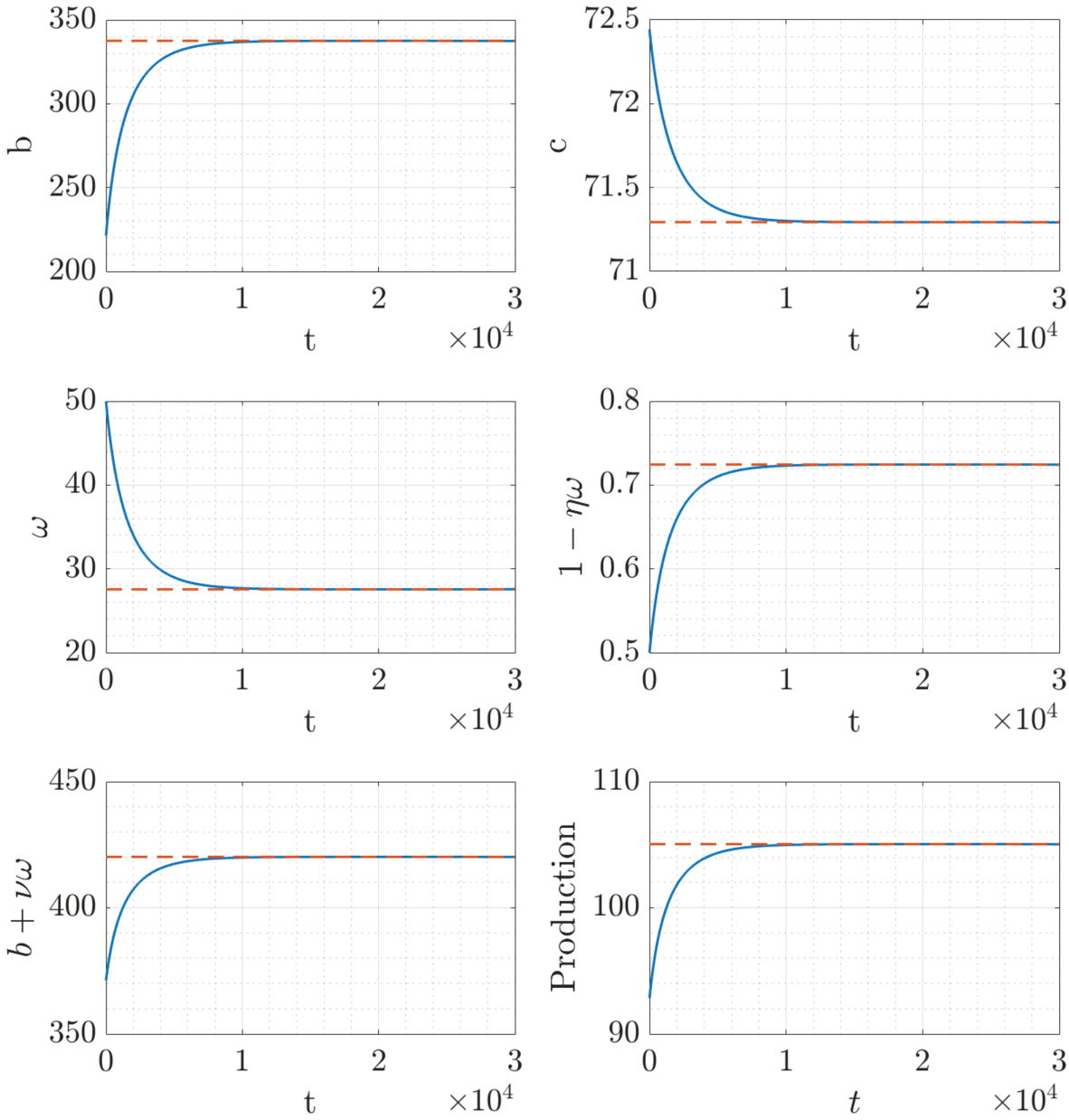

Figure 8: Stable arm converging dynamics towards steady state for initial level of renewable energy above equilibrium: $\omega(0) = \frac{\hat{\omega}}{2} > \omega_m$.

B. Proof of Proposition 1.

The Hamiltonian of the problem writes:

$$H = u(c) + \lambda[A(1-\eta\omega)^{\alpha}(b+\nu\omega)^{\beta} - c - \pi b].$$

Thus the F.O.C lead to:

$$\begin{cases} \frac{\partial H}{\partial c} = 0 \implies u'(c) = \lambda, \\ \frac{\partial H}{\partial b} = 0 \implies A(1-\eta\omega)^{\alpha}\beta(b+\nu\omega)^{\beta-1} - \pi = 0, \\ \frac{\partial H}{\partial \omega} = \lambda\ [-A\alpha\eta(1-\eta\omega)^{\alpha-1}(b+\nu\omega)^{\beta} + A\nu\beta(1-\eta\omega)^{\alpha}(b+\nu\omega)^{\beta-1}] = \rho\lambda - \dot{\lambda}. \end{cases} \tag{1}$$

Therefore, equation (1.2) gives the expression of energy $b+\nu\omega$ as a unique function of ω such that $b+\nu\omega = \left(\frac{A\beta(1-\eta\omega)^{\alpha}}{\pi}\right)^{\frac{1}{1-\beta}}$. Moreover equation (1.3) at steady states writes as:

$$\begin{aligned} &\rho + A\alpha\eta(1-\eta\omega)^{\alpha-1}(b+\nu\omega)^{\beta} - A\nu\beta(1-\eta\omega)^{\alpha}(b+\nu\omega)^{\beta-1} = 0 \\ \iff &\rho + A\alpha\eta(1-\eta\omega)^{\alpha-1}\left(\frac{A\beta\,(1-\eta\omega_m)^{\alpha}}{\pi}\right)^{\frac{\beta}{1-\beta}} - A\nu\beta(1-\eta\omega)^{\alpha}\left(\frac{A\beta\,(1-\eta\omega_m)^{\alpha}}{\pi}\right)^{\frac{\beta-1}{1-\beta}} = 0 \\ \iff &\rho + A\alpha\eta\left(\frac{A\beta}{\pi}\right)^{\frac{\beta}{1-\beta}}(1-\eta\omega)^{\frac{\alpha+\beta-1}{1-\beta}} = \nu\pi \\ \iff &(1-\eta\omega)^{\frac{\alpha+\beta-1}{1-\beta}} = \frac{\nu\ \pi - \rho}{A\alpha\eta\left(\frac{A\beta}{\pi}\right)^{\frac{\beta}{1-\beta}}}. \end{aligned}$$

Hence, if $\nu\pi - \rho > 0$ then the land use equilibrium at steady state writes as:

$$l_m = \eta\omega_m = 1 - \left(\frac{A\alpha\eta\left(\frac{A\beta}{\pi}\right)^{\frac{\beta}{1-\beta}}}{\nu\pi - \rho}\right)^{\frac{1-\beta}{1-\alpha-\beta}}.$$

Regarding the stability of the equilibrium, as $\dot{\omega} = A(1-\eta\omega)^{\alpha}(b+\nu\omega)^{\beta} - c - \pi b$ then at steady state we get that:

$$c_m = A(1-\eta\omega_m)^{\alpha}(b_m+\nu\omega_m)^{\beta} - \pi b_m.$$

Finally as $b = \left(\frac{A\beta(1-\eta\omega_m)^{\alpha}}{\pi}\right)^{\frac{1}{1-\beta}} - \nu\omega$ therefore b on depends on ω. Thus, we can write the problem as a dynamic system of dimension two in only the variables ω and λ as:

$$\begin{cases} \dot{\omega} = A(1-\eta\omega)^{\alpha}(b(\omega)+\nu\omega)^{\beta} - c(\lambda) - \pi b(\omega), \\ \dot{\lambda} = \lambda[\rho + A\alpha\eta(1-\eta\omega)^{\alpha-1}(b+\nu\omega)^{\beta} - A\nu\beta(1-\eta\omega)^{\alpha}(b+\nu\omega)^{\beta-1}]. \end{cases}$$

Hence, at steady state we have that $\frac{\partial\dot{\lambda}}{\partial\lambda} = 0$ and the Jacobian matrix of the system at steady states writes:

$$\mathcal{J} = \begin{pmatrix} \frac{\partial\dot{\omega}}{\partial\omega} & \frac{\partial\dot{\omega}}{\partial\lambda} \\ \frac{\partial\dot{\lambda}}{\partial\omega} & \frac{\partial\dot{\lambda}}{\partial\lambda} \end{pmatrix} = \begin{pmatrix} \frac{\partial\dot{\omega}}{\partial\omega} & -c'(\lambda) \\ \frac{\partial\dot{\lambda}}{\partial\omega} & 0 \end{pmatrix}.$$

Therefore, $\det(\mathcal{J}) = c'(\lambda)\frac{\partial\dot{\lambda}}{\partial\omega} = -\frac{\lambda^{-\frac{1}{\sigma}-1}}{\sigma}\frac{\partial\dot{\lambda}}{\partial\omega}$ and at steady state we get:

$$\dot{\lambda} = \lambda\left[\rho + A\alpha\eta\left(\frac{A\beta}{\pi}\right)^{\frac{\beta}{1-\beta}}(1-\eta\omega)^{\frac{\alpha+\beta-1}{1-\beta}} - \nu\pi\right],$$

which implies that $\frac{\partial\dot{\lambda}}{\partial\omega} = -\lambda A\alpha\eta^2\left(\frac{A\beta}{\pi}\right)^{\frac{\beta}{1-\beta}}\left(\frac{\alpha+\beta-1}{1-\beta}\right)(1-\eta\omega)^{\frac{\alpha+\beta-1}{1-\beta}-1}$ and:

$$\det(\mathcal{J}) = \underbrace{\frac{\lambda^{-\frac{1}{\sigma}}}{\sigma}A\alpha\eta^2\left(\frac{A\beta}{\pi}\right)^{\frac{\beta}{1-\beta}}}_{>0}\underbrace{\left(\frac{\alpha+\beta-1}{1-\beta}\right)}_{\substack{<0 \\ \text{as } \alpha+\beta<1}}\underbrace{(1-\eta\omega)^{\frac{\alpha+\beta-1}{1-\beta}-1}}_{>0} < 0.$$

As the determinant of the Jacobian matrix is strictly negative at steady state, this means that its two eigenvalues are reals of opposite signs which proves the saddle-path stability of steady state equilibrium.

To finish the proof we shall study the comparative statics of the equilibrium with respect to ν, π, η and ρ.

• Be $\psi_1 = \left(A\alpha\eta\left(\frac{A\beta}{\pi}\right)^{\frac{\beta}{1-\beta}}\right)^{\frac{1-\beta}{1-\alpha-\beta}} > 0$, then the renewable energy land use at steady state can be written as $l_m = 1 - \psi_1(\nu\pi-\rho)^{\frac{\beta-1}{1-\alpha-\beta}}$ and thus:

$$\begin{aligned}\frac{\partial l_m}{\partial\nu} &= -\psi_1\left(\frac{\beta-1}{1-\alpha-\beta}\right)\pi(\nu\pi-\rho)^{\frac{\beta-1}{1-\alpha-\beta}-1} \\ &= \psi_1\underbrace{\left(\frac{1-\beta}{1-\alpha-\beta}\right)}_{>0}\pi\underbrace{(\nu\pi-\rho)}_{>0}^{\frac{\beta-1}{1-\alpha-\beta}-1} > 0,\end{aligned}$$

meaning that the more renewable energy produces energy, the more land should be allocated to renewable energy production.

• Similarly, derivating renewable energy land use with respect to the discount rate leads to:

$$\begin{aligned}\frac{\partial l_m}{\partial\rho} &= \psi_1\left(\frac{\beta-1}{1-\alpha-\beta}\right)(\nu\pi-\rho)^{\frac{\beta-1}{1-\alpha-\beta}-1} \\ &= -\psi_1\underbrace{\left(\frac{1-\beta}{1-\alpha-\beta}\right)}_{>0}\underbrace{(\nu\pi-\rho)}_{>0}^{\frac{\beta-1}{1-\alpha-\beta}-1} < 0,\end{aligned}$$

meaning that the more discount rate is important, the less land should be allocated to renewable energy production.

• Now be $\psi_2 = \left(A\alpha\eta(A\beta)^{\frac{\beta}{1-\beta}}\right)^{\frac{1-\beta}{1-\alpha-\beta}} > 0$ then renewable energy land use at steady state can be written as $l_m = 1 - \psi_2\pi^{-\frac{\beta}{1-\alpha-\beta}}(\nu\pi-\rho)^{\frac{\beta-1}{1-\alpha-\beta}}$ and thus:

$$\begin{aligned}\frac{\partial l_m}{\partial \pi} &= -\psi_2\left[\frac{-\beta}{1-\alpha-\beta}\pi^{\frac{-\beta}{1-\alpha-\beta}-1}(\nu\pi-\rho)^{\frac{\beta-1}{1-\alpha-\beta}} + \left(\frac{\beta-1}{1-\alpha-\beta}\right)\pi^{\frac{-\beta}{1-\alpha-\beta}}(\nu\pi-\rho)^{\frac{\beta-1}{1-\alpha-\beta}-1}\right] \\ &= \psi_2\left[\underbrace{\frac{\beta}{1-\alpha-\beta}}_{>0}\pi^{\frac{-\beta}{1-\alpha-\beta}-1}(\underbrace{\nu\pi-\rho}_{>0})^{\frac{\beta-1}{1-\alpha-\beta}} + \underbrace{\left(\frac{1-\beta}{1-\alpha-\beta}\right)}_{>0}\pi^{\frac{-\beta}{1-\alpha-\beta}}(\underbrace{\nu\pi-\rho}_{>0})^{\frac{\beta-1}{1-\alpha-\beta}-1}\right] > 0,\end{aligned}$$

which means that as the price of fossil fuels increases, the land allocated to renewable energy production installed at steady states increases.

• Finally, be $\psi_3 = \left(\frac{A\alpha\left(\frac{A\beta}{\pi}\right)^{\frac{\beta}{1-\beta}}}{\nu\pi-\rho}\right)^{\frac{1-\beta}{1-\alpha-\beta}} > 0$ as from Assumption 2 $\rho < \nu\pi$. With this notation renewable energy land use at steady state writes as $l_m = 1 - \psi_3\eta^{\frac{1-\beta}{1-\alpha-\beta}}$ and thus:

$$\frac{\partial l_m}{\partial \eta} = -\underbrace{\left(\frac{1-\beta}{1-\alpha-\beta}\right)}_{>0}\psi_3\eta^{\frac{1-\beta}{1-\alpha-\beta}-1} < 0,$$

meaning that the more renewable energy needs land to produce energy, the less land should be allocated to renewable energy production at steady state.

C. Proof of Proposition 2.

From the expression of the land allocated to renewable energy we directly have the stock of installed renewable energy on this land being:

$$\omega_m = \frac{1}{\eta}\left[1 - \left(\frac{A\alpha\eta\left(\frac{A\beta}{\pi}\right)^{\frac{\beta}{1-\beta}}}{\nu\pi-\rho}\right)^{\frac{1-\beta}{1-\alpha-\beta}}\right].$$

Moreover, as the expression $b + \nu\omega = \left(\frac{A\beta(1-\eta\omega_m)^\alpha}{\pi}\right)^{\frac{1}{1-\beta}}$ is true at steady state then:

$$b_m = \left[\frac{A\beta\left(1-\eta\omega_m\right)^\alpha}{\pi}\right]^{\frac{1}{1-\beta}} - \nu\omega_m = \left[\frac{A\beta\left(1-\eta\omega_m\right)^\alpha}{\pi}\right]^{\frac{1}{1-\beta}} - \frac{\nu}{\eta}l_m.$$

We study the impact of the land required to produce renewable energy η, the efficiency of renewable energy ν as well as the cost of using fossil fuels π on the energy mix at steady state. We first analyse the level of renewable energy ω_m at steady state and study the implications regarding the use of fossil fuels b_m.

• Be $\psi_1 = \left(\frac{A\alpha\left(\frac{A\beta}{\pi}\right)^{\frac{\beta}{1-\beta}}}{\nu\pi-\rho} \right)^{\frac{1-\beta}{1-\alpha-\beta}} > 0$ as from Assumption 2 $\rho < \nu\pi$. With this notation the stock of renewable energy at steady state writes as $\omega_m = \frac{1}{\eta} - \psi_1 \eta^{\frac{1-\beta}{1-\alpha-\beta}-1}$ and thus:

$$\begin{aligned}\frac{\partial \omega_m}{\partial \eta} &= -\frac{1}{\eta^2} - \left(\frac{1-\beta}{1-\alpha-\beta} - 1\right)\psi_1 \eta^{\frac{1-\beta}{1-\alpha-\beta}-2} \\ &= -\frac{1}{\eta^2} - \underbrace{\left(\frac{\alpha}{1-\alpha-\beta}\right)}_{>0}\psi_1 \eta^{\frac{1-\beta}{1-\alpha-\beta}-2} < 0,\end{aligned}$$

meaning that the more renewable energy needs land to produce energy, the less renewable energy will be installed at steady state.

• Moreover, be $\psi_2 = \left(A\alpha\eta \left(\frac{A\beta}{\pi}\right)^{\frac{\beta}{1-\beta}} \right)^{\frac{1-\beta}{1-\alpha-\beta}} > 0$, then the stock of renewable energy at steady state can be written as:

$$\omega_m = \frac{1}{\eta}\left(1 - \psi_2 (\nu\pi - \rho)^{\frac{\beta-1}{1-\alpha-\beta}}\right),$$

and thus:

$$\begin{aligned}\frac{\partial \omega_m}{\partial \nu} &= -\frac{\psi_2}{\eta}\left(\frac{\beta-1}{1-\alpha-\beta}\right)\pi(\nu\pi-\rho)^{\frac{\beta-1}{1-\alpha-\beta}-1} \\ &= \frac{\psi_2}{\eta}\underbrace{\left(\frac{1-\beta}{1-\alpha-\beta}\right)}_{>0}\pi(\underbrace{\nu\pi-\rho}_{>0})^{\frac{\beta-1}{1-\alpha-\beta}-1} > 0,\end{aligned}$$

meaning that the more renewable energy produces energy, the more renewable energy plants will be installed at steady state.

• Now be $\psi_3 = \left(A\alpha\eta(A\beta)^{\frac{\beta}{1-\beta}}\right)^{\frac{1-\beta}{1-\alpha-\beta}} > 0$ then the stock of renewable energy at steady state can be written as $\omega_m = \frac{1}{\eta}\left(1 - \psi_3 \pi^{-\frac{\beta}{1-\alpha-\beta}}(\nu\pi-\rho)^{\frac{\beta-1}{1-\alpha-\beta}}\right)$ and thus:

$$\begin{aligned}\frac{\partial \omega_m}{\partial \pi} &= -\frac{\psi_3}{\eta}\left[\frac{-\beta}{1-\alpha-\beta}\pi^{\frac{-\beta}{1-\alpha-\beta}-1}(\nu\pi-\rho)^{\frac{\beta-1}{1-\alpha-\beta}} + \left(\frac{\beta-1}{1-\alpha-\beta}\right)\pi^{\frac{-\beta}{1-\alpha-\beta}}(\nu\pi-\rho)^{\frac{\beta-1}{1-\alpha-\beta}-1}\right] \\ &= \frac{\psi_3}{\eta}\left[\underbrace{\frac{\beta}{1-\alpha-\beta}}_{>0}\pi^{\frac{-\beta}{1-\alpha-\beta}-1}\underbrace{(\nu\pi-\rho)}_{>0}^{\frac{\beta-1}{1-\alpha-\beta}} + \underbrace{\left(\frac{1-\beta}{1-\alpha-\beta}\right)}_{>0}\pi^{\frac{-\beta}{1-\alpha-\beta}}\underbrace{(\nu\pi-\rho)}_{>0}^{\frac{\beta-1}{1-\alpha-\beta}-1}\right] > 0,\end{aligned}$$

which means that as the price of fossil fuels increases, the stock of renewable energy plants installed at steady states increases.

Regarding the use of fossil fuels b_m at steady state, the effect of ν and η and π can be directly studied using the previous analysis for ω_m. Indeed, from Proposition 1 we know that $b_m = \left[\frac{A\beta(1-\eta\omega_m)^\alpha}{\pi}\right]^{\frac{1}{1-\beta}} - \nu\omega_m$.

• Therefore deriving with respect to ν leads to:

$$\begin{aligned}\frac{\partial b_m}{\partial \nu} &= \left(\frac{A\beta}{\pi}\right)^{\frac{1}{1-\beta}} \frac{\partial}{\partial \nu}(1-\eta\omega_m(\nu))^{\frac{\alpha}{1-\beta}} - \omega_m - \nu\frac{\partial \omega_m}{\partial \nu} \\ &= -\left(\frac{A\beta}{\pi}\right)^{\frac{1}{1-\beta}} \underbrace{\frac{\alpha}{1-\beta}(1-\eta\omega_m(\nu))^{\frac{\alpha}{1-\beta}-1}\eta\frac{\partial \omega_m}{\partial \nu}}_{>0} - \omega_m - \nu\underbrace{\frac{\partial \omega_m}{\partial \nu}}_{>0} < 0,\end{aligned}$$

meaning that the the technology of renewable energy is efficient or the more there is primary renewable energy the less fossil fuels is needed.

• Similarly, deriving the expression of b_m with respect to η leads to:

$$\begin{aligned}\frac{\partial b_m}{\partial \eta} &= \left(\frac{A\beta}{\pi}\right)^{\frac{1}{1-\beta}} \frac{\partial}{\partial \eta}(1-\eta\omega_m(\eta))^{\frac{\alpha}{1-\beta}} - \nu\frac{\partial \omega_m}{\partial \eta} \\ &= -\left(\frac{A\beta}{\pi}\right)^{\frac{1}{1-\beta}} \frac{\alpha}{1-\beta}(1-\eta\omega_m(\eta))^{\frac{\alpha}{1-\beta}-1}\frac{\partial \eta\omega_m(\eta)}{\partial \eta} - \nu\frac{\partial \omega_m}{\partial \eta} \\ &= \underbrace{\left(\frac{A\beta}{\pi}\right)^{\frac{1}{1-\beta}} \frac{\alpha}{1-\beta}(1-\eta\omega_m(\eta))^{\frac{\alpha}{1-\beta}-1}\psi_5\left(\frac{1-\beta}{1-\alpha-\beta}\right)\eta^{\frac{1-\beta}{1-\alpha-\beta}-1}}_{>0} - \nu\underbrace{\frac{\partial \omega_m}{\partial \eta}}_{<0} > 0,\end{aligned}$$

meaning that as the land needed to produce renewable energy increases, the more fossil fuels is used to produce energy.

• Finally, an increase in the price of fossil fuels reduces the use of fossil fuels in the energy mix as:

$$\begin{aligned}\frac{\partial b_m}{\partial \pi} &= (A\beta)^{\frac{1}{1-\beta}}\frac{\partial}{\partial \pi}\left[\frac{(1-\eta\omega_m)^\alpha}{\pi}\right]^{\frac{1}{1-\beta}} - \nu\frac{\partial \omega_m}{\partial \pi} \\ &= -\underbrace{(A\beta)^{\frac{1}{1-\beta}}\frac{1}{1-\beta}\left[\frac{(1-\eta\omega_m)^\alpha}{\pi}\right]^{\frac{\beta}{1-\beta}}\left[\frac{\pi\alpha\eta(1-\eta\omega_m)^{\alpha-1}\frac{\partial \omega_m}{\partial \pi} + (1-\eta\omega)^\alpha}{\pi^2}\right]}_{>0} - \underbrace{\nu\frac{\partial \omega_m}{\partial \pi}}_{>0} < 0,\end{aligned}$$

which ends the proof of Proposition 2.

D. Proof of Proposition 3.

Here we study the land allocation towards renewable energy that maximizes consumption at steady state. As $c_m = A(1-\eta\omega_m)^{\alpha}(b_m+\nu\omega_m)^{\beta} - \pi b_m$, then, deriving steady state consumption with respect to ω_m leads to:

$$\begin{aligned}\frac{\partial c_m}{\partial \omega_m} &= -A\eta\alpha(1-\eta\omega_m)^{\alpha-1}(b_m+\nu\omega_m)^{\beta} + A(1-\eta\omega_m)^{\alpha}\beta(b_m+\nu\omega_m)^{\beta-1}\left(\frac{\partial b_m}{\partial \omega_m}+\nu\right) - \pi\frac{\partial b_m}{\partial \omega_m}\\ &= -A\eta\alpha(1-\eta\omega_m)^{\alpha-1}\left(\frac{A\beta\,(1-\eta\omega_m)^{\alpha}}{\pi}\right)^{\frac{\beta}{1-\beta}} + \pi\left(\frac{\partial b_m}{\partial \omega_m}+\nu\right) - \pi\frac{\partial b_m}{\partial \omega_m}\\ &= -A\eta\alpha\left(\frac{A\beta}{\pi}\right)^{\frac{\beta}{1-\beta}}(1-\eta\omega_m)^{\frac{\alpha+\beta-1}{1-\beta}} + \nu\pi.\end{aligned}$$

Moreover as:

$$\frac{\partial^2 c_m}{\partial \omega_m^2} = -A\eta^2\alpha\left(\frac{A\beta}{\pi}\right)^{\frac{\beta}{1-\beta}}\frac{1-\alpha-\beta}{1-\beta}(1-\eta\omega_m)^{\frac{\alpha+\beta-1}{1-\beta}-1} < 0,$$

then the stock of renewable energy ω_g which maximizes steady state consumption is such that:

$$\begin{aligned}\frac{\partial c_m}{\partial \omega_m} = 0 \iff & A\eta\alpha\left(\frac{A\beta}{\pi}\right)^{\frac{\beta}{1-\beta}}(1-\eta\omega_g)^{\frac{\alpha+\beta-1}{1-\beta}} = \nu\pi\\ \iff & l_g = \eta\omega_g = 1 - \left(\frac{A\alpha\eta\left(\frac{A\beta}{\pi}\right)^{\frac{\beta}{1-\beta}}}{\nu\pi}\right)^{\frac{1-\beta}{1-\alpha-\beta}},\end{aligned}$$

which ends the proof of Proposition 3.

E. Proof of Proposition 4.

From equation (1.1) we have that $\lambda = u'(c) = c^{-\sigma}$. Therefore, differentiating with respect to time leads to $\dot{\lambda} = -\sigma c^{-\sigma-1}\dot{c}$. Writing equation (1.3) with the previous express of $\dot{\lambda}$ leads to the dynamics of consumption described in the following Euler equation:

$$\dot{c} = \frac{c}{\sigma}\left[A\nu\beta(1-\eta\omega)^{\alpha}(b+\nu\omega)^{\beta-1} - A\eta\alpha(1-\eta\omega)^{\alpha-1}(b+\nu\omega)^{\beta} - \rho\right].$$

Therefore, the dynamics in the accumulation of renewable energy and consumption are given by:

$$\begin{cases}\dot{\omega} = A(1-\eta\omega)^{\alpha}(b(\omega)+\nu\omega)^{\beta} - c - \pi b(\omega),\\ \dot{c} = \frac{c}{\sigma}\left[A\nu\beta(1-\eta\omega)^{\alpha}(b(\omega)+\nu\omega)^{\beta-1} - A\eta\alpha(1-\eta\omega)^{\alpha-1}(b(\omega)+\nu\omega)^{\beta} - \rho\right].\end{cases}$$

As from equation (1.2), $b = \left(\frac{A\beta(1-\eta\omega)^{\alpha}}{\pi}\right)^{\frac{1}{1-\beta}} - \nu\omega$, then the dynamics can be written as the following two dimension dynamic system in ω and c:

$$\begin{cases} \dot{\omega} = A\left(\frac{A\beta}{\pi}\right)^{\frac{\beta}{1-\beta}}(1-\eta\omega)^{\frac{\alpha+\beta-1}{1-\beta}} - \pi\left(\frac{A\beta(1-\eta\omega)^{\alpha}}{\pi}\right)^{\frac{1}{1-\beta}} + \nu\pi\omega - c, \\ \dot{c} = -\frac{c}{\sigma}\left[A\eta\alpha\left(\frac{A\beta}{\pi}\right)^{\frac{\beta}{1-\beta}}(1-\eta\omega)^{\frac{\alpha+\beta-1}{1-\beta}} + \rho - \nu\pi\right], \end{cases}$$

with $b = \left(\frac{A\beta(1-\eta\omega)^{\alpha}}{\pi}\right)^{\frac{1}{1-\beta}} - \nu\omega$, which ends the proof of Proposition 4.

F. Proof of Proposition 5.

The Hamiltonian of the problem writes:

$$H = u(c) + \lambda_{\omega}[A(1-\eta\omega)^{\alpha}(b+\nu\omega)^{\beta} - \theta P - c - \pi b] + \lambda_P[\gamma b - \delta P].$$

Thus, the F.O.C. lead to:

$$\begin{cases} \frac{\partial H}{\partial c} = 0 \implies u'(c) = \lambda_{\omega}, \\ \frac{\partial H}{\partial b} = 0 \implies \lambda_{\omega}[A(1-\eta\omega)^{\alpha}\beta(b+\nu\omega)^{\beta-1} - \pi] + \gamma\lambda_P = 0, \\ \frac{\partial H}{\partial \omega} = \lambda_{\omega}\left[-A\alpha\eta(1-\eta\omega)^{\alpha-1}(b+\nu\omega)^{\beta} + A\nu\beta(1-\eta\omega)^{\alpha}(b+\nu\omega)^{\beta-1}\right] = \rho\lambda_{\omega} - \dot{\lambda}_{\omega}, \\ \frac{\partial H}{\partial P} = -\lambda_{\omega}\theta - \delta\lambda_P = \rho\lambda_P - \dot{\lambda}_P. \end{cases} \tag{2}$$

From equation (2.2) we can express the shadow price of the stock of renewable energy price as a function of the shadow price of pollution as:

$$\lambda_{\omega} = \frac{\gamma}{\pi - A(1-\eta\omega)^{\alpha}\beta(b+\nu\omega)^{\beta-1}}\lambda_P.$$

Substituting λ_{ω} in equation (2.4) leads to the following dimension 4 dynamic system in $(\lambda_P, \lambda_{\omega}, \omega, P)$:

$$\begin{cases} \dot{\omega} = A(1-\eta\omega)^{\alpha}(b+\nu\omega)^{\beta} - \theta P - c - \pi b, \\ \dot{P} = \gamma b - \delta P, \\ \dot{\lambda}_{\omega} = [\rho + A\alpha\eta(1-\eta\omega)^{\alpha-1}(b+\nu\omega)^{\beta} - A\nu\beta(1-\eta\omega)^{\alpha}(b+\nu\omega)^{\beta-1}]\lambda_{\omega}, \\ \dot{\lambda}_P = \left[\rho + \delta + \frac{\gamma\theta}{\pi - A(1-\eta\omega)^{\alpha}\beta(b+\nu\omega)^{\beta-1}}\right]\lambda_P. \end{cases} \tag{3}$$

Thus, at steady state, if $c \neq 0$ then $\lambda_{\omega} \neq 0$ and $\lambda_P \neq 0$ then from equation (3.4) one gets:

$$\begin{aligned}
&\rho+\delta+\frac{\gamma\theta}{\pi-A(1-\eta\omega)^{\alpha}\beta(b+\nu\omega)^{\beta-1}}=0\\
\iff& A(1-\eta\omega)^{\alpha}\beta(b+\nu\omega)^{\beta-1}=\pi+\frac{\gamma\theta}{\rho+\delta}\\
\iff&(b+\nu\omega)^{\beta-1}=\frac{\pi+\frac{\gamma\theta}{\rho+\delta}}{A(1-\eta\omega)^{\alpha}\beta}\\
\iff& b+\nu\omega=\left(\frac{A\beta\left(1-\eta\omega\right)^{\alpha}}{\pi+\frac{\gamma\theta}{\rho+\delta}}\right)^{\frac{1}{1-\beta}}.
\end{aligned}$$

Injecting the previous expression of energy level $b+\nu\omega$ into equation (3.3) at steady state leads to:

$$\begin{aligned}
&\rho+A\alpha\eta(1-\eta\omega)^{\alpha-1}\left(\frac{A\beta\left(1-\eta\omega\right)^{\alpha}}{\pi+\frac{\gamma\theta}{\rho+\delta}}\right)^{\frac{\beta}{1-\beta}}-A\nu\beta(1-\eta\omega)^{\alpha}\left(\frac{A\beta\left(1-\eta\omega\right)^{\alpha}}{\pi+\frac{\gamma\theta}{\rho+\delta}}\right)^{\frac{\beta-1}{1-\beta}}=0\\
\iff&\rho+A\alpha\eta\left(\frac{A\beta}{\pi+\frac{\gamma\theta}{\rho+\delta}}\right)^{\frac{\beta}{1-\beta}}(1-\eta\omega)^{\frac{\alpha+\beta-1}{1-\beta}}=\nu\left(\pi+\frac{\gamma\theta}{\rho+\delta}\right)\\
\iff&(1-\eta\omega)^{\frac{\alpha+\beta-1}{1-\beta}}=\frac{\nu\left(\pi+\frac{\gamma\theta}{\rho+\delta}\right)-\rho}{A\alpha\eta\left(\frac{A\beta}{\pi}\right)^{\frac{\beta}{1-\beta}}}.
\end{aligned}$$

Therefore, if $\nu\left(\pi+\frac{\gamma\theta}{\rho+\delta}\right)-\rho>0$ then the land allocated to renewable energy production at steady state is:

$$l_e=1-\left(\frac{A\alpha\eta\left(\frac{A\beta}{\pi+\frac{\gamma\theta}{\rho+\delta}}\right)^{\frac{\beta}{1-\beta}}}{\nu\left(\pi+\frac{\gamma\theta}{\rho+\delta}\right)-\rho}\right)^{\frac{1-\beta}{1-\alpha-\beta}}.$$

Regarding, the stability of steady state, we compute in the following the coefficient of the Jacobian matrix at steady states from the dynamics of ω, P, c and b.

- As $\dot{\omega}=A(1-\eta\omega)^{\alpha}(b+\nu\omega)^{\beta}-\theta P-c-\pi b$ we can directly compute the coefficient of the Jacobian matrix for ω at steady state and:

$$\begin{cases}
\dfrac{\partial\dot{\omega}}{\partial\omega}=-A\alpha\eta(1-\eta\omega)^{\alpha-1}(b+\nu\omega)^{\beta}+A\beta\nu(1-\eta\omega)^{\alpha}(b+\nu\omega)^{\beta-1}=\rho,\\
\dfrac{\partial\dot{\omega}}{\partial P}=-\theta,\\
\dfrac{\partial\dot{\omega}}{\partial c}=-1,\\
\dfrac{\partial\dot{\omega}}{\partial b}=A\beta(1-\eta\omega)^{\alpha}(b+\nu\omega)^{\beta-1}-\pi=\dfrac{\gamma\theta}{\delta+\rho}.
\end{cases}$$

• As $\dot{P} = \gamma b - \delta P$ we can directly compute the coefficient of the Jacobian matrix for P at steady state and:

$$\begin{cases} \dfrac{\partial \dot{P}}{\partial \omega} = \dfrac{\partial \dot{P}}{\partial c} = 0, \\ \dfrac{\partial \dot{P}}{\partial P} = -\delta, \\ \dfrac{\partial \dot{P}}{\partial b} = \gamma. \end{cases}$$

• In order to compute the coefficient for c we must find the expression of the dynamics of consumption. Differentiating (2.1) with respect to time leads to $\dot{\lambda}_\omega = -\sigma c^{-\sigma-1}\dot{c}$. Thus, writing equation (3.3) with the previous express of $\dot{\lambda}_\omega$ leads to the dynamics of consumption with the following Euler equation:

$$\dot{c} = \frac{c}{\sigma}\left[A\nu\beta(1-\eta\omega)^\alpha(b+\nu\omega)^{\beta-1} - A\eta\alpha(1-\eta\omega)^{\alpha-1}(b+\nu\omega)^\beta - \rho\right].$$

Therefore, the coefficients of the Jacobian matrix for c at steady state are:

$$\begin{cases} \dfrac{\partial \dot{c}}{\partial \omega} = -\dfrac{c}{\sigma}[A\nu^2\beta(1-\beta)(1-\eta\omega)^\alpha(b+\nu\omega)^{\beta-2} + A\eta^2\alpha(1-\alpha)(1-\eta\omega)^{\alpha-2}(b+\nu\omega)^\beta \\ \qquad\qquad + 2A\eta\alpha\beta\nu(1-\eta\nu)^{\alpha-1}(b+\nu\omega)^{\beta-1}], \\ \dfrac{\partial \dot{c}}{\partial P} = \dfrac{\partial \dot{c}}{\partial c} = 0, \\ \dfrac{\partial \dot{c}}{\partial b} = -\dfrac{c}{\sigma}\left[A\nu\beta(1-\beta)(1-\eta\omega)^\alpha(b+\nu\omega)^{\beta-2} + A\eta\alpha\beta(1-\eta\omega)^{\alpha-1}(b+\nu\omega)^{\beta-1}\right]. \end{cases}$$

• Finally, in order to compute the coefficient for b we must find the expression of the dynamics of fossil fuels. From (2.2) we obtained the relation between the shadow price of the stock of renewable energy price and the shadow price of pollution being:

$$\lambda_P = \frac{\pi - A(1-\eta\omega)^\alpha\beta(b+\nu\omega)^{\beta-1}}{\gamma}\lambda_\omega.$$

Therefore, the time derivative of the shadow price of pollution can be written as:

$$\begin{aligned} \dot{\lambda_P} &= -\frac{A\beta}{\gamma}\frac{d}{dt}\left[(1-\eta\omega)^\alpha(b+\nu\omega)^{\beta-1}\right]\lambda_\omega + \frac{\pi - A(1-\eta\omega)^\alpha\beta(b+\nu\omega)^{\beta-1}}{\gamma}\dot{\lambda}_\omega \\ &= -\frac{A\beta}{\gamma}\left[\alpha(1-\eta\omega)^{\alpha-1}\eta\dot{\omega}(b+\nu\omega)^{\beta-1} + (1-\beta)(1-\eta\omega)^\alpha(b+\nu\omega)^{\beta-2}(\dot{b}+\nu\dot{\omega})\right]\lambda_\omega \\ &+ \frac{\pi - A(1-\eta\omega)^\alpha\beta(b+\nu\omega)^{\beta-1}}{\gamma}\dot{\lambda}_\omega. \end{aligned}$$

Thus, by injecting the expressions $\dot{\lambda_P}$ and λ_P in equation (3.4) we get that:

$$-\frac{A\beta}{\gamma}\left[\alpha(1-\eta\omega)^{\alpha-1}\eta\dot{\omega}(b+\nu\omega)^{\beta-1}+(1-\beta)(1-\eta\omega)^{\alpha}(b+\nu\omega)^{\beta-2}(\dot{b}+\nu\dot{\omega})\right]\lambda_\omega$$
$$+\frac{\pi-A(1-\eta\omega)^{\alpha}\beta(b+\nu\omega)^{\beta-1}}{\gamma}\dot{\lambda}_\omega=\left[\theta+(\rho+\delta)\frac{\pi-A(1-\eta\omega)^{\alpha}\beta(b+\nu\omega)^{\beta-1}}{\gamma}\right]\lambda_\omega.$$

Moreover, from (2.1) we know that $\lambda_\omega = u'(c) = c^{-\sigma}$ thus $\dot{\lambda}_\omega = -\sigma c^{-\sigma-1}\dot{c}$ which by substituting in the previous equation leads to the dynamics in b:

$$\dot{b}=\frac{\sigma\frac{\dot{c}}{c}\left[\pi-A\beta(1-\eta\omega)^{\alpha}(b+\nu\omega)^{\beta-1}\right]+\theta\gamma(\rho+\delta)\left[\pi-A(1-\eta\omega)^{\alpha}\beta(b+\nu\omega)^{\beta-1}\right]-A\beta\alpha(1-\eta\omega)^{\alpha-1}\eta\dot{\omega}(b+\nu\omega)^{\beta-1}}{(1-\beta)(1-\eta\omega)^{\alpha}(b+\nu\omega)^{\beta-2}}-\nu\dot{\omega}$$

and thus, the coefficients of the Jacobian matrix for b at steady state are:

$$\begin{cases}\dfrac{\partial\dot{b}}{\partial\omega}=(\rho+\delta)\dfrac{\alpha\eta(1-\eta\omega)^{\alpha-1}(b+\nu\omega)^{\beta-1}+\nu(1-\beta)(1-\eta\omega)^{\alpha}(b+\nu\omega)^{\beta-2}}{(1-\beta)(1-\eta\omega)^{\alpha}(b+\nu\omega)^{\beta-2}},\\ \dfrac{\partial\dot{b}}{\partial P}=\dfrac{\partial\dot{b}}{\partial c}=0,\\ \dfrac{\partial\dot{b}}{\partial b}=\rho+\ \delta.\end{cases}$$

As a result, the Jacobian matrix of the system at steady states writes as:

$$\mathcal{J}=\begin{pmatrix}\rho & -\theta & -1 & \frac{\gamma\theta}{\rho+\delta}\\ 0 & -\delta & 0 & \gamma\\ \frac{\partial\dot{c}}{\partial\omega} & 0 & 0 & \frac{\partial\dot{c}}{\partial b}\\ \frac{\partial\dot{b}}{\partial\omega} & 0 & 0 & \delta+\rho\end{pmatrix}.$$

First of all, we have that $\mathrm{Tr}(\mathcal{J}) = 2\rho > 0$ which means that there is at least one strictly positive eigenvalue. Moreover, let's denote $l = 1-\eta\omega$ the land variable and $\epsilon = b+\nu\omega$ the energy variable then:

$$\begin{aligned}\det(\mathcal{J}) &= \delta\left[\frac{\partial\dot{b}}{\partial\omega}\frac{\partial\dot{c}}{\partial b}-(\delta+\rho)\frac{\partial\dot{c}}{\partial\omega}\right]\\ &= \frac{\delta}{\delta+\rho}\left[\frac{1}{\delta+\rho}\frac{\partial\dot{b}}{\partial\omega}\frac{\partial\dot{c}}{\partial b}-\frac{\partial\dot{c}}{\partial\omega}\right]\\ &= -\frac{\frac{c}{\sigma}\left[\alpha\eta l^{\alpha-1}\epsilon^{\beta-1}+(1-\beta)\nu l^{\alpha}\epsilon^{\beta-2}\right]\left[A\nu\beta(1-\beta)l^{\alpha}\epsilon^{\beta-2}+A\eta\alpha\beta l^{\alpha-1}\epsilon^{\beta-1}\right]}{(1-\beta)l^{\alpha}\epsilon^{\beta-2}}-\frac{\partial\dot{c}}{\partial\omega}\\ &= -\frac{c}{\sigma}\left[A\nu^2\beta(1-\beta)l^{\alpha}\epsilon^{\beta-2}-\frac{A\eta^2\alpha^2\beta}{1-\beta}l^{\alpha-2}\epsilon^{\beta}-2A\alpha\beta\eta\nu l^{\alpha-1}\epsilon^{\beta-1}\right]-\frac{\partial\dot{c}}{\partial\omega}.\end{aligned}$$

After simplifications we get that:

$$\begin{aligned}\det(\mathcal{J}) &= \frac{c}{\sigma}\left[l^{\alpha-2}\epsilon^{\beta}\left(A\eta^2\alpha(1-\alpha)-\frac{A\eta^2\alpha^2\beta}{1-\beta}\right)\right]\\ &= \frac{c}{\sigma}A\alpha\eta^2 l^{\alpha-2}\epsilon^{\beta}\left(1-\alpha-\frac{\alpha\beta}{1-\beta}\right)\\ &= \underbrace{\frac{c}{\sigma}A\alpha\eta^2 l^{\alpha-2}\epsilon^{\beta}}_{>0}\underbrace{\frac{1-\alpha-\beta}{1-\beta}}_{\substack{>0\\ \text{as } \alpha+\beta<1}} > 0.\end{aligned}$$

Therefore, as $\det(\mathcal{J}) > 0$ this means that the product of the four eigenvalues of $\mathcal{J}$ is strictly positive. This means that either the four eigenvalues are strictly positive, either the four eigenvalues are strictly negative or either two eigenvalues are strictly positive and two eigenvalues are strictly positive. Note that as $\mathrm{Tr}(\mathcal{J}) = 2\rho > 0$ then the case in which the four eigenvalues are strictly negative can be excluded. Moreover, the characteristic polynomial of $\mathcal{J}$ writes:

$$\begin{aligned}\Lambda(X) &= \det(\mathcal{J} - X\mathbb{I})\\ &= (-\delta - X)\left[\frac{\partial\dot{b}}{\partial\omega}\left(-\frac{\partial\dot{c}}{\partial b}+X\frac{\partial\dot{\omega}}{\partial b}\right)-(\delta+\rho-X)\left(-X(\rho-X)+\frac{\partial\dot{c}}{\partial\omega}\right)\right]+\gamma\theta\frac{\partial\dot{b}}{\partial\omega}X.\end{aligned}$$

As a result, we have that:

$$\Lambda(0) = \det(\mathcal{J}) > 0,$$

and:

$$\Lambda(-\delta) = -\gamma\theta\frac{\partial\dot{b}}{\partial\omega}\delta < 0,$$

as $\gamma > 0$, $\theta > 0$, $\delta > 0$ and:

$$\frac{\partial\dot{b}}{\partial\omega} = (\rho+\delta)\frac{\alpha\eta(1-\eta\omega)^{\alpha-1}(b+\nu\omega)^{\beta-1}+\nu(1-\beta)(1-\eta\omega)^{\alpha}(b+\nu\omega)^{\beta-2}}{(1-\beta)(1-\eta\omega)^{\alpha}(b+\nu\omega)^{\beta-2}} > 0.$$

This means that Λ has a root in $]-\delta, 0[$. In other words, $\mathcal{J}$ has at least one strictly negative eigenvalue. Thus, the case where $\mathcal{J}$ has four strictly positive eigenvalues can also be excluded. Therefore, by elimination, $\mathcal{J}$ has two strictly positive eigenvalues and two strictly negative eigenvalues, which proves saddle path stability.

To finish the proof we shall study the comparative statics of the equilibrium with respect to θ, γ and δ. In the expression of the land use equilibrium the pollution terms θ, γ and δ are gathered in the term $\frac{\gamma\theta}{\rho+\delta}$ in the numerator and denominator of agricultural land use that is:

$$\kappa_e = \left(\frac{A\alpha\eta \left(\frac{A\beta}{\pi + \frac{\gamma\theta}{\rho+\delta}} \right)^{\frac{\beta}{1-\beta}}}{\nu \left(\pi + \frac{\gamma\theta}{\rho+\delta} \right) - \rho} \right)^{\frac{1-\beta}{1-\alpha-\beta}}.$$

Thereby, as θ or γ increases, the term $\frac{\gamma\theta}{\rho+\delta}$ increases which diminishes the numerator and increases the denominator of κ_e. As a result, agricultural land diminishes and land allocated to renewable energy increases. On the contrary, if δ increases, then the term $\frac{\gamma\theta}{\rho+\delta}$ decreases. Thereby, an increase in pollution natural decay results in a decrease in renewable production land allocation and an increase in agricultural land.

G. Proof of Proposition 6.

From the expression of the land allocated to renewable energy we directly have the stock of installed renewable energy on this land being:

$$\omega_e = \frac{1}{\eta} \left[1 - \left(\frac{A\alpha\eta \left(\frac{A\beta}{\pi + \frac{\gamma\theta}{\rho+\delta}} \right)^{\frac{\beta}{1-\beta}}}{\nu \left(\pi + \frac{\gamma\theta}{\rho+\delta} \right) - \rho} \right)^{\frac{1-\beta}{1-\alpha-\beta}} \right].$$

Moreover, as the expression $b + \nu\omega = \left(\frac{A\beta(1-\eta\omega_e)^\alpha}{\pi + \frac{\gamma\theta}{\rho+\delta}} \right)^{\frac{1}{1-\beta}}$ is true at steady state then:

$$b_e = \left[\frac{A\beta \left(1 - l_e\right)^\alpha}{\pi + \frac{\gamma\theta}{\rho+\delta}} \right]^{\frac{1}{1-\beta}} - \nu\omega_e = \left[\frac{A\beta \left(1 - l_e\right)^\alpha}{\pi + \frac{\gamma\theta}{\rho+\delta}} \right]^{\frac{1}{1-\beta}} - \frac{\nu}{\eta} l_e.$$

Now the comparative statics for ω_m in θ, γ and δ is very straightforward from the previous comparative statics for l_e. Indeed, as $\omega_e = \frac{l_e}{\eta}$ then the monotony of ω_e with respect to θ, γ and δ is the same as the one of l_e. Regarding l_e, the pollution terms θ, γ and δ are both in the term $\frac{\gamma\theta}{\rho+\delta}$ in the numerator of $\left[\frac{A\beta(1-l_e)^\alpha}{\pi + \frac{\gamma\theta}{\rho+\delta}} \right]^{\frac{1}{1-\beta}}$, as well as in the expression of l_e. Yet, as θ or γ increases, the $\frac{\gamma\theta}{\rho+\delta}$ increases, thereby reducing $\left[\frac{A\beta(1-l_e)^\alpha}{\pi + \frac{\gamma\theta}{\rho+\delta}} \right]^{\frac{1}{1-\beta}}$ in the expression of b_e. Moreover, as l_e increases when θ or γ increases then the terms in $-l_e$ in the expression of b_e decreases. As a result, b_e decreases with respect to θ and γ. On the contrary, as δ increases, the $\frac{\gamma\theta}{\rho+\delta}$ decreases, thereby increasing $\left[\frac{A\beta(1-l_e)^\alpha}{\pi + \frac{\gamma\theta}{\rho+\delta}} \right]^{\frac{1}{1-\beta}}$ in the expression of b_e. Moreover, as

l_e decreases when δ increases then the terms in $-l_e$ in the expression of b_e increases. As a result, b_e increases with respect to δ which completes to proof of Proposition 6.

H. Proof of Proposition 7.

As $\dot{\omega} = A(1-\eta\omega)^{\alpha}(b+\nu\omega)^{\beta} - \theta P - c - \pi b$ then at steady state we get that:

$$c_e = A(1-\eta\omega_e)^{\alpha}(b_e+\nu\omega_e)^{\beta} - \pi b_e - \theta P_e.$$

We express steady state consumption as a function of the stock of renewable energy at steady state:

$$\begin{aligned}
c_e &= A(1-\eta\omega_e)^{\alpha}(b_e+\nu\omega_e)^{\beta} - \pi b_e - \theta P_e \\
&= A(1-\eta\omega_e)^{\alpha}(b_e+\nu\omega_e)^{\beta} - \left(\pi + \frac{\theta\gamma}{\delta}\right) b_e \\
&= A(1-\eta\omega_e)^{\alpha}\left[\frac{A\beta\,(1-\eta\omega_e)^{\alpha}}{\pi+\frac{\gamma\theta}{\rho+\delta}}\right]^{\frac{\beta}{1-\beta}} - \left(\pi+\frac{\theta\gamma}{\delta}\right)\left[\frac{A\beta\,(1-\eta\omega_e)^{\alpha}}{\pi+\frac{\gamma\theta}{\rho+\delta}}\right]^{\frac{1}{1-\beta}} - \nu\omega_e \\
&= \left[A\left(\frac{\beta}{\pi+\frac{\gamma\theta}{\rho+\delta}}\right)^{\beta}\right]^{\frac{1}{1-\beta}} (1-\beta)(1-\eta\omega_e)^{\frac{\alpha}{1-\beta}} + \left(\pi+\frac{\theta\gamma}{\delta}\right)\nu\omega_e.
\end{aligned}$$

Therefore, deriving the steady state consumption w.r.t. the stock of renewable energy leads to:

$$\frac{\partial c_e}{\partial \omega_e} = -\alpha\eta\left[A\left(\frac{\beta}{\pi+\frac{\gamma\theta}{\rho+\delta}}\right)^{\beta}\right]^{\frac{1}{1-\beta}} (1-\eta\omega_e)^{\frac{\alpha+\beta-1}{1-\beta}} + \left(\pi+\frac{\theta\gamma}{\delta}\right)\nu.$$

Moreover as $\frac{\partial^2 c_e}{\partial {\omega_e}^2} = -\underbrace{\frac{1-\alpha-\beta}{1-\beta}}_{>0}\alpha\eta^2\left[A\left(\frac{\beta}{\pi+\frac{\gamma\theta}{\rho+\delta}}\right)^{\beta}\right]^{\frac{1}{1-\beta}} (1-\eta\omega_e)^{\frac{\alpha+\beta-1}{1-\beta}-1} < 0$ then the stock of renewable energy ω_{g_e} which maximizes steady state consumption is such that:

$$\begin{aligned}
\frac{\partial c_e}{\partial \omega_e} = 0 &\iff \alpha\eta\left[A\left(\frac{\beta}{\pi+\frac{\gamma\theta}{\rho+\delta}}\right)^{\beta}\right]^{\frac{1}{1-\beta}} (1-\eta\omega_{g_e})^{\frac{\alpha+\beta-1}{1-\beta}} = \left(\pi+\frac{\theta\gamma}{\delta}\right)\nu \\
&\iff l_{g_e} = \eta\omega_{g_e} = 1 - \left(\frac{A\alpha\eta\left(\frac{A\beta}{\pi+\frac{\gamma}{\rho+\delta}\frac{\theta}{}}\right)^{\frac{\beta}{1-\beta}}}{\nu\left(\pi+\frac{\theta\gamma}{\delta}\right)}\right)^{\frac{1-\beta}{1-\alpha-\beta}}.
\end{aligned}$$

which ends the the proof of Proposition 7.

I. Proof of Proposition 8.

As $\dot{P} = \gamma b - \delta P$ then at steady state we get that $P_e = \frac{\gamma b_e}{\delta}$. Therefore:

$$\frac{\partial P_e}{\partial l_e} = \frac{\gamma}{\delta}\frac{\partial b_e}{\partial l_e} = \underbrace{-\frac{\gamma}{\delta}\left[\frac{A\beta}{\pi + \frac{\gamma\theta}{\rho+\delta}}\right]^{\frac{1}{1-\beta}} \frac{\alpha}{1-\beta}(1-l_e)^{\frac{\alpha}{1-\beta}-1}}_{<0} - \frac{\nu}{\eta} < 0,$$

meaning that as land use of renewable energy at steady state increases, the pollution decreases and thus there is no interior stock of renewable energy land allocation that minimizes pollution as there is one that maximizes consumption.

J. Proof of Proposition 9.

Writing the steady states expressions from Proposition 1 for the *market problem* with a price on fossil fuels $\pi' = \pi + \frac{\gamma\theta}{\rho+\delta}$ where π is the price of fossil fuels for the *environmental problem* proves the claim.

K. Proof of Proposition 10.

The Hamiltonian of the *abatement problem* writes as:

$$H = u(c) + \lambda_\omega[A(1-\eta\omega-\xi)^\alpha(b+\nu\omega)^\beta - \theta P - c - \pi b] + \lambda_P[\gamma b - \delta P - f(\xi)].$$

Thus the F.O.C lead to:

$$\begin{cases} \frac{\partial H}{\partial c} = 0 \implies u'(c) = \lambda_\omega, \\ \frac{\partial H}{\partial b} = 0 \implies \lambda_\omega[A(1-\eta\omega-\xi)^\alpha\beta(b+\nu\omega)^{\beta-1} - \pi] + \gamma\lambda_P = 0, \\ \frac{\partial H}{\partial \xi} = 0 \implies -\lambda_\omega A\alpha(1-\eta\omega-\xi)^{\alpha-1}(b+\nu\omega)^\beta - \lambda_P f'(\xi) = 0, \\ \frac{\partial H}{\partial \omega} = \lambda_\omega\ [-A\alpha\eta(1-\eta\omega-\xi)^{\alpha-1}(b+\nu\omega)^\beta + A\nu\beta(1-\eta\omega-\xi)^\alpha(b+\nu\omega)^{\beta-1}] = \rho\lambda_\omega - \dot{\lambda}_\omega, \\ \frac{\partial H}{\partial P} = -\lambda_\omega\theta - \delta\lambda_P = \rho\lambda_P - \dot{\lambda}_P. \end{cases} \tag{4}$$

From (4.2) we can expression the shadow price of the stock of renewable energy price as a function of the shadow price of pollution as

$$\lambda_\omega = \frac{\gamma}{\pi - A(1-\eta\omega-\xi)^\alpha\beta(b+\nu\omega)^{\beta-1}}\lambda_P,$$

and substituting λ_ω in (4.5) leads to the following dimension 4 dynamic system in $(\lambda_P, \lambda_\omega, \omega, P)$:

$$\begin{cases} \dot{\omega} = A(1-\eta\omega-\xi)^\alpha(b+\nu\omega)^\beta - \theta P - c - \pi b, \\ \dot{P} = \gamma b - \delta P, \\ \dot{\lambda}_\omega = [\rho + A\alpha\eta(1-\eta\omega-\xi)^{\alpha-1}(b+\nu\omega)^\beta - A\nu\beta(1-\eta\omega-\xi)^\alpha(b+\nu\omega)^{\beta-1}]\lambda_\omega, \\ \dot{\lambda}_P = \left[\rho + \delta + \frac{\gamma\theta}{\pi - A(1-\eta\omega-\xi)^\alpha\beta(b+\nu\omega)^{\beta-1}}\right]\lambda_P. \end{cases} \tag{5}$$

Thus, at steady state, if $c \neq 0$ then $\lambda_\omega \neq 0$ and $\lambda_P \neq 0$ then from (4.5) we have that:

$$\begin{aligned} & \rho + \delta + \frac{\gamma\theta}{\pi - A(1-\eta\omega-\xi)^\alpha\beta(b+\nu\omega)^{\beta-1}} = 0 \\ \iff & A(1-\eta\omega-\xi)^\alpha\beta(b+\nu\omega)^{\beta-1} = \pi + \frac{\gamma\theta}{\rho+\delta} \\ \iff & (b+\nu\omega)^{\beta-1} = \frac{\pi + \frac{\gamma\theta}{\rho+\delta}}{A(1-\eta\omega-\xi)^\alpha\beta} \\ \iff & b+\nu\omega = \left(\frac{A\beta\,(1-\eta\omega-\xi)^\alpha}{\pi + \frac{\gamma\theta}{\rho+\delta}}\right)^{\frac{1}{1-\beta}}. \end{aligned}$$

Thereby as for the proof of Proposition 5 we get that, if $\nu\left(\pi + \frac{\gamma\theta}{\rho+\delta}\right) - \rho > 0$, the land allocated to agricultural production is given by:

$$\kappa_a = \left(\frac{A\alpha\eta\left(\frac{A\beta}{\pi+\frac{\gamma\theta}{\rho+\delta}}\right)^{\frac{\beta}{1-\beta}}}{\nu\left(\pi+\frac{\gamma\theta}{\rho+\delta}\right)-\rho}\right)^{\frac{1-\beta}{1-\alpha-\beta}} = \left[A\left(\frac{\eta}{\nu}\cdot\frac{\alpha}{(\pi-\pi_e)}\right)^{1-\beta}\left(\frac{\beta}{\pi+\frac{\gamma\theta}{\rho+\delta}}\right)^{\beta}\right]^{\frac{1}{1-\alpha-\beta}}.$$

From (4.3) we get that:

$$\begin{aligned} f'(\xi) &= -\frac{\lambda_\omega}{\lambda_P}A\alpha(1- \eta\omega-\xi)^{\alpha-1}(b+\nu\omega)^\beta \\ &= \frac{\gamma}{A(1- \eta\omega-\xi)^\alpha\beta(b+\nu\omega)^{\beta-1} - \pi}A\alpha(1- \eta\omega-\xi)^{\alpha-1}(b+\nu\omega)^\beta, \end{aligned}$$

and at steady state (5.4) leads to:

$$\frac{\gamma\theta}{A(1- \eta\omega-\xi)^\alpha\beta(b+\nu\omega)^{\beta-1} - \pi} = \rho + \delta.$$

Thereby we get:

$$
\begin{aligned}
f'(\xi) &= \frac{\rho+\delta}{\theta} A\alpha(1- \ \eta\omega - \xi)^{\alpha-1}(b+\nu\omega)^{\beta} \\
&= \frac{\rho+\delta}{\theta} A\alpha(1- \ \eta\omega - \xi)^{\alpha-1} \left(\frac{A\beta\,(1-\eta\omega-\xi)^{\alpha}}{\pi + \frac{\gamma\theta}{\rho+\delta}} \right)^{\frac{\beta}{1-\beta}} \\
&= \frac{\rho+\delta}{\theta} A\alpha \left(\frac{A\beta}{\pi + \frac{\gamma\theta}{\rho+\delta}} \right)^{\frac{\beta}{1-\beta}} \left(\frac{\nu\left(\pi + \frac{\gamma\theta}{\rho+\delta}\right) - \rho}{A\alpha\eta \left(\frac{A\beta}{\pi+\frac{\gamma\theta}{\rho+\delta}} \right)^{\frac{\beta}{1-\beta}}} \right) \\
&= \frac{\rho+\delta}{\theta} \left(\frac{\nu\left(\pi + \frac{\gamma\theta}{\rho+\delta}\right) - \rho}{\eta} \right).
\end{aligned}
$$

Finally, as $f(\xi) = \mu\xi^{\epsilon}$ we get that $f'(\xi) = \mu\epsilon\xi^{\epsilon-1}$ and thus:

$$
\mu\epsilon\xi^{\epsilon-1} = \frac{\rho+\delta}{\theta} \left(\frac{\nu\left(\pi + \frac{\gamma\theta}{\rho+\delta}\right) - \rho}{\eta} \right) \iff \xi_a = \left[\mu\epsilon \cdot \frac{\eta}{\nu} \cdot \frac{\theta}{(\rho+\delta)(\pi-\pi_e)} \right]^{\frac{1}{1-\epsilon}},
$$

which ends the proof of Proposition 10. The stability analysis is equivalent to the one from *environmental problem* in the proof of Proposition 5.

L. Proof of Proposition 11.

First, let's assume that fossil price is such that $\pi > \frac{\rho}{\nu}$. Therefore the problem is well defined for all $\theta > 0$ and:

$$
\begin{aligned}
\kappa_a'(\theta) = -\frac{A\eta\alpha\beta}{\nu} \Bigg[& \frac{1- \ \alpha}{1-\alpha-\beta} \left(\frac{1}{\pi-\pi_e} \right)^{\frac{\alpha}{1-\alpha-\beta}} \frac{\frac{\gamma}{\rho+\delta}}{(\pi-\pi_e)^2} \left(\frac{1}{\pi-\pi_e+\pi_m} \right)^{\frac{\beta}{1-\alpha-\beta}} \\
& + \frac{\beta}{1-\alpha-\beta} \left(\frac{1}{\pi-\pi_e} \right)^{\frac{1-\beta}{1-\alpha-\beta}} \frac{\frac{\gamma}{\rho+\delta}}{(\pi-\pi_e+\pi_m)^2} \left(\frac{1}{\pi-\pi_e+\pi_m} \right)^{\frac{\alpha+2\beta-1}{1-\alpha-\beta}} \Bigg] < 0.
\end{aligned}
$$

Thereby, land allocation to agricultural production decreases as production sensitivity to pollution rises. This land is therefore allocated to mitigations measures and we shall study the trade off in the reallocation of agricultural land. Note that from the above expression, we directly see that κ_a' increases with respect to θ. Thus κ_a is convex, that is $\kappa_a''(\theta) > 0$ for all $\theta > 0$. Moreover:

$$
\begin{aligned}
\kappa_a'(0) = -\frac{A\eta\alpha\beta}{\nu} \Bigg[& \frac{1- \ \alpha}{1-\alpha-\beta} \left(\frac{1}{\pi-\frac{\rho}{\nu}} \right)^{\frac{\alpha}{1-\alpha-\beta}} \frac{\frac{\gamma}{\rho+\delta}}{(\pi-\frac{\rho}{\nu})^2} \left(\frac{1}{\pi} \right)^{\frac{\beta}{1-\alpha-\beta}} \\
& + \frac{\beta}{1-\alpha-\beta} \left(\frac{1}{\pi-\frac{\rho}{\nu}} \right)^{\frac{1-\beta}{1-\alpha-\beta}} \frac{\gamma}{(\rho+\delta)\pi^2} \left(\frac{1}{\pi} \right)^{\frac{\alpha+2\beta-1}{1-\alpha-\beta}} \Bigg] < 0.
\end{aligned}
$$

Regarding land allocation to abatement we have that:

$$\xi_a'(\theta) = \frac{\pi - \frac{\rho}{\nu}}{1-\epsilon}\left[\frac{\mu\eta\epsilon}{\nu(\rho+\delta)}\frac{\theta^\epsilon}{(\pi-\pi_e)^{2-\epsilon}}\right]^{\frac{1}{1-\epsilon}}.$$

Therefore, $\xi_a'(0) = 0$ and $\xi_a'(\theta) > 0$ for all $\theta > 0$. As a result, land allocated to abatement always increase as pollution sensitivity increases, which proves the first part of the claim. The second part of the claim is the evolution of the land allocated to renewable energy as sensitivity increases. Taking the second derivative of abatement policy with respect to pollution sensitivity leads to:

$$\xi_a''(\theta) = \frac{\pi - \frac{\rho}{\nu}}{(1-\epsilon)^2}\left(\frac{\mu\eta\epsilon}{\nu(\rho+\delta)}\right)^{\frac{1}{1-\epsilon}}\left[\frac{\theta^\epsilon}{(\pi-\pi_e)^{2-\epsilon}}\right]^{\frac{\epsilon}{1-\epsilon}}\left[\frac{\epsilon\theta^{\epsilon-1}(\pi-\pi_e)^{2-\epsilon} + \theta^\epsilon(2-\epsilon)(\pi-\pi_e)^{1-\epsilon}\pi_e'}{(\pi-\pi_e)^{4-2\epsilon}}\right].$$

Thus, as $\pi > \frac{\rho}{\nu}$ then:

$$\begin{aligned}
\xi_a''(\theta) \geq 0 &\iff \epsilon\theta^{\epsilon-1}(\pi-\pi_e)^{2-\epsilon} + \theta^\epsilon(2-\epsilon)(\pi-\pi_e)^{1-\epsilon}\pi_e' \geq 0 \\
&\iff \epsilon(\pi-\pi_e) - \theta\frac{\gamma}{\rho+\delta}(2-\epsilon) \geq 0 \\
&\iff \epsilon\pi + \frac{\gamma\theta\epsilon}{\rho+\delta} - \frac{\rho\epsilon}{\nu} - 2\frac{\theta\gamma}{\rho+\delta} + \frac{\gamma\theta\epsilon}{\rho+\delta} \geq 0 \\
&\iff \theta \leq \frac{\epsilon(\rho+\delta)}{2\gamma(1-\epsilon)}\left(\pi - \frac{\rho}{\nu}\right).
\end{aligned}$$

Therefore, ξ_a has one inflection point $\hat{\theta} = \frac{\epsilon(\rho+\delta)}{2\gamma(1-\epsilon)}\left(\pi - \frac{\rho}{\nu}\right) > 0$ as $\pi > \frac{\rho}{\nu}$, bellow which the abatement policy is convex with respect to sensitivity, that is $\xi_a''(\theta) > 0$ for all $\theta < \hat{\theta}$. Finally, as $l_a = 1 - \kappa_a - \xi_a$ then $l_a' = -(\kappa_a' + \xi_a')$ and thus:

$$l_a'(0) = -(\kappa_a'(0) + \xi_a'(0)) = -\kappa_a'(0) > 0,$$

as $\xi_a'(0) = 0$ and $\kappa_a'(0) < 0$, and from Assumption 5 we have that $\kappa_a'(\hat{\theta}) + \xi_a'(\hat{\theta}) > 0$, which implies:

$$l_a'(\hat{\theta}) = -(\kappa_a'(\hat{\theta}) + \xi_a'(\hat{\theta})) < 0.$$

Therefore, as ξ_a' and κ_a' are strictly monotonous and continuous on $[0, \hat{\theta}[$ then there exists one and only one $\tilde{\theta} \in [0, \hat{\theta}[$ such that $l_a'(\tilde{\theta}) = 0$. Moreover, from Assumption 5 we have that:

$$\forall\theta \geq \hat{\theta}\ \xi'(\theta) + \kappa'(\theta) > 0 \iff \forall\theta \geq \hat{\theta}\ l_a'(\theta) < 0.$$

Thus, land allocation towards renewable energy has one and only one extremum that is $\tilde{\theta} \in [0, \hat{\theta}[$, and as κ_a and ξ_a are both convex in $[0, \hat{\theta}[$ then $\kappa_a''(\tilde{\theta}) > 0$ and $\xi_a''(\tilde{\theta}) > 0$. Thereby:

$$l_a'(\tilde{\theta}) = -(\kappa_a''(\tilde{\theta}) + \xi_a''(\tilde{\theta})) < 0,$$

which proves that the threshold $\tilde{\theta}$ for production sensitivity to pollution is a maximum for land allocation to renewable energy and completes the proof of Proposition 11.

M. Proof of Proposition 12.

From Proposition 3 we have that $P_a = \frac{\gamma b_a - f(\xi)}{\delta}$ therefore:

$$\frac{\partial P_a}{\partial \xi} = \frac{\frac{\gamma\nu}{\eta} - f'(\xi)}{\delta} = 0 \iff f'(\xi) = \frac{\gamma\nu}{\eta}.$$

Thus, as $f(\xi) = \mu\xi^\epsilon$ then the abatement policy ξ_P which minimizes pollution is such that:

$$f'(\xi_P) = \frac{\gamma\nu}{\eta} \iff \xi_P = \left(\frac{\eta\mu\epsilon}{\gamma\nu}\right)^{\frac{1}{1-\epsilon}},$$

with:

$$\left.\frac{\partial^2 P_a}{\partial \xi^2}\right|_{\xi=\xi_P} = -f''(\xi_P) = \underbrace{(1-\epsilon)}_{>0}\underbrace{\mu\epsilon\xi_P^{\epsilon-2}}_{>0} > 0,$$

which shows that ξ_P indeed minimizes steady state pollution.

Moreover, be $e_a = b_a + \nu\omega_a$ the energy level at steady state then the consumption at steady state writes as:

$$c_a = A(1 - \xi - \eta\omega_a)^\alpha e_a^\beta - \pi b_a - \theta\left(\frac{\gamma b_a - f(\xi)}{\delta}\right).$$

Finally, as $e_a = \left(\frac{A\beta\kappa_a^\alpha}{\pi + \frac{\gamma\theta}{\rho+\delta}}\right)^{\frac{1}{1-\beta}}$ then $\frac{\partial e_a}{\partial \xi} = \frac{\partial \kappa_a^{\frac{\alpha}{1-\beta}}}{\partial \xi} = 0$ and $\frac{\partial b_a}{\partial \xi} = \frac{\nu}{\eta}$, therefore:

$$\frac{\partial c_a}{\partial \xi} = \frac{\theta}{\delta}f'(\xi) - \frac{\nu}{\eta}\left(\pi + \frac{\gamma\theta}{\delta}\right) = 0 \iff f'(\xi) = \frac{\delta\nu}{\eta\theta}\left(\pi + \frac{\gamma\theta}{\delta}\right).$$

Hence, the abatement policy ξ_c which maximizes consumption is such that:

$$f'(\xi_c) = \frac{\delta\nu}{\eta\theta}\left(\pi + \frac{\gamma\theta}{\delta}\right) \iff \xi_c = \left(\frac{\theta\eta\mu\epsilon}{\delta\nu\left(\pi + \frac{\gamma\theta}{\delta}\right)}\right)^{\frac{1}{1-\epsilon}},$$

with:

$$\left.\frac{\partial^2 c_a}{\partial \xi^2}\right|_{\xi=\xi_c} = \frac{\theta}{\delta}f''(\xi_c) = \underbrace{(\epsilon-1)}_{<0}\underbrace{\frac{\theta}{\delta}\mu\epsilon\xi_c^{\epsilon-2}}_{>0} < 0,$$

which shows that ξ_c indeed maximizes steady state consumption and ends the proof of Proposition 12.

N. Proof of Proposition 13.

Writing the Hamiltonian of the *abatement problem* with the transfert $\tau\xi$ leads to:

$$H = u(c) + \lambda_\omega[A(1-\eta\omega-\xi)^\alpha(b+\nu\omega)^\beta - \theta P - c - \pi b + \tau\xi] + \lambda_P[\gamma b - \delta P - f(\xi)].$$

Thus the F.O.C lead to:

$$\begin{cases} \frac{\partial H}{\partial c} = 0 \implies u'(c) = \lambda_\omega, \\ \frac{\partial H}{\partial b} = 0 \implies \lambda_\omega[A(1-\eta\omega-\xi)^\alpha\beta(b+\nu\omega)^{\beta-1} - \pi] + \gamma\lambda_P = 0, \\ \frac{\partial H}{\partial \xi} = 0 \implies \lambda_\omega[\tau - A\alpha(1-\eta\omega-\xi)^{\alpha-1}(b+\nu\omega)^\beta] - \lambda_P f'(\xi) = 0, \\ \frac{\partial H}{\partial \omega} = \lambda_\omega\ [-A\alpha\eta(1-\eta\omega-\xi)^{\alpha-1}(b+\nu\omega)^\beta + A\nu\beta(1-\eta\omega-\xi)^\alpha(b+\nu\omega)^{\beta-1}] = \rho\lambda_\omega - \dot{\lambda}_\omega, \\ \frac{\partial H}{\partial P} = -\lambda_\omega\theta - \delta\lambda_P = \rho\lambda_P - \dot{\lambda}_P. \end{cases} \tag{6}$$

From (6.2) the expression of the shadow price of the stock of renewable energy price as a function of the shadow price of pollution as:

$$\lambda_\omega = \frac{\gamma}{\pi - A(1-\eta\omega-\xi)^\alpha\beta(b+\nu\omega)^{\beta-1}}\lambda_P,$$

and substituting λ_ω in (6.5) leads to the following dimension 4 dynamic system in $(\lambda_P, \lambda_\omega, \omega, P)$:

$$\begin{cases} \dot{\omega} = A(1-\eta\omega-\xi)^\alpha(b+\nu\omega)^\beta - \theta P - c - \pi b, \\ \dot{P} = \gamma b - \delta P, \\ \dot{\lambda}_\omega = [\rho + A\alpha\eta(1-\eta\omega-\xi)^{\alpha-1}(b+\nu\omega)^\beta - A\nu\beta(1-\eta\omega-\xi)^\alpha(b+\nu\omega)^{\beta-1}]\lambda_\omega, \\ \dot{\lambda}_P = \left[\rho + \delta + \frac{\gamma\theta}{\pi - A(1-\eta\omega-\xi)^\alpha\beta(b+\nu\omega)^{\beta-1}}\right]\lambda_P. \end{cases} \tag{7}$$

Thus, at steady state, if $c \neq 0$ then $\lambda_\omega \neq 0$ and $\lambda_P \neq 0$ then from (6.5) we have that:

$$\begin{aligned} & \rho + \delta + \frac{\gamma\theta}{\pi - A(1-\eta\omega-\xi)^\alpha\beta(b+\nu\omega)^{\beta-1}} = 0 \\ \iff & A(1-\eta\omega-\xi)^\alpha\beta(b+\nu\omega)^{\beta-1} = \pi + \frac{\gamma\theta}{\rho+\delta} \\ \iff & (b+\nu\omega)^{\beta-1} = \frac{\pi + \frac{\gamma\theta}{\rho+\delta}}{A(1-\eta\omega-\xi)^\alpha\beta} \\ \iff & b + \nu\omega = \left(\frac{A\beta\,(1-\eta\omega-\xi)^\alpha}{\pi + \frac{\gamma\theta}{\rho+\delta}}\right)^{\frac{1}{1-\beta}}. \end{aligned}$$

Thereby as for the proof of Proposition 10 we get that, if $\nu\left(\pi + \frac{\gamma\theta}{\rho+\delta}\right) - \rho > 0$, the land

allocated to agricultural production is given by:

$$1-\eta\omega-\xi=\left(\frac{A\alpha\eta\left(\frac{A\beta}{\pi+\frac{\gamma\theta}{\rho+\delta}}\right)^{\frac{\beta}{1-\beta}}}{\nu\left(\pi+\frac{\gamma\theta}{\rho+\delta}\right)-\rho}\right)^{\frac{1-\beta}{1-\alpha-\beta}}=\left[A\left(\frac{\eta}{\nu}\cdot\frac{\alpha}{(\pi-\pi_e)}\right)^{1-\beta}\left(\frac{\beta}{\pi+\frac{\gamma\theta}{\rho+\delta}}\right)^{\beta}\right]^{\frac{1}{1-\alpha-\beta}}.$$

Finally from (6.3) we get that:

$$\begin{aligned}f'(\xi)&=-\frac{\lambda_\omega}{\lambda_P}[A\alpha(1-\eta\omega-\xi)^{\alpha-1}(b+\nu\omega)^{\beta}-\tau]\\&=\frac{\gamma}{A(1-\ \eta\omega-\xi)^{\alpha}\beta(b+\nu\omega)^{\beta-1}-\pi}[A\alpha(1-\eta\omega-\xi)^{\alpha-1}(b+\nu\omega)^{\beta}-\tau],\end{aligned}$$

and at steady state (7.4) leads to:

$$\frac{\gamma\theta}{A(1-\ \eta\omega-\xi)^{\alpha}\beta(b+\nu\omega)^{\beta-1}-\pi}=\rho+\delta.$$

Thereby we get:

$$\begin{aligned}f'(\xi)&=\frac{\rho+\delta}{\theta}\left[A\alpha(1-\eta\omega-\xi)^{\alpha-1}(b+\nu\omega)^{\beta}-\tau\right]\\&=\frac{\rho+\delta}{\theta}\left[A\alpha(1-\ \eta\omega-\xi)^{\alpha-1}\left(\frac{A\beta\,(1-\eta\omega-\xi)^{\alpha}}{\pi+\frac{\gamma\theta}{\rho+\delta}}\right)^{\frac{\beta}{1-\beta}}-\tau\right]\\&=\frac{\rho+\delta}{\theta}\left[A\alpha\left(\frac{A\beta}{\pi+\frac{\gamma\theta}{\rho+\delta}}\right)^{\frac{\beta}{1-\beta}}\left(\frac{\nu\left(\pi+\frac{\gamma\theta}{\rho+\delta}\right)-\rho}{A\alpha\eta\left(\frac{A\beta}{\pi+\frac{\gamma\theta}{\rho+\delta}}\right)^{\frac{\beta}{1-\beta}}}\right)-\tau\right]\\&=\frac{\rho+\delta}{\theta}\left[\left(\frac{\nu\left(\pi+\frac{\gamma\theta}{\rho+\delta}\right)-\rho}{\eta}\right)-\tau\right].\\&=\frac{\rho+\delta}{\theta}\left[\frac{\nu}{\eta}(\pi-\pi_e)-\tau\right].\end{aligned}$$

Finally, as $f(\xi)=\mu\xi^{\epsilon}$ we get that $f'(\xi)=\mu\epsilon\xi^{\epsilon-1}$ and thus:

$$\tau=\frac{\nu}{\eta}(\pi-\pi_e)-\frac{\theta}{\rho+\delta}\frac{\mu\epsilon}{\xi^{1-\epsilon}},$$

which ends the proof of Proposition 13.

Chapter 3

Soil pollution diffusion in a spatial agricultural economy

Abstract

There exists a pressing need to analyze the impact of agriculture on soil fertility. This paper develops a spatial growth model for an agricultural economy, in which pollution diffuses across space. In order to produce, the economy needs fertile soil, naturally bounded by the amount of available land. When regions have not yet reached their maximal soil fertility, they can locally invest in abatement in order to reduce soil pollution. Once a location reaches this maximum of fertile land, the economy is split in two: a fertile region and a polluted region. We analytically show how the polluted region can either stagnate at low levels of fertility, or catch up with the fertile region. Our results are numerically illustrated, including the resiliency of the economy to recover from pollution shocks.

Keywords: Spatial dynamics, Soil pollution diffusion, Agricultural economy, Sturm-Liouville theory, Dynamic programming, Numerical methods.

Journal of Economic Literature: C61, O44, Q15, Q56, R11.

This chapter builds on the eponymous research paper co-written with Carmen Camacho. All errors remain mine.

Contents

List of Figures

1 Introduction

Soil is the complexe mixture of air, water, mineral particles, organic matter and living organisms which sits on Earth's crust top layer. Besides hosting the major part of known and unknown biodiversity, soils perform specific functions and provide with fragile ecosystems services vital to the biosphere durability as well as to human activities. In addition to providing with 99% of the world's food production (Kopittke et al., 2019), soils provide with a broad range of other ecosystems services such as the regulation of green house gaz emissions by acting as a carbon sink or flood mitigation. Needless to say that the value of such services is colossal. In McBratney et al. (2017), the authors estimate that the economic value in the US of soils services reaches $11.4 trillion. Yet, soils and its many ecosystems services are very fragile and are being affected by the human activity in many ways. In this research, we focus in particular on how the agricultural activity and its inappropriate practices, such as the excessive use of fertilizers, increases environmental pressure on soils. Indeed, in 2017, the United Nations Convention to Combat Desertification (UNCCD) estimated that the agricultural sector, by itself, is responsible for a loss in 24 billion tonnes every year in fertile soil (UNCCD, 2017). Among other things, such loss in fertile soil implies worldwide risks in food security, as food demand will keep increasing in the next decades, pushed by global population growth. Reducing the impact of agriculture practices on soil fertility is therefore becoming urgent, and this research proposes a theoretical framework in which is analyzed the impacts of agricultural pollution externalities on soils fertility.

The official definition for soil pollution has been formalized in 2015 by The Intergovernmental Technical Panel on Soils (ITPS) as "the presence of a chemical or substance out of place and/or present at a higher than normal concentration that has adverse effects on any non-targeted organism" (ITPS, 2015).[1] Anthropogenic activities are the main sources of soil pollution and, unfortunately, there is no lack of examples: wars, mining, former factory sites, accidental oil leakage, over use of fertilizers, etc... Concerns are now growing all around the world since the Status of the World's Soil Resources Report identified soil pollution as one of the main threat to soils ecosystems services. In our case, we narrow our analysis research to soil pollution caused by inappropriate agricultural practices such as the over use of fertilizers. Two categories

[1]Note that "soil pollution" shall not be used as a synonym for "soil contamination" as ITPS also formalized the definition of the latter which only occurs when "the concentration of a chemical or substance is higher than would occur naturally but is not necessarily causing harm." (ITPS, 2015).

of pollution emerge from the literature : point-source soil pollution and diffuse soil pollution. On the one hand, point source pollution is defined as pollution "which contaminants are released to the soil, and the source and identity of the pollution is easily identified" (FAO, 2018). Among many examples, let us mention inadequate wastes disposals or accidental chemical leakages. On the other hand, diffuse pollution is defined as "pollution that is spread over very wide areas, accumulates in soil, and does not have a single or easily identified source". Regarding the agricultural activity, the use of fertilizer is the main source of diffuse pollution. To stress on the fundamental difference in nature regarding these two types of population, note that Switzerland disposes of two different ordinances regarding soil pollution regulation : the contaminated-sites ordinance for localized point-source soil pollution, and the soil ordinance for diffuse soil pollution. In this research, we focus our analysis on the second type of pollution, that is diffuse soil pollution, and in the following, any general mentioning of soil pollution will exclusively refer to diffuse soil pollution.

Diffuse soil pollution therefore mostly comes from inappropriate agricultural practices and in particular from the use of nitrogenous fertilizers. Yet, even though we now have a better understanding on the role of nitrogenous fertilizers as being responsible for diffuse soil pollution, their use in the agricultural sector keeps increasing every year around the world. In 1980, the worldwide nitrogenous fertilizer consumption was around 60 million tonnes, and almost doubled in less than 40 years, reaching 110 millions tonnes in 2014.

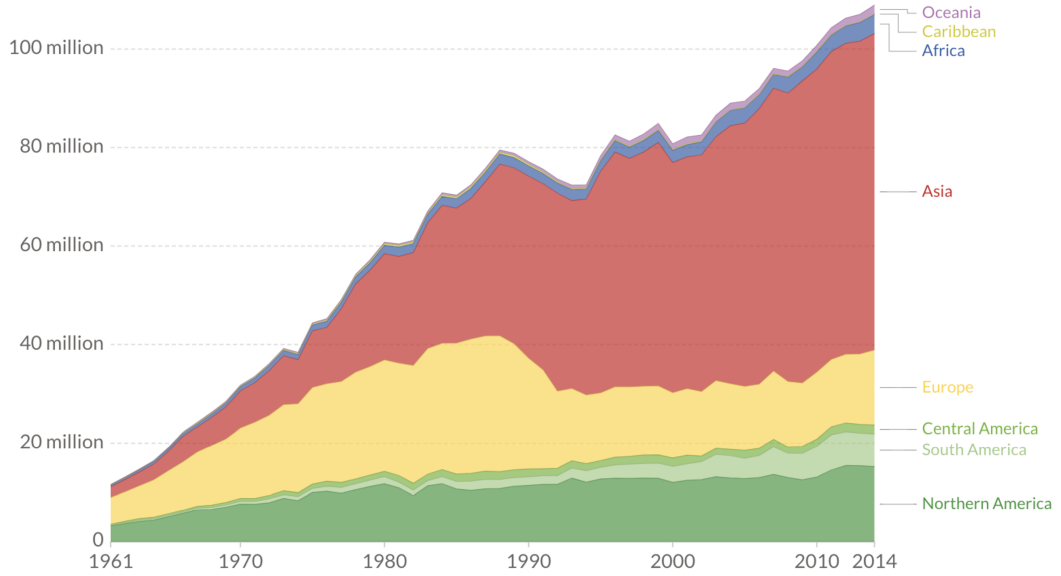

Figure 1: Total nitrogenous fertilizer consumption in tonnes of total nutrient per year from 1961 to 2014. Source : UN Food and Agricultural Organization (FAO, 2015).

Note that if this increase in the use of fertilizers is very clear and pronounced at a global level, this trend highly depends on the local regulations in charge of agricultural practices. For instance, due to a lack of strict environmental regulations in Asia regarding soil pollution, the use of fertilizer in this region have been continuously increasing since the 1960's. This intensive use of fertilizers in Asia, and particularly in China, must be taken very seriously as 19% of all Chinese agricultural soils are now categorized as polluted by the Chinese Environmental Protection Ministry (CCICED, 2015). In contrast, after an even more important growth in the use of fertilizer in Europe between 1960 and 1980, their use abruptly decreased by almost 50% around the year 1990, and took on a rather constant trend in the following decades as shown in Figure 1. Such decrease in the use of nitrogenous fertilizers in Europe can directly be related to the EU Nitrate Directive of 1991 which aimed at "preventing nitrates from agricultural sources polluting ground and surface waters and by promoting the use of good farming practices" (EU Commission, 1991). Among other things, this shows that soil pollution awareness due to agricultural practices, as well as clear political convictions regarding soil conservation, can lead to significative changes in the trend of agricultural practices. Yet, the current European legislations could still be more stringent as soil pollution has been identified as the third threat to soil functions in Europe by The Intergovernmental Technical Panel of Soil (ITPS, 2015).

Hence, our research proposes the theoretical foundation for the analysis of soil pollution diffusion emerging from the lack of regulations regarding agricultural practices, and in particular regarding the use nitrogenous fertilizers responsible for diffuse pollution into soil. In order to understand where we stand, let us mention that the economics of soil conservation has a long tradition of interdisciplinary thinking, borrowing tools and concepts from related disciplines such as ecology or agronomy. For instance, in the early days of soil economics Ciriacy-Wantrup (1968) borrowed from ecology the concept of damage thresholds, therefore leading to an analysis of soil while considering irreversible damages in its fertility due to agricultural production. Yet, the economics of soil conservation did not initially attract all the attention it now deserves, as according to Burt (1981) : "the most obvious reason for this apparent lack of interest in the subject is the view that advances in technology have made soil resources per se of less consequence for agricultural production". However, our new understandings regarding the high sensitivity of soils to agricultural production, precisely led the field of soil economics to analyse the complex interactions between agricultural practices

and soil fertility. As a seminal paper, let us mention Pope et al. (1983), in which the authors analysis the interrelationships among soil loss, topsoil depth, net farm income, and technological progress and provide with the optimal policies in soil conservation which maximizes net farm incomes. Similarly, McConnell (1983) and Barbier (1990) also consider topsoil depth in their analysis. Such approach have the benefit to provide with simple dynamic models, yet are very reductive regarding soils' characteristics. Since, the linkage between agricultural practices and soil quality has grew in complexity. For instance, in Smith et al. (2000) the authors develop a dynamic model for soil quality in order to evaluate optimal cropping systems while considering crop rotation, tillage practices and fertilizers and characterize soils by their content in organic carbon, inorganic carbon, pH, and salt. More recently, the question of soil conservation shifted to the context of developing countries where it is thought that better soil management practices could lead to the highest potential gains.[2] Hence, the economics of soil conservation is by essence interdisciplinary, borrowing concepts to ecology and agronomy, while touching upon different trends in the economic literature such as agricultural, environmental or development economics. Yet, to our knowledge, none has ever focused their research specifically on the impact of diffuse soil pollution due to agricultural practices, and in particular to the use of nitrogenous fertilizers.

This research aims precisely to fill in this gap by analyzing for the first time in the soil economics literature the diffusion process of pollution into soil in a theoretical perspective. To do so, we use a recently developed conceptual framework from a rather novel trend in the economic literature being spatial growth models.[3] We consider an agricultural economy where the diffusion of pollution into soils is governed by Fick's law of motion, stating that the flux of soil pollution concentration at a location is proportional to the pollution concentration gradient at this location (see Brock and Xepapadeas (2008, 2010), Smith et al. (2009), La Torre et al. (2015), or Camacho and Pérez-Barahona (2015)). Moreover, our economy is made of a continuum of locations distributed along the unit circle,[4] and each location is endowed with a given amount of fertile soil. The unique agricultural good is locally managed, and can be either directly consumed or reinvested to abate at least some of the pollution locally generated in the

[2]See for instance Antle et al. (2006), Hagos et al. (2006), de Graaf et al. (2008), Stephens et al. (2012), Barrett et al. (2015), Bevis et al. (2017), or Berazneva et al. (2018).

[3]See Augeraud-Véron et al. (2019) for a very complete review on distributed optimal control models applied to environmental economics.

[4]This is another classic specification used for spatial growth models in order to avoid additional spatial contraints on the domain's boundaries (see for instance Boucekkine et al. (2019)).

agricultural production process. Our model is structurally close to Boucekkine et al. (2018), since production is linear in fertile soil, and to Camacho and Pérez-Barahona (2015), as the locally generated pollution, not only accumulates at the given site, but also diffuses across locations through soils. Yet, there is a key difference with spatial growth models which study the diffusion of wealth or air pollution, being that fertile soil is naturally and locally bounded by the total amount of land that each location disposes for their respective agricultural production. In other words, the local amount of fertile soil cannot exceed the local amount of available land, in contrast with wealth or air pollution which can accumulate indefinitely (or at least does not have a natural upper bound as it the case for soils). Thereby this research presents an original problem to the economics literature by considering fertile soil as a naturally bounded production factor which leads us to consider that locations can succeed, or not, in making fertile all their locally available land.

We describe analytically the optimal policies and resulting spatial-dynamics of the economy in two separate phases. The first phase occurs when no location has yet reached its local upper boundary for fertile soil, that is when all land is locally fertile. In this first phase, policy maker takes into account spatial heterogeneities across the economy, and local optimal consumption levels depend, among other factors, on local abatement efficiency and local production technology. Despite being spatially heterogeneous, consumption grows at the same constant rate at all locations. Similarly, the resulting optimal trajectories in fertile soil at each location grow at a constant rate during this first phase. Once one location reaches its upper boundary in fertile soil, the spatial-dynamics of the economy enters its second phase. In this second phase, the economy is therefore divided in one fertile region, in which locations succeeded in making fertile all their land, and a polluted region, in which locations has not yet reached their upper boundary in fertile soil. The two regions are therefore separated by a pollution frontier which evolves over time and space, according to the optimal decisions taken in both the polluted and fertile region.

In the fertile region, the optimal choice of the policy maker is the autarky, in the sense that each location consume what is locally produced. As a consequence, the fertile locations only abate their own pollution while the other polluted region still experiences diffusion of pollution. Contrary to the well-known results that apply when the production factors are unbounded, the economy can here reach a steady state in long-term situations with two distinct regions: a permanently fertile region, where all

locations have attained their maximum for fertile soil, next to which a polluted region where locations cannot reach their maximum level for fertile soil. Indeed, during the convergence phase, the pollution from the less fertile regions is partially absorbed by the more fertile regions. However, once diffusion towards the fertile region stops, the polluted region may not be able to abate enough to eradicate its own pollution. If this happens, the polluted region can stagnate at low levels of fertile soil and hence never catch up with the fertile region. We analytically show how the emergence of one permanently fertile region next to a permanently polluted region is caused precisely by the diffusive aspect of pollution into soils.

Hence, from a modeling perspective, this research describes for the first time in this literature the case of an economy with two regions, a fertile and a polluted region, separated by a pollution frontier that can evolves geographically with time, accordingly to regions' optimal decisions. We investigate on the evolution of such dynamic pollution frontier between the two regions, as well as on the possible emergence of two distinct and permanent regions respectively polluted and fertile in the long-run steady state. This research also provides with numerical exercices and show that in a spatially homogeneous economy, initial disparities in soil fertility may not vanish with time if the fertile region does not help absorbing the pollution from neighboring locations. Moreover, we also assess numerically the resiliency of the economy to pollution shocks by considering an initial state in which all locations have reached their upper bound in fertile soil and by applying a localized pollution shock to one region (for instance, as if one region suffers from an industrial catastrophe, which increases suddenly its local soil pollution). Such "pollution stress tests" cover different cases depending on the magnitude of the shock, the size of the affected region and the operating technology. Overall, we show that if the economy uses a sufficiently advanced technology, then the pollution shock can be absorbed with time by the economy through optimally localized investments in pollution abatement. In such cases, the economy progressively relaxes back to its initial fully fertile state. However, if technology is not sophisticated enough, then the rather local initial pollution shock can diffuse all across the economy, at the risk of affecting a too large area of the economy, above which the shock can no longer be contained, leading therefore to global collapse.

The rest of the chapter is organized as follows. The spatial growth model is presented in section 2. Section 3 provides with the optimal solution for the policy maker problem, describing the transit between the two phases of the spatial-dynamics as well

as characterizing the dynamics of the pollution frontier between the polluted and the fertile region. In Section 4, we run different numerical exercises, and provide with some dynamic properties of the economy such as its resiliency to pollution shocks. Section 5 concludes. Proofs are gathered in the Appendix.

2 Soil pollution diffusion in a linear growth model

We consider a closed economy, where both land and households are distributed over the unit circle on the plane, $\mathcal{S} = \{(\sin\theta, \cos\theta) \in \mathbb{R}^2 : \theta \in [0, 2\pi]\}$. Each location $\theta \in \mathcal{S}$ is populated by $N(\theta)$ individuals and is endowed with an amount of land $L(t, \theta)$.

Assumption 1. *The spatial distribution of land, $L(\cdot)$ is given and independent of time. Moreover, $L(\cdot)$ is either a constant or a linear function of space.*

Assumption 1 implies that locations cannot increase their total land allocation. Moreover, we suppose that land is composed of both fertile and polluted soil, L_F and L_P respectively, such that $L(\theta) = L_P(t, \theta) + L_F(t, \theta)$. All locations produce a unique agriculture good from the labour of local available fertile soil, according to the following linear production function $Y(t, \theta) = A(\theta)L_F(t, \theta)$, where $A(\theta)$ is the local production technology at location θ. Note that our specification allows us to capture the most general case regarding soil quality, that is local soil can be partly fertile and used for agricultural production, yet even with a non-zero local concentration in pollution. In such framework, the local concentration in soil pollution therefore writes as $\frac{L_P(t,\theta)}{L(\theta)}$ and is 1 when soil is totally polluted, in such case locations cannot locally produce, and is 0 when soil is totally fertile, in such case locations reach their maximum yield. In general, local concentration in pollution lies between 0 and 1, and local productivity levels depends on the proportion of polluted and fertile soil at one location. Hence, we do not consider a binary specification with, on the one hand, completely unusable polluted soil, and on the other hand, fully fertile soil, as the aim of this research is to study precisely the spatial-dynamics of pollution diffusion into soil.

The dynamics of soil pollution at one location is explained by three factors. First, pollution diffuses accordingly to Fick's law of motion, that is pollution diffuses from more polluted locations to less polluted locations with a pollution flux proportional to pollution gradient. The diffusion of soil pollution is therefore captured by $D\frac{\partial^2 L_P}{\partial \theta^2}(t, \theta)$, where D is the diffusion coefficient. As this research proposes a first attempt to assess soil pollution diffusion in a macrodynamic growth model, we shall therefore consider

the simplest form for the diffusion coefficient, that is D is assumed both constant in time and homogeneous in space. We therefore do not consider any seasonal effects nor heterogeneities in soil porosity, which would lead us to study time and space dependent diffusion coefficients.[5] Second, fertile soil deteriorates locally according to its exploitation by the agricultural activity. Indeed, the local agricultural production generates some pollutant as a negative externality, which transforms fertile soil into polluted soil. The local effect is measured as $\nu(\theta)A(\theta)L_F(t,\theta)$, where $\nu(\theta)$ is the local sensitivity of fertile soil with respect to pollution and $A(\theta)L_F(t,\theta)$ local production. Local sensitivity $\nu(\theta)$, can for instance be related to the use of different production technologies more or less pollutant across space, or to a higher or lower level of biodiversity at θ, which are *a priori* heterogeneous in space. Last but not least, soil pollution is reversible. Indeed, as a first approximation, we suppose that polluted soil can be depolluted using an abatement technology, independently of the local pollution level. A more accurate specification for soil pollution dynamics would consider that abatement is feasible as long as the pollution level does not cross a specific pollution threshold, above which pollution damages become irreversible. Such critical zone for pollution reversibility has been widely studied in both the ecologic (Dupouey et al., 2002; Chartier et al., 2006; Gao et al., 2011) and economic (Le Kama et al., 2014) literature. Yet, in our research, we shall not consider critical pollution levels, making therefore pollution irreversibility out of our scope.[6] Hence polluted soil can be reversibly changed in fertile soil through investments in pollution abatement. Hence, if $C(t,\theta)$ denotes total consumption at location θ at time t, then each location θ invests an amount $A(\theta)L_F(t,\theta) - C(t,\theta) \geq 0$ in abatement. Let $\phi(\theta)$ be the local pollution abatement efficiency. Then the spatial dynamics of polluted soil writes:

$$\frac{\partial L_P}{\partial t}(t,\theta) = D\frac{\partial^2 L_P}{\partial \theta^2}(t,\theta) + \nu(\theta)A(\theta)L_F(t,\theta) - \phi(\theta)[A(\theta)L_F(t,\theta) - C(t,\theta)].$$

Therefore, under Assumption 1, one can write that $\frac{\partial L_F}{\partial t}(t,\theta) = -\frac{\partial L_P}{\partial t}(t,\theta)$, and the evolution of fertile soil is described for all $t > 0$ and $\theta \in \mathcal{S}$ by:

$$\begin{cases} \frac{\partial L_F}{\partial t}(t,\theta) = D\frac{\partial^2 L_F}{\partial \theta^2}(t,\theta) + A(\theta)[\phi(\theta) - \nu(\theta)]L_F(t,\theta) - c(t,\theta)N(\theta)\phi(\theta), \\ L_F(0,\theta) = L_F^0(\theta), \ \theta \in \mathcal{S}, \end{cases} \tag{1}$$

[5] Such complex, yet more general, specification for diffusion coefficients could very well be analyzed following an other method from Boucekkine et al. (2020), yet is out of the scope of our research.

[6] Examining irreversible pollution damages would lead us to consider an additional negativity constraint on fertile soils first time derivative, that is $\frac{\partial L_F(t,\theta)}{\partial t} \leq 0$ above a local pollution threshold concentration. Yet, as mentioned, irreversibility is out of the scope of this present research.

where $A(\theta)[\phi(\theta) - \nu(\theta)]$ is the net land productivity. Total consumption, $C(t,\theta)$, is the product of the per-capita consumption $c(t,\theta)$ and the location's time-independent exogenous population $N(\theta)$. Hereafter the chapter utilizes and analyses only L_F. Nevertheless, it is straightforward to obtain the corresponding results for L_P.

Let us now introduce the linear operator $\mathcal{L}$ defined for all functions u in the Hilbert space of function from $\mathcal{S}$ to $\mathbb{R}$ by, $\mathcal{L}u(\theta) := Du''(\theta) + A(\theta)[\phi(\theta) - \nu(\theta)]u(\theta)$. Then (1) can be rewritten as:

$$\frac{\partial L_F}{\partial t}(t,\theta) = \mathcal{L}L_F(t,\theta) - c(t,\theta)N(\theta)\phi(\theta), \tag{2}$$

where the initial distribution of L_F is known, $L_F(0,\theta) = L_F^0(\theta)$ for all $\theta \in \mathcal{S}$. Operator $\mathcal{L}$ is well behaved when applied to twice differentiable functions, measurable in $\mathcal{S}$. We say a function ϕ defined on $\mathcal{S}$, regular and non-identically zero, is an eigenfunction of $\mathcal{L}$, with associated eigenvalue $\lambda \in \mathbb{R}$ if $\mathcal{L}\phi(x) = \lambda\phi(x)$. Coddington and Levinson (1955) proved that there exists a countable set of eigenvalues $\{\lambda_n\}_{n\geq 0}$, which can be ordered as a decreasing sequence. It can be proven that the first eigenvalue of $\mathcal{L}$, λ_0, is an eigenvalue with multiplicity 1, all other eigenvalues have either multiplicity 1 or 2.[7] Besides, e_0, the eigenfunction associated to λ_0, is strictly positive on the unit circle and one can set $\int_0^{2\pi} e_0^2(\theta)d\theta = 1$. Moreover, the eigenfunctions of $\mathcal{L}$ form an orthonormal basis in $L^2(\mathcal{S})$ and the sequence of eigenvalues tends to $-\infty$, while the eigenfunction e_n associated to λ_n has n zeros in $[0, 2\pi]$.[8]

Finally, we assume there exists a policy maker, whose aim is to maximize overall welfare. Welfare is measured as the time integral from time 0 of the present value of the spatial aggregate of individuals' utility. Here, utility depends solely on per capita consumption, c, and it is measured by a constant inter-temporal elasticity of substitution function of parameter $\sigma \in \mathbb{R}$. Knowing that the policy maker discounts time at a constant rate ρ, her problem writes as:

$$\max_c \int_0^\infty e^{-\rho t}\left(\int_0^{2\pi} \frac{c(t,\theta)^{1-\sigma}}{1-\sigma} N(\theta)d\theta\right)dt, \tag{3}$$

subject to (1) and:

$$0 \leq L_F(t,\theta) \leq L(\theta), \tag{4}$$

$$c(t,\theta) \geq 0, \text{ for all } \theta \in \mathcal{S}, \text{ and } t \geq 0. \tag{5}$$

[7] The multiplicity of an eigenvalue is the number of times it appears in this sequence.

[8] See Appendix A for a brief introduction to abstract dynamic systems in infinite dimensions. For further details see Coddinton and Levinson (1955) or Brown et al. (2013).

Our model is structurally close to Boucekkine et al. (2013) and Boucekkine et al. (2018), since production is linear in fertile soil. As in previous works, all land is labored at all locations, independently of the distribution of population. Nevertheless, there is a key difference with all previous work from the literature: the production factor, here fertile soil, is naturally bounded. From this, we shall now give the following definition:

Definition 1. *The economy is said to be in Phase 1 (resp. Phase 2) when the constraint on fertile soil L_F expressed in (4) is not binding (resp. is binding).*

Thus, our present analysis faces new challenges as it leads to the description of optimal trajectories in two separate phases, that is before and after one location locally reaches its boundary, when all soil at this location becomes fertile. Most remarkable, the policy maker will play an active role in Phase 1, during which no location has reached its boundary, by indirectly redistributing consumption from fertile to polluted locations. Finally, we face an additional theoretical challenge, namely the description of the dynamic frontier dividing the region at the maximum of fertile soil, and the region still in transition. Here we make use of Stefan's equation in which the frontier evolves following the gradient of pollution. A detailed description is provided in Section 3.2.

3 Optimal policy and the evolution of fertile soil

This section provides with the optimal solution to the policy maker problem introduced in the previous section. In particular, we show that the economy transits through two phases. In Phase 1, each location's land is divided between fertile and polluted soil. During such phase, the amount of fertile soil evolves steadily at a constant rate, which can either be positive or negative. Phase 2 starts whenever fertile soil at a single location attains the maximum or the minimum value, that is, $L(\theta)$ or 0. We characterize the entire path for optimal consumption and for fertile soil when the model's parameters are heterogeneous in space. We have relegated to the Appendix most technical material as well as all the article's proofs.

3.1 Dynamics within the bounds

Beforehand, we shall make the following assumption regarding discount rate:

Assumption 2. $\rho > \lambda_0(1-\sigma)$, *where* λ_0 *the first eigenvalue of the problem* $\mathcal{L}u = \lambda u$.

In the following, we shall work exclusively under Assumption 2 as it provides with the positivity of the value function, and ensures the finiteness of the inter-temporal utility as in Boucekkine et al., (2018). Moreover, let us define $\langle L_F \rangle(t) := \frac{1}{2\pi}\int_0^{2\pi} L_F(\eta, t)d\eta$, the instantaneous spatial mean value for a given fertile soil distribution $L_F(\cdot, t)$ at time t. We provide next with the optimal solution for fertile soil and consumption in Phase 1, that is, when no location have reached their local maximum of fertility level.[9]

Proposition 1. *Under Assumptions 1 and 2, the optimal spatial dynamics of fertile soil in Phase 1, $L_F^*(t,\theta)$ is the solution of:*

$$\frac{dL_F^*}{dt}(t,\theta) = \mathcal{L}L_F^*(t,\theta) - [\phi(\theta)N(\theta)]^{\frac{\sigma-1}{\sigma}} N(\theta)^{\frac{1}{\sigma}}(\alpha_0 e_0(\theta))^{-\frac{1}{\sigma}} \int_0^{2\pi} L_F^*(t,\eta)\alpha_0 e_0(\theta)d\eta,$$

where $L_F^*(t,\theta) < L(\theta)$ for all $t \geq 0$ and $\theta \in \mathcal{S}$, and the dynamics for its mean value writes as:

$$\langle L_F^* \rangle(t) = \langle L_F^0 \rangle e^{gt},$$

for all $t \geq 0$, where $L_F^0(\theta) = L_F(0,\theta)$ is the initial distribution of fertile soil.

Moreover, optimal consumption c^* can be expressed as:

$$c^*(t,\theta) = [\phi(\theta)\alpha_0 e_0(\theta)]^{-\frac{1}{\sigma}} e^{gt} \int_0^{2\pi} L_F^0(\eta)\alpha_0 e_0(\theta)d\eta, \tag{6}$$

where $\alpha_0 \in \mathbb{R}$ is defined as:

$$\alpha_0 = \left[\frac{\sigma}{\rho - \lambda_0(1-\sigma)} \int_0^{2\pi} [\phi(\eta)e_0(\eta)]^{-\frac{1-\sigma}{\sigma}} N(\eta)d\eta\right]^{\frac{\sigma}{1-\sigma}}.$$

e_0 is the first eigenvector of the problem $\mathcal{L}u = \lambda u$ associated to the first eigenvalues λ_0, and $g = \frac{\lambda_0 - \rho}{\sigma}$ is the growth rate of the economy.

Proposition 1 shows that both fertile soil mean and consumption grow at a constant and homogeneous rate g from $t = 0$. Hence, although consumption varies across locations, consumption grows at the same rate across space, and if g is positive, then consumption increases continuously with time at all locations. In contrast, as land is

[9]Note that although we have separated the presentation of the optimal solution in the two phases for the sake of exposition, the optimization problem is solved globally from $t = 0$ taking into account the eventuality of reaching the upper bound for L_F at certain locations (see Appendix B). Using the optimal conditions found in Appendix B, Appendix C finds the explicit optimal solution in Phase 1, while Appendix F provides us with the optimal solution in Phase 2 that we provide in Section 3.2.

naturally bounded, fertile soil cannot increase forever. Some locations will attain their maximum in a finite time $\tau > 0$. At such time τ, the economy enters Phase 2, that is, when the fertile soil constraint (4) is binding at least at one location. We describe Phase 2 in the following section. Note that, if $g < 0$, then fertile soil tends to zero at all locations, and the economy vanishes. This situation could also be considered as reaching Phase 2, although we opt here to focus on the case of a second phase with $g > 0$ and available fertile soil.

The proposition also reveals the existence of a sustainable level for the time discount rate $\tilde{\rho} = \lambda_0$. If the policy maker weights enough the future generations, $\rho < \tilde{\rho}$, she sacrifices current consumption to increase abatement and guarantee future generations' consumption. In this case $g > 0$ and at least some locations attain the maximum of fertile soil. If $\rho = \tilde{\rho}$, then $g = 0$ and the economy stagnates and remains at the initial situation. When the policy maker is not altruistic enough, $\rho > \tilde{\rho}$, then $g < 0$ and she prefers current consumption to abatement, endangering the future of fertile soil, production and consumption.

As in Boucekkine et al. (2018), the policy maker cannot disregard the heterogeneity of the economy in her optimal decision. Despite weighting the welfare of each individual equally, consumption per capita varies across locations. Note that c^* in (6) depends on the location characteristics via ϕ and e_0. However, since the analytical form of e_0 is typically not computable, we cannot provide a detailed analytical description of the effect of the different factors on c^*. Similarly, when A, ϕ, ν and N are spatially distributed and when $D \neq 0$, the growth rate g in our general set-up depends on the first eigenvalue λ_0 of the $\mathcal{L}$ operator, with $g = \frac{\lambda_0 - \rho}{\sigma}$, and does not have a closed-form formula for heterogeneous spatial characteristics.

Yet, under specific hypothesis on the model's parameters we can provide closed form formulas for the eigenvectors and eigenvalues of the operator. As a result, closed forms are also obtained for growth rate g, the distribution in consumption c^* and in fertile soil L_F^*. In particular, we develop next two applications of the general framework for which solutions are fully analytically tractable. First, we consider a diffusive homogeneous economy, where A, ϕ, ν and N are homogeneous, yet with potentially an heterogeneous initial fertile soil distribution. Secondly, we analyse the role of diffusion by comparing these results to the case of an unconnected economy made of spatially independent locations, that is, when pollution does not diffuse across locations, hence $D = 0$.

Proposition 2. *In a diffusive homogeneous economy, where the distributions for A, ϕ, ν and N are constant in space, optimal fertile soil in Phase 1 can be expressed as:*

$$L_F^*(t,\theta) = \langle L_F^0 \rangle e^{gt} + \sum_{n\geq 1} \langle L_F^0, e_n \rangle e_n(\theta) e^{\lambda_n t}, \quad \forall \theta \in \mathcal{S} \text{ and } \forall t \in [0, \tau[,$$

where L_F^0 is the initial fertile soil distribution, e_n the n^{th} eigenvector of the problem $\mathcal{L}u = \lambda u$ associated to the n^{th} eigenvalue λ_n, with $\lambda_n = A(\phi - \nu) - Dn^2$ for $n \geq 0$ and τ the time at which the economy reaches Phase 2.

Moreover, the optimal growth rate of consumption is independent of the pollution diffusion coefficient D and of population N and writes as:

$$g = \frac{\lambda_0 - \rho}{\sigma} = \frac{A(\phi - \nu) - \rho}{\sigma}.$$

For the homogeneous economy, the expression for the optimal fertile soil distribution is very convenient. Indeed, L_F^* can be written as the sum of its mean value, $\langle L_F^0 \rangle e^{gt}$, and a second term, $\sum_{n\geq 1} \langle L_F^0, e_n \rangle e_n e^{\lambda_n t}$, with zero mean. Since neither g nor L_F^0 depend on the diffusion coefficient D, then the first term does not depend on D either. Hence, the effects of pollution are gathered in the second term, that is, in the eigenvalues λ_n. Note that if $D > A(\phi - \nu)$, then $\lambda_n < 0$ for $n \geq 1$. Hence, if diffusion is strong enough, the second term vanishes to zero with time and fertile soil is only driven by its initial mean value in the long-run. This is all the more true as diffusion D increases.

Next let us consider the case of an homogeneous unconnected economy in which $D = 0$. Here, soil pollution no longer diffuses so that the quality of the soil is independent from one location to another. As a matter of fact, it is as if the economy was made of independent and unconnected locations where the activity of one location does not affects its neighbors. Hence, the spatial dynamic optimal control problem presented in Section 2 reduces to a simpler problem, which is to be solved for each location independently. In what follows we analyze and quantify the gains and losses when locations belong to a diffusive economy with positive growth. We define the consumption transfer distribution as:

$$\Gamma(t,\theta) := c_A(t,\theta) - c_D(t,\theta),$$

where c_A is the consumption distribution in the unconnected economy and c_D the consumption distribution in the diffusive economy. In other words, Γ measures the losses in consumption from entering a diffusive economy. Whenever $\Gamma(t,\theta)$ is positive

at a given (t, θ), location θ would be better off alone at time t, consumption-wise. Obviously, since the contrary is also true, the economy will be made of losers and winners at all times.

Proposition 3. *When A, ϕ, ν and N are homogeneous, the consumption profiles are:*

$$\begin{aligned} c_A(t,\theta) &= \frac{\rho + A(\phi-\nu)(\sigma-1)}{N\sigma\phi} L_F^0(\theta) e^{gt}, \\ c_D(t,\theta) &= \frac{\rho + A(\phi-\nu)(\sigma-1)}{N\sigma\phi} \langle L_F^0 \rangle e^{gt}, \end{aligned}$$

where, L_F^0 is the given initial fertile soil distribution and $\langle L_F^0 \rangle$ its mean value. The two consumption profiles grow at the same rate $g = \frac{A(\phi-\nu)-\rho}{\sigma}$ and the consumption transfer distribution depends on the initial distribution in fertile soil $L_F^0(\theta)$ and writes as:

$$\Gamma(t,\theta) = \frac{\rho + A(\phi-\nu)(\sigma-1)}{N\sigma\phi} \left[L_F^0(\theta) - \langle L_F^0 \rangle \right] e^{gt}.$$

Proposition 3 proves that whether pollution diffuses or not, homogeneous economies grow at the same rate. In both cases, if the net productivity $A(\phi - \nu)$ is not large enough, that is if $A(\phi - \nu) < \rho$, then $g < 0$ and consumption decreases. Therefore, there is an abatement efficiency threshold $\frac{\rho}{A} + \nu$ above which the economy prospers. Hence, even in a diffusive economy, each location needs to abate efficiently so as to compensate its own pollution, or else the economy collapses. In other words, no location can rely on positive spillovers from its neighbors, and this despite diffusion.

However, although consumption growth rates are identical, the distributions in consumption differ. In the unconnected economy, locations' consumption depends solely on their own initial endowment of fertile soil and spatial inequalities consumption-wise across locations persist in time. Note how consumption grows at a constant rate g and does not adjust to current values of fertile soil, building on the initial land endowment as reference. In contrast, consumption distribution in the diffusive economy is homogeneous in space, even starting from an heterogeneous initial distribution L_F^0. Finally, Assumption 2 implies here that $\rho + A(\phi - \nu)(\sigma - 1) > 0$. Therefore, if at location θ, $L_F^0(\theta)$ is above the economy's initial mean value, then $\Gamma(t, \theta) > 0$, and thus location θ always transfers consumption (indirectly). Therefore, the policy maker induces larger abatement efforts to the initially more fertile and productive regions so they can absorb pollution from other locations, which thanks to that, can increase their consumption.

3.2 The dynamic frontier and the final adjustment

The second phase begins the moment one location's fertile soil attains its maximum. Locations at the maximum, divide production between consumption and abatement of instantaneously generated pollution before it settles. This way, fertile soil remains at its maximum value thereafter.

Let us consider $\mathcal{S} = \underline{\mathcal{S}}(t) \cup \bar{\mathcal{S}}(t)$ where $\bar{\mathcal{S}}(t)$ is made of the locations that have reached the upper bound for fertility at time t and locations in $\underline{\mathcal{S}}(t)$ have not reached the boundary yet. Our results hold if $\bar{\mathcal{S}}(t)$ is a convex set or a finite union of convex sets. For simplicity reasons, we proceed as if $\bar{\mathcal{S}}(t)$ is made of a single convex set as Figure 2 shows. In the sequel, we shall omit the time index in $\underline{\mathcal{S}}(t)$ and $\bar{\mathcal{S}}(t)$.

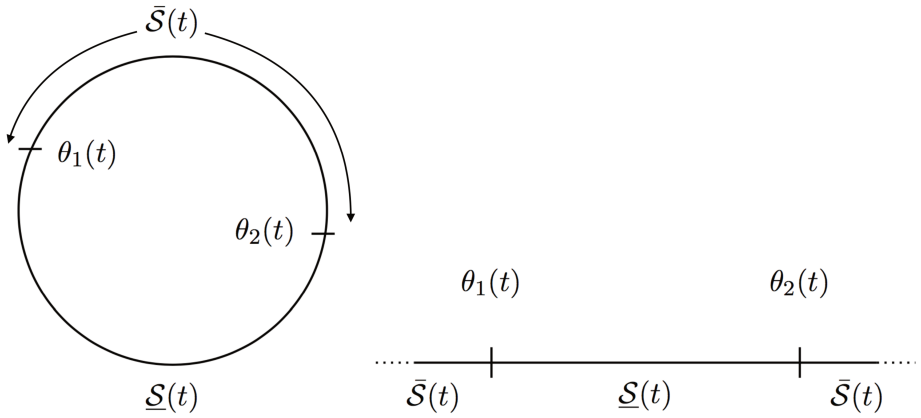

Figure 2: Description of the pollution frontier.

In Physics, the Stefan equation describes the evolution in time of the frontier between two phases of a matter. Typically, it has been applied to describe the frontier between the solid and liquid phases of water.[10] In our problem, we assume that the pollution frontier delimiting the fertile region $\bar{\mathcal{S}}$ from the polluted region $\underline{\mathcal{S}}$ moves according to the Stefan equation, following the spatial gradient of polluted land. If at time $t \geq 0$ $\underline{\mathcal{S}}(t) = [\theta_1(t), \theta_2(t)] \subset \mathcal{S}$, then:

[10]The Stefan condition is expressed as a law of energy conservation, and in the case of water, the moving frontier depends on the change of temperature. Hence, if $u(x,t)$ denotes the temperature of water at location x in a space X at a given time $t \geq 0$, and $\xi(t)$ the frontier between solid and liquid water, then:

$$\eta\rho\dot{\xi}(t) = c_1\frac{\partial u(x^-,t)}{\partial x} - c_2\frac{\partial u(x^+,t)}{\partial x},$$

where $\xi(0) = 0$, so that initially all space is frozen, and water melts when temperature attains an upper bound, that is $u(x,t) \geq U$ for some $U \in \mathbb{R}$. c_1 and c_2 are the coefficients of heat conductivity, ρ is the density of the solid phase and η is the latent heat of melting per unit of mass.

$$\dot{\theta}_1(t) = -D\frac{\partial L_P(t,\theta_1)}{\partial \theta} = D\frac{\partial L_F(t,\theta_1)}{\partial \theta} \quad \text{and} \quad \dot{\theta}_2(t) = -D\frac{\partial L_P(t,\theta_2)}{\partial \theta} = D\frac{\partial L_F(t,\theta_2)}{\partial \theta}.$$

Figures 3 provides with a graphical description of the dynamics of the pollution frontier.

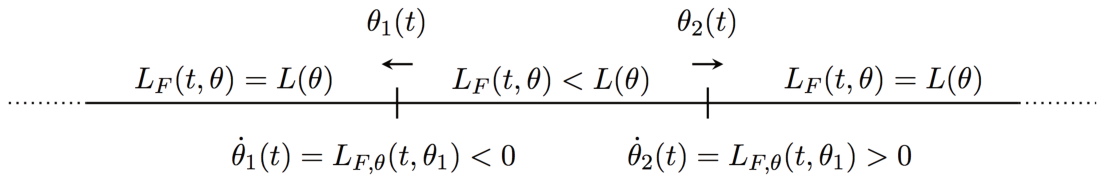

Figure 3: Dynamic pollution frontier

We now provide with the optimal consumption policy in Phase 2, that is, when at least one location fertility is binding, as well as the optimal fertile soil dynamics in the polluted region $\underline{\mathcal{S}}(t)$.

Proposition 4. *Suppose that at time $\tau \geq 0$, at least one location reaches the upper bound for fertile soil. Then, under Assumptions 1 and 2, the optimal spatial dynamics of fertile soil in Phase 2 depend on whether locations have reached their boundary. If at time $t \geq \tau$, $\theta \in \bar{\mathcal{S}}(t)$, then $L_F^*(t,\theta) = L(\theta)$ and optimal consumption is given by:*

$$c^*(t,\theta) = A(\theta)\frac{\phi(\theta) - \nu(\theta)}{\phi(\theta)}\frac{L(\theta)}{N(\theta)}, \quad \textit{for all } t \geq \tau. \tag{7}$$

If on the contrary, $\theta \in \underline{\mathcal{S}}(t)$, then optimal consumption policy can be expressed as:

$$c^*(t,\theta) = (\phi\beta_0 e_0)^{-\frac{1}{\sigma}} \int_{\underline{\mathcal{S}}(t)} L_F^*(t,z)\beta_0 e_0(z)dz, \tag{8}$$

where e_0 is the first eigenvector of the problem $\mathcal{L}u = \lambda u$ on $\mathcal{S}$ and β_0 a function of time such that:

$$\beta_0^{\frac{1-\sigma}{\sigma}} = \frac{\sigma}{\rho - \lambda_0(1-\sigma)} \int_{\underline{\mathcal{S}}(t)} (\phi(z)e_0(z))^{-\frac{1-\sigma}{\sigma}} N(z)dz,$$

and the optimal fertile soil distribution in the polluted region $\underline{\mathcal{S}}$ is solution to the integro-differential equation:

$$\begin{aligned}\int_{\underline{\mathcal{S}}(t)} L_F^*(t,z)e_0(z)dz = &\int_{\underline{\mathcal{S}}(t)} L_F^*(\tau,z)e_0(z)dz\; e^{\frac{\lambda_0-\rho}{\sigma}(t-\tau)} \\ &+ \int_\tau^t e^{\frac{\lambda_0-\rho}{\sigma}(t-s)} \Big(L(\theta_2(s))e_0(2\pi)\dot{\theta}_2(s) - L(\theta_1(s))e_0(0)\dot{\theta}_1(s)\Big)\, ds,\end{aligned}$$

where the evolution of the pollution frontier $[\theta_1(t), \theta_2(t)]$ in time is given by the initial condition $(\theta_1(\tau), \theta_2(\tau))$ and the dynamics $\dot{\theta}_1(t) = D\frac{\partial L_F^*(t,\theta_1)}{\partial \theta}$, $\dot{\theta}_2(t) = D\frac{\partial L_F^*(t,\theta_2)}{\partial \theta}$.

Note that contrary to Phase 1, consumption in the polluted region $\underline{\mathcal{S}}$ does not grow at a constant rate. Among other things, its growth rate is linked to the evolution of the pollution frontier $[\theta_1(t), \theta_2(t)]$, that is the borders of $\underline{\mathcal{S}}$, and to abatement efficiency ϕ. In contrast, consumption in the fertile region $\bar{\mathcal{S}}$ is constant in time, yet heterogeneous in space, as it depends exclusively on locations' local characteristics. More productive locations, those less populated and those with a higher total land endowment consume more. Moreover, optimal consumption policy in $\bar{\mathcal{S}}$, can be rewritten as $\phi(AL - c^*N) = \nu AL$, ensuring that each location in the fertile region abates its own pollution, therefore avoiding pollution diffusion from the surrounding locations in $\underline{\mathcal{S}}$ and no longer contributing to the abatement of their pollution.

Finally, in the long-term in Phase 2, either all locations converge to their own boundary for fertile soil, either there exists a region in which pollution diffuses forever and in which fertile soil never reaches its maximum.

Proposition 5. *In Phase 2, the economy can reach a steady state in which $\mathcal{S} = \bar{\mathcal{S}} \cup \underline{\mathcal{S}}$ at all t, where $\theta_1(t) = \bar{\theta}_1$ and $\theta_2(t) = \bar{\theta}_2$, with $\bar{\theta}_1, \bar{\theta}_2 \in \mathbb{R}$. fertile soil equals total land in $\bar{\mathcal{S}}$, and consumption is given by (7). In the polluted region $\underline{\mathcal{S}}$, the steady state for fertile soil $\bar{L}_F$ is solution to $D\bar{L}_F'' + A(\phi - \nu)\bar{L}_F = 0$.*

Proposition 5 presents one of the main findings of this chapter: in the case of a diffusive economy, that is $D \neq 0$, the polluted region $\underline{\mathcal{S}}$ in Phase 2 may fall in a sort of environmental poverty trap and never catch up with the fertile region. This result is not necessary straightforward as it provides with the existence of an heterogeneous steady state in fertile soil, that is the emergence of fertility patterns, even in the case of an homogeneous economy. Note that the emergence of such soil patterns in the polluted region $\underline{\mathcal{S}}$ is a direct effect of pollution diffusivity as, if $D = 0$, then the steady state for fertile soil in $\underline{\mathcal{S}}$ is $\bar{L}_F = 0$.

4 Numerical experiments

The previous section provides with analytical solutions in fertile soil and consumption in the two phases of the economy. Here, we shall present numerical exercises to shed light on some of the remaining open questions that were not analytically accessible. More precisely, subsection 4.1 studies the dependency of the optimal solution on the spatial heterogeneity of the model components in Phase 1. We explore the case of a

technological central pole and analyse the effect on fertile soil spatial dynamics of variations in abatement efficiency, while considering both homogeneous and heterogeneous soil sensitivities. Subsection 4.2 proposes five exercises that describe the dynamics of the optimal solution in Phase 2, as well as the evolution of the pollution frontier. We first study the convergence towards the fertile economy, that is, when all locations reach their maximum level of fertile soil. Then, we study the resiliency of the fertile economy to pollution shocks. We consider both a uniform technology and a central pole, and discuss on the capacity of the economy to recover from pollution shocks, depending on their size and on the available technology.[11] Regarding our calibration, the discount rate ρ is 3% as in Boucekkine et al. (2018) and Lopez (2008). Using micro-household data, Attanasio and Weber (1993) and Attanasio and Browning (1995) show that σ lies in an interval between 1.25 and 3.33. Here we assume that $\sigma = 2$ following Barro et al. (1995). The amount of available land is 10 at all locations. This means that $L_F(\theta) < 10$ at all locations in Phase 1, and that the economy reaches Phase 2 when at least one location reaches maximum fertile soil, that is here $L_F(\theta) = 10$. Population is also uniformly distributed, with $N(t, \theta) = 1$ for all t and θ. Finally, we set the diffusion parameter D to 1.

4.1 Optimal solution in Phase 1

We study the detrended consumption distribution $c_g^*(\theta) = e^{-gt}c^*(t, \theta)$ and the dynamics of fertile soil for two values of ϕ, the abatement efficiency, and different functional forms for ν, the soil sensitivity to pollution.

Effect of abatement efficiency ϕ. Let us consider here the case of a technological pole around π, and analyze the effect of the abatement efficiency when $\phi = 2$ and $\phi = 3$. Figure 4 shows the given distributions of productivity A, abatement efficiency ϕ, soil sensitivity ν and the resulting optimal detrended consumption c_g.

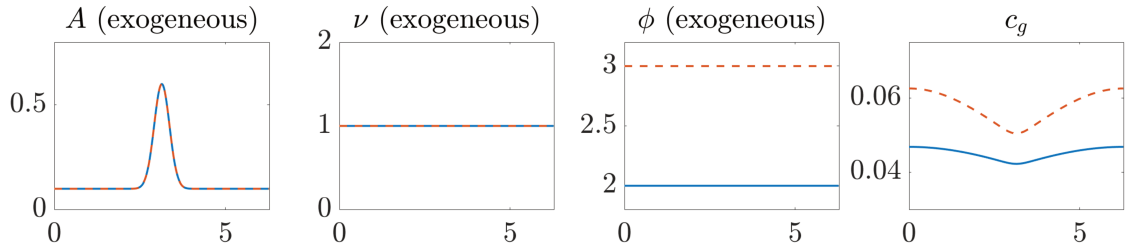

Figure 4: Impact of ϕ on c_g in Phase 1. $\phi = 3$ for dashed lines; $\phi = 2$ fo solid lines.

[11] Subsection 4.1 uses the package Chebfun in Matlab. An algorithm has been developed in Matlab to simulate the optimal solution in Phase 2.

Since net productivity $A(\phi - \nu)$ increases with ϕ, optimal consumption also increases with ϕ at each location. Figure 4 also shows that consumption is heterogeneous and that inequality in consumption becomes larger as abatement efficiency increases. Surprisingly, consumption is lower in the technologically advanced locations. There are two reasons for this phenomenon. First and independently of ϕ, pollution damage $\nu A L_F$ is stronger in the technological pole. As a result, the social planner sacrifices consumption there in order to abate the local excess in pollution. Second, note that the central area can also abate more efficiently since $A\phi$ is larger there. For this reason the policy maker induces these locations to abate even further to act as a pollution sink along the optimal trajectory. In doing so, consumption diminishes locally while heterogeneity increases.

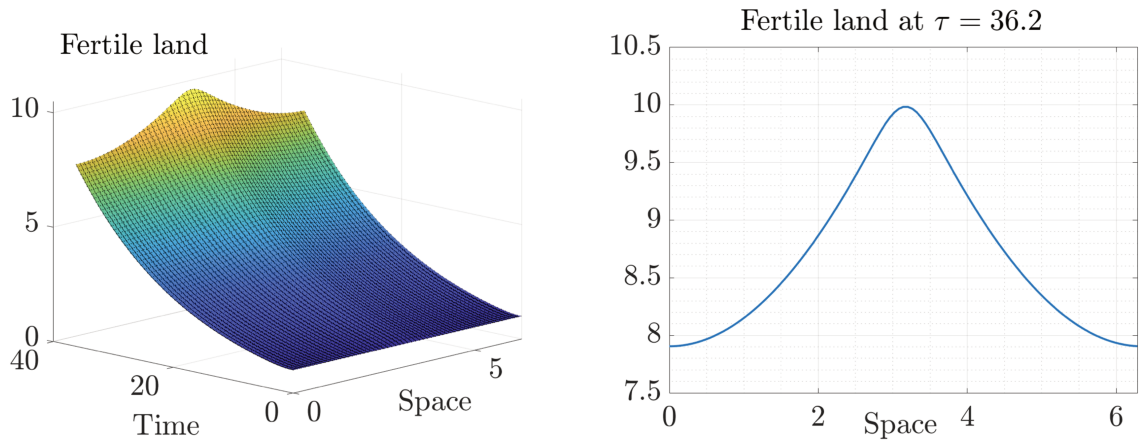

Figure 5: Dynamics of fertile soil in Phase 1 for $\phi = 2$ starting with $L_F^0 = 1$ for all θ.

As abatement increases, the technological pole accumulates more fertile soil and they are first to reach their fertility upper bound (see Figure 5). Moreover, as ϕ increases, this advantage of the core region over the periphery gets even more pronounced. Figure 6 shows that the more efficient the abatement technology is, the more unequal the economy (in terms of L_F). Yet, a higher ϕ reduces the length of Phase 1, compensating somehow the greater inequality it implies.

Proposition 1 proves that g is constant in time and spatially homogeneous in this Phase 1. Our numerical exercises show that g increases with ϕ. Indeed g grows from 6% to 14.1% when ϕ passes from 2 to 3. That is, an increase in 50% in the abatement efficiency implies an increase in 135% in the growth rate, pushing the economy towards Phase 2 at a faster pace. Indeed, when $\phi = 2$ the economy reaches Phase 2 in 36.2 units of time, i.e. $\tau = 36.2$, while $\tau = 14.4$ when $\phi = 3$.

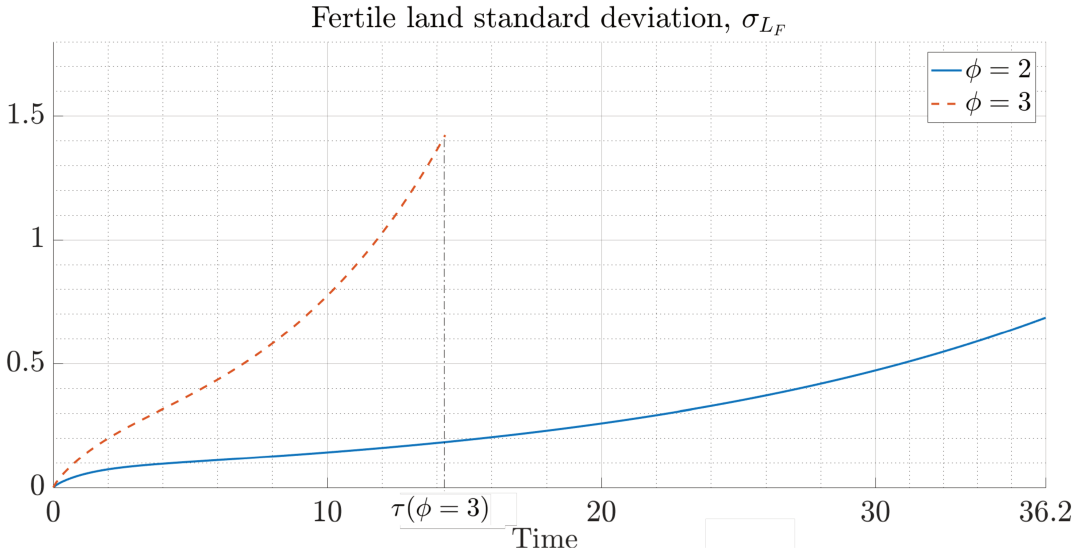

Figure 6: σ_{L_F} as a function of time for $\phi = 2$ and $\phi = 3$.

Soil sensitivite to production. In this example locations with high productivity are also those where soil is more sensitive to pollution. This could reflect situations in which a very efficient production technology causes greater damages to soil, locally eroding the area's resilience to pollution. This dependence of soil sensitivity to productivity is modeled here using a power function: $\nu = \nu_0 A^\gamma$. Figure 7 shows the simulation results for two values of abatement efficiency $\phi = 10$ and $\phi = 11$.

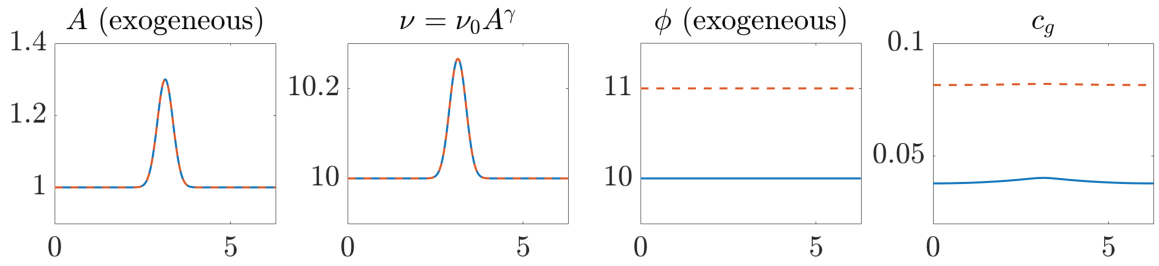

Figure 7: Impact of ϕ on c_g with spatially heterogeneous ν. Dashed lines correspond to $\phi = 11$; solid lines to $\phi = 10$.

As abatement efficiency increases, both detrended consumption and the growth rate increase as in the previous example. Yet, Figure 8 shows that, in this case, the fertile soil distribution when the economy reaches Phase 2 is U-shaped, which is in contrast with the inverted U-shaped distribution of the previous example. Here, abatement is not efficient enough in the sensitive and productive core region to absorb all the pollution that is locally generated. As a result, the first locations to reach the fertile

economy are in the periphery, which are endowed with the least productive, yet least damaging, technology.

Note that this behavior holds only for values of ϕ bellow a specific threshold. Above this threshold, abatement becomes efficient enough to absorb pollution from the core productive region. In such case, the dynamics of fertile soil switches back to the inverted U-shape of the previous example in which the productive region reaches first the fertile economy. In either case, as long as the growth rate is positive, that is for $\lambda_0 > \rho$, one location reaches its fertility upper bound and the economy switches to Phase 2.

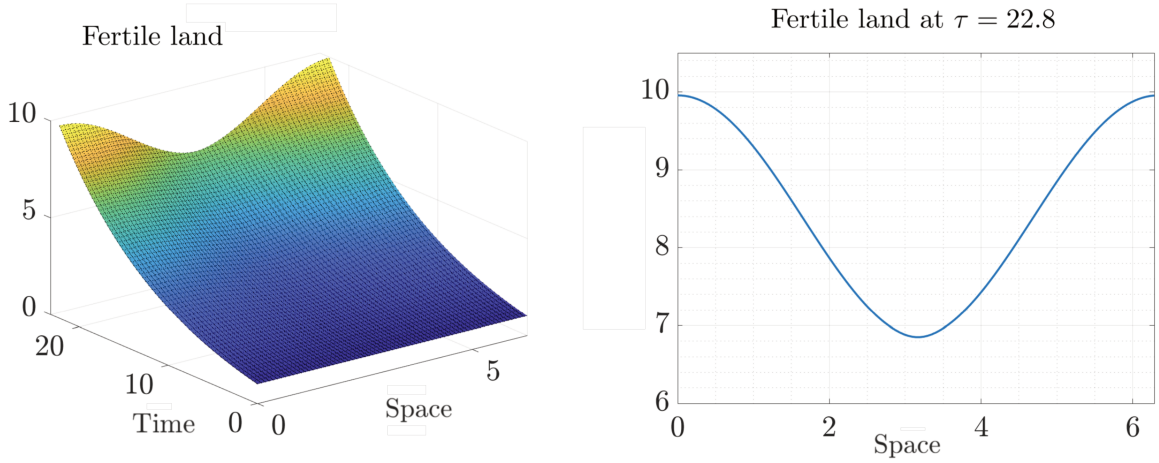

Figure 8: Dynamics of fertile soil in Phase 1 for $\phi = 11$ starting with $L_F^0 = 1$ for all θ.

4.2 Fertile soil dynamics in Phase 2

Proposition 5 shows that despite spatial diffusion, fertile soil in the polluted region $\underline{\mathcal{S}}$ could remain below the maximum forever. We explore numerically the second phase of the dynamics, in which space is divided in two regions one of which has no pollution at all. The first exercise completes the first example of section 4.1, describing the dynamics of fertile soil from the moment Phase 2 is reached, until the fertile economy, that is, until fertile soil attains the maximum at all locations. The second set of exercises investigates on the resiliency of the fertile economy towards pollution shocks and on the existence of a spatially heterogeneous fertile soil steady state. It will be assumed that starting from the zero pollution economy, a region receives a pollution shock. The shock could be thought as a natural or industrial catastrophe which locally pollutes soil on a limited geographic area such as the leak of pollutants from an industrial site or the explosion of a chemical plant.

Usually, when the technological coefficient is constant it is assumed that $A = 1$ for illustration purposes as in Boucekkine et al. (2018) or Camacho and Pérez-Barahona (2015). For the same illustrative reason, when technology is constant we choose $A = 0.2$ to underline that the economy is agricultural and it uses a relatively backward technology. In the cases where A is spatially heterogeneous, A will be an exponential function as we explain below. ϕ is equal to 2, ν is 0.2 and population is homogeneous and equal to 10.

4.2.1 Convergence towards the fertile economy

This exercise presents the continuation of the optimal solution studied in 4.1 and depicted in Figure 5, in which the central region attains Phase 2 at $\tau = 36.2$. From that moment onwards, locations at the maximum of fertile soil only abate to maintain their maximum level and diffusion only takes place across the borders of the fertile area. That is, locations with the largest amount of fertile soil stop absorbing pollution from neighboring locations. For locations in transition towards their maximum, this change comes as a shock and pollution rises. Let us underline that the passage from Phase 1 to Phase 2 was foreseen from $t = 0$ and it is by no means a shock, it is an optimal adaptation pattern. Figure 9 shows how at locations around $\theta = 0$ (or $\theta = 2\pi$), fertile soil drops from 7.9 to 7.4. Then abatement rates increase in $\underline{\mathcal{S}}$ and fertile soil starts growing again so that the polluted region catches up with the fertile one. The right panel in Figure 9 shows the growth rate of fertile soil. Note that in contrast to Phase 1, the growth rate is not in the least constant in time nor spatially homogeneous. Locations where fertile soil had dropped in the most severe manner grow the fastest.

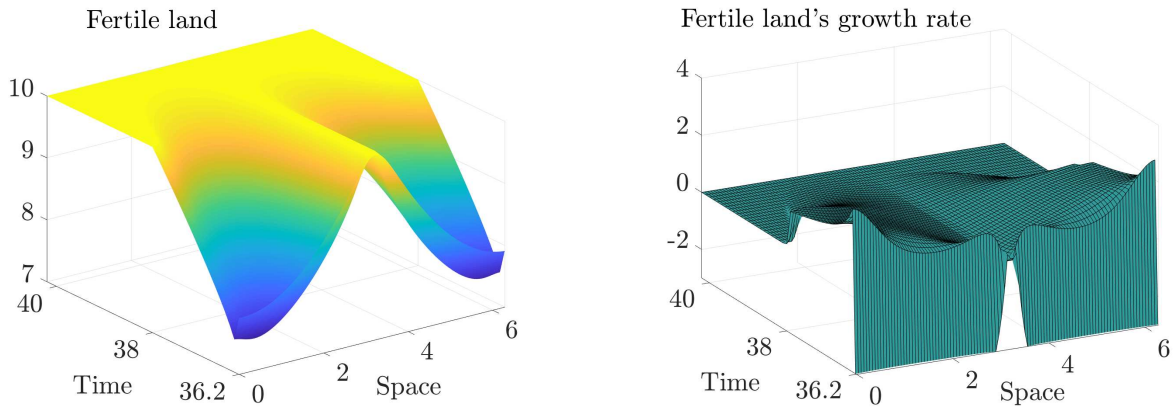

Figure 9: Dynamics in Phase 2 towards the fertile economy for $\phi = 2$.

4.2.2 Resiliency of the fertile economy to pollution shocks

In the following exercises, the economy is subject to different shocks which vary in size and coverage. First, let us compare the effect of a relatively small shock. The central region $[\frac{4.5}{10}2\pi, \frac{5.5}{10}2\pi]$ of size 1 receives a pollution shock, which induces a loss of 1% of its fertile soil, that is, $L_F(0,\theta) = 0.99L(\theta)$ for $\theta \in [\frac{4.5}{10}2\pi, \frac{5.5}{10}2\pi]$. The left column of Figure 10 describes the evolution in time of the pollution frontier between the fertile and the polluted regions after the shock, as well as the spatial dynamics of polluted land when technology A is spatially homogeneous, $A = 0.2$. On the right column, the figure shows the results when A follows an exponential spatial distribution, making the spatial center a technological pole. In this case, $A(\theta) = 0.20 + 2e^{-(\theta-\pi)^2}$. Advancing our results, we will conclude that a shock can be overcome only if the region under ecological stress is endowed with a sufficiently advanced technology.

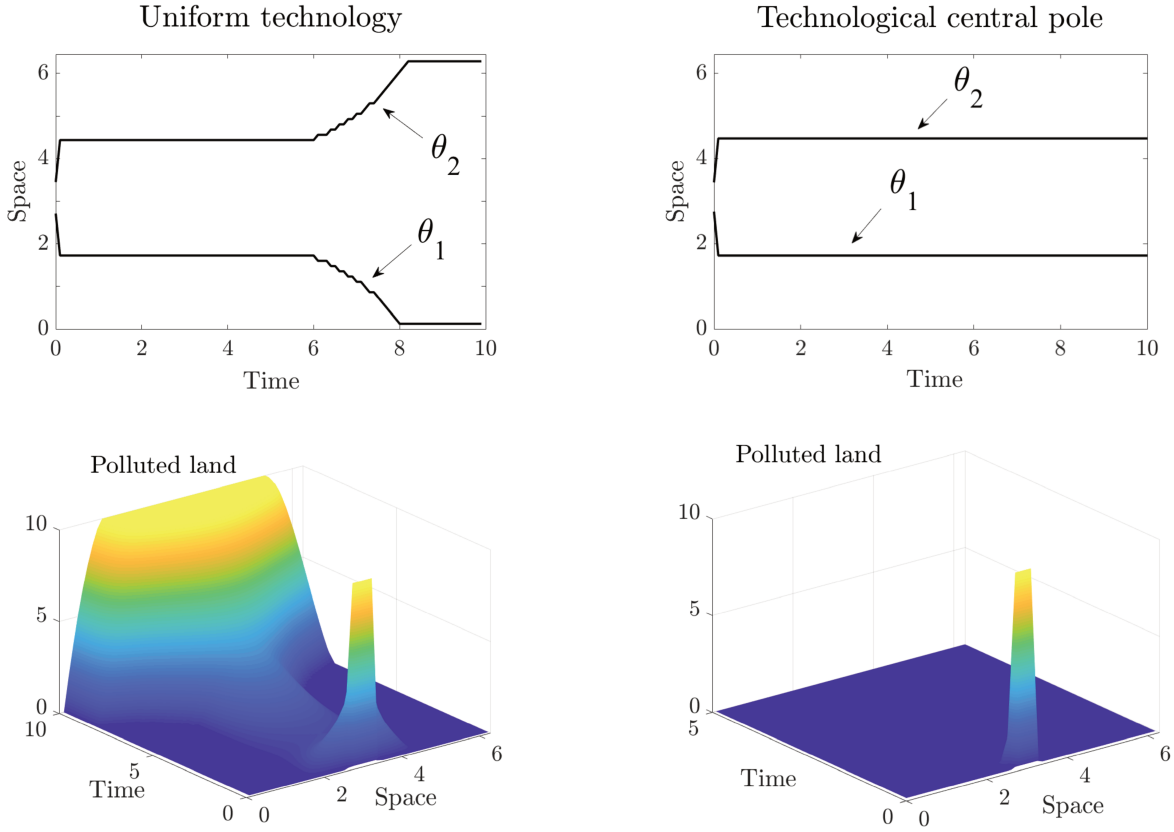

Figure 10: Spatial dynamics for initial shock $L_F(0,\theta) = 0.99L(\theta)$ for $\theta \in [\frac{4.5}{10}2\pi, \frac{5.5}{10}2\pi]$.

Let us analyze the different stages of the evolution of a pollution shock. Right after the shock, polluted land increases, and this is independent on the technology the region uses as Figure 10 shows. Indeed, the remaining fertile soil has to face a large

stock of pollution, trying to preserve consumption in as much as possible, sacrificing abatement temporarily. Additionally, we know that once pollution is present in the soil, it accumulates in time. As a result, after the initial shock, polluted land rockets. We begin by the case of the homogeneous technology, depicted on the left column of Figure 10.

In a second moment after the shock, pollution diffuses over space pushing the frontiers of the polluted region, so that the region with polluted land expands. As the top graphs show in Figure 10, the polluted region becomes stable in size for some time, reducing the level of pollution. Nevertheless, this situation is not stable. Indeed, the fall in polluted land is followed by a very slow and subtle accumulation of pollution in all locations of the polluted region. Once a threshold of total pollution is reached, the region cannot abate enough. As a result, pollution starts diffusing spatially, pushing the frontiers of the polluted region outwards. At that moment there is a massive uprise in pollution everywhere. Indeed, not only local pollution accumulates in time by its own production, but it also receives pollution from neighboring locations. Again, locations tend to preserve consumption, diminishing abatement, which makes pollution increase locally. Noteworthy, in this example, locations at the maximum of fertile soil at the beginning, and which do not abate more than needed locally, end up being highly polluted by the diffusion mechanism.

In sharp contrast, when the shocked region has a technological advantage, locations can overcome the shock by adapting their consumption and abatement during the initial moments (see graphs on the right of Figure 10). Although polluted land increases during the first moments, the central locations are more productive and can produce more using less land and hence polluting less. This mechanism counterbalances the shock, explaining why the central region absorbs all pollution in an extremely short period of time.

In a second example, we subject the economy to an enormous shock both in terms of the area covered and the amount of fertile soil lost. Indeed, in this example, $L_F(0,\theta) = 0.1L(\theta)$ for $\theta \in [\frac{2}{10}2\pi, \frac{8}{10}2\pi]$. That is, the catastrophic region represents 60% of the entire land, and it loses 90% of its fertile soil. Figure 11 shows the results for both a homogeneous and a heterogeneous technology. When technology is spatially homogeneous, the catastrophic region experiences a rise in pollution from the beginning. Augmenting further emissions of pollution, which add to the pre-existing pollution locally, and which diffuse spatially to the adjacent locations. A self-reinforcing

polluting mechanism is triggered. Note that the central region remains at the highest levels of pollution (where almost all land is polluted) forever. Since technology is not advanced enough, the catastrophic region cannot produce enough for its population without worsening the environmental situation. Note how, as in the previous example, with time, pollution diffuses spatially and almost all the economy experiences high levels of pollution after 10 periods of time.

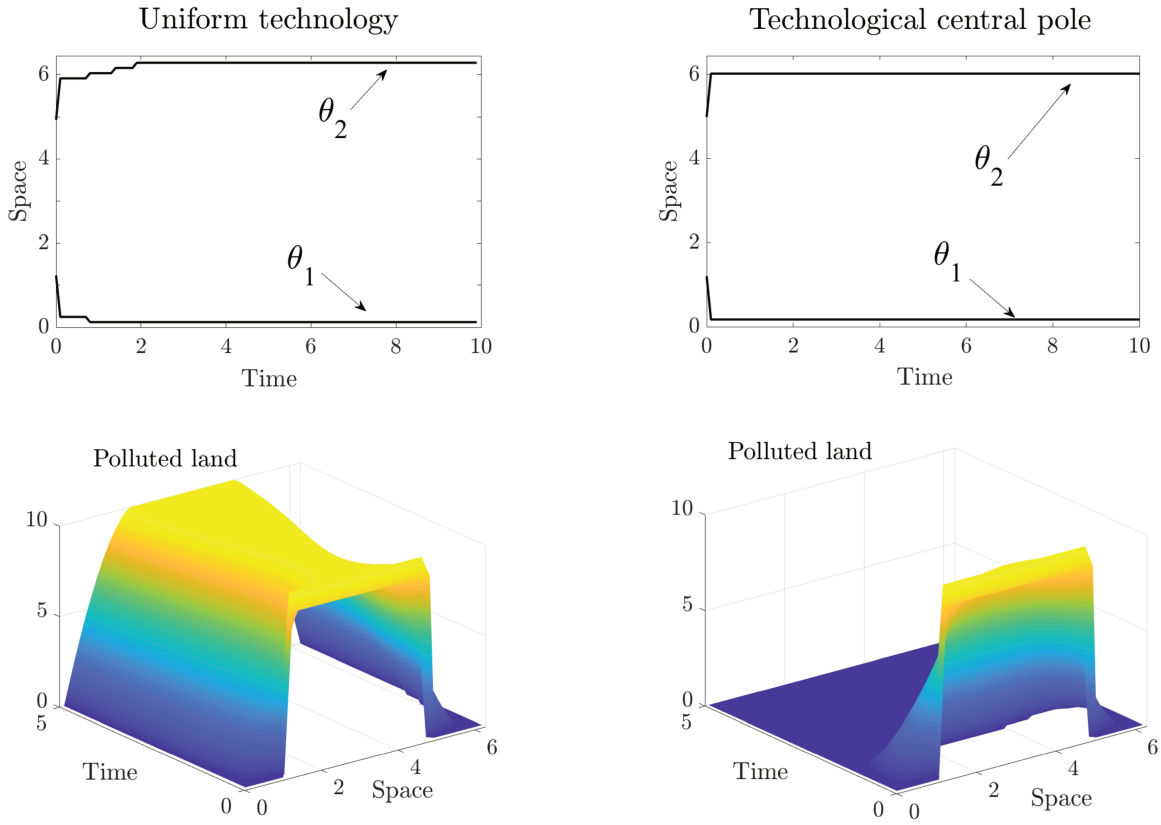

Figure 11: Spatial dynamics for initial shock $L_F(0,\theta) = 0.1L(\theta)$ with $\theta \in [\frac{2}{10}2\pi, \frac{8}{10}2\pi]$.

Finally, let us underline that when technology is sufficiently advanced, the catastrophic region can recover after an adjustment period even after an enormous shock (see right column in Figure 11). After the initial raise in pollution in the shocked region, all locations react, diminishing consumption, abating pollution until they reach the equilibrium. Here, all locations recover the maximum level of fertile soil. Nevertheless, given the size of the shock, recovery takes longer time than in the previous example. Hence, our exercises have shown the existence of non homogeneous steady states for fertile soil, even when all the model's parameters are spatially homogeneous. As advanced, their existence hinges on the size of the region and its technology. Indeed,

a relatively small and backward region cannot absorb nor diffuse enough pollution, accumulating it locally instead.

5 Conclusion

This chapter develops a spatial growth model accounting for the diffusion of pollution into soils. We provide with the explicit optimal trajectories for fertile and polluted soil in space and time, while considering the persistence of pollution into agricultural soils. We faced two major challenges. First, the production factor, fertile soil, is here, locally and naturally bounded by the amount of available land at each location. Second, space can be divided in regions, one of which could have attained the maximum of fertile soil. Borrowing the Stefan's equation from Physics, we have modeled the dynamics of the pollution frontier between the region in which fertile soil is at its maximum, and the region in which there is a share of polluted soil.

The boundedness of the production factor defines two phases in the dynamics of fertile soil. We described a first phase in which all locations have some polluted land, during which fertile soil and consumption grow at the same constant rate at all locations. Eventually, some locations eradicate all pollution and reach their maximum for fertile soil. Here the dynamics change radically. Locations at the maximum stop absorbing pollution coming from the yet struggling and polluted area. As a result, it may be the case that the polluted regions will never reach their potential maximum for fertile soil, remaining forever in a sort of environmental poverty trap, that is at a steady state with some share of polluted soil. This possibility has been analytically proven and numerically explored. We have indeed shown that economies could reach a spatially heterogeneous steady state after a catastrophic pollution shock when their technology is not advanced enough.

Therefore, and surprisingly enough, spatial pollution patterns can emerge even from an economy that is endowed with homogeneous technological and soil characteristics. We think that the emergence of such heterogeneous soil fertility patterns is precisely the effect of diffuse soil pollution in a spatially distributed agricultural economy.

References

[1] Allen, T. and Arkolakis, C. (2014), "Trade and the topography of the spatial economy", *Quarterly Journal of Economics*, 129, 1085-1139.

[2] Aldashev, G., Aldashev, S., and Carletti, T. (2014), "On convergence in the spatial AK growth models", *Working Paper arXiv preprint arXiv*, 1401-4887.

[3] Augeraud-Véron, E., Boucekkine, R. and Veliov, V. (2019), "Distributed optimal control models in environmental economics: a review", *Mathematical Modelling of Natural Phenomena*. 14, 106.

[4] Antle, J. M., Stoorvogel, J. J., Valdivia, R. O. (2006), "Multiple equilibria, soil conservation investments, and the resilience of agricultural systems", *Environ. Dev. Econ.*, 11(4), 477-492.

[5] Attanasio, O. and Browning, M. (1995), "Consumption over the Life Cycle and over the Business Cycle", *American Economic Review*, 85(5), 1118-1137.

[6] Attanasio, O. and Weber, G. (1993), "Consumption, the Interest Rate and Aggregation", *Review of Economic Studies*, 60(3), 631-649.

[7] Ballestra, V. L. (2016), "The spatial AK model and the Pontryagin maximum principle", *Journal of Mathematical Economics*, 67, 87-94.

[8] Barbier, E. B. (1990), "The farm-level economics of soil conservation: the uplands of Java", *Land Econ.*, 66(2), 199-211.

[9] Barrett, S. (1991), "Optimal soil conservation and the reform of agricultural pricing policies", *J. Dev. Econ.*, 36(2), 167-187.

[10] Barrett, C. B. and Bevis, L. E. (2015), "The self-reinforcing feedback between low soil fertility and chronic poverty", *Nat. Geosci.*, 8(12), 907-912.

[11] Barro R., Mankiw, G. and Sala-i-Martin, X. (1995), "Mobility in Neoclassical models of Growth", *American Economic Review*, 85(1), 103-115.

[12] Bensoussan, A., Da Prato, G., Delfour, M. C. and Mitter, S. K. (2007), "Representation and control of infinite dimensional system", *Second edition, Birkhauser, Boston.*

[13] Berazneva, J., Conrad, J., Gerena, D., Lehmann, J. and Woolf, D. (2018), "Agricultural productivity and soil carbon dynamics: a bioeconomic model", *Working Paper.*

[14] Bevis, L. E., Conrad, J. M., Barrett, C. B. and Gray, C. (2017), "State-conditioned soil investment in rural Uganda", *Res. Econ.*, 71(2), 254-281.

[15] Boucekkine, R., Camacho, C. and Zou, B. (2009), "Bridging the gap between growth theory and the new economic geography: The spatial Ramsey model", *Macroeconomic Dynamics*, 13, 20-45.

[16] Boucekkine, R., Camacho, C. and Fabbri, G. (2013), "Spatial dynamics and convergence: The spatial AK model", *Journal of Economic Theory*, 148, 2719-2736.

[17] Boucekkine, R., Fabbri, G., Federico, S. and Gozzi, F. (2018), "Growth and agglomeration in the heterogeneous space: a generalized AK approach", *Journal of Economic Geography*, 0, 1-32.

[18] Boucekkine, R., Fabbri, G., Federico, S. and Gozzi, F. (2020), "From firm to global-level pollution control: the case of transboundary pollution", *Quaderni del Dipartimentodi Economia Politica e Statistica*.

[19] Brito, P. (2001), "A Bentham-Ramsey model for spatially heterogeneous growth", *Working Papers Department of Economics. ISEG, University of Lisboa.*

[20] Brito, P. (2004), "The dynamics of growth and distribution in a spatially heterogeneous world", *Working Papers Department of Economics. ISEG, University of Lisboa.*

[21] Brock, W., Xepapadeas, A. (2008), "Diffusion-induced instability and pattern formation in infinite horizon recursive optimal control", *J. Econ. Dyn. Control*, 32, 2745-2787.

[22] Brock, W., Xepapadeas, A. (2010), "Pattern formation, spatial externalities and regulation in coupled economic-ecological systems", *J. Environ. Econ. Manag.*, 59, 149-164.

[23] Bunce, Arthur C. (1974), "Economics of Soil Conservation", *Ames: Iowa State University Press.*

[24] Burt, O.R. (1981), "Farm level economics of soil conservation in the Palouse area of the Northwest", Am. *J. Agric. Econ.*, 63(1), 83-92.

[25] Camacho, C. and Pérez-Barahona A. (2016), "Land use dynamics and the environment", *Journal of Economic Dynamics and Control*, 52, 96-118.

[26] Camacho, C., Zou, B., and Briani, M. (2008), "On the dynamics of capital accumulation across space", *European Journal of Operational Research*, 186(2), 451-465.

[27] CCICED (2015), *CCICED 2015 Work Report.*

[28] Chartier, P.M. and Rostagno, C.M. (2006), "Soil Erosion Thresholds and Alternative States in Northeastern Patagonian Rangelands", *Rangeland Ecology and Management*, 59(6), 616-624.

[29] Ciriacy-Wantrup, S. V. (1968), "Resource Conservation-Economics and Policies", *Berkeley: University of California Agr. Exp. Sta.*

[30] Coddington, E. A., Levinson, N. (1955), "Theory of Ordinary Differential Equations", *New York: McGraw-Hill.*

[31] d'Albis, H. and Augeraud-VŽron, E. (2009), "The optimal prevention of epidemics", *Georgia Institute of Technology.*

[32] Dupouey, J.J., Dambrine, E., Laffite, J.D. and Moares, C. (2002), "Irreversible Impact of Past Land Use on Forest Soils and Biodiversity", *Ecology*, 83(11), 2978-2984.

[33] EU Commission (1991), Directive 91/676/EEC. "Council Directive of 12 December 1991 concerning the protection of waters against pollution caused by nitrates from agricultural sources", *Official Journal of European Community L375: 1-8.*

[34] Fabbri, G. (2016), "Geographical structure and convergence: A note on geometry in spatial growth models", *Journal of Economic Theory*, 162, 114-136.

[35] Food and Agriculture Organization of the United Nations and Intergovernmental Technical Panel on Soils Status (2015), *Status of the World's Soil Resources Main Report.*

[36] Gao, Y., Zhong, B., Yue, H., Wu, B. and Cao, S. (2011), "A degradation threshold for irreversible loss of soil productivity: a long?term case study in China", *Journal of Applied Ecology*, 48, 1145-1154.

[37] de Graa , J., Amsalu, A., Bodnár, F., Kessler, A., Posthumus, H., Tenge, A. (2008), "Factors influencing adoption and continued use of long-term soil and water conservation measures in developing countries", *Appl. Geography*, 28(4), 271-280.

[38] Hagos, F., Holden, S. (2006), "Tenure security, resource poverty, public programs, and household plot-level conservation investments in the highlands of northern Ethiopia", *Agric. Econ.*, 34(2), 183-196.

[39] Isard, W., Liossatos, P. (1979), "Spatial Dynamics and Optimal Space-time Development", *North-Holland Publishing Company.*

[40] Kopittke, P.M., Menzies, W.N., Wang, P., McKenna, B.A. and Lombi, E. (2019), "Soil and the intensification of agriculture for global food security", *Environment International*, 132.

[41] La Torre, D., Liuzzi, D. and Marsiglio, S. (2015), "Pollution diffusion and abatement activities across space and over time", *Mathematical Social Sciences*, 78, 48-63.

[42] Le Kama, A.A., Pommeret, A. and Prieur, F. (2014), "Optimal Emission Policy under the Risk of Irreversible Pollution", *Journal of Public Economic Theory*, 16(6), 959-980.

[43] Lopez, H. (2008), "The social discount rate : estimates for nine Latin American countries", *The World Bank Policy Research Working Paper Series 4639.*

[44] McBratney, A., Morgan, C. and Jarrett, L. (2017), "The Value of Soil's Contributions to Ecosystem Services", *Global Soil Security*, 227-235.

[45] McConnell, K.E. (1983), "An economic model of soil conservation", *Am. J. Agric. Econ.*, 65(1), 83-89.

[46] Pope, C.A., Bhide, S., Heady, E.O. (1983), "The economics of soil conservation: an optimal control theory approach", *North Central J. Agric. Econ.*, 5(2), 83-89.

[47] Rodríguez-Eugenio, N., McLaughlin, M. and Pennock, D. (2018), *Soil Pollution: a hidden reality.*

[48] Saliba, B.C. (1985), "Soil productivity and farmers' erosion control incentives? A dynamic modeling approach", *Western J. Agric. Econ.*, 10(2), 354-364.

[49] Segarra, E., Taylor, D.B. (1987), "Farm level dynamic analysis of soil conservation: an application to the piedmont area of Virginia", *J. Agric. Appl. Econ.*, 19(2), 61-73.

[50] Smith, E.G., Lerohl, M., Messele, T. and Janzen, H.H. (2000), "The Value of Soil's Contributions to Ecosystem Services", *Journal of Agricultural and Resource Economics*, 25(1), 307-324.

[51] Smith, M., Sanchirico, J., Wilen, J. (2009), "The economics of spatial-dynamic processes: applications to renewable resources", *J. Environ. Econ. Manag.*, 57, 104-121.

[52] Stephens, E. C., Nicholson, C. F., Brown, D. R., et al. (2012), "Modeling the impact of natural resource-based poverty traps on food security in Kenya: The Crops, Livestock and Soils in Smallholder Economic Systems (CLASSES) model", *Food Security*, 4(3), 423-439.

[53] "United Nations Convention to Combat Desertification", (2017), *The Global Land Outlook, first edition.*

[54] Verhulst, P.-F. (1845), "Recherches mathématiques sur la loi d'accroissement de la population", *Nouv. Mem. Acad. R. Sci. B.-lett. Brux.*, 18, 1-45.

[55] Xepapadeas, A. and Yannacopoulos, A. N. (2016), "Spatial growth with exogenous saving rates", *Journal of Mathematical Economics*, 67, 125-137.

Appendices

A. Mathematical Preliminaries

We represent (2) as an abstract dynamical system in infinite dimension.[12] Its solutions belong to $L^2(\mathcal{S})$, defined as:

$$L^2(\mathcal{S}) = \{f : \mathcal{S} \longrightarrow \mathbb{R} \mid \int_0^{2\pi} \mid f(\theta) \mid^2 d\theta < \infty\}.$$

For any two functions f, g in $L^2(\mathcal{S})$, their inner product is defined as $< f, g >= \int_0^{2\pi} f(\theta)g(\theta)d\theta$, and f's norm is then $\mid f \mid^2 =< f, f >= \int_0^{2\pi} f^2(\theta)d\theta$. $L^2(\mathcal{S})$ endowed with the inner product $< \cdot, \cdot >$ is a Hilbert space. Since we cannot take derivatives on all elements of $L^2(\mathcal{S})$, let us define three spaces that will help us defining the domain of $\mathcal{L}$:

$$\begin{aligned}
\mathcal{H}^0_+(\mathcal{S}) &:= \{f \in L^2(\mathcal{S}) : f(\cdot) \geq 0, \text{and } f(\cdot) \neq 0\}, \\
\mathcal{H}^1(\mathcal{S}) &:= \{f \in L^2(\mathcal{S}) : \exists \text{f' in weak sense and belongs to } L^2(\mathcal{S})\}, \\
\mathcal{H}^2(\mathcal{S}) &:= \{f \in L^2(\mathcal{S}) : \exists \text{f' in weak sense and belongs to } \mathcal{H}^1(\mathcal{S})\}.
\end{aligned}$$

Hence, the domain of $\mathcal{L}$ is $\mathcal{H}^2(\mathcal{S})$ and $\mathcal{L}$ is well defined on this domain. Operator $\mathcal{L}$ is self-adjoint since for any two $f, g \in \mathcal{H}^2(\mathcal{S})$, $< \mathcal{L}f, g >=< f, \mathcal{L}^* g >=< f, \mathcal{L}g >$. Note first that the Laplacian operator is closed in its domain, $\mathcal{H}^2(\mathcal{S})$, and it generates a semigroup on $L^2(\mathcal{S})$. Since the second factor in $\mathcal{L}$ is bounded, we can conclude that our operator $\mathcal{L}$ is closed in its domain, $D(\mathcal{L}) = \mathcal{H}^2(\mathcal{S})$ and it generates a C_0 semigroup.

The Laplacian operator generates a C_0 semigroup in the following sense. Let $\mathcal{A}$ be a closed linear operator defined on $L^2(\mathcal{S})$ (for simplicity), and consider the following initial value problem:

$$\begin{aligned}
y'(t) &= \mathcal{A}y(t), \\
y(0) &= y_0 \in L^2(\mathcal{S}), \text{given.}
\end{aligned}$$

If the operator $\mathcal{A}$ is bounded, then the solution to this problem is given by:

$$y(t) = e^{t\mathcal{A}}y_0 := \sum_{j=0}^{\infty} \frac{t^j \mathcal{A}^j y_0}{j!}.$$

[12] A similar account can be found in Boucekkine et al. (2013). For a deeper insight see Bensoussan et al. (2007).

If we define $Z_{\mathcal{A}}(t) = e^{t\mathcal{A}}$, then $Z_{\mathcal{A}}(t+s) = Z_{\mathcal{A}}(t)Z_{\mathcal{A}}(s)$, and $Z_{\mathcal{A}}(0) = 1$. As mentioned in p. 89 in Bensoussan (2007), there is a one-to-one correspondence between the group $(\mathbb{R}, +)$ and the subset $Z_{\mathcal{A}} = \{Z_{\mathcal{A}}(t) : t \in \mathbb{R}\}$ in $L(\mathcal{S})$, or in particular in $L^2(\mathcal{S})$ under composition "$\circ$". So we say that $(Z_{\mathcal{A}}, \circ)$ is a group. When $\mathcal{A}$ is unbounded like in the case of the Laplacian operator, then one can define $Z_{\mathcal{A}}$ only for $t \geq 0$ and $s \geq 0$ in general. We say then that $Z_{\mathcal{A}}$ is a semigroup.

The most useful property of semigroups hinges on the following relationship. The infinitesimal generator $\mathcal{A}$ of Z is the linear operator in $\mathcal{S}$ defined by:

$$D(\mathcal{A}) = \{x \in \mathcal{S} : \text{such that } \lim_{h \to 0^+} \frac{Z(h)x - x}{h} \text{ exists}\},$$

and $\mathcal{A}x = \lim_{h\to 0^+} \frac{Z(h)x-x}{h}$ for all $x \in D(\mathcal{A})$. Then, we have that:

$$\frac{d}{dt}Z(t)x = \mathcal{A}Z(t)x = Z(t)\mathcal{A}x.$$

Given the set of admissible trajectories for L_F, we can define the set of admissible strategies for c, $\mathcal{C}$ as:

$$\mathcal{C}(L_F^0) = \{c \in \mathcal{L}^1_{\text{loc}}(\mathbb{R}^t, L^2(\mathcal{S})^+) : L_F \in \mathcal{H}_0, \text{for all } t \geq 0\}.$$

Finally, the objective functional is:

$$J(L_F^0; c) := \int_0^\infty e^{-\rho t} U(c) dt,$$

where:

$$U(c) = \int_{\mathcal{S}} \frac{c(t,\theta)^{1-\sigma}}{1-\sigma} N(\theta) d\theta.$$

The value function associated to our problem is then:

$$V(L_F^0) := \sup_c J(L_F^0; c).$$

B. Necessary optimal conditions

Although our problem is close to Boucekkine et al. (2013) and Boucekkine et al. (2018), it differs from then in that our problem the productive factor is bounded. In particular, boundedness implies that at a given point in time, the productive factor could be zero or attain its maximum. Most importantly, the policy maker needs to take into account the eventuality

of reaching one of the boundaries, and that the economy could be split in two regions. Not knowing how to deal with the fullfledged problem using dynamic programming alone, the authors resort to an optimal control approach. Hence, first, using Ekeland's variational principle, we obtain the set of necessary conditions for our problem. Then we will go back and forth from optimal control to dynamic programming, being aware of the awkwardness it generates. As said earlier, the inclusion of (moving) frontiers and the possibility two coexisting and unconnected regions make us combine different approaches. We explain next all details.

The set of necessary optimal conditions obtained though the variational principle has the main shortcoming of including a reverse time parabolic partial differential equation, which renders our problem difficult to analyse. For this reason, we resort to dynamic programming to obtain the exact expression of the optimal solution before any location reaches the boundary. Fortunately, and since the optimal solution is unique (see Camacho and Pérez-Barahona, 2015), we can prove that the solution obtained through dynamic programming also satisfies the set of optimal conditions obtained via optimal control when fertile land lies within its boundaries. Then, we shall prove that during this first regime fertile land grows at a constant and spatially homogeneous rate, steadily increasing or decreasing with time. As a result, one location will eventually reach a boundary for fertile land. At that moment, the solution enters in the second phase. Here, some of the locations have attained the maximum level of fertile land, while others are still transiting. Once locations reach the bound, they stop investing in pollution abatement.

In order to apply Ekeland's variational principle, let us write the value function $V(\cdot)$ associated to problem (2)-(5):

$$V(c, L_F, \psi, \mu) = \int_0^{\infty} \int_0^{2\pi} e^{-\rho t} \frac{c(t,\theta)^{1-\sigma}}{1-\sigma} N(\theta) d\theta dt$$

$$- \int_0^{\infty} \int_0^{2\pi} \psi(t) \left(\frac{\partial L_F}{\partial t}(t,\theta) - D \frac{\partial^2 L_F}{\partial \theta^2}(t,\theta) - A(\theta)[\phi(\theta) - \nu(\theta)] L_F(t,\theta) + c(t,\theta) N(\theta) \phi(\theta) \right) d\theta dt$$

$$- \int_0^{\infty} \int_0^{2\pi} \mu(t,\theta) \left(L(\theta) - L_F(t,\theta) \right) d\theta dt - \int_0^{\infty} \int_0^{2\pi} \xi(t,\theta) L_F(t,\theta) d\theta dt.$$

Then, assuming there exists an optimal solution and that any solution to our problem can be written as a deviation from the optimal solution we obtain:

$$c(t,\theta) = c^*(t,\theta) + \epsilon \mathcal{C}(t,\theta),$$

$$L_F(t,\theta) = L_F^*(t,\theta) + \epsilon \mathcal{L}_F(t,\theta).$$

V becomes then a function of ϵ. To optimize $V(\cdot)$ boils down to minimizing the deviation. At the optimal ϵ^*, $\frac{\partial V(\epsilon^*)}{\partial \epsilon} = 0$. We use that the auxiliary variables ψ, μ and ξ are $\mathcal{C}^1$ functions, so that $\psi(t,0) = \psi(t,\pi)$, $\mu(t,0) = \mu(t,\pi)$, $\xi(t,0) = \xi(t,\pi)$; and $\psi_x(t,0) = \psi_x(t,\pi)$, $\mu_x(t,0) = \mu_x(t,\pi)$, $\xi_x(t,0) = \xi_x(t,\pi)$. Since $L_F \in \mathcal{C}^1$, it is also true that $L_F(t,0) = L_F(t,2\pi)$ and $L_{F,x}(t,0) = L_{F,x}(t,2\pi)$. Then, since V is continuously differentiable in c and L_F, after applying integration by parts, we can compute $\frac{\partial V(\epsilon)}{\partial \epsilon}$ as:

$$\begin{aligned}\frac{\partial V(\epsilon)}{\partial \epsilon} = &\int_0^\infty \int_0^{2\pi} e^{-\rho t} c(t,\theta)^{-\sigma} \mathcal{C}(t,\theta) N(\theta) d\theta dt \\ &- \int_0^\infty \int_0^{2\pi} \left[-\psi_t(t,\theta)\mathcal{L}_F(t,\theta) - D\psi_{xx}(t,\theta)\mathcal{L}_F(t,\theta)\right] d\theta dt \\ &- \int_0^\infty \int_0^{2\pi} \left[A(\theta)[\phi(\theta) - \nu(\theta)]\psi(t,\theta)\mathcal{L}_F(t,\theta) + \mathcal{C}(t,\theta)N(\theta)\phi(\theta)\right] d\theta dt \\ &+ \int_0^\infty \int_0^{2\pi} \left[\mu(t,\theta) - \xi(t,\theta)\right] \mathcal{L}_F(t,\theta) d\theta dt,\end{aligned}$$

with $\lim_{t\to\infty} \psi(t,\theta) L_F(t,\theta) = 0$, for all $\theta \in \mathcal{S}$. Along with the transversality condition, we obtain the following condition on L_F and ψ:

$$\psi(t,\theta)\nabla_\theta L_F(t,\theta) \mid_0^{2\pi} = \nabla_\theta \psi(t,\theta) L_F(t,\theta) \mid_0^{2\pi}, \tag{9}$$

where ∇_θ is the space integral of $\mathcal{L}$.

Collecting the terms multiplying $\mathcal{C}$ and $\mathcal{L}_F$, and detrending ψ, we obtain the following set of necessary optimal conditions for all $\theta \in \mathcal{S}$ and for all $t > 0$:

$$\begin{cases} \psi(t,\theta) = \frac{1}{\phi(\theta)} c(t,\theta)^{-\sigma}, \\ \psi_t(t,\theta) + D\psi_{xx}(t,\theta) + A(\theta)[\phi(\theta) - \nu(\theta)]\psi(t,\theta) - \rho\psi(t,\theta) + \mu(t,\theta) - \xi(t,\theta) = 0, \\ \mu(t,\theta)\left(L(\theta) - L_F(t,\theta)\right) = 0, \\ \xi(t,\theta) L_F(t,\theta) = 0. \end{cases}$$

Recalling that $\mathcal{L}\psi(t,\theta) = D\psi_{xx}(t,\theta) + A(\theta)[\phi(\theta) - \nu(\theta)]\psi(t,\theta)$, we can rewrite the second equation as:

$$\psi_t(t,\theta) + \mathcal{L}\psi(t,\theta) - \rho\psi(t,\theta) + \mu(t,\theta) - \xi(t,\theta) = 0.$$

Note that if L_F lies within its bounds, then both $\mu(t,\theta)$ and $\xi(t,\theta)$ are identically zero. Hence, we can provide a set of necessary conditions when fertile land is between the lower and the upper bound, at all locations.

$$(I)\begin{cases} \frac{\partial L_F}{\partial t}(t,\theta) = \mathcal{L}L_F(t,\theta) - c(t,\theta)N(\theta)\phi(\theta), \\ \psi(t,\theta) = \frac{1}{\phi(\theta)}c(t,\theta)^{-\sigma}, \\ \psi_t(t,\theta) + \mathcal{L}\psi(t,\theta) - \rho\psi(t,\theta) = 0, \\ \lim_{t\to\infty}\psi(t,\theta)L_F(t,\theta) = 0. \end{cases}$$

Hence (I) describes the optimal dynamics of the economy when no location has reached a bound.

The second phase is triggered whenever a location reaches the upper bound for fertile land.[13] In this case, we assume that $\mathcal{S} = \underline{\mathcal{S}} \cup \bar{\mathcal{S}}$, where $\bar{\mathcal{S}}$ is the set of locations that have reached the upper bound. Hence, for all $\theta \in \bar{\mathcal{S}}$:

$$L_F(t,\theta) = L(\theta), \;\; L_{F,t}(t,\theta) = 0 \;\text{ and }\; L_{F,xx}(t,\theta) = 0,$$

which implies that $c(t,\theta) = A(\theta)\frac{\phi(\theta)-\nu(\theta)}{\phi(\theta)}\frac{L(\theta)}{N(\theta)}, \forall t \geq 0$.

However, when analizing the set of optimal conditions in $\underline{S}$, we need to pay special attention to the border. The border condition (9) becomes:

$$\psi(t,\theta)\nabla_\theta L_F(t,\theta) \mid_{\theta_1(t)}^{\theta_2(t)} = \nabla_\theta\psi(t,\theta)L_F(t,\theta) \mid_{\theta_1(t)}^{\theta_2(t)} . \tag{10}$$

Hence, in the second phase at all t:

$$(II)\begin{cases} \frac{\partial L_F}{\partial t}(t,\theta) = \mathcal{L}L_F(t,\theta) - c(t,\theta)N(\theta)\phi(\theta), \\ \psi(t,\theta) = \frac{1}{\phi(\theta)}c(t,\theta)^{-\sigma}, \\ \psi_t(t,\theta) + \mathcal{L}\psi(t,\theta) - \rho\psi(t,\theta) = 0, \forall\theta \in \underline{\mathcal{S}}, \\ \psi(t,\theta)\nabla_\theta L_F(t,\theta) \mid_{\theta_1(t)}^{\theta_2(t)} = \nabla_\theta\psi(t,\theta)L_F(t,\theta) \mid_{\theta_1(t)}^{\theta_2(t)}, \\ \lim_{t\to\infty}\psi(t,\theta)L_F(t,\theta) = 0, \\ \text{and:} \\ L_F(t,\theta) = L(\theta), \;\; L_{F,t}(t,\theta) = 0 \;\text{ and }\; L_{F,xx}(t,\theta) = 0, \\ c(t,\theta) = A(\theta)\frac{\phi(\theta)-\nu(\theta)}{\phi(\theta)}\frac{L(\theta)}{N(\theta)}, \forall\theta \in \bar{\mathcal{S}}. \end{cases}$$

[13] When fertile land reaches the lower bound, dynamics are similar to the case of the upper bound except that consumption becomes zero at locations with zero fertile land.

C. Proof of Proposition 1. Optimal solution in Phase 1.

As explained in Appendix 5, we cannot be sure that the optimal solution we obtain using dynamic programming focusing on the time period before the border is reached coincides with the optimal solution of a policy maker that considers the problem globally, that is, taking into consideration the second phase. What we do here is to prove that actually, the explicit solution one obtains using dynamic programming for the first phase fulfill the set of necessary conditions obtained via optimal control. This way, we overcome to problems. First, one cannot find an explicit solution to the set of necessary conditions. Second, one cannot be sure that the solution provided by dynamic programming takes into account Phase 2. By proving that both strategies coincide, we can obtain an explicit optimal solution.

As previously explained, we will apply dynamic programming to answer the following question: before a single location reaches the frontier, what would be the optimal solution indicated by dynamic programming ? Remember that in this case the policy does not take into account the possibility of changing regime in the future. Nevertheless, we prove in this appendix that the specific solution we find verifies the set of necessary optimal conditions obtained through optimal control.

In Phase 1, the Hamilton-Jacobi-Bellman (HJB) equation associated to the previous optimal control problem can be written as:

$$\rho v(L_F) = \langle\, L_F, \mathcal{L}\nabla v(L_F)\,\rangle \; + \sup_c \left\{ \langle\, \frac{c^{1-\sigma}}{1-\sigma} N, \mathbb{1}\,\rangle \; - \langle\, \phi c N, \nabla v(L_F)\,\rangle \right\}.$$

Let $\hat{c} := \text{argmax}\left\{ \langle\, \frac{c^{1-\sigma}}{1-\sigma} N, \mathbb{1}\,\rangle \; - \langle\, \phi c N, \nabla v(L_F)\,\rangle \right\}$. $\hat{c}$ verifies that:

$$\hat{c}^{-\sigma} N = \phi N \nabla v(L_F) \iff \hat{c} = [\phi \nabla v(L_F)]^{-\frac{1}{\sigma}}.$$

Therefore:

$$\begin{aligned}
&\sup_c \left\{ \langle\, \frac{c^{1-\sigma}}{1-\sigma} N, \mathbb{1}\,\rangle \; - \langle\, \phi c N, \nabla v(L_F)\,\rangle \right\} = \langle\, \frac{\hat{c}^{1-\sigma}}{1-\sigma} N, \mathbb{1}\,\rangle \; - \langle\, \phi \hat{c} N, \nabla v(L_F)\,\rangle \\
&= \langle\, \frac{1}{1-\sigma} [\phi \nabla v(L_F)]^{-\frac{1}{\sigma}} N, \mathbb{1}\,\rangle \; - \langle\, \phi N [\phi \nabla v(L_F)]^{-\frac{1}{\sigma}}, \nabla v(L_F)\,\rangle \\
&= \frac{1}{1-\sigma} \langle\, [\phi \nabla v(L_F)]^{-\frac{1-\sigma}{\sigma}} N, \mathbb{1}\,\rangle \; - \langle\, [\phi \nabla v(L_F)]^{-\frac{1-\sigma}{\sigma}} N, \mathbb{1}\,\rangle \; = \frac{\sigma}{1-\sigma} \langle\, [\phi \nabla v(L_F)]^{-\frac{1-\sigma}{\sigma}} N, \mathbb{1}\,\rangle .
\end{aligned}$$

We look for a solution that can be written as:

$$v = \frac{\langle\, L_F, \alpha_0 e_0\,\rangle^{\,1-\sigma}}{1-\sigma}, \tag{11}$$

with $\alpha_0 \in \mathbb{R}$. Hence if v is defined by (11), then $\nabla v(L_F) = \langle L_F, \alpha_0 e_0 \rangle^{-\sigma} \alpha_0 e_0$. Plugging this solution in the HJB equation leads to the following equation in α_0:

$$\frac{\rho}{1-\sigma} \langle\ L_F, \alpha_0 e_0\ \rangle^{\ 1-\sigma} = \langle\ L_F, \langle L, \alpha_0 e_0 \rangle^{-\sigma} \mathcal{L} \alpha_0 e_0\ \rangle\ + \frac{\sigma}{1-\sigma} \langle L_F, \alpha_0 e_0\ \rangle^{\ 1-\sigma} \langle\ (\phi \alpha_0 e_0)^{-\frac{1-\sigma}{\sigma}} N, \mathbb{1}\ \rangle$$
$$= \lambda_0 \langle L_F, \alpha_0 e_0 \rangle^{1-\sigma} + \frac{\sigma}{1-\sigma} \langle L_F, \alpha_0 e_0\ \rangle^{\ 1-\sigma} \int_0^{2\pi} (\phi(\eta) \alpha_0 e_0(\eta))^{-\frac{1-\sigma}{\sigma}} N(\eta) d\eta.$$

Dividing by $\langle\ L_F, \alpha_0 e_0\ \rangle^{\ 1-\sigma}$:

$$\frac{\rho}{1-\sigma} = \lambda_0 + \frac{\sigma}{1-\sigma} \int_0^{2\pi} (\phi(\eta) \alpha_0 e_0(\eta))^{-\frac{1-\sigma}{\sigma}} N(\eta) d\eta$$

$$\iff \frac{\rho - \lambda_0(1-\sigma)}{\sigma} = \alpha_0^{-\frac{1-\sigma}{\sigma}} \int_0^{2\pi} (\phi(\eta) e_0(\eta))^{-\frac{1-\sigma}{\sigma}} N(\eta) d\eta.$$

Since by Assumption 2:

$$\rho - \lambda_0(1-\sigma) > 0,$$

then α_0 obtains as:

$$\alpha_0 = \left[\frac{\sigma}{\rho - \lambda_0(1-\sigma)} \int_0^{2\pi} (\phi(\eta) e_0(\eta))^{-\frac{1-\sigma}{\sigma}} N(\eta) d\eta \right]^{\frac{\sigma}{1-\sigma}}.$$

Moreover, we have that:

$$L_F' = \mathcal{L} L_F - (\phi N)^{\frac{\sigma-1}{\sigma}} N^{\frac{1}{\sigma}} (\alpha_0 e_0)^{-\frac{1}{\sigma}} \langle\ L_F, \alpha_0 e_0\ \rangle\ .$$

Thus $\forall \Phi \in \mathcal{D}(\mathcal{L})$:

$$\begin{aligned} \frac{d}{dt} \langle\ L_F, \Phi\ \rangle\ &= \langle\ \mathcal{L} L_F, \Phi\ \rangle\ - \langle\ L, \alpha_0 e_0\ \rangle\ \langle\ (\phi N)^{\frac{\sigma-1}{\sigma}} N^{\frac{1}{\sigma}} (\alpha_0 e_0)^{-\frac{1}{\sigma}}, \Phi\ \rangle \\ &= \langle\ L_F, \mathcal{L} \Phi\ \rangle\ - \langle\ L, \alpha_0 e_0\ \rangle\ \langle\ (\phi N)^{\frac{\sigma-1}{\sigma}} N^{\frac{1}{\sigma}} (\alpha_0 e_0)^{-\frac{1}{\sigma}}, \Phi\ \rangle\ . \end{aligned}$$

In particular, for $\Phi = \alpha_0 e_0$:

$$\begin{aligned} \frac{d}{dt} \langle\ L_F, \alpha_0 e_0\ \rangle\ &= \langle\ L_F, \lambda_0 \alpha_0 e_0\ \rangle\ - \langle\ L_F, \alpha_0 e_0\ \rangle\ \langle\ (\phi N)^{\frac{\sigma-1}{\sigma}} N^{\frac{1}{\sigma}} (\alpha_0 e_0)^{-\frac{1}{\sigma}}, \alpha_0 e_0\ \rangle \\ &= [\lambda_0 - \langle\ (\phi N)^{\frac{\sigma-1}{\sigma}} N^{\frac{1}{\sigma}} (\alpha_0 e_0)^{-\frac{1}{\sigma}}, \alpha_0 e_0\ \rangle\ ] \langle\ L_F, \alpha_0 e_0\ \rangle\ . \end{aligned}$$

Let g be $g := \lambda_0 - \langle\ (\phi N)^{\frac{\sigma-1}{\sigma}} N^{\frac{1}{\sigma}} (\alpha_0 e_0)^{-\frac{1}{\sigma}}, \alpha_0 e_0 \rangle$. Then we can write the expression above as:

$$\frac{d}{dt} \langle\ L_F, \alpha_0 e_0\ \rangle\ = g \langle\ L_F, \alpha_0 e_0\ \rangle.$$

which can be solved as:

$$\langle\ L_F, \alpha_0 e_0\ \rangle\ = \langle\ L_F^0, \alpha_0 e_0\ \rangle\ e^{gt}, \tag{12}$$

where L_F^0 is the initial distribution for fertile soil. Optimal consumption can be expressed as:

$$c^* = [\phi \nabla v(L_F)]^{-\frac{1}{\sigma}} = \phi^{-\frac{1}{\sigma}} [\langle\ L_F, \alpha_0 e_0\ \rangle\ ^{-\sigma} \alpha_0 e_0\ \rangle\ ]^{-\frac{1}{\sigma}} = \phi^{-\frac{1}{\sigma}} \langle\ L_F, \alpha_0 e_0\ \rangle\ (\alpha_0 e_0)^{-\frac{1}{\sigma}}.$$

Using (30) we obtain optimal consumption in terms of the initial distribution of fertile land, the model parameters and g:

$$c^* = \phi^{-\frac{1}{\sigma}} (\alpha_0 e_0)^{-\frac{1}{\sigma}} \langle\ L_F^0, \alpha_0 e_0\ \rangle\ e^{gt}.$$

Finally when we obtained the expression of α_0, it was shown that:

$$\frac{\rho - \lambda_0(1-\sigma)}{\sigma} = \int_0^{2\pi} (\phi(z) N(z) \alpha_0 e_0(z))^{-\frac{1-\sigma}{\sigma}} N(z)^{\frac{1}{\sigma}} dz.$$

Therefore, a simpler expression of g can be derived as:

$$g = \lambda_0 - \int_0^{2\pi} (\phi(z) N(z) \alpha_0 e_0(z))^{-\frac{1-\sigma}{\sigma}} N(z)^{\frac{1}{\sigma}} dz = \lambda_0 - \frac{\rho - \lambda_0(1-\sigma)}{\sigma} = \frac{\lambda_0 - \rho}{\sigma}.$$

With this explicit solution in hand, the next step is to prove that it actually verifies the set of necessary conditions in (I). We claim that:

$$c^*(t,\theta) = (\phi(\theta)\alpha_0 e_0(\theta))^{-\frac{1}{\sigma}} e^{gt} \int_0^{2\pi} L_F^0(z) \alpha_0 e_0(z) dz,$$

is the optimal solution in Phase 1. As said, let us prove next that actually this solution verifies the optimal necessary conditions (I). Since $\psi(t,\theta) = \frac{1}{\phi(\theta)} c(t,\theta)^{-\sigma}$, then:

$$\psi(t,\theta) = \alpha_0 e_0(\theta) e^{-\sigma g t} \left(\int_0^{2\pi} L_F^0(z) \alpha_0 e_0(z) dz \right)^{-\sigma}, \tag{13}$$

and its partial derivatives are:

$$\begin{aligned}
&\psi_t(t,\theta) = -\sigma g \psi(t,\theta), \\
&\psi_x(t,\theta) = \alpha_0 e_0'(\theta) e^{-\sigma g t} \left(\textstyle\int_0^{2\pi} L_F^0(z) \alpha_0 e_0(z) dz \right)^{-\sigma}, \\
&\psi_{xx}(t,\theta) = \alpha_0 e_0''(\theta) e^{-\sigma g t} \left(\textstyle\int_0^{2\pi} L_F^0(z) \alpha_0 e_0(z) dz \right)^{-\sigma}.
\end{aligned}$$

Substituting into:

$$\psi_t(t,\theta) + \mathcal{L}\psi(t,\theta) - \rho\psi(t,\theta) + \mu(t,\theta) = 0,$$

checking that $\mathcal{L}\psi(t,\theta) = \lambda_0\psi(t,\theta)$, and letting $\mu(t,\theta) \equiv 0$, we do obtain that the solution in (34) satisfies the optimality condition whenever $g = \frac{\lambda_0 - \rho}{\sigma}$.

Finally, once we have proven that both solutions coincide, we close this proof showing that aggregated land grows at rate g. Since $\langle\, L_F, \alpha_0 e_0 \,\rangle = \langle\, L_F^0, \alpha_0 e_0 \,\rangle\, e^{gt}$ then:

$$\int_0^{2\pi} L_F(t,\theta)e_0(\theta)d\theta = \int_0^{2\pi} L_F^0(\theta)e_0(\theta)e^{gt}d\theta \iff \int_0^{2\pi} \left[L_F(t,\theta) - L_F^0(\theta)e^{gt}\right] e_0(\theta)d\theta = 0.$$

Defining $\underline{e_0} := \min_{[0,2\pi]} e_0(\theta)$ and $\bar{e_0} := \max_{[0,2\pi]} e_0(\theta)$, the following inequalities obtain:

$$\underline{e_0} \int_0^{2\pi} \left(L_F(t,\theta) - L_F^0(\theta)e^{gt}\right) d\theta \leq \int_0^{2\pi} \left(L_F(t,\theta) - L_F^0(\theta)e^{gt}\right) e_0(\theta)d\theta = 0, \tag{14}$$

and:

$$\bar{e_0} \int_0^{2\pi} \left(L_F(t,\theta) - L_F^0(\theta)e^{gt}\right) d\theta \geq \int_0^{2\pi} \left(L_F(t,\theta) - L_F^0(\theta)e^{gt}\right) e_0(\theta)d\theta = 0. \tag{15}$$

Hence, since $e_0(\theta) > 0\ \forall\theta \in [0, 2\pi]$, then (14) and (15) imply that $\bar{e_0} > 0$ and $\underline{e_0} > 0$. As a result, (14) and (15) imply that:

$$\int_0^{2\pi} \left(L_F(t,\theta) - L_F^0(\theta)e^{gt}\right) d\theta \leq 0, \text{ and } \int_0^{2\pi} \left(L_F(t,\theta) - L_F^0(\theta)e^{gt}\right) d\theta \geq 0,$$

which implies that $\int_0^{2\pi} \left(L_F(t,\theta) - L_F^0(\theta)e^{gt}\right) d\theta = 0$. Dividing by the length of the interval, the result in terms of mean values obtains: $\langle L_F(t)\rangle = e^{gt}\langle L_F^0\rangle$.

D. Proof of Proposition 2. The homogeneous and diffusive economy.

We decompose fertile soil on the eigenvector basis as:

$$L_F = \sum_{n\geq 0} \langle L_F, e_n\rangle e_n(\theta) \tag{16}$$

and look for the expression of the coefficients $\langle L_F, e_n\rangle$ for $n \geq 0$.

Recall that A, ϕ and $\nu, N \in \mathbb{R}$. Thus, the eigenvalue problem can be written as the following second order linear ordinary differential equation with constant coefficients:

$$u'' + \frac{A(\phi - \nu) - \lambda}{D} u = 0. \tag{17}$$

Any function $u(\theta) = C_1 \cos\left(\theta\sqrt{\frac{A(\phi-\nu)-\lambda}{D}} + C_2\right)$, whith $(C_1, C_2) \in \mathbb{R}^2$ is a solution to (17). Note that since our problem is 2π periodic, solutions obvioulsy need to verify $u(0) = u(2\pi)$. Imposing this boundary condition, we obtain that:

$$\cos(C_2) = \cos\left(2\pi\sqrt{\frac{A(\phi-\nu)-\lambda}{D}} + C_2\right),$$

which holds if and only if:

$$2\pi\sqrt{\frac{A(\phi-\nu)-\lambda_n}{D}} + C_2 = C_2 + 2n\pi, \text{ with } n \in \mathbb{Z} \implies \sqrt{\frac{A(\phi-\nu)-\lambda_n}{D}} = n.$$

Therefore, the n^{th} eigenvalue of the problem and the associated n^{th} eigenvector are:

$$\lambda_n = A(\phi-\nu) - Dn^2, \tag{18}$$

and:

$$\begin{aligned} e_n(\theta) &= C_1 \cos\left(\theta\sqrt{\frac{A(\phi-\nu)-\lambda_n}{D}} + C_2\right) = C_1 \cos\left(\theta\sqrt{\frac{A(\phi-\nu)-A(\phi-\nu)+Dn^2}{D}} + C_2\right) \\ &= C_1 \cos(\theta n + C_2). \end{aligned} \tag{19}$$

Here we need to analyze separatedly the cases $n = 0$ and $n > 0$:

1. When $n = 0$, we have that $\lambda_0 = A(\phi-\nu)$. As a result:

$$g = \frac{\lambda_0 - \rho}{\sigma} = \frac{A(\phi-\nu)-\rho}{\sigma}.$$

From (19), $e_0(\theta) = e_0 = C_1\cos(C_2)$ is spatially homogeneous. As a result, $\langle L_F, e_0\rangle e_0$ can be written as:

$$\langle L_F, e_0\rangle e_0 = \langle L_F^0, e_0\rangle e_0 e^{gt} = e_0^2 \int_0^{2\pi} L_F^0(\theta)d\theta\ e^{gt}.$$

Since eigenvectors form an orthonormal basis, we have that in particular $\int_0^{2\pi} e_0^2 d\theta = 1$, which implies that $e_0^2 = \frac{1}{2\pi}$. As a result, we can write:

$$\langle L_F, e_0\rangle e_0 = \langle L_F^0, e_0\rangle e_0 e^{gt} = \langle L_F^0\rangle e^{gt}.$$

2. For $n \geq 1$, since the dynamics of fertile soil writes:

$$L_F' = \mathcal{L}L_F - (\phi N)^{\frac{\sigma-1}{\sigma}} N^{\frac{1}{\sigma}} (\alpha_0 e_0)^{-\frac{1}{\sigma}} \langle\ L_F, \alpha_0 e_0\ \rangle,$$

and $\langle L_F, e_0\rangle = \langle L_F^0, e_0\rangle e^{gt}$, then:

$$\begin{aligned}\frac{d}{dt}\langle\ L_F, e_n\ \rangle &= \langle\ \mathcal{L}L_F, e_n\ \rangle - \langle\ L_F, \alpha_0 e_0\ \rangle\ \langle\ (\phi N)^{\frac{\sigma-1}{\sigma}} N^{\frac{1}{\sigma}} (\alpha_0 e_0)^{-\frac{1}{\sigma}}, e_n\ \rangle \\ &= \langle\ L_F, \mathcal{L}e_n\ \rangle - \langle\ L_F, \alpha_0 e_0\ \rangle \beta_n = \lambda_n \langle\ L_F, e_n\ \rangle - \langle\ L_F^0, \alpha_0 e_0\ \rangle\ e^{gt}\beta_n\end{aligned}$$

with $\beta_n = \langle\ (\phi N)^{\frac{\sigma-1}{\sigma}} N^{\frac{1}{\sigma}} (\alpha_0 e_0)^{-\frac{1}{\sigma}}, e_n\ \rangle$. As ϕ, N, and e_0 are spatially homogeneous:

$$\begin{aligned}\beta_n &= (\phi N)^{\frac{\sigma-1}{\sigma}} N^{\frac{1}{\sigma}} (\alpha_0 e_0)^{-\frac{1}{\sigma}} \int_0^{2\pi} e_n(\theta) d\theta = (\phi N)^{\frac{\sigma-1}{\sigma}} N^{\frac{1}{\sigma}} (\alpha_0 e_0)^{-\frac{1}{\sigma}} \int_0^{2\pi} C_1 \cos(\theta n + C_2)\, d\theta \\ &= (\phi N)^{\frac{\sigma-1}{\sigma}} N^{\frac{1}{\sigma}} (\alpha_0 e_0)^{-\frac{1}{\sigma}} \left[\frac{C_1}{n} \sin(\theta n + C_2)\right]_0^{2\pi} = 0.\end{aligned}$$

Therefore:

$$\frac{d}{dt}\langle\ L_F, e_n\ \rangle = \lambda_n \langle\ L_F, e_n\ \rangle,$$

and:

$$\langle L_F, e_n\rangle = \langle L_F^0, e_n\rangle e^{\lambda_n t}.$$

Substituting $\langle\ L_F, e_0\ \rangle\ e_0$ and $\langle\ L_F, e_n\ \rangle\ e_n$ into (16), L_F can be written as $L_F(t,\theta) = \langle L_F^0\rangle e^{gt} + \sum_{n\geq 1} \langle L_F^0, e_n\rangle e_n e^{\lambda_n t}$, which proves our claim.

E. Proof of Proposition 3. Consumption transfers.

This proof is structured in three steps. First, we obtain the optimal solution for the policy maker problem in the un-connected economy. Second, we do the same for the diffusive economy. In the third step, we use the previous results to compute consumption transfers.

1. We obtain optimal consumption $c_A(t)$ in the unconnected economy. Here, the social planner solves the following problem for each location:

$$\max_{c_A(t)} \int_0^\infty \frac{c_A^{1-\sigma}(t,\theta)}{1-\sigma} N e^{-\rho t} dt \tag{20}$$

subject to:

$$\begin{cases} \dot{L}_F(t,\theta) = A(\phi - \nu) L_F(t,\theta) - \Phi N c_A(t,\theta), \\ L_F(0,\theta) = L_F^0(\theta) \geq 0 \end{cases} \tag{21}$$

for all $t > 0$ and $\theta \in S^1$, with $N, A, \phi, \nu, \Phi \in \mathbb{R}$. The easiest way to solve problem (20)-(21) is to define the associated Hamiltonian and to obtain a set of Pontryagin conditions. The Hamiltonian associated to (20)-(21) writes as $\mathcal{H}(c_a, L_F, \lambda, t) = \frac{c_A^{1-\sigma}}{1-\sigma} N e^{-\rho t} + \lambda[A(\phi - \nu)L_F - \Phi N c_A]$. Taking the first order conditions of $\mathcal{H}$ with respect to c_A and L_F, we obtain:

$$\begin{cases} \frac{\partial \mathcal{H}}{\partial c_A} = 0 \implies c_A^{-\sigma} N e^{-\rho t} = \lambda \phi N. \\ \frac{\partial \mathcal{H}}{\partial L_F} = -\dot{\lambda} \implies -\dot{\lambda} = \lambda A(\phi - \nu), \end{cases}$$

plus the transversality condition $\lim_{t\to\infty} L_F(t,\theta)\lambda(t) = 0$. Let us define $\tilde{\lambda} = \lambda e^{\rho t}$. Then we can express the dynamics of the co-state variable as $\dot{\tilde{\lambda}} = -\tilde{\lambda}\,(A(\phi - \nu) - rho)$. Since $\tilde{\lambda} = \frac{c_A^{-\sigma}}{\phi}$, then $\dot{\tilde{\lambda}} = -\frac{\sigma c_A^{-\sigma-1}\dot{c_A}}{\phi}$ and $\frac{\dot{\tilde{\lambda}}}{\tilde{\lambda}} = -\sigma \frac{\dot{c_A}}{c_A}$.

Let us define g_A as $c_A's$ growth rate, i.e. $g_A := \frac{\dot{c_A}}{c_A}$, and as a result:

$$g_A = \frac{A(\phi - \nu) - \rho}{\sigma},$$

and $c_A(t,\theta) = c_A(0,\theta)e^{gt}$. Note that $g_A = g$, which proves that location's consumption in the unconnected and the diffusive economy grow at the same rate. Hereafter we will write g.

Finally, note that:

$$\dot{L}_F(t,\theta) = A(\phi - \nu)L_F(t,\theta) - \phi N c_A(t,\theta) \iff \frac{\dot{L}_F(t,\theta)}{L_F(t,\theta)} = A(\phi - \nu) - \phi N \frac{c_A(t,\theta)}{L_F(t,\theta)}.$$

Hence $\frac{\dot{L}_F(t,\theta)}{L_F(t,\theta)} = g$ along the balanced growth path, and as a result $L_F(t,\theta) = L_F(0,\theta)e^{gt} = L_F^0(\theta)e^{gt}$, and:

$$c_A(t,\theta) = \frac{A}{N\sigma\phi}\left[\frac{\rho}{A} + (\phi - \nu)(\sigma - 1)\right] L_F(t,\theta) = \frac{A}{N\sigma\phi}\left[\frac{\rho}{A} + (\phi - \nu)(\sigma - 1)\right] L_F^0(\theta)e^{gt}.$$

2. Proposition 1 provided us with the trajectory for optimal consumption in the diffusive economy, c_D:

$$c_D(t,\theta) = e^{gt}(\phi\alpha_0 e_0(\theta))^{-\frac{1}{\sigma}} \int_0^{2\pi} L_F^0(\eta)\alpha_0 e_0(\eta)d\eta,$$

with:

$$\alpha_0 = \left[\frac{\sigma}{\rho - A(\phi - \nu)(1 - \sigma)} \int_0^{2\pi} N(\phi e_0(\eta))^{-\frac{1-\sigma}{\sigma}} d\eta\right]^{\frac{\sigma}{1-\sigma}}$$

and where $e_0(\cdot)$ the first eigenvector of the problem $\mathcal{L}u = \lambda u$. In Appendix D we proved that

e_0 is spatially homogeneous, so that:

$$\begin{aligned}\alpha_0 e_0 &= \left[\frac{\sigma}{\rho - A(\phi-\nu)(1-\sigma)}\int_0^{2\pi} N(\phi e_0)^{-\frac{1-\sigma}{\sigma}} d\eta\right]^{\frac{\sigma}{1-\sigma}} e_0 \\ &= \left[\frac{2\pi\sigma N(\phi e_0)^{-\frac{1-\sigma}{\sigma}}}{\rho - A(\phi-\nu)(1-\sigma)}\right]^{\frac{\sigma}{1-\sigma}} e_0 = \frac{1}{\phi}\left[\frac{2\pi\sigma N}{\rho - A(\phi-\nu)(1-\sigma)}\right]^{\frac{\sigma}{1-\sigma}}.\end{aligned}$$

Therefore, we can prove that c_D is homogeneous in space and obtain the following expression:

$$\begin{aligned}c_D(t,\theta) &= e^{gt}(\phi\alpha_0 e_0)^{-\frac{1}{\sigma}}\int_0^{2\pi} L_F^0(\eta)\alpha_0 e_0 d\eta \\ &= e^{gt}\left[\frac{2\pi\sigma N}{\rho - A(\phi-\nu)(1-\sigma)}\right]^{\frac{1}{\sigma-1}}\frac{1}{\phi}\left[\frac{2\pi\sigma N}{\rho - A(\phi-\nu)(1-\sigma)}\right]^{\frac{\sigma}{1-\sigma}}\int_0^{2\pi} L_F^0(\eta)d\eta \\ &= e^{gt}\frac{\rho - A(\phi-\nu)(1-\sigma)}{2\pi\sigma N\phi}\int_0^{2\pi} L_F^0(\eta)d\eta = \frac{\rho - A(\phi-\nu)(1-\sigma)}{N\sigma\phi}\langle L_F^0\rangle e^{gt}.\end{aligned}$$

3. Finally, let us compute consumption transfers. Using our previous results, $\tau(t,\theta)$ obtains:

$$\begin{aligned}\tau(t,\theta) &= c_A(t,\theta) - c_D(t,\theta) = \frac{\rho + A(\phi-\nu)(\sigma-1)}{N\sigma\phi}L_F^0(\theta)e^{gt} - \frac{\rho + A(\phi-\nu)(\sigma-1)}{N\sigma\phi}\langle L_F^0\rangle e^{gt} \\ &= \frac{\rho + A(\phi-\nu)(\sigma-1)}{N\sigma\phi}\left[L_F^0(\theta) - \langle L_F^0\rangle\right]e^{gt}.\end{aligned}$$

F. Proof of Proposition 4. Optimal solution in Phase 2.

In order to obtain the optimal trajectories in $\underline{S}(t)$, we need to start by defining the interior product in $\underline{S}(t)$. For any two functions f, g in $\mathcal{H}^2(\underline{\mathcal{S}}(t))$, we define their interior product as:

$$\langle\ f, g\ \rangle_{\underline{S}} = \int_{\theta_1(t)}^{\theta_2(t)} f(z)g(z)dz.$$

In Phase 2, the HJB equation is:

$$\rho v(L_F) = \langle\ L_F, \mathcal{L}\nabla v(L_F)\ \rangle_{\underline{S}} + \sup_c\left\{\langle\ \frac{c^{1-\sigma}}{1-\sigma}N, \mathbb{1}\ \rangle_{\underline{S}} - \langle\ \phi cN, \nabla v(L_F)\ \rangle_{\underline{S}}\right\}.$$

Let $\hat{c} := \text{argmax}\left\{\langle\ \frac{c^{1-\sigma}}{1-\sigma}N, \mathbb{1}\ \rangle_{\underline{S}} - \langle\ \phi cN, \nabla v(L_F)\ \rangle_{\underline{S}}\right\}$. As in Appendix C, $\hat{c}$ verifies that $\hat{c} = [\phi\nabla v(L_F)]^{-\frac{1}{\sigma}}$.

As in Phase 1, we also look in Phase 2 for a solution that can be written as $v = \frac{\langle\ L_F, \beta_0 e_0\ \rangle_{\underline{S}}^{1-\sigma}}{1-\sigma}$, where β_0 is this time a continuous function of time. e_0 is the first eigen-

vector associated to eigenvalue λ_0 of the eigenvalue problem: $\mathcal{L}u = \lambda u$ on S. Note that we are borrowing the first eigenvector and eigenvalue from the problem on S and not restricting the eigenvalue problem to $\underline{S}$.

Operator $\mathcal{L}$ is self-adjoint on $\underline{S}$ only under certain assumptions. Indeed:

$$\begin{aligned}\langle\, \mathcal{L}L_F, \nabla v(L_F)\,\rangle_{\underline{S}} &= \int_{\theta_1(t)}^{\theta_2(t)} \mathcal{L}L_F(z)\nabla v(L_F)(z)dz \\ &= \nabla_\theta L_F(z)\nabla v(L_F)\,|_{\theta_1(t)}^{\theta_2(t)} - \int_{\theta_1(t)}^{\theta_2(t)} \nabla_\theta L_F(z)\nabla_\theta(\nabla v(L_F)(z))dz \\ &= \nabla_\theta L_F(z)\nabla v(L_F)\,|_{\theta_1(t)}^{\theta_2(t)} - L_F(z)\nabla_\theta(\nabla v(L_F))\,|_{\theta_1(t)}^{\theta_2(t)} + \int_{\theta_1(t)}^{\theta_2(t)} L_F(z)\mathcal{L}\nabla v(L_F)(z)dz.\end{aligned}$$

Hence:

$$\langle\, \mathcal{L}L_F, \nabla v(L_F)\,\rangle_{\underline{S}} = \langle\, L_F, \mathcal{L}(\nabla v(L_F))\,\rangle_{\underline{S}} + \nabla_\theta L_F(z)\nabla v(L_F)\,|_{\theta_1(t)}^{\theta_2(t)} - L_F(z)\nabla_\theta(\nabla v(L_F))\,|_{\theta_1(t)}^{\theta_2(t)},$$

and our operator is self-adjoint if and only if:

$$\nabla_\theta L_F(z)\nabla v(L_F)\,|_{\theta_1(t)}^{\theta_2(t)} = L_F(z)\nabla_\theta(\nabla v(L_F))\,|_{\theta_1(t)}^{\theta_2(t)}\,. \tag{22}$$

Note that (22) coincides with (10), implying that operator $\mathcal{L}$ is self-adjoint in the subset of optimal solutions.

Proceeding like in Appendix C, we substitute $\hat{c}$ into the HJB equation and impose that the solutions must be optimal, that is, that they verify (22):

$$\begin{aligned}&\frac{\rho}{1-\sigma}\langle\, L_F, \beta_0 e_0\,\rangle_{\underline{S}}^{1-\sigma} = \langle\, L_F, \langle L, \beta_0 e_0\rangle^{-\sigma}\mathcal{L}\beta_0 e_0\,\rangle_{\underline{S}} + \frac{\sigma}{1-\sigma}\langle L_F, \beta_0 e_0\,\rangle_{\underline{S}}^{1-\sigma}\langle\, (\phi\beta_0 e_0)^{-\frac{1-\sigma}{\sigma}}N, \mathbb{1}\,\rangle_{\underline{S}} \\ &= \lambda_0\langle L_F, \beta_0 e_0\rangle^{1-\sigma} + \frac{\sigma}{1-\sigma}\langle L_F, \beta_0 e_0\,\rangle_{\underline{S}}^{1-\sigma}\int_{\underline{S}}(\phi(\eta)\beta_0 e_0(\eta))^{-\frac{1-\sigma}{\sigma}}N(\eta)d\eta.\end{aligned}$$

Hence, dividing on both sides by $\langle\, L_F, \beta_0 e_0\,\rangle_{\underline{S}}^{1-\sigma}$:

$$\frac{\rho}{1-\sigma} = \lambda_0 + \frac{\sigma}{1-\sigma}\int_{\underline{S}}(\phi(\eta)\beta_0 e_0(\eta))^{-\frac{1-\sigma}{\sigma}}N(\eta)d\eta$$

$$\iff \frac{\rho - \lambda_0(1-\sigma)}{\sigma} = \beta_0^{-\frac{1-\sigma}{\sigma}}\int_{\underline{S}}(\phi(\eta)e_0(\eta))^{-\frac{1-\sigma}{\sigma}}N(\eta)d\eta.$$

By Assumption 2, $\rho - \lambda_0(1-\sigma) > 0$, so that:

$$\beta_0^{\frac{1-\sigma}{\sigma}} = \frac{\sigma}{\rho - \lambda_0(1-\sigma)}\int_{\underline{S}}(\phi(z)e_0(z))^{-\frac{1-\sigma}{\sigma}}N(z)dz = \frac{\sigma}{\rho - \lambda_0(1-\sigma)} < (\phi(z)e_0(z))^{-\frac{1-\sigma}{\sigma}}N(z), \mathbb{1} >_{\underline{S}}\,. \tag{23}$$

As a result, we can write $\hat{c}$ as:

$$\hat{c} = [\phi \nabla v(L_F)]^{-\frac{1}{\sigma}} = (\phi \beta_0 e_0)^{-\frac{1}{\sigma}} < L_F, \beta_0 e_0 >_{\underline{S}} . \tag{24}$$

Taking the logarithm of (23) and derivating, we obtain β_0's growth rate:

$$\begin{aligned} \frac{1-\sigma}{\sigma} \frac{\beta_{0,t}(t)}{\beta_0(t)} &= \frac{d}{dt} \ln \int_{\underline{S}} (\phi(z) e_0(z))^{-\frac{1-\sigma}{\sigma}} N(z) dz \\ &= \frac{N(\theta_2(t))[\phi(\theta_2(t)) e_0(\theta_2(t))]^{-\frac{1-\sigma}{\sigma}} \dot{\theta}_2(t) - N(\theta_1(t))[\phi(\theta_1(t)) e_0(\theta_1(t))]^{-\frac{1-\sigma}{\sigma}} \dot{\theta}_1(t)}{\int_{\underline{S}} (\phi(z) e_0(z))^{-\frac{1-\sigma}{\sigma}} N(z) dz}. \end{aligned} \tag{25}$$

Replacing $\hat{c}$ in the original state equation for L_F, we obtain that:

$$L'_F = \mathcal{L} L_F - \phi N \, (\phi \beta_0 e_0)^{-\frac{1}{\sigma}} \langle \, L_F, \beta_0 e_0 \, \rangle_{\underline{S}}. \tag{26}$$

Let us multiply (26) by $\beta_0 e_0$, and compute the interior product restricting our analysis to optimal solutions that verify (22):

$$\begin{aligned} \langle \, \frac{d}{dt} L_F, \beta_0 e_0 \, \rangle_{\underline{S}} &= \langle \, \mathcal{L} L_F, \beta_0 e_0 \, \rangle_{\underline{S}} - \langle \, (\phi N)^{\frac{\sigma-1}{\sigma}} N^{\frac{1}{\sigma}} (\beta_0 e_0)^{-\frac{1}{\sigma}}, \beta_0 e_0 \, \rangle_{\underline{S}} \langle \, L_F, \beta_0 e_0 \, \rangle_{\underline{S}} \\ &= \langle \, L_F, \beta_0 \mathcal{L} e_0 \, \rangle_{\underline{S}} - \langle \, (\phi N \beta_0 e_0)^{\frac{-(1-\sigma)}{\sigma}} N^{\frac{1}{\sigma}}, \mathbb{1} \, \rangle_{\underline{S}} \langle \, L_F, \beta_0 e_0 \, \rangle_{\underline{S}} \\ &= \lambda_0 \langle \, L_F, \beta_0 e_0 \, \rangle_{\underline{S}} - \langle \, (\phi N \beta_0 e_0)^{\frac{-(1-\sigma)}{\sigma}} N^{\frac{1}{\sigma}}, \mathbb{1} \, \rangle_{\underline{S}} \langle \, L_F, \beta_0 e_0 \, \rangle_{\underline{S}}. \end{aligned}$$

Note that we cannot solve the problem unless we transform $\langle \, \frac{d}{dt} L_F, \beta_0 e_0 \, \rangle_{\underline{S}}$. Indeed, when the interior product changes with time, it is not straightforward to proceed as in Appendix C. Note that:

$$\begin{aligned} \frac{d}{dt} \langle \, L_F, \beta_0 e_0 \, \rangle_{\underline{S}} &= \frac{d}{dt} \int_{\theta_1(t)}^{\theta_2(t)} L_F \beta_0 e_0 dz \\ &= \int_{\theta_1(t)}^{\theta_2(t)} \frac{d}{dt} L_F \beta_0 e_0 dz + \int_{\theta_1(t)}^{\theta_2(t)} L_F \frac{d}{dt} \beta_0 e_0 dz + L_F(\theta_2(t)) \beta_0(t) e_0(\theta_2(t)) \dot{\theta}_2(t) \\ &- L_F(\theta_1(t)) \beta_0(t) e_0(\theta_1(t)) \dot{\theta}_1(t) \\ &= \langle \, \frac{d}{dt} L_F, \beta_0 e_0 \, \rangle_{\underline{S}} + \langle \, L_F, \beta_{0,t} e_0 \, \rangle_{\underline{S}} + L_F(\theta_2(t)) \beta_0(t) e_0(\theta_2(t)) \dot{\theta}_2(t) \\ &- L_F(\theta_1(t)) \beta_0(t) e_0(\theta_1(t)) \dot{\theta}_1(t). \end{aligned}$$

We finally obtain that:

$$\begin{aligned}\langle\ \frac{d}{dt}L_F, \beta_0 e_0\ \rangle_{\underline{S}} = \frac{d}{dt}\langle\ L_F, \beta_0 e_0\ \rangle_{\underline{S}} - \frac{\beta_{0,t}}{\beta_0}\langle\ L_F, \beta_0 e_0\ \rangle_{\underline{S}} \\ - L_F(\theta_2(t))\beta_0(t)e_0(\theta_2(t))\dot{\theta}_2(t) + L_F(\theta_1(t))\beta_0(t)e_0(\theta_1(t))\dot{\theta}_1(t).\end{aligned} \tag{27}$$

Replacing (22) and (27) into (26):

$$\begin{aligned}\frac{d}{dt}\langle\ L_F, \beta_0 e_0\ \rangle_{\underline{S}} = \left[\lambda_0 - \langle\ (\phi N)^{\frac{\sigma-1}{\sigma}} N^{\frac{1}{\sigma}} (\beta_0 e_0)^{-\frac{1}{\sigma}}, \beta_0 e_0\ \rangle_{\underline{S}} + \frac{\beta_{0,t}}{\beta_0}\right]\langle\ L_F, \beta_0 e_0\ \rangle_{\underline{S}} \\ + L_F(\theta_2(t))\beta_0(t)e_0(\theta_2(t))\dot{\theta}_2(t) - L_F(\theta_1(t))\beta_0(t)e_0(\theta_1(t))\dot{\theta}_1(t).\end{aligned} \tag{28}$$

Using (23), and removing the time variable for simplicity:

$$\frac{d}{dt}\langle\ L_F, \beta_0 e_0\ \rangle_{\underline{S}} = \left[\frac{\lambda_0 - \rho}{\sigma} + \frac{\beta_{0,t}}{\beta_0}\right]\langle\ L_F, \beta_0 e_0\ \rangle_{\underline{S}} + \beta_0\left(L_F(\theta_2)e_0(\theta_2)\dot{\theta}_2 - L_F(\theta_1)e_0(\theta_1)\dot{\theta}_1\right). \tag{29}$$

We can solve (29) in two stages:

1. First, we solve the homogeneous equation:

$$\begin{aligned}\langle\ L_F, \beta_0 e_0\ \rangle_{\underline{S}} &= \langle\ L_F, \beta_0 e_0\ \rangle_{\underline{S}(\tau)} e^{\int_\tau^t \left(\frac{\lambda_0-\rho}{\sigma} + \frac{\beta_{0,t}}{\beta_0}\right)ds} \\ &= \langle\ L_F(\tau), \beta_0(\tau)e_0\ \rangle e^{\frac{\lambda_0-\rho}{\sigma}(t-\tau)} e^{\int_\tau^t \frac{\beta_{0,t}}{\beta_0}ds} = \langle\ L_F(\tau), \beta_0(\tau)e_0\ \rangle e^{\frac{\lambda_0-\rho}{\sigma}(t-\tau)} e^{\ln\beta_0|_\tau^t} \\ &= \langle\ L_F(\tau), \beta_0(\tau)e_0\ \rangle e^{\frac{\lambda_0-\rho}{\sigma}(t-\tau)} e^{\ln\beta_0|_\tau^t} = \langle\ L_F(\tau), \beta_0(\tau)e_0\ \rangle e^{\frac{\lambda_0-\rho}{\sigma}(t-\tau)} \frac{\beta_0(t)}{\beta_0(\tau)} \\ &= \langle\ L_F(\tau), \alpha_0 e_0\ \rangle\ e^{\frac{\lambda_0-\rho}{\sigma}(t-\tau)} \frac{\beta_0(t)}{\alpha_0}\end{aligned} \tag{30}$$

where $L_F(\tau)$ is the distribution of fertile soil at the time the second phase is triggered and $\underline{S}(\tau) = \mathcal{S}$. By continuity, it is also true that $\beta_0(\tau) = \alpha_0$.

2. Then we solve the non-homogeneous equation trying a solution of the type:

$$\langle\ L_F, \beta_0 e_0\ \rangle_{\underline{S}} = m(t)e^{\frac{\lambda_0-\rho}{\sigma}t}\beta_0(t) \tag{31}$$

whose time derivative is:

$$\begin{aligned}\frac{d}{dt}\langle\ L_F, \beta_0 e_0\ \rangle_{\underline{S}} &= \dot{m}(t)e^{\frac{\lambda_0-\rho}{\sigma}t}\beta_0 + m(t)\frac{\lambda_0-\rho}{\sigma}e^{\frac{\lambda_0-\rho}{\sigma}t}\beta_0 + m(t)e^{\frac{\lambda_0-\rho}{\sigma}t}\beta_{0,t}(t) \\ &= e^{\frac{\lambda_0-\rho}{\sigma}t}\beta_0\left[\dot{m}(t) + m(t)\left(\frac{\lambda_0-\rho}{\sigma} + \frac{\beta_{0,t}(t)}{\beta_0(t)}\right)\right].\end{aligned} \tag{32}$$

If (31) is a solution, then it has to verify (29). Replacing $\langle\ L_F, \beta_0 e_0\ \rangle_{\underline{S}}$ by (31) and $\frac{d}{dt}\langle\ L_F, \beta_0 e_0\ \rangle_{\underline{S}}$ using (32), we get that:

$$\dot{m}(t) = e^{-\frac{\lambda_0-\rho}{\sigma}t}\left(L_F(\theta_2)e_0(\theta_2)\dot{\theta}_2 - L_F(\theta_1)e_0(\theta_1)\dot{\theta}_1\right),$$

that is:

$$m(t) = \int_\tau^t e^{-\frac{\lambda_0-\rho}{\sigma}s}\left(L_F(\theta_2(s))e_0(\theta_2(s))\dot{\theta}_2(s) - L_F(\theta_1(s))e_0(\theta_1(s))\dot{\theta}_1(s)\right)ds.$$

Plugging m back into (31), and taking into account that $\langle\ L_F, \beta_0 e_0\ \rangle_{\underline{S}(\tau)} = \langle\ L_F(\tau), \alpha_0 e_0\ \rangle$, we obtain that the solution for $\langle\ L_F, \beta_0 e_0\ \rangle_{\underline{S}}$ is:

$$\begin{aligned}\langle\ L_F, \beta_0 e_0\ \rangle_{\underline{S}} = {} & \frac{\beta_0(t)}{\alpha_0}\langle\ L_F(\tau), \alpha_0 e_0\ \rangle\ e^{\frac{\lambda_0-\rho}{\sigma}(t-\tau)} \\ & + e^{\frac{\lambda_0-\rho}{\sigma}t}\beta_0(t)\int_\tau^t e^{-\frac{\lambda_0-\rho}{\sigma}s}\left(L_F(\theta_2(s))e_0(\theta_2(s))\dot{\theta}_2(s) - L_F(\theta_1(s))e_0(\theta_1(s))\dot{\theta}_1(s)\right)ds,\end{aligned}$$

or:

$$\begin{aligned}\langle\ L_F, \beta_0 e_0\ \rangle_{\underline{S}} = {} & \beta_0(t)\langle\ L_F(\tau), e_0\ \rangle\ e^{\frac{\lambda_0-\rho}{\sigma}(t-\tau)} \\ & + \beta_0(t)\int_\tau^t e^{\frac{\lambda_0-\rho}{\sigma}(t-s)}\left(L_F(\theta_2(s))e_0(\theta_2(s))\dot{\theta}_2(s) - L_F(\theta_1(s))e_0(\theta_1(s))\dot{\theta}_1(s)\right)ds.\end{aligned}$$

With this solution for $\langle\ L_F, \beta_0 e_0\ \rangle_{\underline{S}}$, we can obtain the optimal solution for consumption:

$$c^* = [\phi\nabla v(L_F)]^{-\frac{1}{\sigma}} = \phi^{-\frac{1}{\sigma}}[\langle\ L_F, \beta_0 e_0\ \rangle_{\underline{S}}^{-\sigma}\beta_0 e_0]^{-\frac{1}{\sigma}} = (\phi\beta_0 e_0)^{-\frac{1}{\sigma}}\langle\ L_F, \beta_0 e_0\ \rangle_{\underline{S}}. \tag{33}$$

Note that c^* is the optimal solution of our problem on $\underline{S}$ but the dynamic programming technique does not allow us to introduce the border conditions, $\dot{\theta}_1$ and $\dot{\theta}_2$. For this reason, we will mix here as in Appendix C dynamic programming and optimal control.

Let us prove next that c^* can be the optimal solution in Phase 2 under certain conditions, i.e. that c^* verifies the optimal necessary conditions (II). According to (II), optimal consumption in Phase 2 needs to be equal to $(\phi\lambda)^{-1/\sigma}$.[14] On the other hand, the candidate we have just obtained is $c^* = (\phi\nabla v(L_F))^{-1/\sigma}$. Hence, to prove that c^* is the optimal solution for consumption, it remains to prove that $\lambda = \nabla v(L_F)$.

Since $\lambda(t,\theta) = \frac{1}{\phi(\theta)}c(t,\theta)^{-\sigma}$, then substituting c^* using (33), we have that:

$$\lambda(t,\theta) = \beta_0 e_0\langle\ L_F, \beta_0 e_0\ \rangle_{\underline{S}}^{-\sigma}. \tag{34}$$

[14] With an abuse of notation, let us denote by λ the co-state variable associated to L_F also in Phase 2. Since both phases cannot co-exist, there will not be any conflict.

From (34), the partial derivative of λ with respect to t is:

$$\lambda_t(t,\theta) = -\sigma\beta_0 e_0\langle\ L_F, \beta_0 e_0\ \rangle_{\underline{S}}^{-\sigma-1}\frac{d}{dt}\langle\ L_F, \beta_0 e_0\ \rangle_{\underline{S}} + \beta_{0,t}e_0\langle\ L_F, \beta_0 e_0\ \rangle_{\underline{S}}^{-\sigma}.$$

Note that we also know that $\mathcal{L}\lambda(t,\theta) = \lambda_0\lambda(t,\theta)$. Substituting λ_t and $\mathcal{L}\lambda$ into the optimal condition for λ:

$$\lambda_t(t,\theta) + \mathcal{L}\lambda(t,\theta) - \rho\lambda(t,\theta) = 0,$$

we have:

$$\begin{aligned}
&-\sigma\beta_0 e_0\langle\ L_F, \beta_0 e_0\ \rangle_{\underline{S}}^{-\sigma-1}\tfrac{d}{dt}\langle\ L_F, \beta_0 e_0\ \rangle_{\underline{S}} + \beta_{0,t}e_0\langle\ L_F, \beta_0 e_0\ \rangle_{\underline{S}}^{-\sigma} + (\lambda_0 - \rho)\,\beta_0 e_0\langle\ L_F, \beta_0 e_0\ \rangle_{\underline{S}}^{-\sigma} = 0,\\
&-\sigma\beta_0 e_0\langle\ L_F, \beta_0 e_0\ \rangle_{\underline{S}}^{-\sigma-1}\tfrac{d}{dt}\langle\ L_F, \beta_0 e_0\ \rangle_{\underline{S}} + \left(\lambda_0 - \rho + \tfrac{\beta_{0,t}}{\beta_0}\right)\beta_0 e_0\langle\ L_F, \beta_0 e_0\ \rangle_{\underline{S}}^{-\sigma} = 0,\\
&-\sigma\tfrac{d}{dt}\langle\ L_F, \beta_0 e_0\ \rangle_{\underline{S}} + \left(\lambda_0 - \rho + \tfrac{\beta_{0,t}}{\beta_0}\right)\langle\ L_F, \beta_0 e_0\ \rangle_{\underline{S}} = 0,\\
&\tfrac{d}{dt}\langle\ L_F, \beta_0 e_0\ \rangle_{\underline{S}} = \tfrac{1}{\sigma}\left(\lambda_0 - \rho + \tfrac{\beta_{0,t}}{\beta_0}\right)\langle\ L_F, \beta_0 e_0\ \rangle_{\underline{S}}.
\end{aligned}$$

Hence, the solutions coming from the two approaches are identical if and only if:

$$\begin{aligned}
&\left[\frac{\lambda_0 - \rho}{\sigma} + \frac{\beta_{0,t}}{\beta_0}\right]\langle\ L_F, \beta_0 e_0\ \rangle_{\underline{S}} + \beta_0\left(L_F(\theta_2)e_0(\theta_2)\dot{\theta}_2 - L_F(\theta_1)e_0(\theta_1)\dot{\theta}_1\right)\\
&\qquad = \frac{1}{\sigma}\left(\lambda_0 - \rho + \frac{\beta_{0,t}}{\beta_0}\right)\langle\ L_F, \beta_0 e_0\ \rangle_{\underline{S}}.
\end{aligned}$$

The condition above can be simplified to:

$$\frac{1-\sigma}{\sigma}\frac{\beta_{0,t}}{\beta_0}\langle\ L_F, \beta_0 e_0\ \rangle_{\underline{S}} = \beta_0\left(L_F(\theta_2)e_0(\theta_2)\dot{\theta}_2 - L_F(\theta_1)e_0(\theta_1)\dot{\theta}_1\right). \tag{35}$$

In order to better understand our results, let us rewrite (25) as:

$$\frac{1-\sigma}{\sigma}\frac{\beta_{0,t}(t)}{\beta_0(t)} = \frac{N(\theta_2)[\phi(\theta_2)e_0(\theta_2)]^{-\frac{1-\sigma}{\sigma}}\dot{\theta}_2 - N(\theta_1)[\phi(\theta_1)e_0(\theta_1)]^{-\frac{1-\sigma}{\sigma}}\dot{\theta}_1}{\langle\ (\phi e_0)^{-\frac{1-\sigma}{\sigma}}N, \mathbb{1}\ \rangle_{\underline{S}}}.$$

Replacing $\frac{\beta_{0,t}}{\beta_0}$ into (35) using the expression above, we obtain that:

$$\begin{aligned}
&\dot{\theta}_2\left(\beta_0 L_F(\theta_2)e_0(\theta_2) - \frac{\langle\ L_F, \beta_0 e_0\ \rangle_{\underline{S}}}{\langle\ (\phi e_0)^{-\frac{1-\sigma}{\sigma}}N, \mathbb{1}\ \rangle_{\underline{S}}}N(\theta_2)\left(\phi(\theta_2)e_0(\theta_2)\right)^{\frac{\sigma-1}{\sigma}}\right)\\
&= \dot{\theta}_1\left(\beta_0 L_F(\theta_1)e_0(\theta_1) - \frac{\langle\ L_F, \beta_0 e_0\ \rangle_{\underline{S}}}{\langle\ (\phi e_0)^{-\frac{1-\sigma}{\sigma}}N, \mathbb{1}\ \rangle_{\underline{S}}}N(\theta_1)\left(\phi(\theta_1)e_0(\theta_1)\right)^{\frac{\sigma-1}{\sigma}}\right).
\end{aligned} \tag{36}$$

We can rewrite (36) using the definition of θ_i, i.e. $\dot{\theta}_i = DL_{F,\theta}(\theta_i)$, and using that:

$$\lambda(\theta) = \beta_0 e_0(\theta) \langle\ L_F, \beta_0 e_0\ \rangle_{\underline{S}}^{-\sigma}$$

and:

$$\begin{aligned}
\beta_0 &= \left(\frac{\sigma}{\rho - \lambda_0(1-\sigma)}\right)^{\frac{\sigma}{1-\sigma}} \langle\ (\phi e_0)^{-\frac{1-\sigma}{\sigma}} N, \mathbb{1}\ \rangle_{\underline{S}}^{\frac{\sigma}{1-\sigma}} \\
&L_{F,\theta}(\theta_2) e_0(\theta_2) \left(L(\theta_2) - \frac{\sigma}{\rho - \lambda_0(1-\sigma)} N(\theta_2) \phi(\theta_2)^{\frac{\sigma-1}{\sigma}} \lambda(\theta_2)^{\frac{-1}{\sigma}}\right) \\
&= L_{F,\theta}(\theta_1) e_0(\theta_1) \left(L(\theta_1) - \frac{\sigma}{\rho - \lambda_0(1-\sigma)} N(\theta_1) \phi(\theta_1)^{\frac{\sigma-1}{\sigma}} \lambda(\theta_1)^{\frac{-1}{\sigma}}\right).
\end{aligned} \tag{37}$$

(37) needs to be completed with the spatial boundary conditions that ensure that our operator is self-adjoint:

$$\nabla_\theta L_F(z) \nabla v(L_F)\ |_{\theta_1(t)}^{\theta_2(t)} = L_F(z) \nabla_\theta (\nabla v(L_F))\ |_{\theta_1(t)}^{\theta_2(t)}, \tag{38}$$

that is:

$$L_{F,\theta}(\theta_2)\lambda(\theta_2) - L_{F,\theta}(\theta_1)\lambda(\theta_1) = L(\theta_2)\lambda_\theta(\theta_2) - L(\theta_1)\lambda_\theta(\theta_1). \tag{39}$$

Hence, the optimal solution for the co-state variable in Phase 2 is given by the following system made of a PDE for the shadow price of fertile land, two boundary conditions on λ and λ_θ at θ_1 and θ_2 plus a transversality condition:

$$(III) \begin{cases}
\lambda_t(t,\theta) + \mathcal{L}\lambda(t,\theta) - \rho\lambda(t,\theta) = 0, \ \ \forall t \geq \tau, \ \text{ and } \ \forall \theta \in \underline{S}, \\
L_{F,\theta}(\theta_2) e_0(\theta_2) \left(L(\theta_2) - \frac{\sigma}{\rho - \lambda_0(1-\sigma)} N(\theta_2) \lambda(\theta_2)^{\frac{\sigma-1}{\sigma}} \psi(\theta_2)^{\frac{-1}{\sigma}}\right) \\
\qquad = L_{F,\theta}(\theta_1) e_0(\theta_1) \left(L(\theta_1) - \frac{\sigma}{\rho - \lambda_0(1-\sigma)} N(\theta_1) \phi(\theta_1)^{\frac{\sigma-1}{\sigma}} \lambda(\theta_1)^{\frac{-1}{\sigma}}\right), \ \ \forall t \geq \tau, \\
L_{F,\theta}(\theta_2)\lambda(\theta_2) - L_{F,\theta}(\theta_1)\lambda(\theta_1) = L(\theta_2)\lambda_\theta(\theta_2) - L(\theta_1)\lambda_\theta(\theta_1), \ \ \forall t \geq \tau, \\
\lim_{t\to\infty} \lambda L_F = 0, \ \ \forall \theta \in \underline{S}.
\end{cases}$$

G. Proof of Proposition 5. Steady states in Phase 2.

If at time $\tau' \geq 0$, a steady state is attained, then $\dot{\theta}_1(t) = \dot{\theta}_2(t) = 0$ for all $t \geq \tau'$. Let us denote the steady state solution $(\bar{L}_F, \bar{\psi}, \bar{\theta}_1, \bar{\theta}_2)$. At the steady state, the left hand side of (39) is zero. Since $L_F(\bar{\theta}_i) = L(\bar{\theta}_i)$ for $i = 1, 2$, (39) implies that:

$$L(\bar{\theta}_1) e_{0,\theta}(\bar{\theta}_1) = L(\bar{\theta}_2) e_{0,\theta}(\bar{\theta}_2).$$

By definition of the steady state, $\bar{L}_F$ is the solution of:

$$\mathcal{L}\bar{L}_F = \phi N \left(\phi\beta_0 e_0\right)^{-\frac{1}{\sigma}} \langle\ \bar{L}_F, \beta_0 e_0\ \rangle_{\underline{S}},$$

with $\bar{L}_F(\bar{\theta}_1) = L(\bar{\theta}_1)$ and $\bar{L}_F(\bar{\theta}_2) = L(\bar{\theta}_2)$. Besides, we know that $\bar{L}_{F,\theta}(\bar{\theta}_2) = \bar{L}_{F,\theta}(\bar{\theta}_1) = 0$. $\bar{c}$ will obtain using that $\bar{\lambda} = \frac{1}{\phi(\theta)}\bar{c}^{-\sigma}$. Regarding $\bar{\lambda}$, it verifies that:

$$\mathcal{L}\bar{\psi} - \rho\bar{\psi} = 0. \tag{40}$$

$\bar{c}(\bar{\theta}_1)$ and $\bar{c}(\bar{\theta}_2)$ follow from (36):

$$\bar{c}(\bar{\theta}_1) = \frac{\rho - \lambda_0(1-\sigma)}{\sigma}\frac{L_F(\bar{\theta}_1)}{N(\bar{\theta}_1)\phi(\bar{\theta}_1)},$$

$$\bar{c}(\bar{\theta}_2) = \frac{\rho - \lambda_0(1-\sigma)}{\sigma}\frac{L_F(\bar{\theta}_2)}{N(\bar{\theta}_2)\phi(\bar{\theta}_2)}.$$

And the border conditions for $\bar{\lambda}$ in (40) are:

$$\bar{\lambda}(\bar{\theta}_1) = \frac{1}{\phi(\bar{\theta}_1)^{1-\sigma}}\left(\frac{\rho - \lambda_0(1-\sigma)}{\sigma}\frac{L_F(\bar{\theta}_1)}{N(\bar{\theta}_1)}\right)^{-\sigma},$$

$$\bar{\lambda}(\bar{\theta}_2) = \frac{1}{\phi(\bar{\theta}_2)^{1-\sigma}}\left(\frac{\rho - \lambda_0(1-\sigma)}{\sigma}\frac{L_F(\bar{\theta}_2)}{N(\bar{\theta}_2)}\right)^{-\sigma}.$$

Hence the steady state $(\bar{L}_F, \bar{\lambda}, \bar{\theta}_1, \bar{\theta}_2)$ is the solution to:

$$(IV)\begin{cases} \mathcal{L}\bar{L}_F = \phi N \left(\phi\beta_0 e_0\right)^{-\frac{1}{\sigma}} \langle\ \bar{L}_F, \beta_0 e_0\ \rangle_{\underline{S}}, \\ \bar{L}_F(\bar{\theta}_1) = L(\bar{\theta}_1),\ \ \bar{L}_F(\bar{\theta}_2) = L(\bar{\theta}_2), \\ L_\theta(\bar{\theta}_1) = 0,\ \ L_\theta(\bar{\theta}_2) = 0, \\ \mathcal{L}\bar{\psi} - \rho\bar{\psi} = 0, \\ \bar{\psi}(\bar{\theta}_1) = \frac{1}{\phi(\bar{\theta}_1)^{1-\sigma}}\left(\frac{\rho-\lambda_0(1-\sigma)}{\sigma}\frac{L_F(\bar{\theta}_1)}{N(\bar{\theta}_1)}\right)^{-\sigma}, \\ \bar{\psi}(\bar{\theta}_2) = \frac{1}{\phi(\bar{\theta}_2)^{1-\sigma}}\left(\frac{\rho-\lambda_0(1-\sigma)}{\sigma}\frac{L_F(\bar{\theta}_2)}{N(\bar{\theta}_2)}\right)^{-\sigma}. \end{cases}$$

Recall that in Phase 2 $\rho < \lambda_0 = \max_{\lambda\in\sigma(\mathcal{L})}\lambda$. As $\bar{\lambda}$ is an eigenvector, then we have that $\bar{\lambda} \neq 0$, meaning that there exists a non-zero steady state that we characterize in the following. Since

the eigenvectors of $\mathcal{L}$ are orthogonal then:

$$\langle\, \bar{\lambda}, e_0 \,\rangle_{\underline{S}} = 0 \iff \langle\, \frac{\bar{c}^{-\sigma}}{\phi}, e_0 \,\rangle_{\underline{S}} = 0 \iff \langle\, \frac{[\langle \bar{L}_F, \beta_0 e_0 \,\rangle_{\underline{S}} (\phi\beta_0 e_0)^{-\frac{1}{\sigma}}]^{-\sigma}}{\phi}, e_0 \,\rangle_{\underline{S}} = 0$$
$$\iff \langle\, \bar{L}_F, \beta_0 e_0 \,\rangle_{\underline{S}}^{-\sigma} \beta_0 \langle\, e_0, e_0 \,\rangle_{\underline{S}} = 0 \iff \langle\, \bar{L}_F, \beta_0 e_0 \,\rangle_{\underline{S}} = 0.$$

The last equality obtains because $\beta_0 \neq 0$ and $\langle\, e_0, e_0 \,\rangle_{\underline{S}} = 1$. Finally, since $\bar{L}_F$ is a solution to:

$$\mathcal{L}\bar{L}_F = \phi N \left(\phi\beta_0 e_0\right)^{-\frac{1}{\sigma}} \langle\, \bar{L}_F, \beta_0 e_0 \,\rangle_{\underline{S}},$$

and since $\langle\, \bar{L}_F, \beta_0 e_0 \,\rangle_{\underline{S}} = 0$, we have that $\bar{L}_F \in ker\mathcal{L}$, *i.e.* $\bar{L}_F$ is a solution to:

$$\mathcal{L}\bar{L}_F = 0 \iff D\bar{L}_F'' + A(\phi - \nu)\bar{L}_F = 0.$$

Conclusion

The economic stakes throughout this thesis are the optimal, inter-temporal and intra-spatial use and preservation of natural resources. Optimal policies are analyzed by the mean of different methods of dynamic optimization, both analytically and numerically. We focus more particularly on the problem of intermittent renewable energy storage in the first chapter, then is assessed the question of land use raised by today's on-going development of land intensive climate change mitigation policies in the second chapter, to finally study the environmental concerns regarding diffuse soil pollution due to inappropriate agricultural practices in the third chapter. Hence, as other works from the field of natural resources economics, this thesis proposes research at the frontier of other disciplines, whether it is other social sciences such as geography, or natural sciences, such as physics or ecology. More particularly, this thesis focuses on analyzing the dynamics and interactions between economic policies on the one hand, and extra-economic dynamics on the other hand being, technological dynamics, geographic dynamics, and environmental dynamics.

Technological issues and their interactions with optimal economic policies are analyzed from various angles in this thesis. Indeed, this research focuses on the optimal technological policies for either the development of renewable energy or the storage of such resource, but it also addresses the question of pollution abatement technology, whether it is air or soil pollution. Geographical dynamics are also at the core of this thesis. For instance, the availability of renewable energy can vary from one geographical location to another, therefore affecting economic policies regarding either energy storage policies or land allocation policies for renewable energy production. Also, the economic activity is itself subject to ever-growing geographical pressures, in particular with today's development of land intensive, yet necessary, climate change mitigations policies. Reciprocally, the economic activity can also transform geographic areas, by being for instance responsible for the emergence of regions more or less polluted than others. Finally, the environmental dynamics provide with a general framework for the different research topics considered in this thesis. Indeed, we analyse the stochastic nature of renewable energy availability, along with the stakes of pollution accumulation due to the use of fossil fuels, or the spatial dynamics and implications of diffuse pollution through agricultural soils.